Unexpected Longevity Factors

Elisa Enriquez Hesles
B.S., College of William & Mary, 2014

A Dissertation presented to the Graduate Faculty
of the University of Virginia in Candidacy for the Degree of
Doctor of Philosophy

Department of Biochemistry and Molecular Genetics
University of Virginia
January 9, 2023

Abstract

Caloric restriction (CR), without malnutrition, is the most robust intervention used to increase the "healthspan" and extend the lifespan in model organisms ranging from yeast to mammals. It has been proposed that CR attenuates growth and improves cellular resistance to stress, thus leading to longevity. Longevity *via* CR hinges on extrinsic factors and intrinsic pathways at an organism's disposal. *Saccharomyces cerevisiae* (budding yeast) represents a well-studied model organism to enrich our understanding of how extrinsic factors and intrinsic pathways can activate longevity pathways. Over the years, scientists have learned a lot about aging pathways from altering genes and the environmental conditions in this single cell eukaryote. It has been shown that temperature, carbon source, metabolite availability, and pH all matter in regulating the longevity of yeast. At the molecular level, new canonical aging pathways and metabolites have emerged with clear links to growth and nutrient signaling including the sirtuins, mechanistic target of rapamycin (mTOR), AMP-activated protein kinase (AMPK), polyamines, and nicotinamide adenine dinucleotide (NAD^+). Our overarching goal is to add to the understanding of these mechanisms by which CR extends lifespan. One of those mechanisms appears to be through the unexpected underutilization of amino acids, such as methionine, suggesting a link between CR (glucose restriction), amino acid restriction, and methionine restriction (MetR), either at the level of transport or reduced catabolism relative to Non-Restriction (NR) conditions. In Chapter II, I focus on the unexpected similarities and common pathways between CR and MetR. In Chapter IV, I show that this low consumption of amino acids in CR, contrasts with the high demand of amino acids in the Non-Restriction (NR) condition suggesting that they are limiting for longevity in the context of NR. In Chapter III, I demonstrate how yeast chronological lifespan (CLS) assays can be used to study quiescence, and I conduct experiments to show that yeast is an organism with negligible senescence.

Acknowledgements

This project represents various years of time and effort. I am extremely appreciative of my advisor, Jeff Smith. I've learned much about leadership and science through his outstanding mentorship. I could not have done it without him. A special thanks to all the other Smith lab members, past and present including Ryan Fine and Nazif Maqani, Natalia, Agata Kalita. I want to thank the current Smith lab team for sharing the journey with me, especially Lindsey Power, Mani Dinda, and Carolyn Smith, it has been great to work with all of you. I also must thank Bill Petri, a dear mentor, for his continued support through my time in the program and his presence on the stands of the soccer pitch. I can always count on him. Thank you so much for your endless support and friendship. I must also thank my committee members Drs. Marty Mayo, David Auble, Kevin Lynch, and Dave Kashatus for their suggestions and support. I want to give Marty a special shoutout for always helping trouble shoot experiments and his willingness to share his vast knowledge of cellular metabolism. While at UVA, I was fortunate to be funded through the Cell and Molecular Biology (CMB) Training Grant, the Double Hoo, and the Robert Wagner Award. I thank faculty who were also involved in my training and growth as a scientist and leader including Drs. Eyleen O'Rourke, Norbert Leitinger, Janet Cross, Thurl Harris, Lili Powell, and Diane Whaley. I thank all the administrative staff, especially Debbie Sites, Carolyn Smith, Bill Garmer, and Nancy Rush. I want to thank my Ragged Mountain running family and UVA women's club soccer, and my Net six and Chill Soccer team. These groups were an important part of my identity as a graduate student. Finally, I want to thank my support system, my family for always being present. I wish you all happy, long, and healthy lives.

List of Abbreviations

ADE	Adenine
CFUs	Colony Forming Units
CLS	Chronological Lifespan
CR	Calorie Restriction
CRCM	Caloric Restriction Conditioned media
DNA	Deoxyribonucleic Acid
DR	Dietary Restriction
KO	Knock-Out
MET	Methionine
MetR	Methionine Restriction
mRNA	Messenger RNA
NQ	Non-quiescent
NR	Non-Restriction
NRCM	Non-Restriction Conditioned media
OCM	One-Carbon Metabolism
OD	Optical Density
Q	Quiescent
RLS	Replicative Life Span
RNA	Ribonucleic Acid
SC	Synthetic Complete
SGD	Saccharomyces Genome Database
TSP	Transsulfuration pathway
YKO	Yeast Knock Out
YPD	Yeast extract Peptone Dextrose

List of Tables and Figures

Table of Contents

Chapter I
Introduction to Aging

The purpose of Chapter I is describing the importance and evolution of the aging research field. It will highlight the tradeoff between growth and longevity, which is the principal theme in this dissertation. After covering some historical background, Chapter I will then shift to how scientists have turned to more malleable methods of modulating lifespan: dietary interventions and pharmaceuticals. Finally, Chapter I will discuss the role of yeast as a model system and preview relevant molecular pathways including the one-carbon metabolism (OCM) pathway.

The Aging Field Today

Biological aging is characterized by the progressive decline in an organism's ability to respond and adapt to the environment. This loss of physiological integrity leads to loss of autonomy and increased vulnerability to disease and injury (Lopez-Otin et al., 2013). Because of this, aging is the leading risk factor for most chronic diseases such as cardiovascular disease, cancer, arthritis, and neurodegeneration (Niccoli & Partridge, 2012).

Increased life expectancy has led to a higher number of older individuals. As the U.S. population continues to grow older, the prevalence of these diseases will only increase. In the medical system, healthcare providers, along with their patients, manage these diseases as they arise currently, offering disease management options to these patients and their families (Kaeberlein, 2019). In the scientific community, National Institute of Aging (NIA) investigators are seeking to understand the aging process at the cellular level and target its conserved hallmarks (Figure 1.1) in the hope to slow down the aging process, reduce disease development, and retain a healthy population across older generations. By doing so, scientists hope to extend "healthspan," which is defined as the number of years that an individual lives in the absence of serious conditions (Kaeberlein, 2018; Olshansky, 2018). This hypothesis of therapeutically targeting the biological aging process to slow down the decline in tissue function is termed the Geroscience Hypothesis (Austad, 2016). A better understanding of the aging process would transform medical care from reactive disease management toward preventative care (Kaeberlein, 2019). It would also take us closer to "rectangularizing" the survival curve, meaning increased average lifespan.

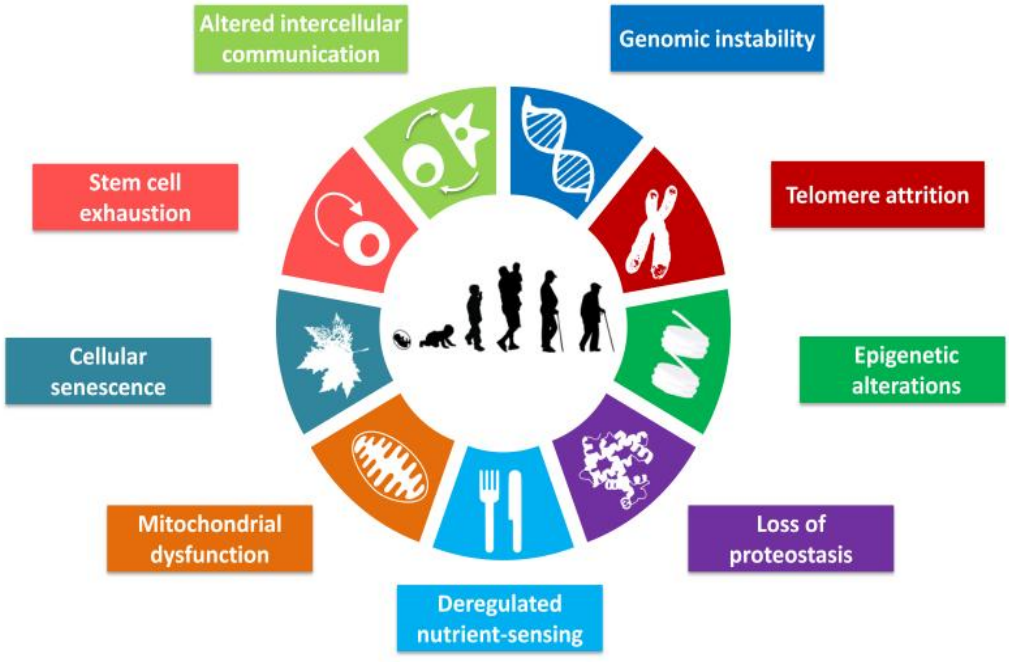

Figure 1.1 The iconic image of the 9 hallmarks of aging. *In a highly cited 2013 review by Carlos Lopez-Otin et al. authors describe 9 molecular-level defects associated with mammalian aging that are also frequently observed in simpler eukaryotic models including yeast. These have become molecular-level assessments of biological aging. The hallmarks are in no hierarchical order and describe typical characteristics of aging cells include genomic instability, telomere attrition, epigenetic alterations, loss of proteostasis, deregulated nutrient sensing, mitochondrial dysfunction, cellular senescence, stem cell exhaustion and intercellular communication. This image represents a broad paradigm of aging, uniting biology of aging scientists working toward a common goal (Gems & de Magalhaes, 2021). Although it offers a good starting point, it lacks explanatory power of what precisely causes aging (Gems & de Magalhaes, 2021).*

Re-thinking Aging as a Malleable Cell Process

Until recently, aging seemed to lack plasticity; it was thought that aging just happened in an unprogrammed manner. Because of this mindset we discounted its scientific investigation (Kenyon, 2011). In addition, although advancements in science

and medicine over the last century improved human mean lifespan, maximum lifespan seemed to remain constant (Blagosklonny, 2010). Scientists in the field of geroscience eventually began to re-think the malleability of aging due to the key discovery of longevity genes (Bartke & Quainoo, 2018).

The field of aging research intensified as soon as scientists realized that the aging process consists of biologically regulated pathways that can be dissected, analyzed, and controlled. In 1993, Cynthia Kenyon described a mutant in the *C. elegans daf-2* gene that lives two times longer than wild type (Kenyon et al., 1993). These studies demonstrated that there truly was a significant genetic component to the aging process. This news attracted wide attention as it also hinted at the malleability of our own aging process (Bartke & Quainoo, 2018). Follow-up studies revealed that these longevity genes centered around insulin signaling pathway. For example, the DAF-2 protein is homologous to Insulin-like growth factor receptor (IGF-1) in mammals and influences the conserved FOXO transcription factor (*DAF-16*) (Kimura et al., 1997; Sun et al., 2017). Importantly, this pathway regulates glucose metabolism and promotes growth in response to food intake. Thus, attenuating these pathways induced a physiological state resembling food shortage response (Kishimoto et al., 2018).

Brown-Borg *et al.* (Andrzej Bartke lab) was the first group to publish that the Ames dwarf mutation (causing dwarfism) allowed mice to live longer (Brown-Borg et al., 1996). The Ames dwarf mouse has a loss of function mutation in the *PROP-1* transcription factor gene that causes an underdeveloped anterior pituitary gland which is responsible for the secretion of growth hormone (GH), prolactin, and thyroid stimulating hormone (Brown-Borg et al., 1996). Relevant to the previous discussion, IGF-1 was

found to function downstream of GH, as impaired GH led to a decline in the levels of IGF-1 factor in circulation of the mice. Studies of the Ames mouse provided more evidence for the role of growth pathways in longevity and contributed to the development of interventions to counter this IGF-1/insulin pathway (Brown-Borg, 2006).

There is evidence that attenuation of the GH pathway *via* secretion or receptor defects correlates with physiological benefits in humans (reviewed extensively in Bartke & Quainoo, 2018). Multiple studies have linked beneficial polymorphisms in the human IGF-1R gene that increase an individual's probability to become a centenarian (Bonafe et al., 2003; Milman et al., 2014; Suh et al., 2008). Attenuation of growth *via* these signals essentially reduces the rate of aging and decreases age-associated diseases. In contrast, acromegaly—a hormonal disorder involving too much GH in humans—predisposes an individual to various health problems and early mortality (Wright et al., 1970).

In summary, genes that limit growth tend to enhance longevity in multiple model organisms, and in humans, delay the onset of age-related disease. Thus, a major goal to advance healthspan became to attenuate growth pathways. How is attenuating growth pathways in an organism promoting health?

Attenuating Growth Pathways

Valter Longo and others proposed lifespan extension occurred in model organisms because the organisms shifted the investment of energy from growth and reproduction to multiple stress resistance systems (Bartke et al., 2013; Fabrizio et al., 2003; Fabrizio et al., 2001). This strategy of survival describes Thomas Kirkwood's 1977 Disposable Soma Theory of aging (Figure 1.2). The Disposable Soma Theory states that an organism has limited resources that it can allocate to growth or maintenance of tissues

(Gavrilov & Gavrilova, 2002). Findings suggest that GH suppression may have beneficial effects on cellular response and antioxidant defenses. For example, GH suppression increased glutathione levels and upregulated heat shock proteins in mouse tissues (Brown-Borg, 2006). Furthermore, cells isolated from the long-lived Ames mouse were more stress resistant in culture when exposed to hydrogen peroxide and other stressors compared to cells from their normal littermates (Salmon et al., 2005). In tandem with the Theory of 'Disposable Soma', the Theory of Hyperfunction describes aging as a continuation of developmental and reproductive programs that are not fully turned off during completion (Blagosklonny, 2021). George Williams saw instances of this (i.e. the benefits of an allele on fitness during development compared to its later negative effect) and named it antagonistic pleiotropy (Austad & Hoffman, 2018; Williams, 1957). To mitigate the detrimental impacts of antagonistic pleiotropy, scientists study interventions, which diminish cell growth pathways. Two interventions commonly studied are Caloric Restriction (CR) and Methionine Restriction (MetR).

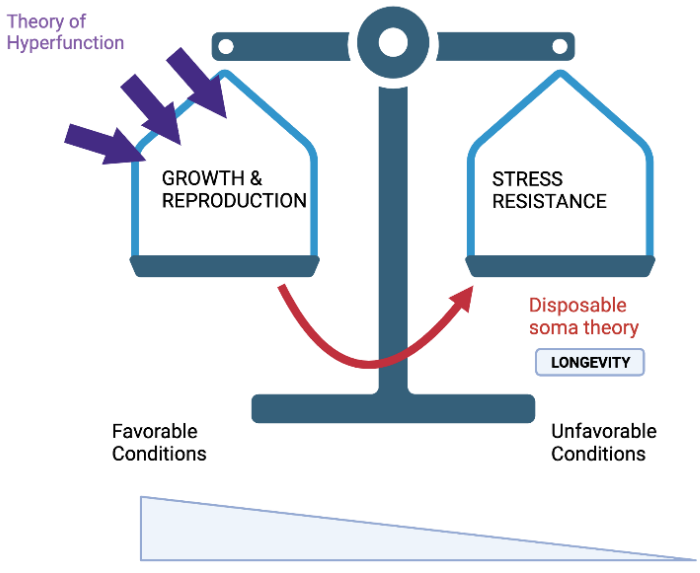

Figure 1.2 Disposable Soma Theory, Theory of Hyperfunction and Antagonistic Pleiotropy. *In favorable conditions with little stress and abundant resources, organisms that allocate more energy and resources to grow and reproduce outcompete the slow growers. These fast-growing organisms do not invest in repair and maintenance of somatic cells. In unfavorable conditions, organisms invest in survival and resilience and fare better in the long run as described in the Disposable Somatic Maintenance Theory. Schematic adapted from (Pitt & Kaeberlein, 2015).*

Calorie Restriction (CR)

CR is a well-studied dietary regimen and understanding its mechanism is central for this thesis. CR extends lifespan in a wide variety of model organisms ranging from the budding yeast, *Saccharomyces cerevisiae*, to non-human primates, implying that conserved cellular processes and pathways must mediate the beneficial effects, or somehow be impacted by the dietary regimen (Fontana et al., 2010). Indeed, conserved processes including autophagy, TOR signaling, and AMPK signaling have each been implicated in regulating aging in most models of CR, including yeast (Kapahi et al., 2017). Furthermore, CR promotes a metabolic program that enhances mitochondria function (Martin-Montalvo & de Cabo, 2013), improving proteasomal activity (da Cunha et al., 2011), and activating superoxide dismutase against reactive oxygen species (Agarwal et al., 2005). CR has also been shown to rejuvenate aspects of progenitor cells in muscle tissue (Cerletti et al., 2012). In humans it has been shown that long-term CR inhibits the IGF-1/insulin pathway in different tissues (Mercken et al., 2013). CR has also been tested in humans in the Comprehensive Assessment of Long-term Effects of Reducing Intake of Energy (CALERIE™) Phase-2 randomized trial (Rochon et al., 2011). This study consisted of evaluating the effects of reducing individuals' food intake by 25% of their base line diet (Rochon et al., 2011). It was conducted over a two-year

period to assess the benefits of CR and separate them from benefits of weight loss (Belsky et al., 2017). The results showed that achieving a mean of ~11% CR lowered "biological age," independent of weight loss with system-wide benefits (Belsky et al., 2017). Subsequent studies have revealed that intermittent fasting (IF) (de Cabo & Mattson, 2019) and alternate-day fasting (ADF) (Stekovic et al., 2019) recapitulate benefits similar to CR, specifically improved cardiovascular parameters and body composition (Stekovic et al., 2019). In studying CR, great advancements continue to be made in determining the role of metabolism, diet composition, sex dimorphisms, and timing of feeding on longevity.

Methionine Restriction

MetR is a dietary regimen that specifically limits intake of the amino acid, methionine. Methionine plays a role in various biological processes including protein synthesis, methylation, and glutathione production. It has been shown that an isocaloric diet with MetR can extend longevity in rodents, fruit flies, and yeast (Lee et al., 2014; Orentreich et al., 1993; Richie et al., 1994; Sun et al., 2009). The mechanisms underlying the lifespan extension effects of MetR are not yet fully understood, but several theories have been proposed. A review by Kitada *et al.* highlights that MetR mediates benefits by reducing oxidative stress via autophagy, promoting polyamine synthesis, H_2S production, and lowering mitochondrial free radical leakage (Kitada et al., 2021). For example, MetR has been shown to increase polyamine levels in the liver of mice (Bárcena et al., 2018). MetR has also been shown to decrease mTOR signaling (Kitada et al., 2020), which is a central regulator of cell growth and metabolism (Kim & Guan, 2019). MetR and/or cysteine restriction—another sulfur amino derived from methionine—improves several

hallmarks of aging. For example, in model organisms, their restriction reverses age-related DNA methylation loss (Mattocks et al., 2017), improves protein folding machinery (Nichenametla et al., 2022), and induces mitophagy (Plummer & Johnson, 2019). Not restricting these sulfur-containing amino acids in the diet has consequences outside laboratory studies. For example, epidemiological studies suggest that methionine intake may increase T2DM risk in humans (Dong et al., 2022).

Summary of Project Aims

Given the difficulty of CR adherence, research has focused on understanding changes in pathways and the mechanism of action underlying CR lifespan extension to facilitate the development of new interventions that mimic the beneficial effects of CR without having to drastically restrict calories. Rapamycin (mTOR inhibition), Metformin (AMP- activated Protein Kinase (AMPK) activation), Sodium-Glucose Cotransporter-2 (SGLT) inhibitors, and other pharmacological agents show great promise in improving various health parameters (La Grotta et al., 2022; Novelle et al., 2016). Senolytics are also potential agents that are just beginning to be explored as healthspan-improving interventions (Kirkland & Tchkonia, 2020). To add to the list of possible interventions, NIA scientists are objectively evaluating selected soluble molecules and other drugs in genetically heterogeneous mice via the intervention testing program (ITP) to identify promising candidates for trials in humans (Macchiarini et al., 2021).To this end, a better understanding of the interplay between interventions and intrinsic aging pathways is warranted. One of the most informative model organisms for these studies is the budding yeast. Our goal is to use *Saccharomyces cerevisiae* to identify novel conserved pathways, factors, metabolic programs, and genes that contribute to CR lifespan extension or are causative for aging. It is an exciting time to be a scientist in this field as underlying cellular mechanisms remain to be untangled.

Yeast as a Model System to Explore Intrinsic Cellular Pathways Described in the Hallmarks of Aging

Model organisms have a crucial role in elucidating the underlying mechanisms of CR and generating CR-mimetics. Model organisms are used because of their short

lifespan, easy maintenance, and environmental and genetic manipulations (Taormina et al., 2019). Yeast, worms, fruit flies, killifish or mammalian models such as mice, monkeys, and dogs are helping dissect pathways activated in aging processes (Taormina et al., 2019). *Saccharomyces cerevisiae* became and continues to be an important low-cost model system to understand cellular intrinsic pathways of aging in higher organisms (Jazwinski, 2005). As single-cell organisms, yeast do not exhibit signs of age-associated diseases that involve organs, but they do offer a way to study the conserved molecular pathways involved in the aging process. First, budding yeast is unparalleled in the ease of genetic manipulation and the variety of available genetic and genomics tools available, as highlighted by the yeast gene knockout (YKO) collection(Winzeler EA, 1999). Second, for aging studies, we perform start to finish whole lifespan experiments within 3 to 4 weeks, and in high throughput. Third, the small genome size (6,000 genes) allows us to heavily multiplex Next-generation sequencing libraries, which again increases throughput and statistical power of having multiple biological replicates. Fourth, this model organism also facilitates manipulation of the surrounding environment. For example, the use of synthetic complete media (SC), which consists of defined levels of amino acids and nutrients, allows scientists to test for nutritional factors mediating longevity. In addition, yeast screens became a common tool to identify and study molecular pathways. In fact, sirtuins, NAD^+ metabolism, and mTOR, were widely studied and sometimes discovered in yeast (Croft et al., 2020; Heitman et al., 1991). To understand the general principles undermining the aging process, scientists rely on Replicative Aging and Chronological Aging models (Postnikoff & Harkness, 2014).

Two models of aging in yeast: RLS and CLS

Yeast Replicative Lifespan (RLS)

Saccharomyces cerevisiae is a unicellular eukaryote that reproduces asymmetrically so a mother cell can be isolated from daughters it produces (Sinclair & Guarente, 1997). The way that some yeast and bacteria divide has earned them the reputation of potentially being immortal and immune to senescence (Sheldrake, 2022). RLS is defined as the number of cell divisions a cell undergoes before it reaches irreversible cell cycle arrest (R. K. Mortimer & J. R. Johnston, 1959). In this model, senescence is obtained when the mother cell can no longer divide despite abundant resources. This model is helpful to understand the conserved process of aging of *dividing cells* (Wasko & Kaeberlein, 2014). There are various techniques to use to isolate and study replicative "old" mother cells. To quantify RLS, individual mother cells can be manually arrayed onto the surface of an agar plate using a dissection microscope and then each daughter cell counted and removed after each division (Robert K. Mortimer & John R. Johnston, 1959; Taormina et al., 2019). Budding scars on the surface of mother cells can also be counted by staining with calcofluor white. In addition, scientists can "capture" and visualize cells in real-time using channels in a microfluidics system (Jo & Qin, 2016). This model of aging is analogous to replicative lifespan of primary mammalian cells, like fibroblast cells (Steinkraus et al., 2008). These mammalian cells shorten their telomeres with each passage because they do not express the enzyme telomerase. This drives senescence. Since yeast constitutively express telomerase, a yeast cell's telomeres do not significantly shorten, therefore they become senescent *via* other means (D'Mello & Jazwinski, 1991; Wierman & Smith, 2014). Budding yeast offers a

way to study replicative aging mechanisms independent of telomere attrition (Wierman & Smith, 2014). This is advantageous as RLS can be a good model system to study hallmarks of aging such as DNA instability in actively proliferating cells.

In studying aging using RLS, *SIR2* (silent information regulator 2) emerged as an anti-aging gene that mediates lifespan at least partially by controlling rDNA stability (Gottlieb & Esposito, 1989; Kennedy et al., 1995; Smith & Boeke, 1997; Wierman & Smith, 2014). Sir2p represses transcription at heterochromatic domains and its histone deacetylase activity is driven by NAD^+ availability, linking longevity to metabolism (Imai et al., 2000; Smith & Boeke, 1997). Since its discovery in yeast, Sir2p has been shown to regulate lifespan in many other species by modulating hallmarks of aging including changes in genome instability, and epigenetic alterations (Wierman & Smith, 2014). In yeast, deletion of Sir2 increased rDNA instability, augmenting the formation of toxic extra-chromosomal rDNA circles (ERCs), and decreased viability (Kaeberlein et al., 1999). Interestingly, although *SIR2* is required for yeast RLS extension under CR conditions (Lin et al., 2000), it may not be required for the CR effect in chronological lifespan (Smith Jr. et al., 2007). In fact, loss of Sir2p activity pushes cells toward nutrient storage in the form of glycogen and trehalose *via* gluconeogenesis, which promotes stress resistance and long-term survival in the stationary phase (Casatta et al., 2013).

Yeast Chronological Lifespan

Whereas RLS analyzes proliferating cells in the exponential phase of growth, CLS analyzes the aging of non-dividing stationary phase cells (Figure 1.3). CLS is defined as the number of days that a non-dividing yeast cell survives in the stationary-phase liquid culture (Fabrizio & Longo, 2003). In chronological aging, ERCs do not play

a role in CLS (Ashrafi et al., 1999). Interestingly, cells that have undergone chronological aging have reduced RLS due to cellular damage during stationary phase (Ashrafi et al., 1999). Most of these CLS experiments utilize glucose and begin when a small number of cells are inoculated in a liquid culture and grown at 30°C. Herein, yeast undergo rapid proliferation when cells utilize fermentable carbon sources in the media if available. Fermentation is preferred even in the presence of oxygen. This is termed the Crabtree effect and it is like the Warburg effect in cancer cells (Hammad et al., 2016). As the cells run out of glucose and transition to the stationary phase, cells shift their metabolism to catabolize non-fermentable products. Herein the cells rely on oxidative phosphorylation and their mitochondria. This metabolic shift is termed the diauxic shift and it becomes critical in CLS. During this transition the cells increase endogenous stress defense mechanisms contributing to cell survival (Casatta et al., 2013). Specifically, cells increase gluconeogenesis, reduce acetic acid in the media, and accumulate trehalose (Casatta et al., 2013). Once they enter the stationary phase, cells stop dividing and enter quiescence—a temporary state of cell cycle arrest (Sun & Gresham, 2021). The most commonly fermentable carbon source used is glucose. As the cells exhaust glucose during fermentation, they must shift their transcription and metabolism to the TCA cycle and oxidative phosphorylation in response to changes in carbon source availability--the ethanol that has accumulated from fermentation. CLS assays can also be performed with other non-fermentable carbon sources like acetate and glycerol. With these non-fermentable carbon sources, these cells are forced to activate mitochondrial-based metabolism from the start, thus extending CLS (Smith Jr. et al., 2007).

Once in stationary phase, CLS is assessed by measuring the ability to re-enter the replicative growth phase and produce colony forming units (CFUs). This traditional method established by Valter Longo as well as newer methods will be reviewed extensively in Chapter III. This chronological model has been informative in the aging of post-mitotic tissues (Fontana et al., 2010). Furthermore, yeast is a model system where we can readily study quiescence pathways. These quiescent pathways are important because they tap into genetic programs of resiliency and survival instead of growth and reproduction (Figure 1.3)(Jazwinski, 2002). Quiescence is a state something that is akin to estivation in mammals, dauer stage in *C. elegans*, or diapause in killifish. In these organisms, urgency exists to appropriately respond to environmental cues in these two ways: to ensure reproduction now or later. It is thought that by tapping into these programs or inhibiting growth pathways, we can potentially extend our own longevity (Jazwinski, 2002). Thus, yeast CLS presents a model system to study pathways and signals that promote quiescence and ultimately longevity in non-dividing cells. Because yeast cells shift their metabolism towards oxidative phosphorylation, CLS also can be used to study the mitochondrial contributions to longevity regulation. Mitochondrial dysfunction has been identified as a major hallmark of aging (Lopez-Otin et al., 2013). Previous work in yeast, has shown that non-fermentable carbon sources that force respiration extend CLS, thus emphasizing its importance.

In CLS, the media is usually not replaced and therefore cells compete for finite nutrient resources. This aging model has been criticized because cells may not be "aging," but instead starving (Nagarajan et al., 2014). However, others show that the cell death that eventually occurs in stationary phase cultures is not simply due to starvation

(Fabrizio & Longo, 2003). It has also been argued that CLS in yeast is not a good model for organismal aging, yet the same pathways that drive successful transition into quiescence in yeast are the ones studied in mammalian aging (Leontieva & Blagosklonny, 2011). Both models of aging in yeast have been important in helping scientists understand the underlying mechanisms of CR (Fabrizio & Longo, 2007; Lin et al., 2000). We view both to be important for a comprehensive view of the aging process and discovery of novel genes and concepts. They even may represent each side of the balance in Figure 1.3.

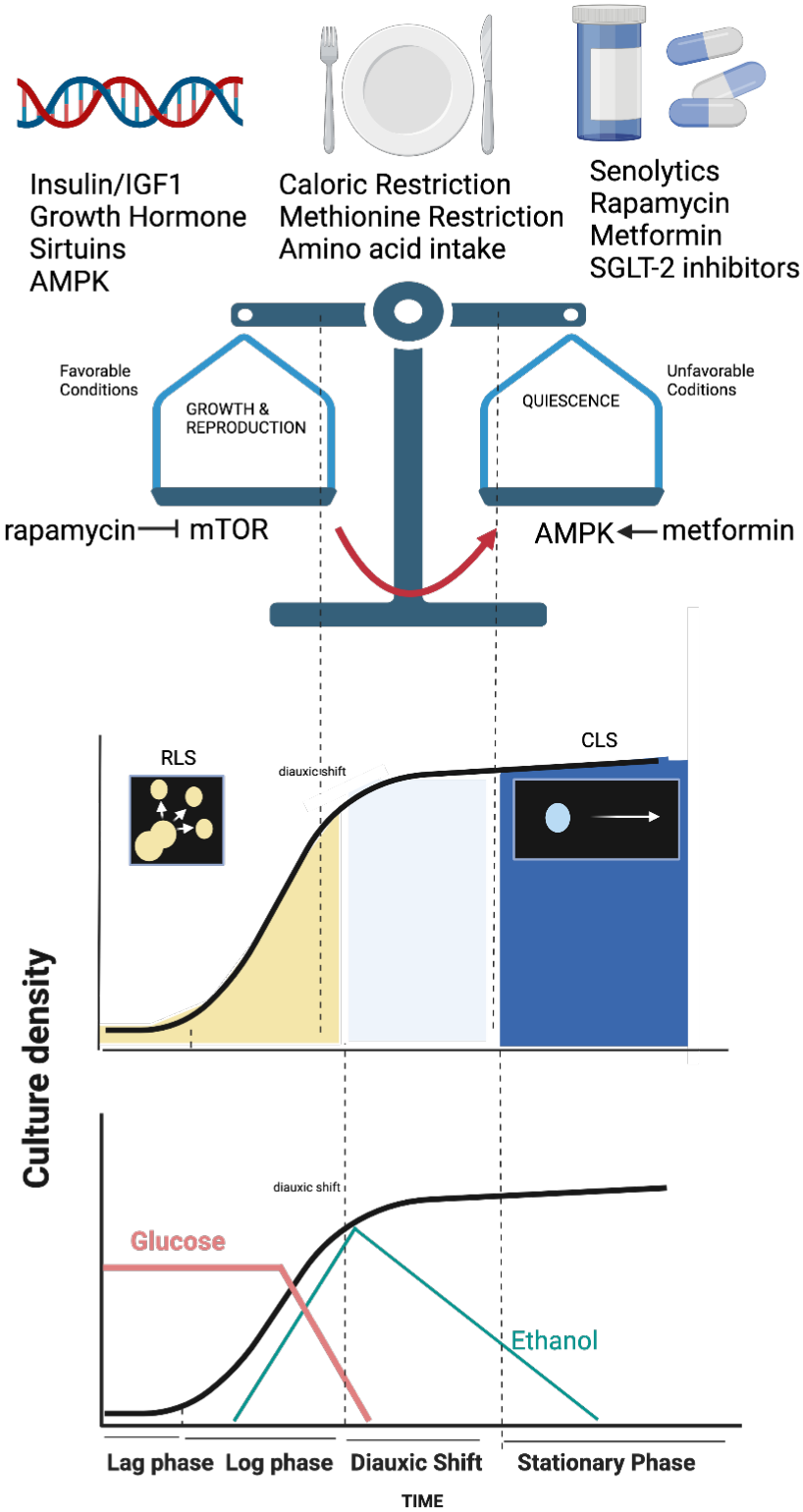

Figure 1.3 Metabolism of RLS and CLS to study mechanisms of aging and quiescence. *List of intrinsic factors (Growth Hormone, Sirtuins, Insulin/IGF), dietary interventions (Caloric Restriction, Methionine Restriction, Amino Acid intake), and*

pharmaceuticals (SGLT-2, Rapamycin, Metformin). Diagram shows that these play a role in shifting the balance between growth/reproduction and quiescence/longevity. Replicative lifespan (RLS) is defined as the number of daughter cells produced before reaching senescence. Cells in RLS are studied in the exponential growth phase. When glucose is used, exponentially growing cells generate energy through glycolysis and fermentation to regenerate NAD^+. CLS is studied once the cells enter stationary phase and they are no longer dividing. One of the reasons that yeast live so long in the stationary phase is that they adapt to the low nutrient environment and enter a temporary state of quiescence—a program to ensure survival when the conditions call for it. Herein, the cells change their metabolism during the diauxic shift. Specifically, the cells shift their energy from growth and reproduction and enter a non-dividing quiescent state. In this non-dividing quiescent state, cells are more resilient and activate important pathways for survival including autophagy (Alvers et al., 2009; Matecic et al., 2010). Interestingly, stationary phase cells are more resistant to stress than dividing cells in log phase (Calahan et al., 2011), exemplifying the resilience-vs-growth tradeoff.

Caloric Restriction in Yeast

CR condition consists of reducing glucose concentration of the starting media from 2% in non-restriction (NR) to 0.5% in CR. Lowering glucose limits the growth, but also extends the longevity of cells in liquid culture (Figure 1.4). This attenuation of growth reflected by the cell culture density perfectly emulates the tradeoff between growth and longevity previously discussed (Figure 1.2). In nutrient-favorable conditions, NR, proliferating cells allocate resources toward cell division. In nutrient unfavorable conditions, such as CR, cells shift their metabolism towards stress resistance. Even in this unicellular eukaryote, lower growth is also accompanied by an increase in cell resistance to elevated temperatures (Smith Jr. et al., 2007), and increase in reactive oxygen species (ROS) defense (Agarwal et al., 2005). Drawing on evolutionary theory, I propose that CR

and NR utilize a different metabolic strategy given the environmental challenge, which has implications on CLS.

First, CR-treated cells expend less energy on proliferation and growth, and instead, cells allocate resources towards stress resistance. For example CR cells accumulate trehalose—a reserve carbohydrate—*via* gluconeogenesis, which contributes to proteostasis, oxidative damage protection, and life extension (Kyryakov et al., 2012). In the CR condition, cells also adapt to utilize an alternative carbon source to build remaining biomass. AMPK activation allows for the utilization of such carbon sources (Jazwinski, 2002). Indeed, it was observed that acetic acid generated from fermentation did not accumulate in CR treated cells indicating conversionof acetate into acetyl-CoA due to AMPK activation (Wierman et al., 2015). This makes sense as carbon source is limiting under CR. In these CR conditions, shifting metabolism toward gluconeogenesis and respiration allows the cell to survive in stationary phase and to maintain a quiescence state (Smith et al., 2007).

In contrast, NR-treated cells allocate resources towards rapid growth and reproduction, taking advantage of the favorable nutrient conditions (Figure 1.4 A & B). In favorable conditions, there is less selection for homeostasis and maintenance. However, activating this strategy may have detrimental effects for longevity as George Williams' 1957 antagonistic pleiotropy theory describes (Austad & Hoffman, 2018; Williams, 1957). Studying NR and CR in yeast has enabled new intrinsic pathways of aging to be discovered. One central pathway is the one-carbon metabolism (OCM) which will be discussed below.

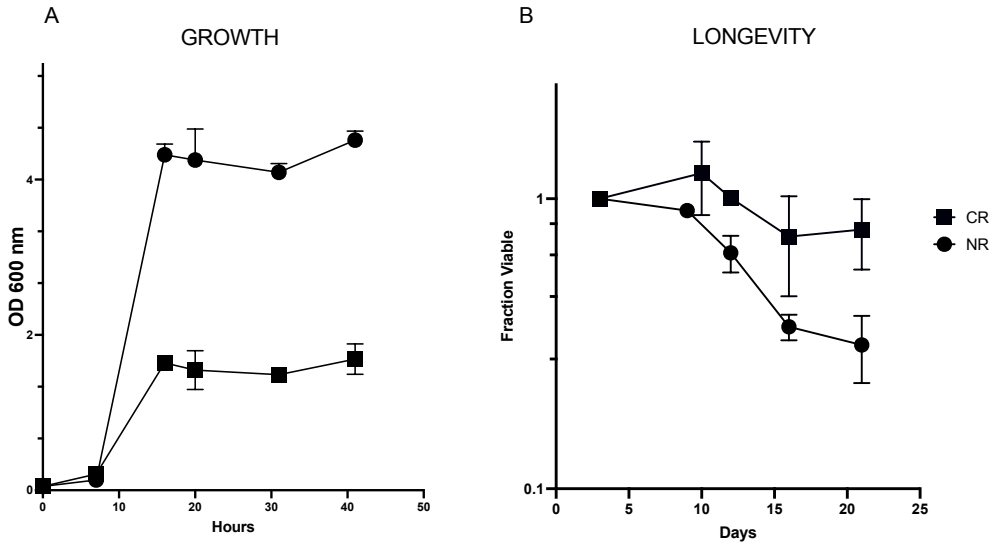

Figure 1.4 CR extends longevity while diminishing liquid culture growth. *A) Liquid culture growth assay of CR-treated cells compared to NR-treated cells. CR condition consists of reducing glucose level of the starting media from 2% in NR to 0.5% in CR. Cells were inoculated in liquid cultures and growth was measured. Absorbance of 3 biological replicates was monitored using a spectrophotometer at 600 nm wavelength. An example of CLS of these two conditions is seen in B).*

One-Carbon Metabolism (OCM) in Aging

The OCM pathway is a central metabolic hub where interconnecting biochemical reversible reactions from the folate, methionine cycle, and transsulfuration pathway (TSP) meet (Lionaki et al., 2022). Its core function is to deliver one-carbon units (1C)—important building blocks for anabolic pathways to maintain homeostasis in proliferating cells (Suh et al., 2016). This 1C transfer from one molecule to another is facilitated through tetrahydrofolate (Lionaki et al., 2022). Based on mammalian systems, parallel pathways occur in the mitochondria, in the nucleus, and in the cytosol, each with similar inputs, outputs, cofactors, and enzymatic reactions (Lionaki et al., 2022). In the nucleus, dTMP synthesis is generated to support DNA replication during S-phase of the cell cycle

(Anderson & Stover, 2009). These indispensable series of reactions have been well established to regulate nucleotide synthesis, amino acids homeostasis, and methionine availability for epigenetic regulation (Lionaki et al., 2022). The OCM pathway relies on the availability of micronutrients as substrates for these growth pathways. Nutrients such as methionine, choline, betaine, threonine, L-serine, glycine, selenium, and retinoic acid are directly and indirectly involved in this biochemical network (Suh et al., 2016) (Figure 1.5)

The methionine cycle is connected to the OCM (Figure 1.5). Methionine can be used to synthesize taurine and glutathione which protects a cell from oxidative stress. Methionine can derive synthesis of S-adenosylmethionine (SAM), which is the universal donor substrate for DNA methylation and histone methylation (Suh et al., 2016). Interestingly, SAM is also a precursor for synthesis of the polyamines, spermidine and spermine, which have been shown to have life extension properties (Suh et al., 2016). SAM donates a methyl group to methylation reactions and becomes S-adenosylhomocysteine (SAH). In the process, SAH can then turn into homocysteine which then becomes remethylated into methionine or reacts with L-serine to become cystathionine *via* the TSP, which has been shown to be upregulated in long-lived humans (Mota-Martorell et al., 2021). Elevated levels of homocysteine are indicative of OCM imbalance and these levels have been associated with aging (Suh et al., 2016). Past studies show that SAH supplementation can mimic MetR and activate autophagy by inhibiting the enzyme that converts methionine to SAM (methionine adenosyltransferase), thus reducing SAM levels (Ogawa et al., 2022).

There are increasing reports that the OCM may be a shared pathway that regulates mechanisms of longevity (Lionaki et al., 2022). For example, folate and OCM have been hypothesized to alleviate unrepaired DNA damage by providing nucleotides to growing cells by supporting *de novo* nucleotide synthesis (Duthie et al., 2002). Various genetic and environmental manipulations of the pathways have impacted lifespan in various model organisms (Lionaki et al., 2022). The Ames dwarf mouse, which is long-lived, has higher levels of OCM enzymes (Suh et al., 2016). Relevant to this dissertation, a study showed that depletion of ribosomal proteins increased RLS in yeast (Maitra et al., 2020b). Noteworthy, reduction of these ribosomal proteins specifically reduced the levels of the OCM proteins, correlating with lifespan extension (Maitra et al., 2020b). Why would reducing OCM metabolism increase lifespan if it's critical? This extension due to reduced translation actually makes sense in the context of the tradeoff between growth and longevity, as the OCM pathway has been linked to growth and proliferation pathways—it is especially critical in cancer cells. Specifically, attenuation of growth *via* OCM pathway perturbation has been shown to extend lifespan, including work from this thesis project (Chapter IV).

One-Carbon Metabolism and Proliferating cells

OCM is critical to proliferating cells. In fact, pregnant mothers are encouraged to increase their folate intake to preserve the flow of 1C units that fuel critical building blocks for fetal growth (Korsmo & Jiang, 2021). These building blocks ensure proper neuronal development of the fetus (Lionaki et al., 2022). Aberrant cell growth also relies on this hub to be successful (Newman & Maddocks, 2017). For example, misregulated and hyperactivated OCM proteins like Shmt2p often fuel cancer as outputs of this cycle

are in high demand (Kim et al., 2015; Newman & Maddocks, 2017). Multiple drugs are designed to inhibit this cycle but are contraindicated in pregnancy. It has been shown that restricting components linked with OCM, like methionine, improves cancer patient outcomes (Gao et al., 2019). Interestingly, more and more studies are pointing towards the OCM being equally important to non-proliferating tissues in regulating longevity (Suh et al., 2016). In our studies, we showed that mutations in both mitochondrial OCM and cytoplasmic OCM genes extended yeast CLS in NR conditions (Enriquez-Hesles et al., 2021; Matecic et al., 2010).

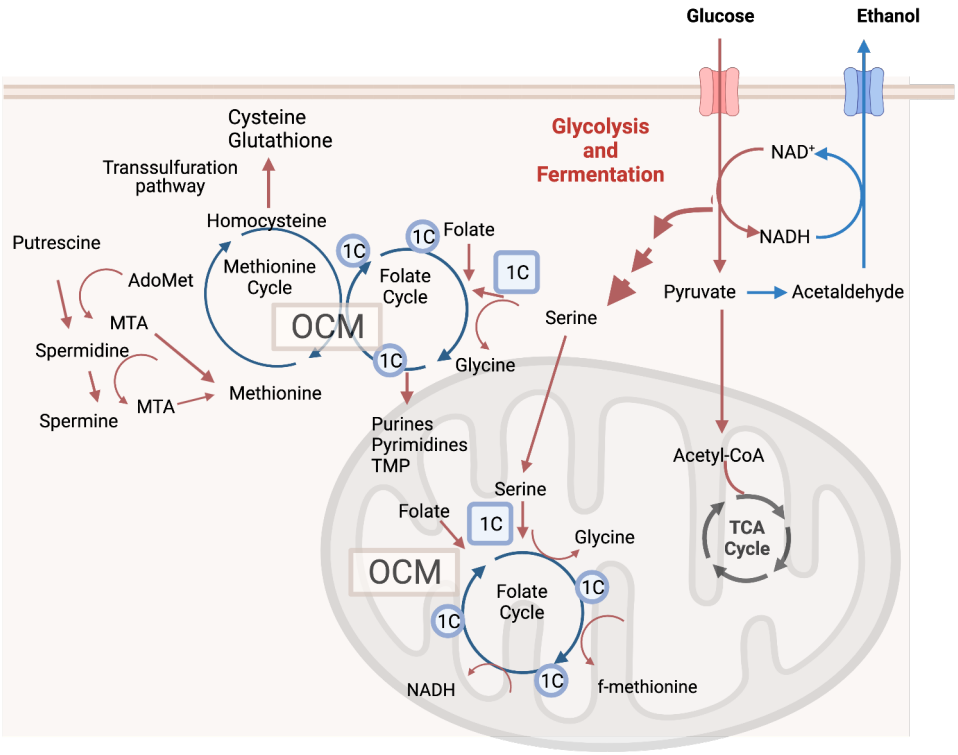

Figure 1.5 Schematic of intracellular pathways mediating longevity with a focus on the one-carbon metabolism (OCM) and associated pathways. *One-carbon metabolism (OCM), like the name implies, consists of the transfer of methyl groups to within the folate and methionine cycles. This occurs in the mitochondria and in the cytoplasm. The polyamine biosynthesis pathways and the transsulfuration pathway (TSP) are also involved. The OCM is crucial for early development as the methyl groups are used for a*

range of building blocks including nucleotides and methylation of DNA and protein. Key metabolites discussed throughout the dissertation are depicted in the diagram including L-serine, polyamines (spermidine, putrescine, spermine, and MTA). Metabolite abbreviations are as follows. 5'-methylthioadenosine (MTA), S-adenosyl-L-methionine (AdoMet).

Back to Dissertation

Aging is an important field of study and great advances have been made since the discovery of longevity genes. Throughout this dissertation, CR with NR studies were conducted using CLS in budding yeast as a model system. Specifically, the dissertation explores extrinsic factors and nutrients influencing intrinsic pathways discussed with a focus on growth-longevity trade-off. The central hypothesis is that CR and NR cells employ two different strategies. While CR cells invest in resilience, NR cells invest in growth. This strategic approach in CR-treated cells leads to underutilization of nutrients, enhanced mitochondrial function, and increased longevity. In contrast, under glucose abundant conditions, the NR-treated cells invest in growth pathways depleting nutrients and losing viability at a faster rate compared to CR cells. Targeting growth pathways like the OCM pathway or reducing methionine in NR (MetR) attenuates growth and reproduces longevity employed by CR cells. The loss of OCM enzymes does not extend longevity in CR cells because this pathway, along with other growth-promoting pathways, is already attenuated under this condition.

Chapter II

Yeast as a model to understand CR and MetR in Chronological Lifespan

Abstract

Longevity hinges on extracellular and intracellular resources at the cell's disposal. Yeast represents a well-studied model organism to enrich our understanding of how genes and environment activate longevity pathways. Cynthia Kenyon's initial experiments provided the first evidence that shows how individual genes can mediate longevity (Kenyon et al., 1993). More recent studies show that genetic background matters in longevity across different model organisms (Korstanje et al., 2021; Mattison et al., 2017). Here, we investigate the mechanism by which CR in the form of reducing the glucose concentration in the growth media, extends chronological lifespan (CLS) in budding yeast. There is an increasing body of evidence suggesting that CR and methionine restriction (MetR) extend lifespan through overlapping pathways and metabolic patterns (Hepowit et al., 2021; Hine et al., 2015; Ogawa et al., 2022; Ogawa et al., 2016; Zou et al., 2020). In this study, we discovered that both CR and MetR augment polyamine synthesis. This generated accumulation of the geroprotector, spermidine, which promotes the cellular process of autophagy in various organisms and by regulating mitochondria function (Tobias Eisenberg et al., 2009; Jing et al., 2018; Messerer et al., 2023). Through metabolomic analysis we show that methionine auxotrophic strain BY4741, which genetically mimics MetR by deletion of the *MET15* gene (*met15Δ0*), activates polyamine synthesis under NR glucose conditions. Similarly, CR glucose conditions activate polyamine synthesis in a *MET15+* strain that is not methionine restricted. Therefore, both conditions that extend CLS (glucose restriction and methionine restriction) also increase polyamine biosynthesis.

Introduction

Genetics, diet composition, and environment make a difference in longevity

CR was thought to be a universal intervention for longevity based on numerous studies in model organisms. Investigators also wondered whether CR worked in humans, so they put it to the test when they conducted long-term CR on nonhuman primates. In two iconic and parallel studies where 30% CR was employed (Colman et al., 2009; Mattison et al., 2012), the robustness of CR came into question when the NIH study showed that CR did not extend lifespan of rhesus monkeys, a result that contradicted the Wisconsin study (Mattison et al., 2017). To make sense of these discrepancies, the investigators focused on understanding the study design differences, including the genetics (Mattison et al., 2017). Although both studies utilized Rhesus monkeys (*Macaca mulatta)*, the animals from Wisconsin and NIH were from different origins and as such differed slightly in genetic background. This result prompted follow up mice studies by the Jackson laboratories that also concluded that genetic background matters in aging (Korstanje et al., 2021) and that sex of an organism plays a role in response to CR (Mitchell et al., 2016). Thus, genetic variations in different species and humans require further investigation. Furthermore, follow-up studies by Rafael de Cabo and others in mice have since determined that macronutrient composition is important and even timing of the food intake can have consequences, both of which differed in the NIH and Wisconsin monkey studies (Mattison et al., 2017). NIH had naturally sourced food, while Wisconsin focused on a semi-purified diet (Mattison et al., 2017). It has been clear from NIH and Wisconsin models that the aging phenotype depends on the interplay of genes and environmental conditions. Although revelation of diet composition refocused the

scientific community, yeast scientists studying chronological aging were more attuned to the finding that longevity was sensitive to even slight changes in diet composition and/or other extrinsic factors(Santos et al., 2020). For example, our laboratory and others have shown that temperature, carbon source, metabolite availability, and pH, all impact chronological lifespan (CLS) of yeast (Burtner et al., 2009; Smith Jr. et al., 2007). Interestingly, non-fermentable carbon sources in the environment extend yeast chronological lifespan (Smith Jr. et al., 2007). In addition, it's been shown that decreasing glucose in the media (CR) or alteration of one amino acid can have lasting impacts on the chronological lifespan of yeast. For example, limiting methionine (MetR) in the diet can promote longevity (Ruckenstuhl et al., 2014).

Genes also play a role in longevity of yeast. The mutation in the *LEU2* seems to make cells incapable of leucine import (Cohen & Engelberg, 2007). Others have also shown that CLS is sensitive to leucine, showing that both supplemental leucine and restoring leucine prototrophy (conversion of *leu2* to *LEU2*) extends lifespan (Alvers et al., 2009). In addition, strains containing deletion in *met15/met17* or *met2* greatly extend lifespan (Ruckenstuhl et al., 2014). This is the genetic mimicking of methionine restriction mentioned above. The *met15/17*Δ mutant has limited endogenous methionine biosynthesis and is termed semi-auxotrophic for methionine, while *met2*Δ is fully auxotrophic and depends on methionine derived from the environment for survival (Ruckenstuhl et al., 2014).

To address the variability surrounding CLS, John Hartman's lab conducted a large-scale study demonstrating that CLS extension is dynamic and context dependent (Santos et al., 2021). They found that CLS depends on multiple genetic and

environmental factors including auxotrophic mutations, ploidy, media composition, and aeration(Santos et al., 2021). The study also provides a possible explanation for why outcomes from various CLS genetic screens have differed across independent laboratories. Specifically, Hartman *et al.* confirmed that mutations in *leu2* or *lys2* shortens CLS, while *met15/met17* extends it, and that auxotrophic influences were not complemented by further supplementation (Smith et al., 2016). Because longevity is sensitive to these factors, the field and individual labs have tried to standardize the media and conditions (Santos et al., 2021), although differences between laboratories remain. Hartman suggests that to avoid variation, these CLS assays should be done in a prototrophic context with an optimized media composition that they developed, mimicking DMEM used in mammalian cell culture (Santos et al., 2020).

BY4741 strain background

The BY4741 (MATa *his3Δ1 leu2Δ0 met15Δ0 ura3Δ*) strain background is derived from S288C and was used in the yeast gene knockout (YKO) collection. It has been frequently used for genetic screens and other studies of replicative and chronological aging. As described above, *met15*Δ acts as a mimic of dietary methionine restriction (Johnson & Johnson, 2014). The CLS of BY4741is also highly sensitive to changes in glucose concentration, thus making it useful for investigating mechanisms underlying CR (Choi et al., 2017; Hepowit et al., 2021; Matecic et al., 2010; Ocampo et al., 2012; Smith Jr. et al., 2007; Wierman et al., 2017). Previous data show that CR may induce MetR as methionine remains underutilized in the media and that CR downregulates methionine transporters (Enriquez-Hesles et al., 2021; Zou et al., 2020). Ruckenstuhl *et al.* also concluded that TOR inhibition and MetR work partially through the same anti-aging

pathway, which includes autophagy activation (Ruckenstuhl et al., 2014). Indeed it's been shown that in MET^+ cells under CR conditions stimulating S-adenosyl-L-methionine (AdoMet) synthesis, or S-adenosyl-L-homocysteine (AdoHyc) supplementation extends lifespan *via* activation of AMPK (Ogawa et al., 2016). Others have pointed out that in a MET^+ strain, CR suppresses the biosynthesis of methionine, SAM and cysteine from asparagine, throughout a CLS time course (Mohammad & Titorenko, 2021). CR-dependent extension of yeast RLS has also been shown to be abrogated by methionine supplementation (Zou et al., 2020). Finally, studies have shown that CR (low glucose) limits intracellular methionine levels (Mohammad & Titorenko, 2021), while others have shown that limiting methionine enhances autophagy (Plummer & Johnson, 2019), which is also switched on during CR (Ruckenstuhl et al., 2014).

This would all be consistent with MetR and CR sharing overlapping mechanisms. Herein, we conducted our own metabolomic analysis on genetic and dietary MetR, CR conditions in BY4741 (methionine auxotroph), SY1083 (*MET15*$^+$ version of BY4741), and FY4 (fully prototrophic strain). Analysis shows that MetR (*met15/met17*Δ) and CR may extend lifespan, at least partially, by upregulating the polyamine synthesis pathway.

Results

Metabolomics is a powerful method for understanding an organisms' active biochemical pathways or changes between conditions. It also provides insight into the interaction between genotype and the environment. To help understand CR, we initially performed a pilot experiment for untargeted metabolomics with cell extracts from BY4741 in CR and NR conditions at day 5. This experiment yielded preliminary evidence for increased intracellular metabolites in CR like spermine (polyamine),

cadaverine (polyamine and lysine metabolism), pipecolic acid (lysine metabolism), and glutathione —all of which have been implicated in oxidative stress protection, autophagy, and ultimately longevity (Figure 2.1A and B) (Hobbs & Gilmour, 2000; V. Olin-Sandoval et al., 2019). Intracellular proline was also elevated in our data set (Figure 2.1). This amino acid protects cells from osmotic and lipid peroxide-induced oxidative stress (Takagi, 2008). Lysine was also detected in CR cell extracts consistent with increased lysine harvesting discussed further in Chapter IV (V. Olin-Sandoval et al., 2019). Glutathione and spermine were present in the CR, but not detected in the NR (Figure 2.1A & B). 5'-methylthioadenosine (MTA), a byproduct of polyamine biosynthesis, was also among the most elevated metabolites in CR (Figure 2.1C). High levels of putrescine (a compound related to polyamines) and gamma-aminobutyric acid (GABA) were present in NR compared to CR (Figure 2.1B). These results suggested that CR was augmenting polyamine synthesis. The BY4741 yeast strain used in the experiment was deleted for *MET15/MET17*, making it a methionine semi-auxotroph. We therefore could not rule out that the apparent upregulated polyamine flux under CR condition was related to the *met15/met17*Δ mutation. However, the experiment did inspire additional experimentation.

A

CAS	Metabolite	CR:NR
70-18-8	Glutathione (reduced) *	
4350-09-8	5-Hydroxytryptophan	
154-02-9	5-Hydroxytryptophol	
71-44-3	Spermine *	
	Naphthalene	
143-07-7	Lauric acid	
2457-80-9	MTA *	7.80
73-24-5	Adenine	7.00
63-68-3	Methionine *	6.12
462-94-2	Cadaverine *	4.62
6205-08-9	N-Acetylornithine	3.65
50-99-7	Glucose and other aldohexoses	3.51
56-87-1	Lysine *	2.57
535-75-1	Pipecolic acid *	2.28
147-85-3	Proline *	2.27
3226-65-1	Methionine sulfoxide *	1.75

B

CAS	Metabolite	NR:CR
51-35-4	Hydroxyprolines	
550-33-4	Purine riboside	
627-01-0	N-Ethylglycine	
1187-84-4	Methylcysteine	
6753-62-4	N-Methylglutamic acid	
1445-07-4	Pseudouridine	
56-81-5	Glycerol	9.70
5949-29-1	Citric acid/isocitric acid	6.61
13095-48-2	2-Hydroxyglutaric acid	6.45
616-45-5	2-Pyrrolidinone	6.30
123-76-2	delta-Aminolevulinic acid	6.13
617-48-1	Malic acid	5.18
110-60-1	Putrescine *	5.00
820-11-1	3-Phosphoglyceric acid	4.57
56-40-6	Glycine	4.30
58-61-7	Adenosine	4.16
50887-69-9	Orotic acid	3.77
58-96-8	Uridine	3.62
97-14-3	N-Acetylserine	3.56
34363-28-5	Glycerol 1-phosphate	3.15
141-43-5	Ethanolamine	2.93
1190-94-9	5-Hydroxylysine	2.77
488-81-3	Pentitols	2.71
72-18-4	Valine	2.68
5934-29-2	Histidine	2.58
56-12-2	gamma-Aminobutyric acid (GABA) *	2.43
56-45-1	Serine	2.43
617-31-2	2-Hydroxyvaleric acid	2.34
828-01-3	3-Phenyllactic acid	2.18
52-90-4	Dehydroalanine	1.83
582-60-5	5,6 - Dimethylbenzimidazole	1.72
61-90-5	Leucine	1.71
3909-12-4	Threonic acid/Erythronic acid	1.61
60-18-4	Tyrosine	1.53
443-79-8	Isoleucine/Leucine	1.40

C

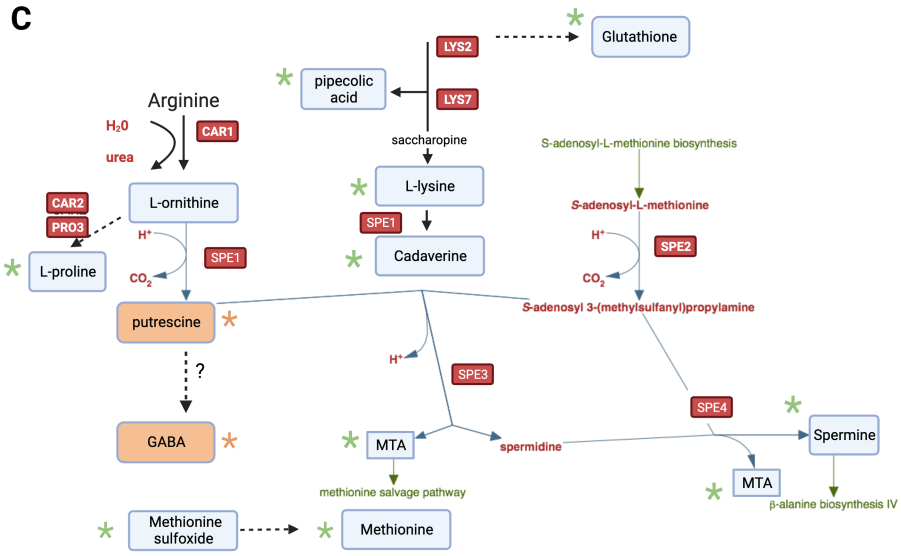

Figure 2.1 BY4741 yeast strain augments polyamine biosynthesis. *A) Table of ranked metabolites showing enrichment of metabolites present in CR compared to NR in BY4741 at day 5. All reported values are log_2 transformed ratios; data are the mean of six biological replicates at day 5. Blanks represent metabolites detected in CR, but not detected in NR-treated cells. B) Table of ranked metabolites showing enrichment of metabolites present in NR compared to CR. Blanks represent metabolites detected in NR,*

but not detected in CR-treated cells. C) Schematic of superpathway of polyamine biosynthesis, highlighting relevant polyamine metabolites detected in metabolomics analysis (Asterisk). Enzymes are depicted in red box; metabolites are in boxes; other related compounds appear in red text. Green text depicts other major pathways that are associated with polyamine biosynthesis. Green Asterisk and blue box are metabolites that are more abundant in CR in (A). For example, 5'-methylthioadenosine (MTA) is more abundant in the CR. MTA is a major byproduct of the polyamine synthesis pathway and is also the principal substrate for the methionine salvage pathway. In this pathway MTA is recycled back into methionine. Metabolites (highlighted in orange box) were detected in greater abundance in the NR and shown in (B). For example, putrescine and gamma-Aminobutyric acid (GABA). This schematic was made by modifying an image from the website of Saccharomyces Genome Database (SGD).

To further test the idea that cells were salvaging methionine during CR *via* polyamine synthesis and the methionine salvage pathway, we conducted a more detailed metabolomic analysis using LC-MS/MS platform, this time utilizing BY4741(*met15*Δ), SY1083 (*MET15*$^{+}$), and FY4 (fully prototrophic strain) under NR and CR conditions. In these experiments we also reduced both methionine and cysteine levels in exogenous media to mimic dietary MetR. 5 mg/L methionine and 25 mg/L of cysteine was added for MetR as opposed to xx and xx for NR. Cysteine is reduced in the media because methionine can be generated from cysteine in yeast. Cell extracts were prepared during log phase growth and day 5 as described in the Experimental Procedures in collaboration with Duke. Metabolite data were normalized to protein levels measured from the extracts. The following analysis describes data obtained from day 5 (stationary phase), which is when the cells are chronologically aging.

Enrichment and pathway analysis of the top 38 metabolites (Figure 2.2A) more abundant in BY4741 (*met15*Δ) compared to SY1083 (*MET15*$^{+}$) was performed using

MetaboAnalyst (Chong et al., 2019), in which pathway impact (relative circle size) is a measure that considers the centrality of a metabolite in the pathway (Figure 2.2 B&C). The most significantly enriched categories (shaded red) were related to arginine and proline metabolism, alanine aspartate and glutamate metabolism, and cysteine and methionine metabolism. These also had high pathway impact scores (x-axis). The significance is indicated in Figure 2.2A with a red asterisk indicating significance between BY4741/SY1083 and black asterisks indicating significance for 1083 CR/1083 NR. Noteworthy, methionine was not detected while aspartate was high which coincided with recent studies showing low intracellular methionine in low glucose conditions (Mohammad & Titorenko, 2021). We wanted to establish if the ratios of the BY4741/SY1083 enriched metabolites were similar to the ratio of 1083 CR/1083 NR and created a scatter plot with 1083 CR/1083 NR on the x-axis and BY4741/SY1083 on the y-axis (Figure 2.3A). The correlation coefficient is 0.3239 showing there is a weak, but significant, association. The fit is probably heavily weighted by a couple metabolites like MTA and adenine. The correlation would be weaker without them. Using MetaboAnalyst software we created our own schematic of metabolites, with red showing the detected and measured metabolites (Figure 2.3B). The darker the shade of red the higher the significance. We conclude that CR in the form of glucose restriction appears to undergo a metabolic shift towards polyamine biosynthesis and methionine salvage that overlaps with genetic methionine restriction.

A

Metabolites	41 NR /1083 NR	1083 CR /1083 NR
MTA * *	14.30	10.05
Aminomalonic acid	8.54	4.14
Methionine sulfoxide *	8.45	2.21
Adenine * *	7.36	6.70
Proline	5.10	1.05
3-Phenyllactic acid	5.05	4.28
gamma-Aminobutyric acid (GABA) * *	4.15	1.87
beta-Hydroxybutyric acid	3.86	3.78
Glycerol	3.28	0.38
dicrotalic acid	3.25	1.45
Cysteine *	2.87	0.38
Alanine	2.63	0.96
Glucose *	2.42	6.95
Indolelactic acid	2.36	2.45
Thymine	2.33	4.12
Adenosine/Inosine *	2.33	1.18
Asparagine *	2.27	1.22
Disaccharide	2.23	0.70
Aspartic acid *	2.22	12.43
Ketopentose-5-phosphate	2.16	1.30
n-Acryloylglycine	2.15	4.28
Phenylalanine	2.12	1.34
Stearamide	2.11	0.38
n-Methylalanine	2.08	0.43
Homocysteine	2.04	0.48
Isoleucine	2.00	0.78
Spermidine * *	1.90	3.91
2-Isopropylmalic acid	1.88	0.61
Gluconic acid	1.85	1.52
3-Cyano-L-alanine	1.80	0.71
Threonine	1.77	2.59
Putrescine	1.71	0.96
Cysteinylglycine *	1.67	2.58
Unknown metabolite	1.65	1.26
Threonic acid	1.64	0.63
Erythronic acid	1.64	0.63
1-Methylhydantoin	1.55	0.88

B

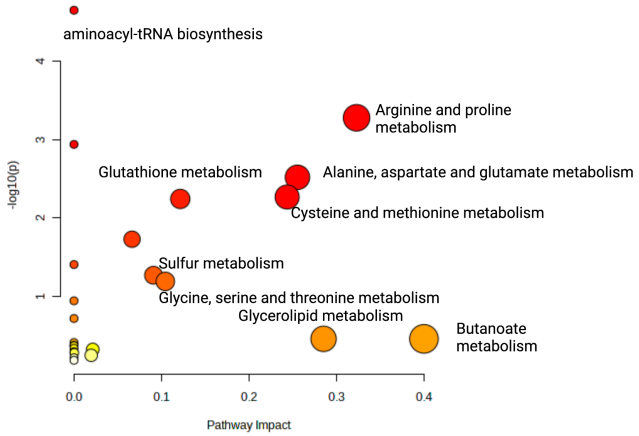

C

Pathway	p value	-log(p)	FDR	Impact
Aminoacyl-tRNA biosynthesis	3.10E-05	4.5082	0.002265	0
Arginine and proline metabolism	6.38E-04	3.195	0.023299	0.32298
Cyanoamino acid metabolism	0.001296	2.8873	0.03154	0
Alanine, aspartate and glutamate metabolism	0.003501	2.4558	0.063894	0.2554
Cysteine and methionine metabolism	0.006403	2.1936	0.079986	0.24361
Glutathione metabolism	0.006574	2.1822	0.079986	0.12149
Valine, leucine and isoleucine biosynthesis	0.020614	1.6858	0.21498	0.06635
beta-Alanine metabolism	0.04188	1.378	0.38215	0

Figure 2.2 Intracellular metabolites converge on polyamine biosynthesis in BY4741 NR and SY1083 CR. *A) Table of ranked metabolites showing enrichment of metabolites present in BY4741 compared to SY1083 (methionine prototroph), and SY1083 CR/ SY1083 NR. All reported values are log_2 transformed ratios; data are the mean of biological replicates at day 5. B&C) MetaboAnalyst software was used for Enrichment and Pathway Analysis of metabolites with a BY4741NR/SY1083 NR ratio greater than 1.5. The names of KEGG pathways with $p<0.05$ are highlighted. Pathway impact is a measure that considers the centrality of a metabolite in the pathway. Circle size is proportional to pathway impact value and darker red color indicates more significant changes.*

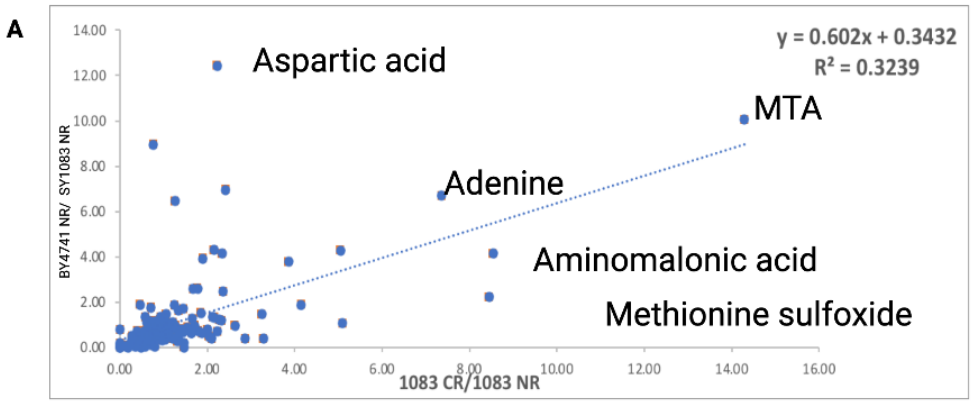
A
y = 0.602x + 0.3432
R² = 0.3239
Aspartic acid
MTA
Adenine
Aminomalonic acid
Methionine sulfoxide
BY4741 NR/ SY1083 NR
1083 CR/1083 NR
0.00
2.00
4.00
6.00
8.00
10.00
12.00
14.00
16.00

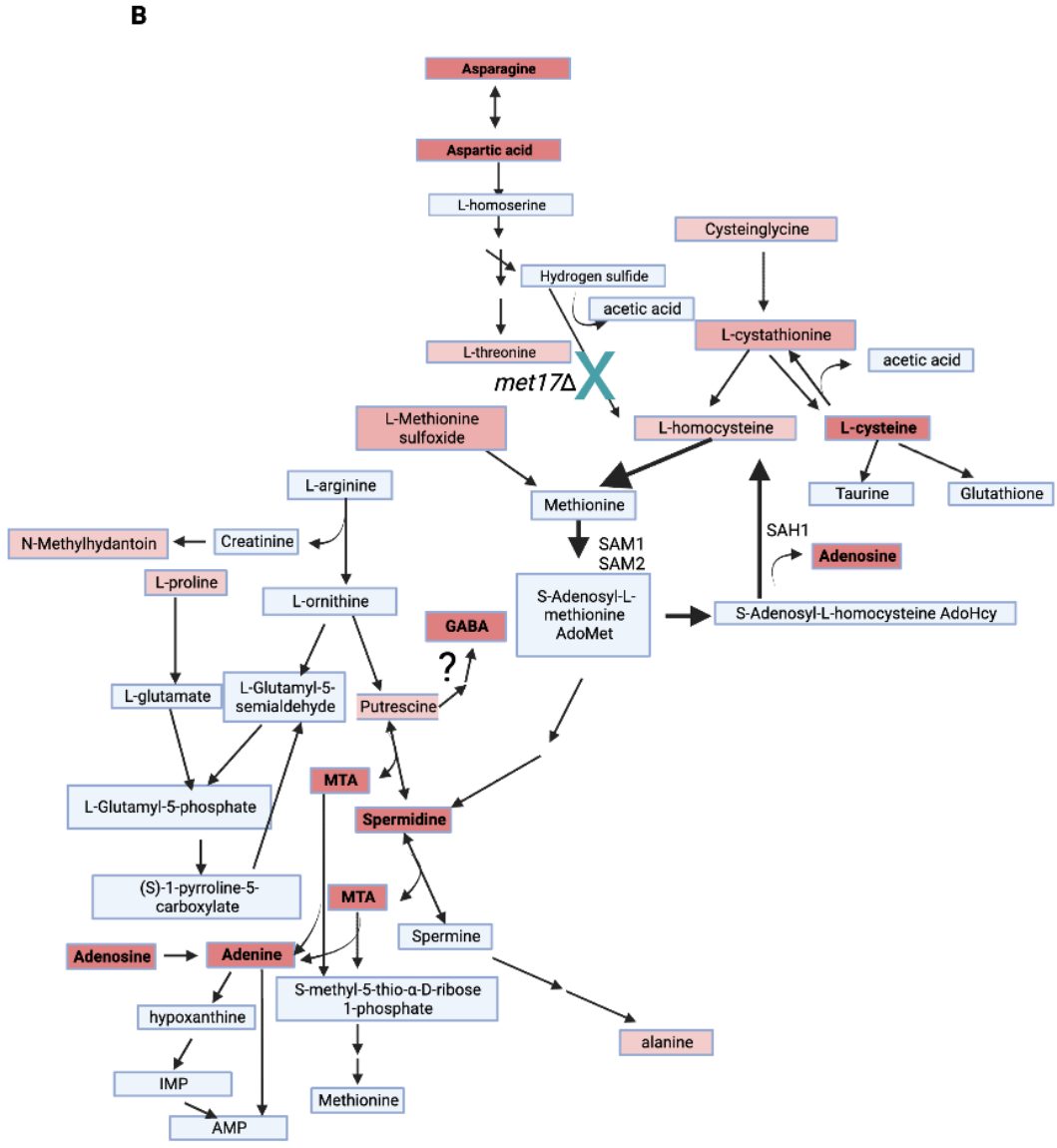
B
Asparagine
Aspartic acid
L-homoserine
Cysteinglycine
Hydrogen sulfide
acetic acid
L-threonine
met17Δ
L-cystathionine
acetic acid
L-Methionine sulfoxide
L-homocysteine
L-cysteine
L-arginine
Methionine
Taurine
Glutathione
N-Methylhydantoin
Creatinine
SAM1
SAM2
SAH1
Adenosine
L-proline
L-ornithine
S-Adenosyl-L-methionine AdoMet
S-Adenosyl-L-homocysteine AdoHcy
GABA
?
L-glutamate
L-Glutamyl-5-semialdehyde
Putrescine
MTA
L-Glutamyl-5-phosphate
Spermidine
(S)-1-pyrroline-5-carboxylate
MTA
Spermine
Adenosine
Adenine
S-methyl-5-thio-α-D-ribose 1-phosphate
hypoxanthine
alanine
IMP
Methionine
AMP

Figure 2.3 Intracellular metabolites converge on polyamine biosynthesis in BY4741 NR and SY1083 CR. *A) Scatter plot showing the relationship between enriched pathways with methionine auxotroph BY4741/ SY1083 and SY1083 CR /SY1083 NR. The best fit line and spearman's rank correlation coefficient r is shown alongside the regression line. The figure shows there is a weak correlation between methionine restriction and CR B) Schematic of polyamine synthesis pathway, highlighting relevant polyamine metabolites detected in metabolomics analysis. Measured metabolites are bolded and red shade indicates significance. Arrows represent steps in reactions. Question mark refers to possible uninvestigated pathway/enzyme in yeast.*

Discussion

Context is everything

Recent CR studies have shown that calories are not the only relevant factor in mediating lifespan. Equivocal results across model organisms have refocused the field into investigating the context in which CR is performed. In addition to low calorie intake, timing of food intake and the genetic background of an organism have emerged as important factors in the effectiveness of CR (Mitchell et al., 2019; Mitchell et al., 2016; Rothschild et al., 2014; Varady & Hellerstein, 2007; Zhang et al., 2021). Thus, these factors need to be considered when performing CR studies in any model organism.

CR and MetR work in similar pathways

Budding yeast has been used extensively to gain insight into the mechanisms of both CR and MetR. There is an increasing body of evidence that suggests that CR and MetR extend lifespan through similar pathways. Although various studies propose various mechanisms underlying methionine restriction, all have overlooked polyamine biosynthesis. Methionine levels and CR (glucose levels) may coordinate longevity through similar pathways in yeast (Zou et al., 2020). For example, both MetR and CR

induce autophagy (Aris et al., 2013; Ruckenstuhl et al., 2014). Interestingly, CR down-regulates transcription and translation of methionine biosynthetic enzymes and transporters (Zou et al., 2020). Consistent with low intracellular methionine in CR cells, we previously reported that cells treated with CR may be restricting entry of amino acids, including methionine (Enriquez-Hesles et al., 2021). Furthermore, endogenous formation of hydrogen sulfide (H_2S) is a molecule derived from the TSP pathway that is indispensable for lifespan extension through CR and sulfur amino acid restriction (Hine et al., 2015).

In this study, we set out to understand the similarities between CR and MetR. Our untargeted metabolomic approach shows that both CR MET^+ and BY4741 induce polyamine synthesis, which is a well-known supplement. The novelty of our work is that the synthesis pathway is induced by both conditions. We hypothesize that BY4741 augments this pathway in a compensatory way to regenerate methionine from MTA—a byproduct of polyamine synthesis. Indeed, MTA was our top hit in the BY4741 background compared to the equivalent strain with methionine prototrophy (MET^+). It has been reported that in a *met15/met17*Δ mutant, MTA metabolism is a significant factor in the metabolism of methionine and that MTA usage to salvage methionine accounts for 15% of the methionine used by the cell (Chattopadhyay et al., 2006). This could be even greater when the cells enter the diauxic shift and enter quiescence. Surprisingly, we found that CR (with methionine prototrophy) had a similar metabolic profile with MTA also being near the top. This would predict that CR and genetic methionine restriction may mediate longevity *via* similar metabolism and metabolites.

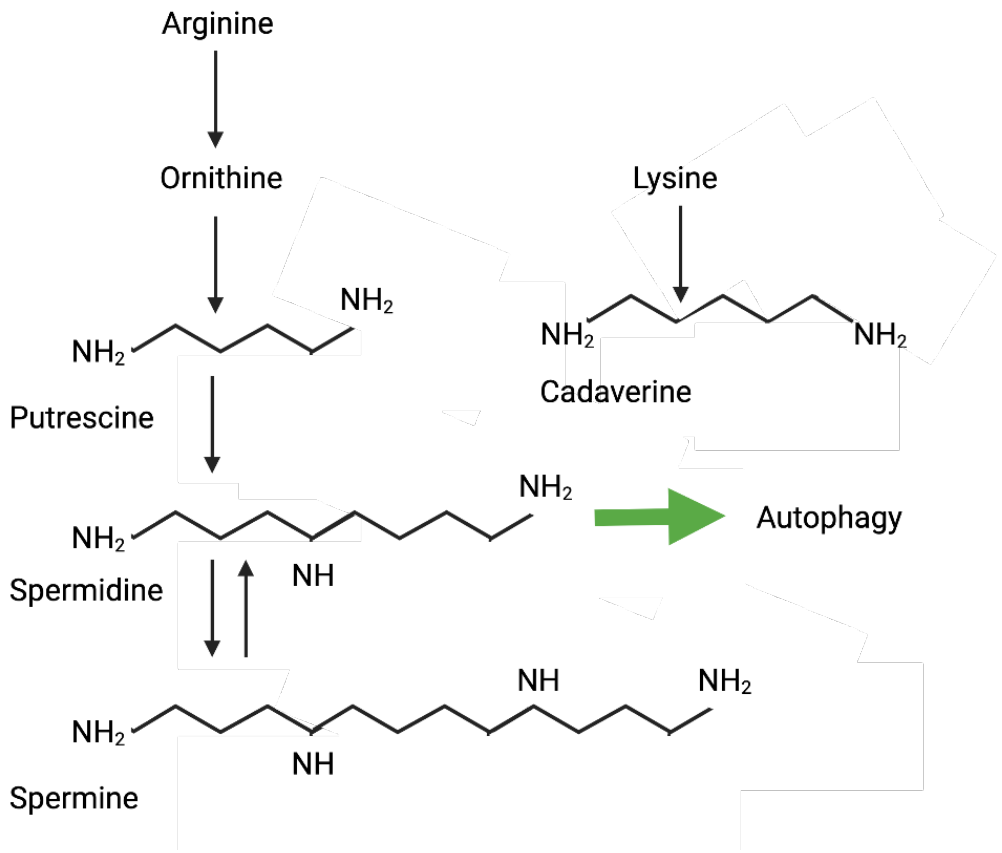

Figure 2.4 The most common polyamines. *Polyamines are low molecular weight proteins present across phyla (Michael, 2016). First, arginine is cleaved by arginase to form ornithine and urea (not shown above) (Karp et al., 2019; Wu et al., 2017). Putrescine is generated from ornithine, which then can make spermidine and spermine. Lysine makes cadaverine. These are molecules with roles in longevity.*

Polyamines and aging

Polyamines, consisting of spermidine, spermine, and putrescine, are a class of small molecules composed of multiple amine groups (Figure 2.4) (Minois et al., 2011). Spermidine was first described in yeast as an anti-aging compound (T. Eisenberg et al., 2009). It was shown to be increased during CLS in wild-type yeast and it remained elevated in replicative old yeast cells (T. Eisenberg et al., 2009). The concentration of polyamines varies by strain and by culture conditions (Tabor & Tabor, 1985).

Supplementation not only increased lifespan in *Saccharomyces cerevisiae*, but also *C. elegans* and *Drosophila* (T. Eisenberg et al., 2009). Spermidine treatment induces autophagy in all model systems tested (T. Eisenberg et al., 2009). In yeast, spermidine reduced acetylation of chromatin and induced transcription of autophagy genes (Tobias Eisenberg et al., 2009). Autophagy is a self-recycling mechanism that degrades intracellular macromolecules and organelles. It has been described as a point of convergence in longevity (Bareja et al., 2019). In various model organisms, polyamines have also been shown to have roles in cell growth, survival, and proliferation (Tobias Eisenberg et al., 2009). Due to this finding, scientists have postulated that polyamine availability, like sugars, could induce a cell response to nutrient availability (Minois et al., 2011). Their levels have been implicated in the pathophysiology of aging and cancer, but beneficial or harmful effects seem to be context dependent.

Polyamines can be obtained from the diet, cellular synthesis, or the microbiome. Specifically, polyamines are derived from amino acids: arginine, ornithine, methionine, and lysine (Figure 2.4). In BY4741 yeast, we were able to detect intracellular spermidine, spermine, putrescine, and cadaverine (Figure 2.1). Polyamines are elevated in CR and low in NR. In our pilot data set (Figure 2.1), putrescine was elevated in NR compared to CR, but this was done in BY4741. Putrescine is a precursor of spermine and spermidine. However, NR cells accumulate high levels of putrescine but fail to accumulate spermine and spermidine. Why? Studies using transgenic mice models have shown that high levels of putrescine are accompanied by depleted spermine and spermidine, meaning that putrescine does not automatically replenish low levels of other polyamines in this model system (Suppola et al., 2001). An alternative mechanism for low levels of polyamines in

our system could be exported out of the cell. TPO1-4 excrete polyamines at acidic pH (at which yeast cells usually grow) but uptake them into the yeast cell at pH 8 (Minois et al., 2011). In our system, media pH is relatively more acidic in NR compared to CR and could contribute to lower intracellular levels of polyamines. In CR, in the context of genetic MetR there may be hyperactivation of the pathway and this forces conversion of putrescine to spermidine and spermine. This would result in lower levels of putrescine.

GABA is also elevated in NR treated cells. GABA in yeast has been shown to be produced from glutamate or taken up from the environment (Bach et al., 2009). This GABA has also been shown to be stored within cells as a nitrogen source and converted to succinate (Bach et al., 2009). Although there are no reports of GABA being produced in yeast from putrescine, there is evidence that this happens in bacteria and the central nervous system in mammals (Jakoby & Fredericks, 1959; Sequerra et al., 2007). In yeast, putrescine could potentially be used to elevate GABA levels through an unidentified enzyme.

Future Directions

In a previous genetic screen to define genes important for CLS, scientists confirmed long-lived mutants were mutants defective in the highly conserved *de novo* purine biosynthesis pathway (the *ADE* genes), which ultimately produces IMP and AMP (Matecic et al., 2010). Blocking this pathway extended lifespan to the same degree as calorie (glucose) restriction (Matecic et al., 2010). Follow-up studies show that there were shared gene expression changes induced by CR and *ade4* mutation (Wierman et al., 2015). Additionally, CR did not further extend CLS of the *ade4*Δ mutant, suggesting they could share certain mechanisms of lifespan extension (Wierman et al., 2015). *ADE*

mutants could also promote longevity through polyamines. Critical experiments for the lab moving forward should include testing whether polyamine biosynthesis or the methionine salvage pathways are required for the lifespan extension induced by MetR or CR.

As mentioned briefly, urea can be produced in the process of making ornithine from arginine. The ornithine cycle reported in yeast (Chan & Cossins, 1972) might play an unidentified role in polyamine synthesis, however there are no studies investigating its effect on longevity or polyamine biosynthesis.

Experimental procedures

Yeast strains and media

S. cerevisiae strains used in this study were BY4741 (*MAT***a** *his3*Δ*1 leu2*Δ*0 met15*Δ*0 ura3*Δ*0)*, FY4 (*MAT***a** prototrophic), SY1083 (*MAT***a** *his3*Δ*1 leu2*Δ*0 ura3*Δ*0)* in the BY4741 background (Winzeler EA, 1999). Synthetic complete (SC) growth medium was used for all experiments except for the use of MetR where methionine and cysteine were reduced. 5 mg/L methionine and 25 mg/L of cysteine was added for MetR. Glucose was added to a final concentration of either 2.0% (non-restricted [NR]) or 0.5% (calorie restricted [CR]). All cultures (10 mL) were grown at 30°C in 15 mL glass culture tubes with loose fitting metal caps on a New Brunswick Scientific roller drum.

Metabolomics

We conducted untargeted GC/MS analysis of 90 yeast lysate samples in collaboration with James Baine at Duke University. Using SY1083, BY4741, and FY4, prepared 50 mL of MetR (methionine restriction), NR (2 % glucose), and CR (0.5%

glucose) media for each sample (5 biological replicates per condition). Then inoculated the media with O/N cultures to 0.03 OD_{600nm}. After inoculation, we mixed and divided the 50 mL culture to 3 glass test tubes (sterile) and placed them in the roller drum at 30˚C. Three of the tubes contained ±15 mL. Two of the three would be used to collect cells from Log phase growth (Figure 2.4). All 30 mL was used for log phase to ensure enough cells were recovered. The third tube was used to collect cells (4 mL) at day 5 of the CLS experiment. Log phase cells were allowed to grow for 6-8 hours in the roller drum. The OD_{600nm} (of the two tubes were read and averaged) and then the first tube culture was transferred to a 15 mL conical tube (precleaned with methanol) and the culture was spun at 1400 rpm for 5 minutes at 4˚C. Then 200ul of the conditioned media was collected at this point and stored at -20˚C. The second 15 ml tube of log phase cells was treated the same and the pellets were combined. Pellet was rinsed once with 3 mL of ice-cold PBS. Aspirate supernatant and add 300 µl of ice-cold deionized water containing 0.6 % formic acid to the cell pellets. Transfer 400 µl * of volume to a 2 mL Reinforced tube (cat 15-340-162) and acid-washed glass beads (Sigma G8772-1KG). There was about 100 µl of PBS remaining in the tube after aspiration. Used Parafilm to wrap the top of the reinforced tube containing cells, beads, and formic acid to prevent leaking during the bead beating step. Kept everything on ice. Bead beat 3 cycles of 20 seconds on 30 seconds off at the Cold Room 4˚C. Removed the beads and collected sample by poking a small hole at the bottom of these reinforced tube with a needle. Spun down tube at 1400 rpm into a disposable culture class tube (Cat 14-961-27). This had been precleaned with methanol. Resuspended the cell debris and supernatant and removed 20 µl and stored it at -20˚C for protein quantification with nanodrop later. For this quantification step, spun 20

µl at 4˚C at 4000rpm and then quantified protein present in supernatant using A280 protein settings. Removed 300 µl from the glass tubes containing cell debris, proteins, metabolites. Added 300 µl or 250 µl (1:1 volume) of cold acetonitrile, vortex, and store at -80 °C. For the samples collected at Day 5: collect 4 mL of culture and washed cell pellet with ice-cold PBS as above. For BY4741 strain re-suspended pellet in 250 µl of 0.6% formic acid. For SY196, re-suspended in 300 µl of formic acid. For SY1085 re-suspended in 250 µl of 0.6% formic acid. These differences in amount of formic acid used may account for the differences in protein concentrations that we see in the samples. Aliquoted 300 µl for the metabolomic analysis and shipped on dry ice to the Metabolomics Laboratory at Duke (Figure 2.5).

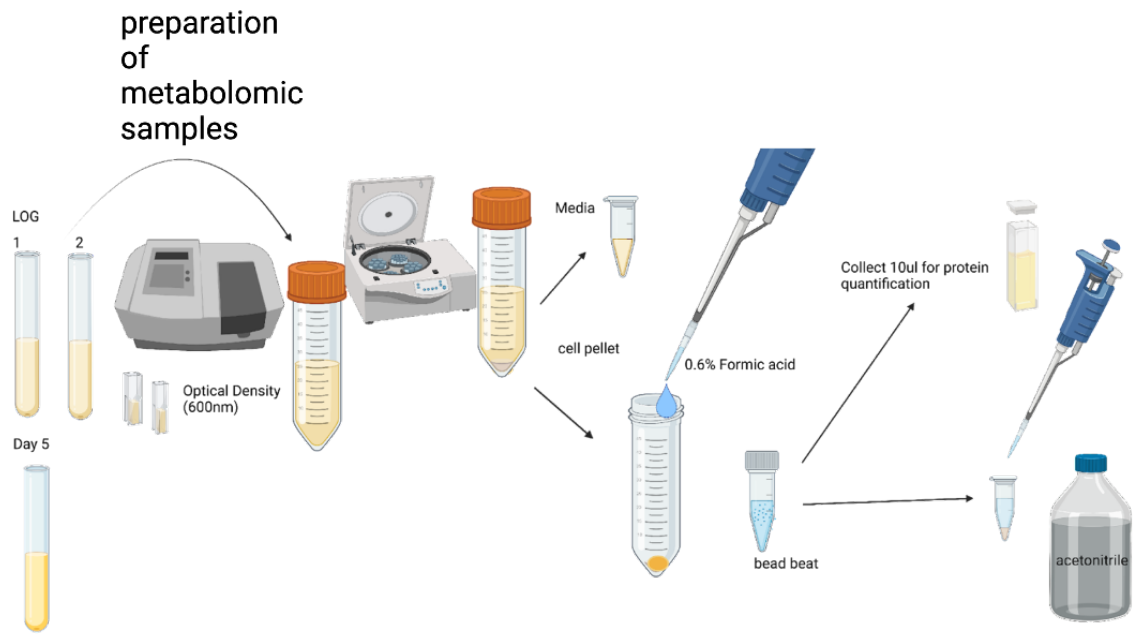

Figure 2.5 Untargeted metabolomic protocol. *Schematic shows quenching of metabolites using formic acid and acetonitrile in cells grown to log phase or day 5. Five biological replicates were analyzed for each condition and strain. These samples were analyzed by our collaborators over at Duke University.*

Chapter III

Yeast senescence and a new micro-colony counting estimation assay combined with the use of counting software for the optimization of yeast quiescence assays

Abstract

As *Saccharomyces cerevisiae* yeast cells chronologically age, their viability and ability to re-enter the cell cycle diminishes, thus making chronological lifespan (CLS) a valuable model system for studying mechanisms of quiescence, including responses to cell-intrinsic or cell-extrinsic manipulations. CLS focuses on a population of quiescent cells that was generally thought of as uniform (Burhans & Weinberger, 2007). However this clonal population is surprisingly heterogeneous in terms of cell size, resilience, trehalose content, budding state, and metabolism (Svenkrtova et al., 2016). To study quiescence, multiple groups have developed tools to study the different subpopulations in the stationary phase cultures. In doing so, some publications have generated conflicting nomenclature to classify these cells. Currently, there is no real consensus on the different subpopulations or whether a senescent population exists in the stationary phase. This Chapter is divided into two parts. Within the first part, we report our own findings of quiescence and explore the possibility of a senescent population in the stationary phase. In the second part, we introduce a low-cost semi-automated microcolony counting method for quantitative yeast CLS assays to study quiescence.

Part 1

Introduction

Aging depends on the interplay of genes and environmental conditions. Yeast has been a well-studied organism for understanding conserved aging pathways. It is an important model organism in the aging field that has contributed to the understanding of the underlying mechanisms and key pathways of the cellular aging process (Kaeberlein et al., 2007; Kaeberlein et al., 2001). To understand the general principles underlying the aging process, we rely on Replicative Aging and Chronological Aging models. Replicative lifespan is defined as the number of cell divisions a cell undergoes before it reaches proliferative senescence. In this model system, senescent cells can be isolated *via* the Mother Enrichment Program or with a mini-chemostat aging device (Yang & Pon, 2022), which our lab typically utilizes. Senescence is obtained when the mother cell can no longer divide despite abundant resources. This model is helpful to understand the process of biological aging and the limits of dividing cells in higher eukaryotes. Chronological lifespan (CLS) is defined as the number of days that a non-dividing cell survives in the stationary phase with limited nutrients. Within aging studies, CLS in budding yeast is an important and well-established tool for determination of cell viability over time (Fabrizio & Longo, 2007; Hu et al., 2013; Longo et al., 1996).

In CLS, a heterogeneous cell population resides in a low metabolic rate and in a non-dividing state waiting for more favorable environmental conditions (López-Maury et al., 2008). These assays involve growing liquid cultures into stationary phase, whereby nutrient depletion, and other alterations in the growth medium trigger drastic changes in transcription, metabolism, and other cellular processes that promote exit from the cell

cycle and establishment of a quiescence-like state. Traditional CLS assays monitor cell "viability" by measuring the reproductive capacity of these cells, or simply put quiescence. Aliquots are taken from the liquid cultures at different time points and then plated onto solid nutrient-rich plates to assess colony forming units (CFUs). In this model of aging, proliferative capacity decreases over time (Figure 3.2B). Measuring re-growth is an indirect measure of viability for these aged cells (Chadwick et al., 2016). It is possible that cells could remain viable but lose the ability to re-enter the cell cycle. This would represent a senescent population in the CLS model. Are there senescent cells present in chronologically aged yeast? A large senescent population in the stationary phase would indicate that CLS assays are missing important viability data. Therefore, we set out to fill this gap in knowledge by monitoring viability with propidium iodide (PI) and SYTO 9 in parallel with the traditional assay of CFUs of the same liquid cultures. We hypothesized that as the cell culture chronologically aged, the population of cells would deteriorate in a stepwise process where cells would lose quiescence and transition to a senescent state before undergoing apoptosis. Therefore, as cells chronologically age, we expected to observe an increase in senescent cells within a culture as cells lose their ability to re-enter the cell cycle. However, in contrast with our expectations, our experiments suggest that senescence is negligible in chronologically aged yeast populations as suggested by others (Cooper, 1994). In our system, the bottom line is an alive yeast cell is a quiescent cell.

Quiescence and Aging

Quiescent cells are non-dividing cells that remain metabolically active in G_0, and are able to return to the cell cycle given the appropriate external stimuli (Gray et al.,

2004). Aging is associated with progressive decline of quiescence that results in inappropriate cell division or decline of regeneration ability (Sousounis et al., 2014), as has been shown during neurodegeneration and cancer (Kirkland & Tchkonia, 2017; Lee et al., 2018; Sen et al., 2016). Therefore, enhancing quiescence may provide a powerful anti-aging strategy, analogous to the current strategy of eliminating senescent cells (Kirkland & Tchkonia, 2017). Similar to complex multicellular organisms, stationary phase yeast cells enter a quiescent state in G0, making yeast well-suited to study quiescent conserved mechanisms in CLS (Dhawan & Laxman, 2015). We conduct CLS by growing liquid cultures into stationary phase and then monitoring cell viability over time by diluting and then spreading aliquots of the cultures onto rich YPD agar plates to quantify colony forming units (CFUs). This assay also allows us to measure quiescence by determining a cell's ability to re-enter the cell cycle when nutrients become available. By contrast, cellular senescence is defined by cells that lose their replicative potential and cannot be measured using the traditional CLS assay designed by Valter Longo (Fabrizio et al., 2004).

Senescence and Aging

A major hallmark of aging is accumulation of senescent cells (Lopez-Otin et al., 2013). Senescent cells lose their self-renewal capacity, arrest in growth, and acquire a phenotype that is resistant to apoptosis (Iske et al., 2021). In response to a variety of stressors, senescent cells accumulate in many tissues with aging (Kirkland & Tchkonia, 2017). In chronologically aged tissues, this accumulation may cause bystander senescence and tissue dysregulation that contribute to age-associated diseases (Iske et al., 2021). There is a large effort in the aging field focused on identifying and studying

senescence. This is especially the case when senescent cells acquire a senescence-associated secretory phenotype (SASP) that promotes damage and compromises the health of nearby tissue (Coppe et al., 2010). These senescent cells themselves appear to be immune to these harmful signals (Hu et al., 2022). In addition, further characterization of these senescent cells shows organelle dysfunction (mitochondrial and lysosome), distinct transcriptional signatures with upregulated cell cycle arrest genes including p21, p16, and p53 (Iske et al., 2021). Because of this, p53, B-galactosidase, Lamin B, p21, and p16 are common senescent markers that have emerged to identify and target senescent cells and their SCAPS (Senescent cell anti-apoptotic pathways) (Gonzalez-Gualda et al., 2021). Scientists are trying to leverage knowledge to promote quiescence and prevent senescence across different contexts.

Potential advantages of senescence in yeast

In the case of a yeast population, it is unlikely that the presence of senescent cells would be advantageous for survival. However, senescent cells may be beneficial if they secrete beneficial factors that support the survival of other cells. These senescent cells may act as a reservoir of nutrients and energy that can be utilized for other cells within the population. More research needs to be conducted to test the role, if any, for these senescent cells. I propose that senescence is short-lived in yeast. It has been shown that cells enter senescence sharply (Fehrmann et al., 2013) and perhaps cells undergo another abrupt transition to cell death.

Using Yeast as a Model System to Study Quiescence

Cell quiescence is incompletely understood. The nature of quiescence has been hard to characterize since there are no clear markers of quiescence other than proliferative capacity. Yeast represents a model system that could help us obtain a greater understanding of the pathways and general principles that regulate quiescence. Yeast presents an ideal model to study quiescence because the entire culture can enter quiescence as cells transition to stationary phase. It is likely that quiescence establishment, like aging pathways, is evolutionarily conserved. Budding yeast has yielded vast knowledge for fundamental eukaryotic cellular processes including cell cycle, protein trafficking (Feyder et al., 2015; Schekman, 2002), autophagy (Ohsumi, 2014; Tooze et al., 2017), and nutrient signaling (Loewith & Hall, 2011). The system could be utilized to guide quiescence studies in other organisms. Can yeast also help us understand senescence? Senescence happens in microbes and is often argued to be a universal feature across phyla even in unicellular organisms (Cooper, 1994; Moger-Reischer & Lennon, 2019). It's well established that proliferative senescent cells can be isolated from replicative aging populations, these cells that have ceased to bud have been reported to survive and remain metabolically active before eventual lysis (Robert K. Mortimer & John R. Johnston, 1959; Steinkraus et al., 2008). Although senesce seems to be present in RLS, is senescence prevalent in CLS?

Results

It had been previously reported that in YPD grown cells, a stationary phase population could be separated into a dense and less dense fraction (Allen et al., 2006). The dense cells, termed quiescent or 'Q' cells exhibited all the expected features of quiescent cells including high proliferative capacity compared to Non-quiescent or 'NQ'

cells (Allen et al., 2006; Aragon et al., 2008; Werner-Washburne et al., 2012). Based on the reports of NQ cells in CLS, we wondered how vast this population was— could we be missing senescence by just looking at CFUs ability (Figure 3.2 panel A). We were intrigued by the possibility that the number of senescent cells would rise as the yeast culture chronologically aged. We hypothesized that as the cell culture chronologically aged, the population of cells would deteriorate in a stepwise process where cells would lose quiescence and transition to a senescent state before undergoing apoptosis. Based on this rationale and its implications, we attempted to isolate these different populations by gradient-density centrifugation as previously reported, using Caloric Restricted cells (CR) as a positive control, which should be enriched for dense "Q" cells.

To begin our studies in quiescence, we tried to isolate dense cells using iodixanol gradient as described in Quasem *et al.* (see materials and methods)(Quasem et al., 2017).The data in Figure 3.1 were obtained by growing the cells at 24, 48, 72, and 144 hours and then taking the same number of cells and separating them with a 50% iodixanol gradient. At 24 hours, only NQ cells were detected with no Q-cell pellet in both CR and NR conditions. At 48 hours and later, a small pellet of Q cells was detected in the NR condition. However, there were no pellets observed in CR, suggesting absence of Q cells in CR cells. This suggested that the definition of dense Q cells as the long-lived quiescent population was not universally correct. Therefore, we shifted our approach to study quiescence and senescence back to using CLS assays.

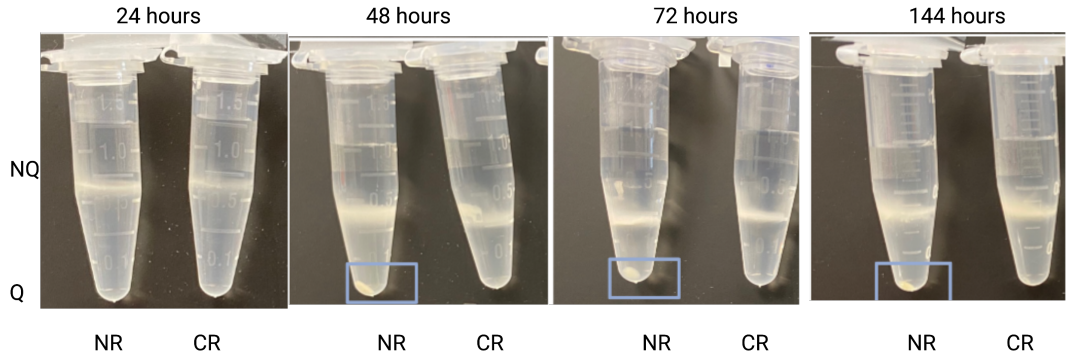

Figure 3.1 Density is not a reliable isolation method for quiescent cells *(A) BY4741 yeast cells were grown in synthetic complete (SC) media in NR (2.0% glucose) or CR (0.5% glucose). Specific number of cells were isolated from liquid cultures and then layered onto pre-made iodixanol density solution and centrifuged to separate populations of different densities. Iodixanol gradient separation of non-quiescent (NQ) and quiescent (Q) yeast cells in a microfuge tube in NR conditions and CR conditions. Box represents detection of Q cells. 50% iodixanol gradient is sufficient for separation of NQ and Q yeast cells.*

Traditionally, viability in CLS is monitored by returning cells to rich media plates and counting colony forming units (CFUs)—a measure of quiescence or proliferative capacity (Figure 3.2 panel A shows schematic of the typical output of a CLS assay). Since their introduction in 1996 (Longo et al., 1996), CLS assays continue to be a useful model to study chronological aging of non-dividing cells, a class that includes neurons. More recently, a subset of these CLS assays measuring regrowth capacity have been used to study mechanisms of quiescence. Like others have noted, it does not account for the possibility that yeast cells may enter a senescent state in which the cells remain viable, but are unable to re-enter the cell cycle (Alvers et al., 2009). Alvers *et al.* used FUN-1 to detect viability of cells (Millard et al., 1997) and found that the cell viability measurements with the dye were similar to viability based on colony formation. To supplement these past studies using FUN-1 fluorescent dye, we monitored uptake of PI

and SYTO 9 in combination with flow cytometry. PI is a well-established method for monitored cell viability since intact membranes of viable cells exclude the dye (Davey & Hexley, 2011). On the other hand, SYTO 9 is a nucleic acid that is cell permeable and thus labels every yeast cell in a population regardless of viability status (x-axis) (Figure 3.2 panel B). In this experiment, we used 4.0% glucose condition (short-lived) and a 0.5% glucose condition (long-lived) and measured CLS by CFUs or flow cytometry. We hypothesized that cells exposed to lower glucose would minimize senescence and retain quiescence more effectively than cells exposed to higher levels of glucose. Flow cytometry distinguishes dead cells within a population that are permeable to PI (loss of plasma membrane integrity) plotted on the y-axis from total live cells with SYTO 9. A representative biological replicate is shown at day 8 and day 20. At day 8, cells are labeled with SYTO 9 and only 22.53% of cells are PI^+, the remaining SYTO 9 $^+$ population should be viable (Figure 3.2 panel B). Later at day 20, the viability decreases as expected, with 96.03% of the cells being PI^+ consistent with less viability (Figure 3.2 panel B). In conjunction with the flow cytometry approach, we monitored cell quiescence using a CLS assay (Figure 3.2 D). We expected to observe loss of quiescence and accumulation of senescence in the stationary phase (Figure 3.2 panel C). If many senescent cells were indeed present, then the percentage of viable cells from flow cytometry should be greater than the fraction of 'viable' cells obtained from CLS CFU assay (Figure 3.2 panel C). The difference between these two metrics should represent the cell population that remains viable but unable to re-enter the cell cycle, in other words, senescence. However, the data surprisingly showed that there was negligible

senescence in chronological aged yeast cultures (Figure 3.2 panel D). This is indicated as no significant differences between the curves.

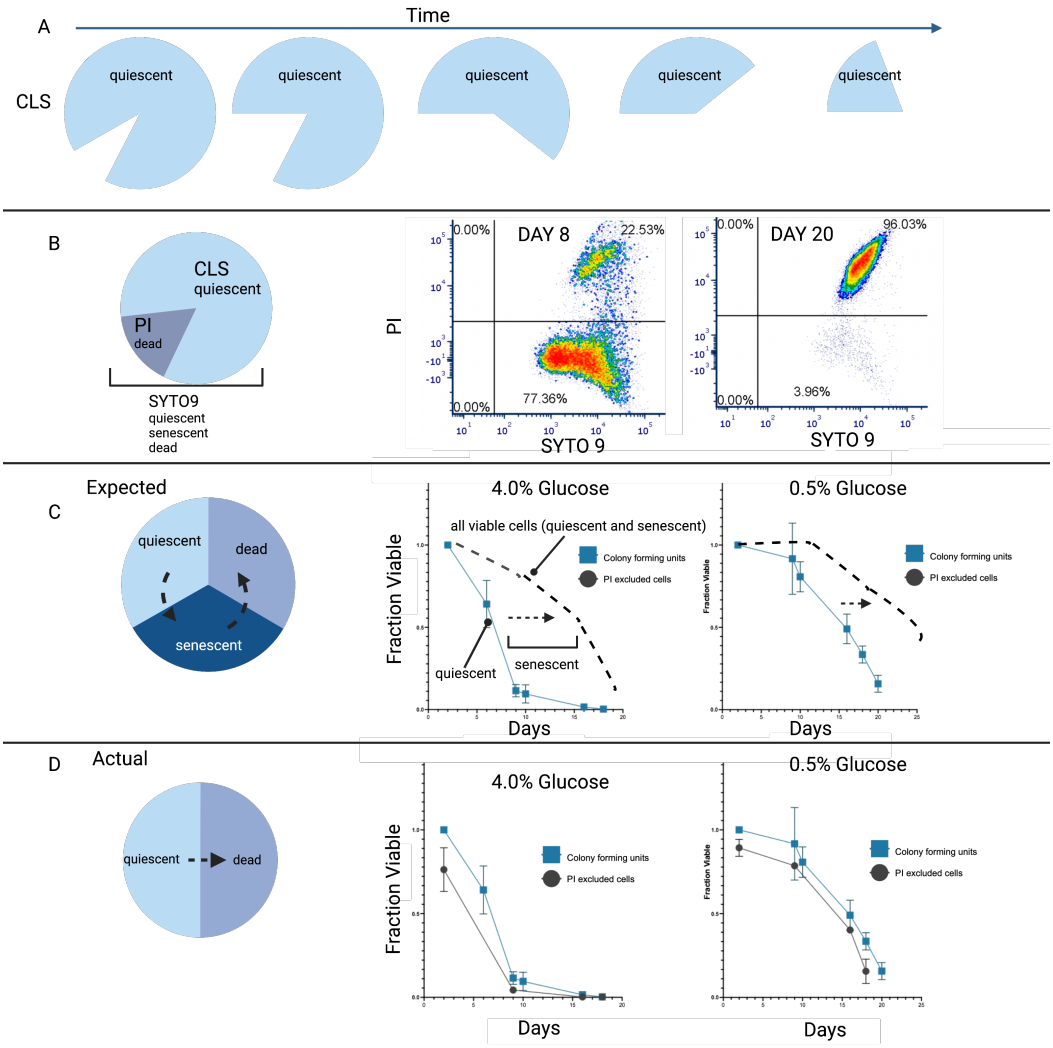

Figure 3.2 Senescent cells are rare in chronological aging yeast cultures*. A) Schematic of CLS assays focusing on quiescent population and omitting potential senescent population. B) Schematic showing that SYTO 9 dye yields total population, while PI yields metric regarding dead cells. Representative data obtained from flow cytometry where SYTO 9 is on the x-axis and PI is on the y-axis C) Initial hypothesis and model of stepwise decline from quiescence, senescence, to death. D) Actual model of quiescence without senescence. CLS and flow cytometry data plotted on the same graph where*

fraction viable is on the y-axis and time is on the x-axis. BY4741 strains in SC medium using 4.0% glucose or 0.5% glucose over a 20-day period.

Discussion

CLS is a direct measure of cell quiescence since quiescent cells are primarily defined by having the potential to re-enter the cell division cycle. By contrast, 'senescent' cells lack cell proliferative capacity, yet remain viable. Human chronological aging has been associated with increasing cellular senescence due to a variety of stresses (Chaib et al., 2022). In mammalian systems, senescent cells have been described to acquire abnormal function which deteriorates organismal health (Chaib et al., 2022). However, in yeast CLS, proliferative capacity decreases over time, yet it is unclear if there is a senescent or viable but not culturable (VBNC) population accruing in the population with the passage of time (Palkova et al., 2014). Could quiescent cells lose quiescence, and then transition to a senescence state, like mammalian cells? To begin to identify senescence we sought to separate quiescent cells from senescent cells in CR cells. Surprisingly, there seemed to be no enrichment of quiescent "Q" cells observed in CR (Figure 3.1), a condition that enhances quiescence as defined by non-dividing but still viable. Hartman and others suggest that quiescence is more complex and completely context dependent (Miles et al., 2023; Peselj et al., 2022; Santos et al., 2021). Due to this result, we decided to use proliferative capacity rather than buoyant density as a primary metric. Publications from the Titorenko and Laporte laboratories also re-examined properties attributed to these Q cells and ultimately demonstrated that proliferative capacity is often similar between NQ and Q cells (Goldberg et al., 2009; Laporte et al., 2011). Others have shown that proliferative capacity correlates with mitochondrial morphology and not cell density

(Laporte et al., 2018). The bottom line is that density is an unreliable marker for quiescence. To identify potential cellular senescence, we turned to answer this question by employing the gold standard criteria of cell cycle re-entry.

To fill this gap in knowledge, we monitored viability with PI and SYTO 9 in parallel with the traditional CLS assay measuring CFUs from the same liquid cultures. When we conducted a small experiment with both short-lived and long-lived conditions and BY4741 strains. We expected to observe viability exceeding proliferative capacity in the yeast population. However, in our study we showed CLS and viability data tracking almost perfectly which suggested that there were a small number of senescent cells (at most). Alvers *et al*. reached similar conclusions when comparing FUN-1 staining and CLS (Alvers et al., 2009). In our data, we observed that viability was slightly lower than reproductive capacity at each time point, which is theoretically impossible. Instead, we think that measured viability *via* flow cytometry is lower due to two reasons. First, in CLS we did not account for the number of dead cells in the population at the start of the experiment. Instead we normalize to 100% at day 4. In contrast the flow cytometry measurement is able to detect dead cells even on day 4. Second, this lower quantity of viable cells could be due to a small subpopulation of viable yet stressed cells uptaking PI as has been reported previously (Davey & Hexley, 2011). This underestimation of viability certainly could contribute to the results in this study, but the small number of senescent cells remain possible.

This evidence that yeast cultures do not accumulate a detectable population of senescent cells is, perhaps, not surprising given yeast's life history. Budding yeast are a short-lived species that can produce many daughter cells, so perhaps in this system there

is no advantage of maintaining senescent cells in the population. For example, organisms that have regenerative capacity like hydra escape senescence (Dańko et al., 2015). Undergoing apoptosis may have a much greater benefit for the population (Ruckenstuhl et al., 2010). Sheldrake and others think that unicellular organisms unlike multicellular organisms are potentially immortal and 'carry the potential of unending life", termed the "potential immortality paradigm—essentially making senescence unlikely (Sheldrake, 2022). Future experiments should focus on trying to induce senescence in budding yeast with specific stressors such as hydrogen peroxide or DNA damaging agents. If successful, then yeast could represent a unique model system to study senescence induction similar to hydra (Bellantuono et al., 2015).

Part 2

Introduction

Measuring cell viability in the form of CFUs is widely used by yeast researchers, and not just for CLS assays. Over the years, various laboratories have improved, modified, or diverged from this traditional CLS method initially described by Longo *et al.* 1996. For example, with the rise of expensive liquid handling robots, specialized plate readers, and imaging systems, outgrowth of yeast cultures or colonies for CLS assays have become more automated (Shah et al., 2007), but not always accessible to many labs. Here, we describe our own in-house modified assembly line of the traditional CLS assay that has allowed for us to realize a greater economy of scale. The modifications are focused on miniaturization of the system with the use of a standard tetrad dissection microscope, a compact digital camera, and automated imaging of microcolonies using a

modified version of open source OrganoSeg software. Herein, we show that our method is comparable with traditional means of conducting CLS assays. The main advantage of our protocol consists of increasing resource efficiency by miniaturizing the system and thus increasing resource efficiency by 36-fold—We fit 36 dilution spots onto one agar plate, rather than each dilution being spread onto an individual plate. Additionally, the protocol is adaptable in a variety of settings with minimal equipment needed, making yeast quantitative CLS studies accessible to practically any yeast lab. Understanding regrowth capacity mechanisms has implications far beyond the yeast system, so we want to share this innovative protocol that easily tests viability and maintenance of cellular quiescence.

The Traditional CLS Assay

CLS is defined as the number of days that non-dividing quiescent yeast cells can survive at stationary phase (Longo et al., 1996). The original method of monitoring viability of non-dividing cells in the stationary phase was an effective protocol developed by Valter Longo and was readily adopted by many yeast laboratories, including ours. Longo conducted these studies by growing liquid cultures exponentially until they depleted most nutrients. In response to this depletion, cells transitioned into a quiescent state where cells are no longer dividing but retained that potential. At this point, Longo then took an aliquot of the aged liquid cell culture, diluted these aliquots in sterile water and plated it onto YPD rich media plates (maximum ~300 colonies per plate), and allowing them to grow for three days (Fabrizio & Longo, 2003). He then counted the number of colonies that regrew. With increasing time, the ability of cells to re-enter the cell cycle diminished. Thus, monitoring the loss of regrowth capacity became an

indicator of cellular aging. This method became known as chronological lifespan assays (CLS). This assay involves using single plates for each dilution replicates and counting colonies manually to calculate the fraction viable from the initial population. This is a labor-intensive task using numerous petri dishes, agar, and media components.

Results

Differentiation from the Original Method

Since initial characterization of the CLS protocol in 1996, there have been several strategies developed to build upon this original method. For example, to test viability more directly, multiple groups have established variations of this assay or developed a variety of different strategies to measure stationary-phase viability such as plate readers, PI, fluorescent cell counter, semi-quantitative CLS assays, methylene blue, and phloxine B (Belak et al., 2018; Chadwick et al., 2016; Garay et al., 2014; Murakami & Kaeberlein, 2009; Murakami et al., 2008). Others have also stuck with using regrowth as a CLS measurement but introduced expensive robotic or spot imaging assays. Our lab initially shifted to conducting a semi-quantitative method using spot assays, since it was an inexpensive way to conduct CLS and there appeared to be strong correlation between the quantitative and semi-quantitative (Smith et al., 2007; Smith Jr. et al., 2007). Although these qualitative spot assays were informative and visually effective, they lacked a quantitative component to discern small changes in longevity with statistics. When we switched to the qualitative spot assay method, we observed that in the dilution spots, the most diluted sample contained micro-colonies. If the plates were only incubated for 16-20 hours and these dilution spots were observed under a microscope at 30x magnification, each dilution spot in the microscope field looked very similar to a petri

dish agar plate (Figure 3.3A). We were able to merge traditional CLS with spot assays to return to a quantitative method.

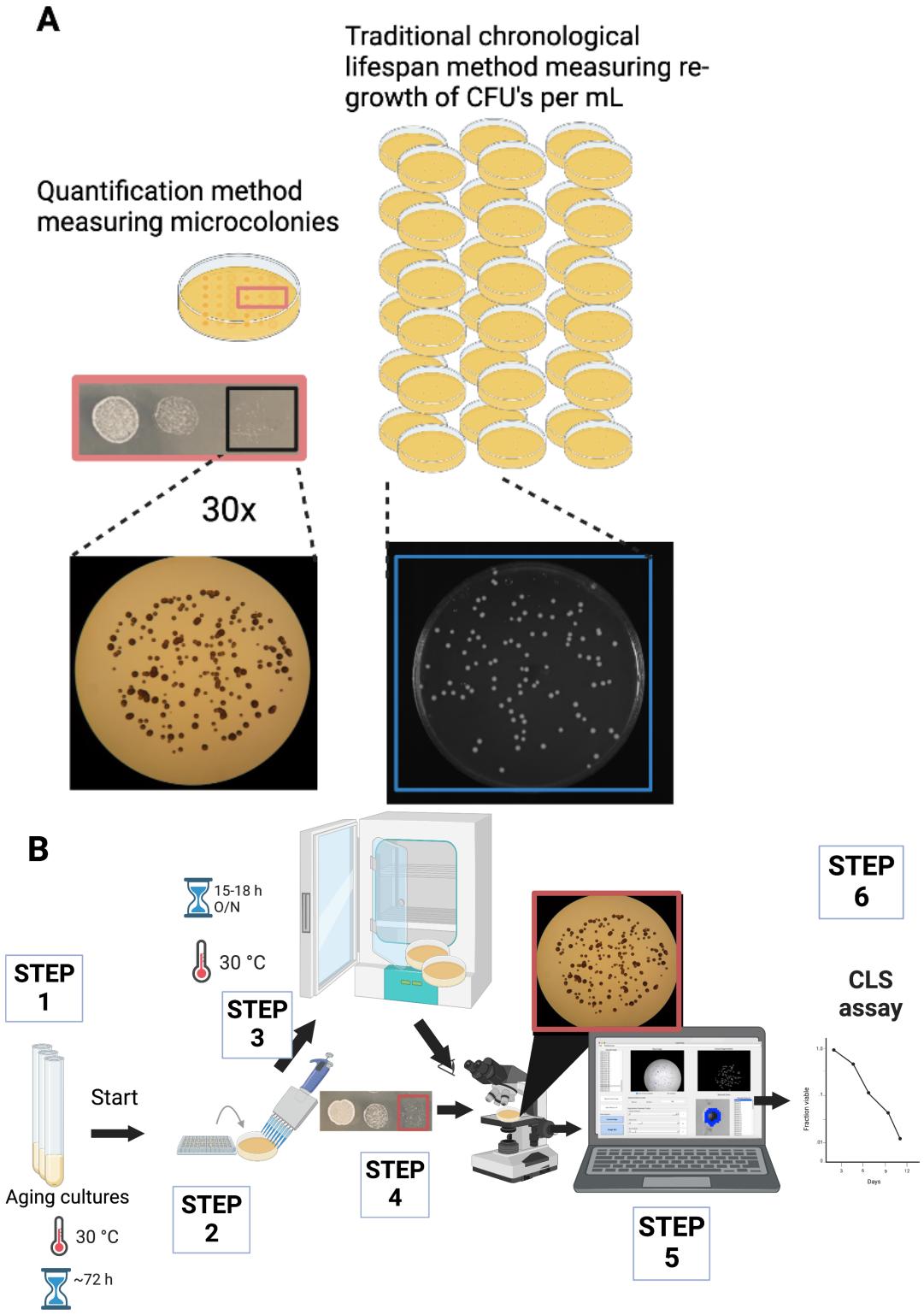

Figure 3.3 CLS assays. *A) Image of dilution spots after 16 hours of incubation compared to the plate-method used in Longo's Traditional method B) Schematic of steps 1-6.*

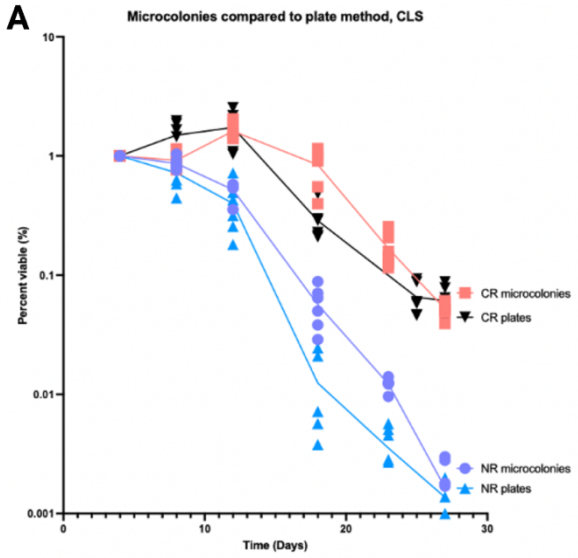

B

Condition	Mean Lifespan (days)	SEM	95% Confidence interval
NR Microcolonies	13.90	0.38	13.15~ 14.65
NR plates	13.07	0.20	12.67~ 13.47
CR Microcolonies	19.38	0.42	18.56 ~ 20.21
CR plates	18.96	0.13	18.70~ 19.21

Figure 3.4 Comparing methods*. Survival curves representing the viability of three biological replicates, microcolonies compared with survival curves representing the viability of three biological replicates using the traditional method (plates) in NR and CR conditions. E) Microcolony method compared to the traditional plate method. Mean lifespan in days was calculated using Online Application for Survival Analysis Software (OASIS 2), which reports standard error of the mean (SEM) and 95% confidence intervals.*

Here, we describe the relatively simple, flexible, low-resource protocol combined with image-based cell counting estimation assay to facilitate CLS (Figure 3.3B). First, we've modified the assay to count imaged micro-colonies, instead of colonies, where each petri dish can now accommodate 12 samples (with three dilution spots each) or 36 dilution spots total (Figure 3.3A). This quantitative method uses 1/12 of the resources of a traditional CLS assay (Figure 3.3A). We conducted an experiment with CR and NR conditions where the traditional method was run in parallel with our microcolony method. These results were comparable with traditional ways of conducting CLS. It is a

reliable assay that can increase scientific output, with fewer resources from the lab and time commitment by the user. (Figure 3.4 A & B). So, what does this new method entail?

Like the traditional method, this protocol involves taking single yeast colonies from agar plates, inoculating into 10 mL liquid cultures, then aging them while turning in a roller drum at a constant temperature. At each time point, an aliquot of the liquid culture is collected, serially diluted 10-fold and then spotted onto rich growth medium plates (YPD) to obtain bright field microscopy images using a digital camera placed close to the oculus of the microscope (we use a model similar to the Sony Cyber-Shot DSC-H70 16.1 MP Digital Still Camera with 10x Wide-Angle Optical Zoom G Lens and 3.0-inch LCD) (Figure 3.4 A-C). The microscope isa Nikon Eclipse E400.

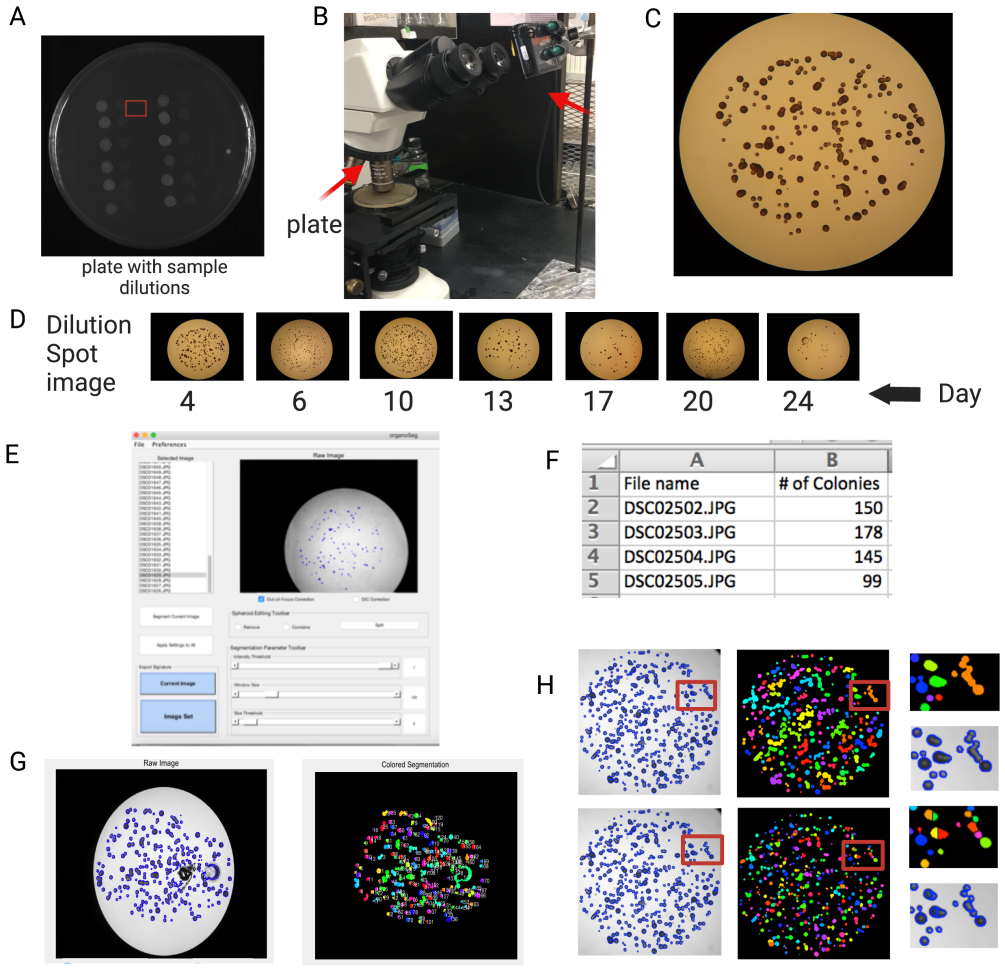

Figure 3.5 Microcolonies and OrganoSeg. *A) plate with sample dilutions after 16 hours of growth. B) Camera set-up for capturing images of dilution spots at 30x, image acquired from microscope of (C) micro-colonies resembling agar plate. D) Dilution of 3rd dilution spot from day 4 to day 24, showing a decrease in viability. E) OrganoSeg software depicting user interface and the data acquisition form the MATLAB based program. F) &G) Output includes the spherical objects detected in each image (The blue around the colonies represents the colonies being detected. H) Function within the program allows segmentation of colonies.*

For subsequent steps, we now use an image-based program to digitally count microcolonies, which expedites the data analysis process (Figure 3.4 D -H). We have adapted OrganoSeg (based on MATLAB), an open-source software used to quantify images of 3-D spheroid and organoids cultures, to count microcolonies. This MATLAB-based software uses grayscale-converted images (tif, jpng, png) to quantify spheroids (Figure 3.4 E). It is comparable with Fiji image analysis, CellProfiler, OpenCFU, and AutoCellSeg (based on MATLAB)(Carpenter et al., 2006; Geissmann, 2013). OrganoSeg is an automated colony segmentation system, a user-friendly tool that allows analysis of a large image number. It was originally developed by Kevin Janes' lab in the UVA Department of Biomedical Engineering to count 3-D organoid and spheroids (Borten et al., 2018). For the yeast CLS assays, OrganoSeg is easy to use as it only requires the adjustment of a size parameter. It has parameters where one can omit artifacts (Figure 3.4 G). Furthermore, it has a sphere-splitting function that is useful if two or more colonies begin overlapping on the agar (Figure 3.4H).

Discussion

Herein, we describe the CLS assay using micro-colonies as an effective, low resource method for quantifying viability and colony re-growth. First, we show the microcolony protocol yields similar outputs to manual counting methods, allowing the researcher to increase sample size and replicate number (Figure 3.2 D & E). Using microcolonies instead of colonies, we have developed this method into a high-throughput assay. With this assay, we speculate that mutants, environmental manipulations, and toxicity studies should easily be tested for viability and maintenance of quiescence. The CLS methodology will continue to be a valuable tool, which continues to provide insights into the basic aging and quiescent mechanisms conserved across eukaryotes.

Protocol (Refer to Figure 3.3C)

Step 1: Preparation of CLS

Prepare 2% glucose YPD agar plates. After the plates have been poured, they must be allowed to dry at least 2 days before plating the dilution spots in Part 2. Wet plates will not work.

1. Obtain yeast strains from frozen stocks and streak for single colonies onto YPD [Bacto yeast extract (10 g L−1), Bacto peptone (20 g L−1), tryptophan (0.32 g L−1), 2% glucose] agar plates.
2. Allow cells to grow at 30˚C for 48 hours.
3. Select a single colony and inoculate into 5 mL of SC (2% glucose) liquid medium in 18-mm glass culture test tubes with loose metal caps. Allow cultures to reach stationary phase by growing them O/N at 30˚C on a New Brunswick Scientific roller drum ~50 r. p. m. to maintain cells in suspension.

4. Inoculate 200ul of the overnight culture into 10 mL of SC medium. Samples are prepared in triplicate to serve as biological replicates of the lifespan analysis for each condition or strain. Mark the top of the test tube with a number and record sample type in a notebook.
5. Maintain the cultures at 30˚C with constant agitation on a roller drum for the entire experiment. Day of inoculation is day 0.

   Step 2: Taking a time-point in chronological lifespan assays (See image below).

   First time point can be acquired at day four of culture (in SC media, the cells should be in the stationary phase). Viability should be monitored every three to four days for two to three weeks or until most colonies are unable to regrow in the rich YPD plate. The length of an experiment can be terminated by plating the dilutions and looking at the YPD plate after O/N growth. For example, if colonies can only be detected at 0.01 dilution spot, then most cells have died, and those samples can be removed from the experiment. Time points should be taken more often for shorter-lived strains (~10-15 days). Frequency will detect short-lived strains that tend to gasp, including *snf1Δ*, *gcn5Δ*.

    1. Obtain a 96 clear well plate. Prepare by adding 180ul of sterile water to wells. For each sample, 3 dilution wells are needed. For multiple samples, use the suggested template (Figure 3.4 A).
    2. Remove the aging glass culture tubes from the roller drum in the incubator.
    3. Vortex and then collect a 20 ul aliquot of culture with a pipette and place in the first well containing water. Repeat for remaining samples. Keep everything sterile.

4. Using a multichannel pipette, take 20 ul of the inoculated first well and conduct 10-fold dilutions for the second and third well. The first well for each is a tenfold dilution of the culture, the second well is 100-fold dilution and the third is 1000-fold (Figure 3.4B).
5. 2.5µl of 1:10, 1:100, and 1:1,000 dilutions of the cultures were spotted onto yeast extract-peptone-dextrose (YPD) plates. With a multichannel pipette, mix and transfer 2.5 ul of each well into a YPD plate. If the template is followed, a YPD plate can fit 12 replicates or 36 dilution spots. Name the plates, and the number of tubes it contains. Plate one should be named, P1, 1-6 on one side, and 7-12 on the other (Figure 3.4 C &D and 3.5). An important point is to avoid touching the agar with the tip of the pipette since it introduces artifacts that will interfere with counting (Figure 3.3G).
6. Check to make sure 2.5ul is on the plate for each condition and that there is no overlap between drops. Printing out a paper grid on the countertop and placing the plate on top of the grid, will facilitate separation. Allow spots to dry before moving.
7. Return the CLS cultures into the 30˚C incubator when finished with the inoculations.
8. Place the plate in a 30˚C incubator. Allow colonies to grow for 16-24 hours to allow for micro-colony formation.

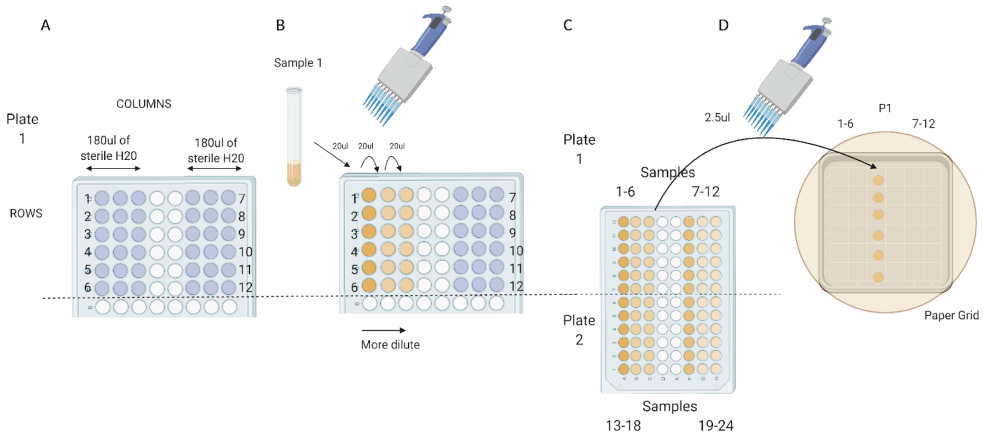

Figure 3.6 Collecting a time point *A) 96-well plate was prepared with 180ul of sterile water in the first three and last three wells of each row. B) First and sixth column wells of every plate were inoculated with 20 ul of cells taken from cultures in order. With a multichannel pipette, 20 ul was added to the second column or seventh column, then thoroughly mixed. Then 20 ul of the second column was added to the third column or eighth column. This was done for sample number 1-12 and for the rest of the plates. C) Plates were labeled. 2.5 ul were then collected from each well starting with the most dilute. For example, the third column of sample one was plated first, then the second, and then the first. These were plated onto a rich media plate with the aid of a paper grid placed under the plastic petri dish to direct placement of each drop without overlap. The layout of the 96-well plate directly matches the placement of 2.5 ul.*

Step 3 Image acquisition

Overview: To capture micro-colonies in these dilution spots, we utilize a dissecting microscope, where images of dilution spots with micro-colonies are obtained and subsequently counted (Figure 3.3B).

1. Remove plate from the incubator and using a microscope place the plate on stage and obtain pictures of the dilution spot. In the beginning of the experiment when the cells are the most viable, take a picture of the most diluted spot of each sample. This will change over time as the population loses viability. The rule of

thumb is to move to the next dilution when there are 5 or less colonies in a dilution spot. Capture Images of the dilution spots using a Nikon Eclipse E400 tetrad dissection microscope at 30x magnification. One picture per condition. Record what dilution was captured. At the first time point, growth should be detected in most conditions at the most diluted spot, 1:1000.

2. Download the images into a folder, naming it with the date of the experiment and day number. Rename images. Open MATLAB and then OrganoSeg.
3. Using the OrganoSeg software, select 'File', 'new set of images to analyze', open and select all the JPG images. Select 'yes' when prompted 'to convert image to optimal size, to improve segmentation'.
4. To begin counting, adjust the size threshold between 0-20, depending on colony size using 'Segmentation Parameter Toolbar.' Click "Apply Settings to All images." Spheroids detected will be on the left of the screen. Trouble shooting; If there are artifacts in the gel, try unchecking the 'out-of–focus correction' on the main screen. If the colonies are too small, return the plate to the incubator, until they are bigger to detect. If they are too big and begin overlapping, attempt to correct by using the 'Split function,' which segments two joined colonies. To export into an excel file, click on the Image set below "Export Signature." Obtain output files from software into an excel document or scroll through OrganoSeg manually and record total spheroids for each image (Figure 3.4).
5. For ease, use the same order in plating the sample and collecting images.
6. Repeat Part 2 and 3 for next time point.

Step 4: Data Analysis

1. For CLS assays, several time points are obtained. The time points for the given experiments were taken on days: 4, 6, 10, 13, 17, 20, 24, 27, 31. Depending on the strains or experimental conditions, time points could be collected less or more frequently. For example, if a short-lived mutant (10 days) is assayed, then it is important to conduct time-points more frequently. In contrast if a long-lived mutant is analyzed then taking time points every 4-5 days is sufficient.
2. Normalize the data by comparing the number of micro-colony forming units to the initial measurements (usually day 3 or 4) to obtain percent viability, time point 1 for each sample should be 100% viability.
3. Generate chronological lifespan curves by plotting the fraction viable cells as a function of time.
4. Calculate the % viability for each well based on the viability of the first time point. For these data will generate a survival curve. The equation used to calculate % viability is: = # of microcolonies ((obtained with OrganoSeg)* # dilution spot(1, 0.1. or 0.01)/ # of microcolonies) x 100 obtained at the first time point.
5. In excel, plot the average of each sample as a function of time.
6. Mean lifespans (days), standard errors of the means (SEM), and 95th percentile confidence intervals of the means (95% CI) can be calculated using OASIS, an online platform for Kaplan-Meier survival curve analysis and other statistical analysis (Han et al., 2016). There is a specific format to input the data that requires a number of dead objects at each time point. To obtain the number of dead objects we took the average number of microcolony forming units for each condition at each time point. The first average of the first time point represents the

total number of "individuals" in a population. The average of the next time point was subtracted from the previous. This in essence would represent the total individuals that died between time points. If the average exceeds the average of the previous time point, which can happen in CLS assays due to growth, then that would yield a negative number. OASIS would interpret this as objects coming back to life and the program gives an error. To prevent this from happening, we remove the numbers by equating them to 0. This would indicate that no deaths occurred between time points. A representative template is provided with examples of negative numbers and adjustments necessary to use OASIS.

7. At the completion of the experiment, a survival curve will be obtained and resemble those in Figure 3, which were conducted in BY4741 background in SC 2% glucose media. We plot Fraction Viable on the y-axis and time on the x-axis.

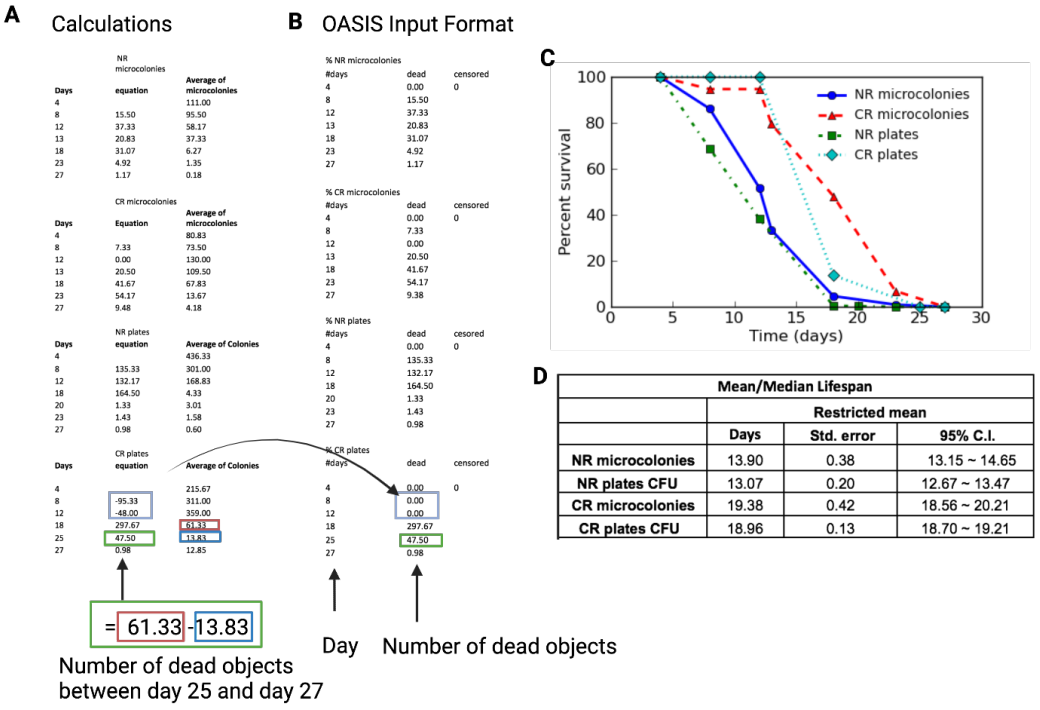

D

Mean/Median Lifespan			
	Restricted mean		
	Days	Std. error	95% C.I.
NR microcolonies	13.90	0.38	13.15 ~ 14.65
NR plates CFU	13.07	0.20	12.67 ~ 13.47
CR microcolonies	19.38	0.42	18.56 ~ 20.21
CR plates CFU	18.96	0.13	18.70 ~ 19.21

***Figure 3.7 Data processing and input format for basic survival analysis in OASIS**. A) Shows calculations of colony forming units to input into OASIS B). C) and D) represent the data output obtained from running the analysis (Han et al., 2016).*

Other Methods

Viability and Flow cytometry

LIVE/DEAD® FungaLight™ Yeast Viability Kit (L34952) contains solutions of our SYTO 9 green, fluorescent nucleic acid stain and the red-fluorescent nucleic acid stain, PI. The excitation/emission maxima for these dyes are 480/500 nm for SYTO® 9 stain and 490/635 nm for PI. Follow LIVE/DEAD ® FungaLightTM Yeast Viability Kit Instructions: Collect 0.5 OD of cells for each sample and centrifuge samples at 10,000 g for 2 minutes to pellet cells. Prepare at least 4 extra tubes to prepare for controls (stained with PI, stained with SYTO 9, no dye, and killed control). Remove the supernatant. Wash once and resuspend in 1 ml of PBS. Transfer this 1 ml to a plastic tube for flow cytometry analysis with LSR Fortessa or FACSCaliburB. To prepare one killed control sample by resuspending cell pellet in 1 mL of 70% isopropyl alcohol and incubating it for 30 minutes. After incubation, wash once with PBS and resuspend in 1 ml of PBS. For all samples, check to have approximately 1 million cells in each vial. For staining procedure, add 1 µL of SYTO 9 dye from the Viability kit to tube, which will only contain SYTO 9. Add 1 µL of PI from the Viability kit to a tube, which will only contain PI. These will be controls. Add 1 µL of PI and 1 µL of SYTO 9 to the rest of the tubes, except for the unstained control which receives no dye. After stain is added, each tube should be vortex and protected from the light. Cells were then analyzed by flow cytometry without washing.

Q cells

BY4741 yeast cells were grown in synthetic complete (SC) media in NR (2.0% glucose) or CR (0.5% glucose). Specific number of cells were isolated from liquid cultures (OD of 0.5-1.0 spun and resuspended in 0.5 ml of SC-glucose) and then this 0.5 mL was layered gently onto pre-made iodixanol density solution of 1 ml and centrifuged to separate populations of different densities. Iodixanol gradient separation of non-quiescent (NQ) and quiescent (Q) yeast cells in a microfuge tube in NR conditions and CR conditions. For this experiment ~50% iodixanol gradient is sufficient for separation of NQ and Q yeast cells.

Chapter IV

A cell non-autonomous mechanism of yeast chronological aging regulated by caloric restriction and one-carbon metabolism

Abstract

Caloric restriction (CR) improves healthspan and lifespan of organisms ranging from yeast to mammals. Understanding the mechanisms involved will uncover future interventions for aging-associated diseases. In budding yeast, *Saccharomyces cerevisiae*, CR is commonly defined by reduced glucose in the growth medium, which extends both replicative and chronological lifespan (CLS). We found that conditioned media collected from stationary-phase CR cultures extended CLS when supplemented into non-restricted (NR) cultures, suggesting a potential cell-nonautonomous mechanism of CR-induced lifespan regulation. Chromatography and untargeted metabolomics of the conditioned media, as well as transcriptional responses associated with the longevity effect, pointed to specific amino acids enriched in the CR conditioned media (CRCM) as functional molecules, with L-serine being a particularly strong candidate. Indeed, supplementing L-serine into NR cultures extended CLS through a mechanism dependent on the one-carbon metabolism pathway, thus implicating this conserved and central metabolic hub in lifespan regulation.

Introduction

In *Saccharomyces cerevisiae*, Caloric Restriction (CR) involves reducing glucose in the growth medium, which extends both replicative (RLS) and chronological lifespan (CLS). Specifically, CR is typically characterized by reducing the initial glucose concentration in the growth medium from 2% (non-restricted; NR) to 0.5% or lower, or reducing overall amino acids (Jiang et al., 2000; Lin et al., 2002). Glucose restriction robustly extends both yeast replicative lifespan (RLS) and chronological lifespan (CLS) (Jiang et al., 2000; Lin et al., 2002; Reverter-Branchat et al., 2004; Smith Jr. et al., 2007), the latter of which is defined by the number of days that non-dividing cells maintain proliferative capacity in liquid culture after entering stationary phase, quantified upon transfer to fresh nutrient media (Fabrizio & Longo, 2003; MacLean et al., 2001). In the stationary phase, the cells remain in this non-dividing state and are considered a model for the aging of quiescent stem cells, or post-mitotic cells like neurons or muscle fiber cells (Jones & Rando, 2011; Longo et al., 2012; Ruetenik & Barrientos, 2018).

Before cells enter the stationary phase, they go through an important transition termed the 'diauxic shift'. Herein, glucose becomes limiting toward the end of exponential growth, and cells reconfigure their metabolism and enact cell protection systems for survival. For example, cells switch from fermentative (metabolism of glucose to ethanol) to mitochondrial-driven oxidative metabolism. This 'diauxic shift' into stationary phase of growth is also accompanied by dramatic changes in transcription, translation, and metabolic profiles that facilitate slower cell growth using non-fermentable carbon sources such as ethanol and organic acids produced during fermentation (DeRisi et al., 1997; Gasch et al., 2000). During this transition, long-term survival in CLS largely hinges on an adaptive response to nutrient depletion, consisting of cell cycle arrest, called quiescence (Allen et al., 2006; Gray et al., 2004). CR optimizes this transition.

In CLS, the initial glucose concentration in cultures has a profound impact on long-term cell survival in the stationary phase. It was surprising that glucose restriction extended the yeast CLS even when the glucose was rapidly utilized (Smith Jr. et al., 2007). This suggested that intrinsic changes occur in a cell during the diauxic shift that has lasting effects on longevity. CR enhances several processes that occur during the diauxic shift, including Snf1 (AMPK) signaling (Wierman et al., 2017), mitochondrial respiration and ATP production (Choi & Lee, 2013; Ocampo et al., 2012; Smith Jr. et al., 2007; Tahara et al., 2013), accumulation of the storage carbohydrate trehalose (Kyryakov et al., 2012), and improved G1 cell cycle arrest (Weinberger et al., 2007).

Independent of CR, there are several other conserved genetic and environmental manipulations that extend CLS, such as inhibition of TOR signaling (Powers et al., 2006) and methionine restriction (Johnson & Johnson, 2014; Ruckenstuhl et al., 2014). Fully understanding intracellular and extracellular responses underlying the complex adaptive transition into quiescence, and how CR influences these responses, are of central interest. In budding yeast as in other unicellular organisms, the impact of environmental and genetic modifications on individual cell survival is usually expected to occur through cell-autonomous mechanisms. These cell autonomous mechanisms *depend* on the intrinsic cellular events, such as direct changes in gene expression, metabolism, and stress response. However, regulation of survival can also be cellular *independent* and can be mediated *via* cell non-autonomous mechanisms driven by cell-derived extracellular factors (Burtner et al., 2009; Fabrizio et al., 2004). For example, high acetic acid concentrations released from cells into the media and the accompanying low pH are associated with sustained growth signals that lead to cell cycle progression, replication stress, and reduced CLS (Ruckenstuhl et al., 2010; Weinberger et al., 2010). Furthermore, acetic acid induced stress

can activate nutrient sensing growth pathways that lead to elevated superoxide (Weinberger et al., 2010). These examples illustrate the life-shortening and the life-extending effects of the cell non-autonomous mechanisms in budding yeast.

Longevity-associated cell non-autonomous mechanisms are classically described from rodent models, where circulating extracellular factors have been identified from heterochronic parabiosis experiments to mediate beneficial effects or detrimental effects to each parabiont (McCay et al., 1957). For example, mesencephalic astrocyte-derived neurotrophic factor (MANF) from younger mice protects against liver damage in the older mice. In contrast, Senescence-Associated Secretory Phenotype (SASP) from aged mice has been shown to negatively contribute to the health of the young mouse (Conboy et al., 2013). Interestingly MANF's overexpression extends lifespan in *Drosophila* (Sousa-Victor et al., 2019). Furthermore, some factors that act in a cell-autonomous manner, such as the insulin-like signaling transcription factor FOXO, can impact organismal longevity *via* cell non-autonomous mechanisms (Hwangbo et al., 2004; Qin & Hubbard, 2015), raising the possibility that cell non-autonomous processes are more widespread than previously thought.

Despite budding yeast being single cell organisms, they utilize proteins and metabolites for cell-cell communication associated with mating, differentiation, and sporulation. Recognition of opposite haploid mating types (a-cells or α-cells) occurs *via* the extracellular pheromone peptides a-factor and α-factor (Haber, 2012), whereas pseudohyphal growth in dense cultures or colonies is mediated by quorum sensing *via* the amino acid derived aromatic alcohols, tryptophol and phenylethanol (Chen & Fink, 2006). Chronological aging of *S. cerevisiae*, which occurs in densely crowded cultures and is highly sensitive to gene-nutrient interactions (Smith et al., 2016), would also seem subject to cell non-autonomous mechanisms. Indeed, unidentified high

molecular weight (>5,000 Da) extracellular factors from old stationary phase cultures have been implicated in stimulating survival of other old cells (Herker et al., 2004).

Similarly, our lab observed that conditioned media isolated from glucose-restricted stationary phase cultures, referred to as CR-conditioned media (CRCM) throughout this chapter, extended CLS when supplemented into non-restricted cultures (Wierman et al., 2015), suggesting the presence of one or more extracellular proteins, peptides, or metabolites that contribute to lifespan regulation. We were interested in elucidating these factors to provide new insights about CR mechanisms.

Results

Conditioned media from CR stationary phase cultures contain longevity factors.

As previously shown (Smith Jr. et al., 2007), BY4741 yeast cells grown in 2% glucose (NR) have a short CLS compared to 0.5% glucose (CR) growth conditions. However, when we conducted media swap experiments where the conditioned media was exchanged after five days, we observed a change in CLS as monitored by spot viability assays (Figure 4.1A & 4.2B). In this experiment, cells grown under CR conditions have a shorter lifespan once exposed to NRCM compared to CR conditions (Figure 4.1B). In addition, the initially grown cells in CR condition live less once exposed to NRCM compared to the CR control (Figure 4.1B). Importantly, this conditioned media is obtained at day 5, where the glucose in the media has been depleted, completely consumed by the cells. This suggests that there are extracellular factors within the CR media that promote longevity, and perhaps negative factors that hinder longevity in NR.

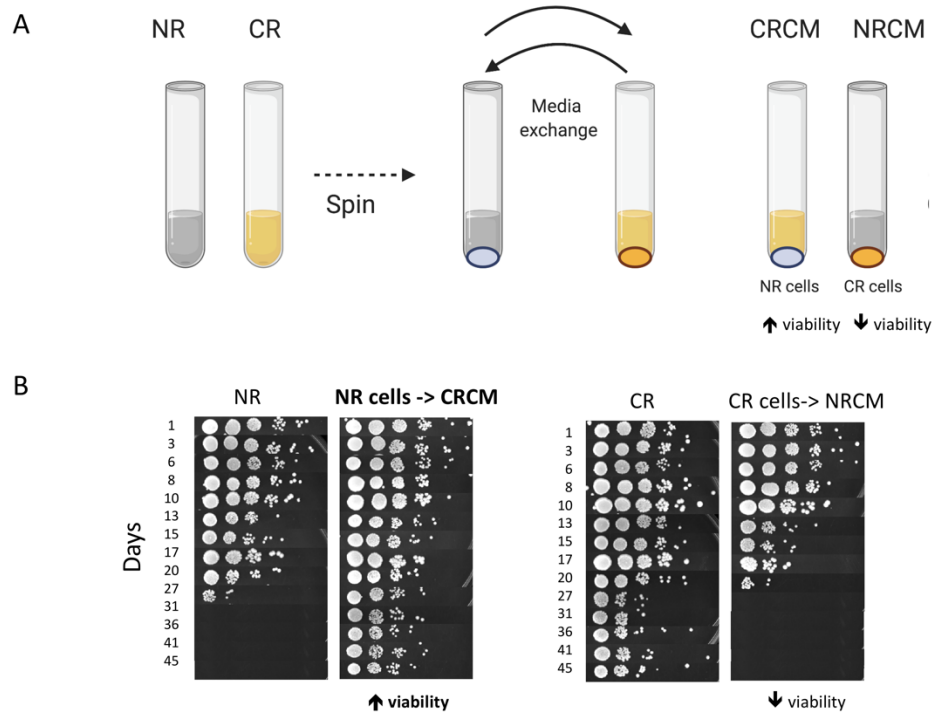

Figure 4.1. Media swap experiments show longevity factors in the media*. (A) Schematic of conditioned media swap experiments conducted at day 5 post-inoculation. BY4741 was grown to stationary phase in SC media containing 2% (NR) or 0.5% (CR) glucose. Cells were pelleted by centrifugation and the conditioned media (NRCM or CRCM) was removed, filtered, and then added back to cells. CR cells received NRCM and NR cells received CRCM media. Control conditions received the same CRCM and NR control cells received the same NRCM. (B) Qualitative chronological lifespan (CLS) assays used to monitor viability starting at day 1 post-media switch. This was created by Daniel Smith.*

We reasoned that using concentrated media would increase the chances of detecting longevity activity if the factors were low abundance molecules. Herein, we collected and concentrated CRCM and NRCM from day 5 stationary phase cultures of BY4741 (Figure 4.2 A). Concentration and supplementation of CR and NR conditioned media at the time of inoculation yielded similar results as the media swap experiment. To test this, we utilized 10 mL cultures and added a small percentage of concentrated media at the time of inoculation. We then monitored

viability *via* a microcolony viability assay (see (Wierman et al., 2017) and Chapter III Experimental Procedures). As shown in Figure 4.2B and C, the CRCM concentrate addition significantly extended CLS of BY4741 when diluted 1:50 (2% vol/vol) or 1:100 (1% vol/vol) in NR (non-restricted) SC media, while NRCM concentrate had a minor effect only at 2% (vol/vol).

Since BY4741 is auxotrophic for histidine, leucine, methionine, and uracil, we next confirmed that concentrated CRCM isolated from this strain could also extend the CLS of a prototrophic strain, FY4, when supplemented into NR. As shown in (Figure 4.2D and E), CR extended the CLS of FY4 as did the supplementation of CRCM derived from BY4741.

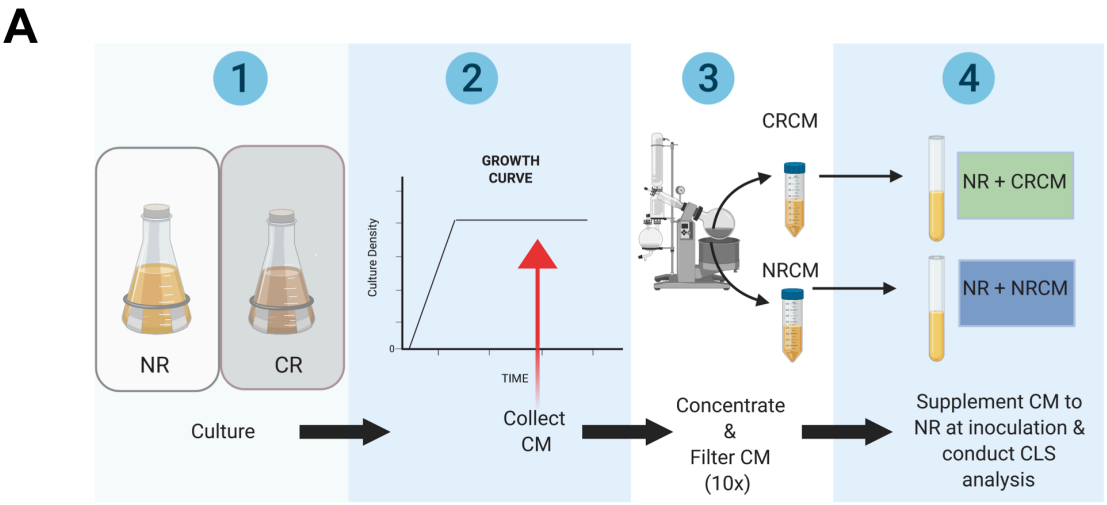

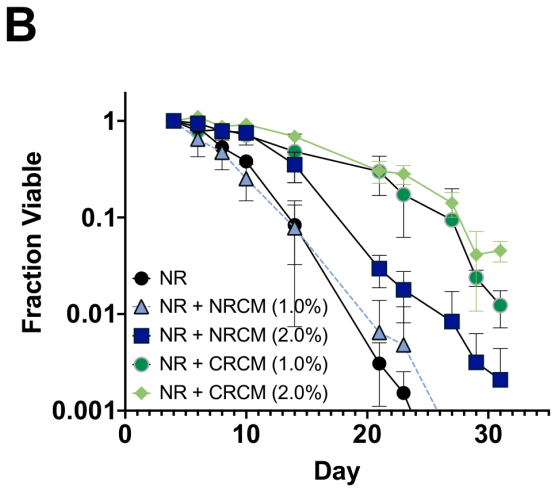

C

Condition	Mean Lifespan (days)	SEM	95% Confidence Interval
NR BY4741	10.84	0.26	10.33 ~ 11.35
NR BY4741 + NRCM 1.0%	10.21	0.27	9.68 ~ 10.74
NR BY4741 + NRCM 2.0%	15	0.31	14.40 ~ 15.60
NR BY4741 + CRCM 2.0%	18.37	0.39	17.61 ~ 19.13
NR BY4741 + CRCM 1.0%	19.41	0.37	18.69 ~ 20.13

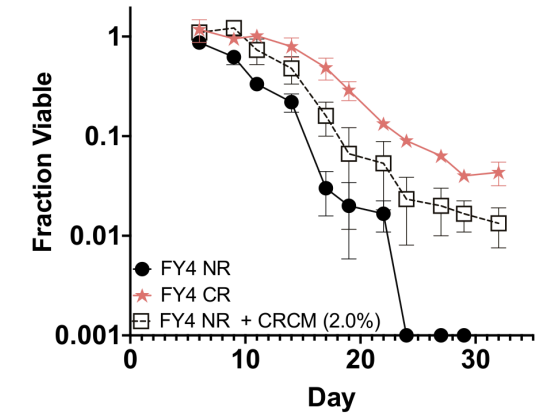

E

Condition	Mean Lifespan (days)	SEM	95% Confidence Interval
NR FY4	11.71	0.27	11.18 ~ 12.23
NR FY4 + CRCM	15.03	0.29	14.45 ~ 15.60
CR FY4	16.61	0.37	15.89 ~ 17.34

Figure 4.2. Longevity factors are present in conditioned media from calorie restricted yeast cultures*. (A) Schematic of conditioned media CLS experiments. BY4741 was grown to stationary phase in SC media containing 2% (NR) or 0.5% (CR) glucose. Cells were pelleted by*

centrifugation and the conditioned media (NRCR or CRCM) then concentrated 10-fold with a Büchi Rotavap apparatus and supplemented into small 15 mL NR cultures of BY4741 or FY4. (B) Quantitative chronological lifespan (CLS) assay. Concentrated CRCM and NRCM was supplemented at 1% or 2% (vol/vol) into NR cultures at time of inoculation. To measure the fraction of viable cells over time, micro-colony forming units were counted after 18 hours of regrowth after spotting onto YPD plates. Error bars indicate standard deviations (n=3). (C) Mean lifespan in days was calculated using Online Application for Survival Analysis Software (OASIS 2), which reports standard error of the mean (SEM) and 95% confidence intervals. (D) Quantitative CLS assay showing effect of CRCM at 2% (vol/vol) on prototrophic strain FY4. (E) Statistical analysis of results from panel D.

Fractionation of CRCM isolates CLS factor activities separate from acetic acid

The preliminary experiments in Figures 4.1 and 4.2 provided evidence of longevity factors enriched in the media of CR cultures, thus raising the question of their chemical nature and identities. An earlier study concluded that chronologically aged yeast cells release large (>5 kD) heat-stable compounds into the media that improve viability of other cells in the population (Herker et al., 2004). To determine if CRCM contained such factors, we treated it with Proteinase K, DNase I, RNase A, phenol/chloroform, autoclaving, or freezing, but none of these treatments attenuated CLS extension observed (data not shown). Instead, CRCM activity was found to be smaller than 5,000 daltons, as the fraction passing through an Amicon Ultra-4 centrifugal filter unit (5,000 MW cutoff) had CLS extending activity equivalent to the starting material (Figure 4.3A). This result demonstrated that the CR-associated longevity factor(s) described here were different from the previously described higher molecular weight factors (Herker et al., 2004).

To get a better sense of the size of the active CLS-modifying molecules in the CR conditioned media we used size exclusion chromatography. To do this, we rigorously

concentrated 150 mL of NRCM or CRCM down to a final volume of 2.5 mL (60-fold). Precipitates were then removed by centrifugation, and the remaining soluble material fractionated through a Sephadex G-10 column, which has a size exclusion limit of ~700 Da. Fractions that eluted with water were added to NR SC cultures of BY4741 at a 1:5 ratio and CLS extension detected using a qualitative spot test assay (Figure 4.3B). At day 11, there was a clear peak of improved viability at fractions 21 and 22 for the CRCM, suggesting the active compounds were smaller than 700 Da (Figure 4.3B). We considered the possibility that toxic levels of acetic acid in the NRCM could potentially mask longevity factor activity in the fractions. However, acetic acid peaked at fractions 18-19 in these columns, distinct from the CRCM longevity peaked at fractions 21-22 (Figure 4.3C, red arrows). Instead, the reduced day 11 viability with NRCM fractions 16-18 was potentially due to elevated acetic acid (Figure 4.3B and C). Based on this size exclusion chromatography and the resistance to various treatments such as heat, phenol extraction, nuclease digestion, etc., we concluded that the longevity factor(s) in CRCM were small water-soluble compounds separable from acetic acid.

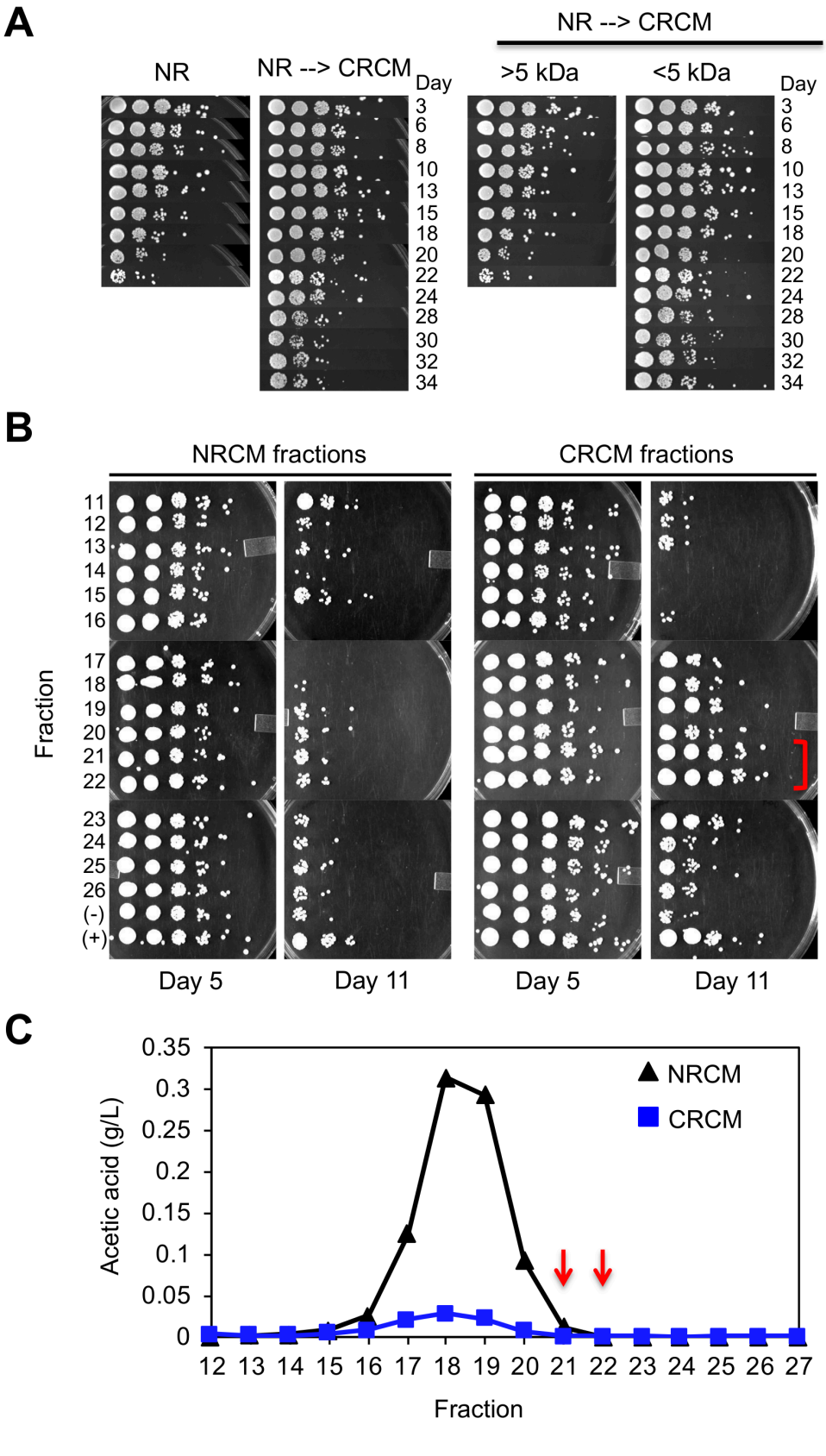
A
NR
NR --> CRCM
Day
3
6
8
10
13
15
18
20
22
24
28
30
32
34
NR --> CRCM
>5 kDa
<5 kDa
Day
3
6
8
10
13
15
18
20
22
24
28
30
32
34
B
NRCM fractions
CRCM fractions
Fraction
11
12
13
14
15
16
17
18
19
20
21
22
23
24
25
26
(-)
(+)
Day 5
Day 11
Day 5
Day 11
C
Acetic acid (g/L)
0.35
0.3
0.25
0.2
0.15
0.1
0.05
0
NRCM
CRCM
12 13 14 15 16 17 18 19 20 21 22 23 24 25 26 27
Fraction

Figure 4.3. Chromatographic sizing and separation of longevity factor activity in CRCM. Figure created by Maggie Wierman. *(A) Left panel: Qualitative CLS assay showing improved viability when supplementing CRCM into non-restricted BY4741 cultures. Right panel: CRCM was first separated into high MW (>5 kDa) or low MW (<5 kDa) fractions using an Amicon Ultra-4 centrifugal filter unit, then supplemented into non-restricted BY4741 cultures. Longevity activity was retained in the low MW fraction. (B) Size exclusion chromatography of NRCM and CRCM was performed using a Sephadex G-10 column (700 dalton MW cutoff). Fractions were added to non-restricted BY4741 cultures at the time of inoculation, and viability tracked over time with qualitative spot assays. The effects of fractions 11 to 26 are shown for days 5 and 11. The longevity peak fractions for CRCM are bracketed in red. (C) Acetic acid concentration (g/L) was measured for each fraction. Red arrows indicate the fractions (21 and 22) with longevity activity in CRCM.*

CRCM-enriched metabolites and induced genes indicate amino acids modulate CLS

Knowing that the extracellular longevity factors were small molecules, we next utilized a comparative metabolomics approach to generate metabolite profiles for the CR and NR conditioned media (Figure 4.4A and 4.4B), reasoning that differential abundance of extracellular metabolites could be a source of CRCM longevity factors. Enrichment and pathway analysis of metabolites more abundant in the CRCM compared to NRCM was performed using MetaboAnalyst (Chong et al., 2019), in which pathway impact (relative circle size) is a measure that considers the centrality of a metabolite in the pathway (Figure 4.4B). The most significantly enriched categories (shaded red), were related to amino acids, including L-alanine, L-aspartate, and L-glutamate metabolism, as well as L-glycine, L-serine, and L-threonine biosynthesis, both of which had the two highest pathway impact scores (x-axis).

To gain additional insights about candidate factors that were potentially functional, we also performed transcriptomics analysis on BY4741 cells grown in NR SC media supplemented with CRCM, NRCM, or water as a control (Figure 4.4C). The goal was to identify cell responses

to gain more clues about the identity of functional longevity factors. Following inoculation into these conditions, we harvested cells at 6 hrs (log phase), 24 hrs (late diauxic shift), and 96 hrs (stationary phase), then performed RNA-seq on isolated mRNAs from three biological replicates. Principal component analysis (PCA) indicated the major variance within the data was the time points (Figure 4.4D), consistent with the massive transcriptional changes that occur during the transition into stationary phase (DeRisi et al., 1997; Gasch et al., 2000). In early log phase cells, there were no significantly upregulated or downregulated genes in the CRCM- or NRCM-supplemented samples as compared to the H_2O-supplemented control (FDR <0.05), consistent with earlier microarray analysis from our lab showing that CR (0.5% glucose) had little effect on gene expression during early log phase (Wierman et al., 2015). At the 24 hr time point, however, CRCM-supplemented samples diverged from the NRCM- and H_2O-supplemented controls in a PCA plot (Figure 4.4D). We also observed that when focusing on 24 and 96 time points, CRCM was more different than the NR. This is different when comparing the NR supplemented with the NRCM. This showed many more differentially regulated genes than the NRCM-treated samples (Figure 4.4E). As a side note, since we do not observe much gene expression early in log phase, we suggest that changes observed in previous studies were likely because these cultures had to progress to the point where glucose had become limiting, thus triggering the initiation of the diauxic shift.

At the 96 hr time point, gene expression for the NRCM samples was also clearly differentiated from the H_2O-supplemented control, though there were still many genes exclusively altered in the CRCM samples.

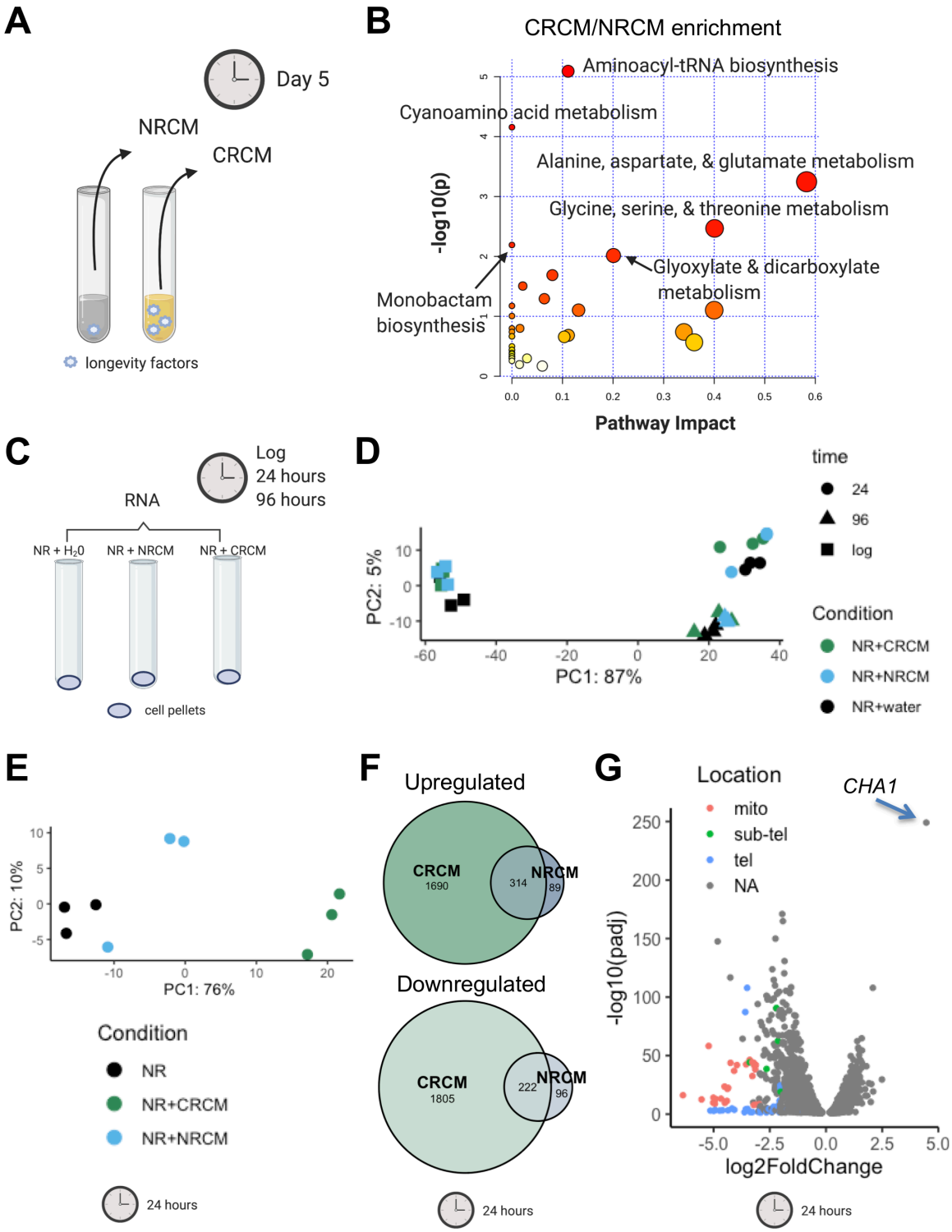

Figure 4.4. Metabolomic and RNA-seq analysis point toward amino acid metabolism. *(A) Schematic of conditioned medium collection used for untargeted metabolomics analysis after five days of SC cultures grown with 2.0% (NR) or 0.5% glucose (CR). (B) MetaboAnalyst software was used for Enrichment and Pathway Analysis of metabolites with a CR/NR ratio greater than*

1.0. The names of KEGG pathways with p<0.05 are highlighted. Pathway impact is a measure that considers the centrality of a metabolite in the pathway. Circle size is proportional to pathway impact value and darker red color indicates more significant changes. (C) Schematic of cell conditions (NR, NR + 2.0 % NRCM, and NR + 2.0% CRCM) collected for RNA-seq analysis at 6 hours (log phase), 24 hours, and 96 hours. Three biological replicates were performed for each condition. (D) Principal component analysis of RNA-seq samples at log, 24, and 96 hour conditions of NR, NR+ NRCM, and NR+ CRCM. (E) Principal component analysis of RNA-seq samples collected at 24 hours. (F) Venn diagram of differentially expressed genes (up or down; FDR<0.05) for NRCM- or CRCM-supplemented samples, as compared to the NR + H2O control at 24 hours. (G) Volcano plot displaying differential expressed genes between the NR + CRCM and NR + H2O samples at 24 hours. The y-axis indicates the p-adjusted value and x-axis the log2 fold change. Red, green, and blue denote genes located in the mitochondrial genome, sub-telomeric, or telomeric regions, respectively. The most upregulated gene CHA1 is highlighted by an arrow.

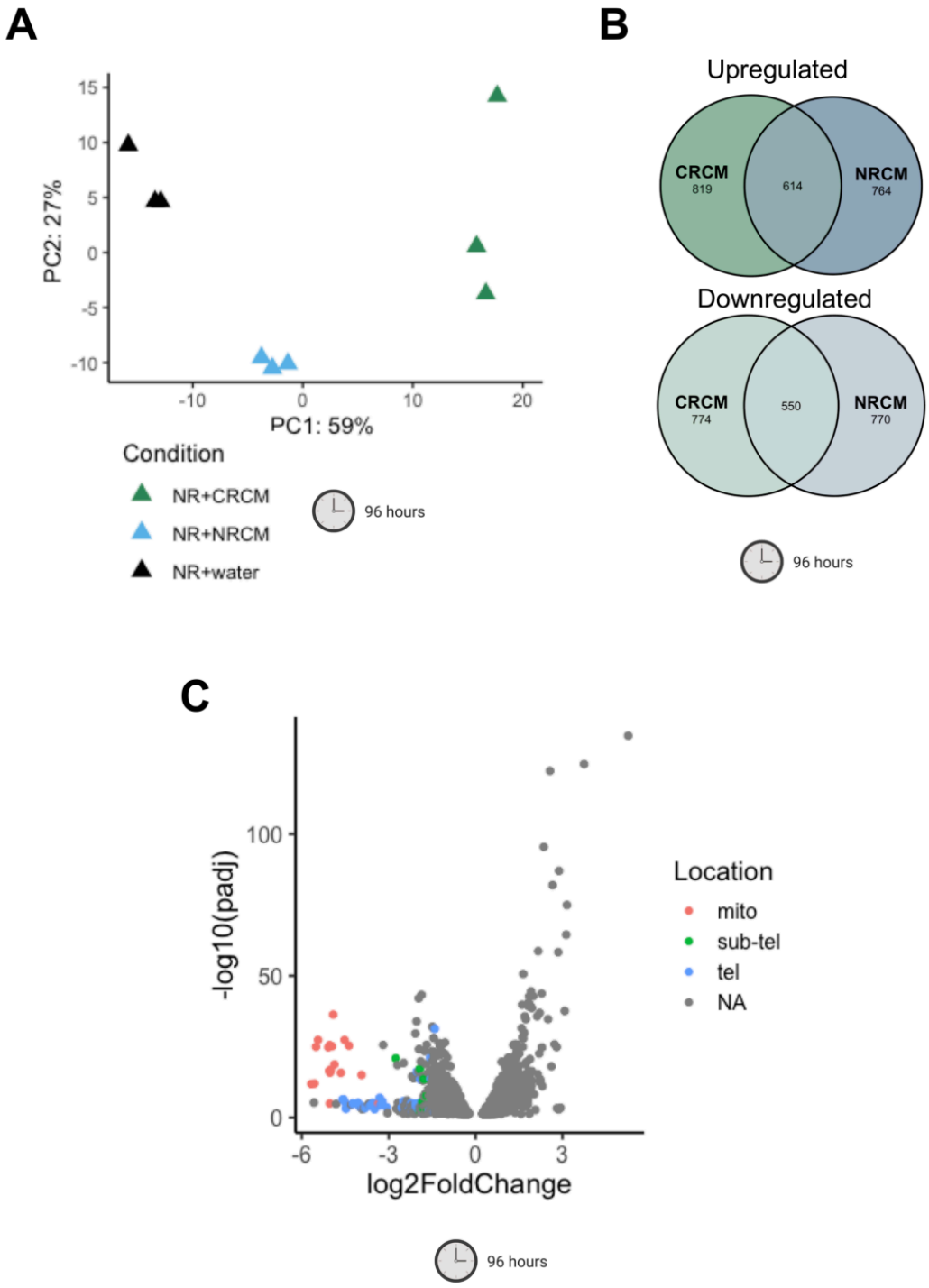

Figure 4.5. Metabolomic and RNA-seq analysis point toward amino acid metabolism.

A) Principal component analysis of RNA-seq samples collected at 96 hours. B) Overview of transcription data. Venn diagram of number of significantly differentially expressed genes

(FDR<0.05) and the overlap between each set of genes. Show the numbers of up-regulated and down-regulated genes between NRCM/NR and CRCM/NR at 96 hours. C) Volcano plot displaying differential expressed genes between NR + CRCM and NR at 96 hours. The vertical axis (y-axis) corresponds to the p-adjusted value and the horizontal axis (x-axis) displays the log 2-fold change value. Red, green, and blue denote location of genes in the mitochondria, sub-telomeric region or telomere region. All points are significant with adjusted p value > 0.05. Positive x-values represent up-regulation and negative x-values represent down-regulation in NR + CRCM compared to NR.

GO biological process complete	REFLIST (6026)	Hits	Expected	Fold enrichment	P-value
alpha-amino acid catabolic process (GO:1901606)	42	19	5.11	3.72	2.93E-02
carboxylic acid catabolic process (GO:0046395)	89	35	10.83	3.23	1.21E-04
cellular amino acid catabolic process (GO:0009063)	56	22	6.81	3.23	3.68E-02
organic acid catabolic process (GO:0016054)	90	35	10.95	3.2	1.51E-04
small molecule catabolic process (GO:0044282)	145	44	17.64	2.49	1.34E-03
alpha-amino acid metabolic process (GO:1901605)	179	51	21.77	2.34	8.84E-04
monocarboxylic acid metabolic process (GO:0032787)	160	45	19.46	2.31	6.79E-03
drug metabolic process (GO:0017144)	197	53	23.96	2.21	2.60E-03

Table 4.1 Gene Ontology term enrichment from RNA-seq analysis point toward amino acid metabolism. *GO terms of 96hr upregulated genes (>1.5 fold) in CRCM compared to NR control. GO terms that show at least 2-fold enrichment. The differentially expressed genes upregulated by NR+CRCM showed enriched biological process terms related to amino acids.*

At 96 hours for the CRCM-supplemented cultures, the top GO term was alpha-amino acid catabolic process (Table 4.1), consistent with the MetaboAnalyst results indicating amino acid metabolism. Interestingly, there were a number of telomeric and sub-telomeric ORFs that were more tightly repressed in the CRCM-treated cells compared to the NR control at 24 and 96

hr (Figures 4.4G, 4.5C), suggesting that the general transcriptional repression associated with chromatin condensation in quiescent cells may be enhanced by supplementing with CRCM (Laporte et al., 2016; Swygert et al., 2019). At 24 hours, the top GO terms for CRCM-upregulated genes were related to mitochondrial function and respiration, consistent with a more robust metabolic transition during the diauxic shift (Table 4.2). Furthermore, at 24 hours, the *CHA1* gene clearly stood out as the most significantly upregulated (4.4G). *CHA1* encodes a L-serine deaminase that produces pyruvate in the mitochondria, giving us a clue to the importance of amino acids in longevity and anapleurotic reactions that replenish the TCA cycle intermediates (Petersen et al., 1988; Ramos & Wiame, 1982). In previous studies, *CHA1* was upregulated in response to high concentrations of L-serine and L-threonine in the media (Godard et al., 2007; Lee et al., 2013). Together, the extracellular metabolite analysis and effects on gene expression during the diauxic shift and stationary phase pointed toward amino acids, especially L-serine, as a major component in the CRCM.

GO biological process complete	REFLIST (6026)	Hits	Expected	Fold enrichment	P-value
mitochondrial translation (GO:0032543)	118	75	15.8	4.75	2.14E-19
respiratory chain complex IV assembly (GO:0008535)	28	16	3.75	4.27	4.59E-02
mitochondrial respiratory chain complex IV assembly (GO:0033617)	28	16	3.75	4.27	4.59E-02
mitochondrial gene expression (GO:0140053)	148	80	19.82	4.04	1.50E-17
cytochrome complex assembly (GO:0017004)	41	22	5.49	4.01	2.95E-03
mitochondrial respiratory chain complex assembly (GO:0033108)	47	25	6.29	3.97	6.37E-04
peptidyl-lysine modification (GO:0018205)	116	40	15.53	2.57	3.78E-03
transcription by RNA polymerase II (GO:0006366)	156	47	20.89	2.25	8.72E-03
rRNA processing (GO:0006364)	280	77	37.5	2.05	1.60E-04
nucleic acid-templated transcription (GO:0097659)	236	64	31.61	2.02	3.20E-03
transcription, DNA-templated (GO:0006351)	236	64	31.61	2.02	3.20E-03

Table 4.2 Gene Ontology term enrichment from RNA-seq analysis point toward mitochondrial genes. *GO terms of 24hr upregulated genes (>1.5 fold) in CRCM compared to NR control. Statistics: Test type: Fisher, Correction: Bonferroni. GO terms that show at least 2-fold enrichment. The differentially expressed genes upregulated by NR+CRCM showed enriched biological process terms related to mitochondrial activation.*

When we conducted untargeted metabolomics of the media, amino acids were enriched in the CR media compared to the NR media with serine being our top hit (Table 4.3). To further confirm these amino acids, we were interested in gaining more insight into amino acid metabolism.

Metabolite in media	CR/NR ratio
*Serine	12.16
N-Acetylglycine	6.17
*Asparagine	5.70
*Aspartic acid	5.61
Kynurenic acid	4.05
Methionine sulfoxide	4.05
*Tryptophan	3.95
Pyridoxamine	3.48
gamma-Aminobutyric acid	3.35
*Phenylalanine	2.90
3-Indolelactic acid/tryptophan	2.71
Annotation unknown	2.66
*Glutamic acid	2.29
Mesaconic acid	2.05
Annotation unknown	2.04
Annotation unknown	2.01

Table 4.3 Metabolite Profiles for CR and NR conditioned media. Data generated by Nazif Maqani. *BY4741 cells were grown, and media was isolated on day 5. Top metabolites in the media show an enrichment of amino acids in the CRCM compared to NRCM.*

Amino Acids were depleted from NR conditioned stationary phase media.

We next profiled all 20 standard amino acids from BY4741 CRCM and NRCM concentrates, as well as unconditioned (fresh) SC media that was concentrated 10-fold in the same manner (Figure 4.6A). All but 6 amino acids (alanine, cysteine, glutamine, glycine, proline, and valine) were significantly depleted to varying degrees in NRCM concentrate, relative to unconditioned SC concentrate. One of the most intriguing results was that CR strongly attenuated the depletion, indicating that amino acid levels were generally higher in CRCM than NRCM. L-serine is an excellent example of this relationship (Figure 4.6A). The CR/NR abundance ratios for lysine, asparagine, and L-serine were each 10-fold or higher in the CRCM (Figure 4.7A), but still less than the level in unconditioned starting SC concentrate (Figure 4.6A). Notably, the branched chain amino acids (BCAAs) —leucine and valine —were significantly more abundant in CRCM concentrate than SC (Figures 4.6A), with isoleucine trending in the same direction. Another amino acid where we see an increase relative to unconditioned starting material is L-glutamine in BY4741. We conducted similar studies for prototrophic strain FY4 and obtained similar results (Figure 4.6B, 4.7B)

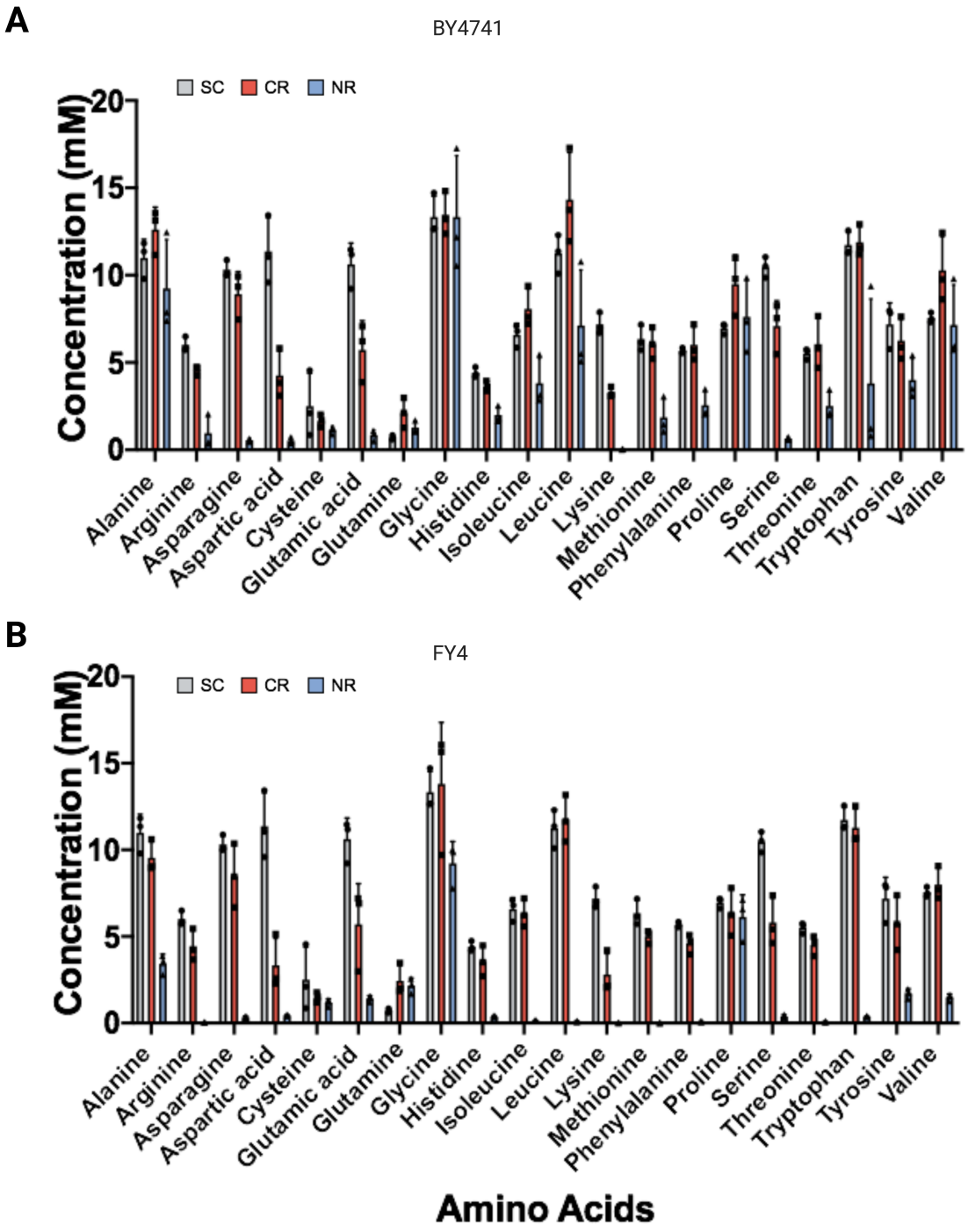

Figure 4.6 CR conditioned media is enriched for multiple amino acids *(A) Quantification of amino acids in concentrated NRCM and CRCM from stationary phase BY4741 cultures, or the concentrated unconditioned SC media. Amino acids were separated with a ZipChip and quantified by mass spectrometry. Error bars indicate standard deviation (n=3), and individual*

data points are displayed. (B) Quantification of amino acids in concentrated NRCM and CRCM from stationary phase FY4 cultures, or unconditioned SC media.

A

BY4741	
Amino acid	Ratio CR/NR
Lysine *	87.68
Asparagine *	16.07
Serine *	10.94
Aspartic acid *	8.09
Glutamic acid *	6.81
Arginine *	4.77
Methionine *	3.28
Tryptophan *	3.13
Threonine *	2.41
Phenylalanine *	2.35
Isoleucine *	2.11
Leucine *	2.01
Histidine	1.82
Glutamine	1.67
Tyrosine	1.56
Cysteine	1.46
Valine	1.44
Alanine	1.36
Proline	1.25
Glycine	1.01

B

FY4	
Amino acid	Ratio CR/NR
Methionine *	485.26
Leucine *	127.59
Lysine *	124.56
Arginine *	120.37
Threonine *	59.9
Phenylalanine *	55.38
Isoleucine *	44.03
Tryptophan *	30.04
Asparagine *	24.91
Serine *	15.18
Histidine *	9.32
Aspartic acid *	7.5
Valine *	5.39
Glutamic acid *	4.02
Tyrosine *	3.39
Alanine *	2.8
Glycine *	1.5
Cysteine	1.26
Glutamine	1.13
Proline	1.04

C

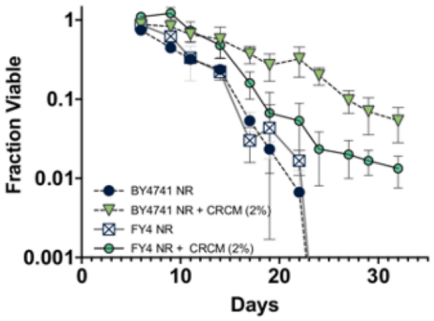

E

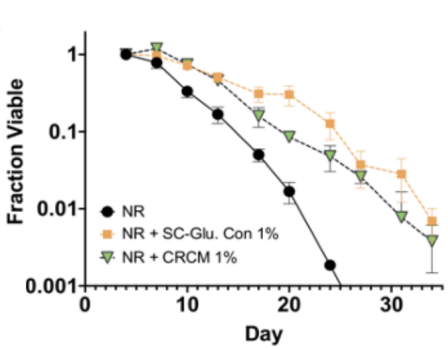

D

Condition	Mean Lifespan (days)	SEM	95% Confidence interval
NR BY4741	11.09	0.36	10.39 ~ 11.80
NR CRCM BY4741	17.19	0.51	16.19 ~ 18.19
NR FY4	11.71	0.27	11.18 ~ 12.23
NR CRCM FY4	15.03	0.29	14.45 ~ 15.60

F

Condition	Mean lifespan (days)	SEM	95% Confidence interval
NR	11.16	0.24	10.69 ~ 11.63
SC-Glu Con 1%	16.6	0.39	15.84 ~ 17.37
CR Con 1%	14.19	0.29	13.63 ~ 14.75

Figure 4.7 Amino acids are enriched in the CRCM in FY4 and BY4741 and CRCM supplementation extends lifespan. *(A) Amino acid abundance ratios between BY4741 CRCM and NRCM are sorted from highest to lowest from previous figure (B) Amino acid abundance ratios between FY4 CRCM and NRCM sorted from highest to lowest from previous figure.*

*Significant differences in panels A and B are indicated (*p≤0.05) using a student t-test. (C) Quantitative CLS of BY4741 and FY4, each supplemented with CRCM isolated from BY4741 at 2% (vol/vol). (D) Mean CLS statistics from panel E calculated using OASIS 2. (E) Quantitative CLS of BY4741 supplemented with CRCM or unconditioned SC concentrate at 1% (vol/vol). (F) Mean CLS statistics from panel G calculated using OASIS 2. All CLS assays were run in biological triplicates.*

The effect of increased BCAA's and alanine was somewhat lost in the prototrophic FY4 strain, suggesting the *leu2*Δ mutation in BY4741 could be a contributing factor (Figure 4.6B). Otherwise, the pattern of CR rescuing amino acid depletion from the media was recapitulated with FY4, though stronger NR depletion rendered CR/NR ratios more extreme (Figure 4.7A and 4.7B). Accordingly, the CRCM concentrate isolated from prototrophic BY4741 stationary phase cultures was also effective at extending FY4 CLS (Figure 4.7C and D). Based on these results we hypothesized that part of the CR-longevity effect consists of altering amino acid metabolism to prevent depletion from the CR media. Similarly, the observed NR-shortening effect could be due to amino acid depletion. Taken together, this difference of the higher amino acid levels in CRCM concentrate could therefore explain why it was more effective than NRCM concentrate at extending CLS of NR cultures. Consistent with amino acid limitation in NR, simply

supplementing the concentrated unconditioned SC 1% media without glucose into NR cultures also extended CLS (Figure 4.7E and F).

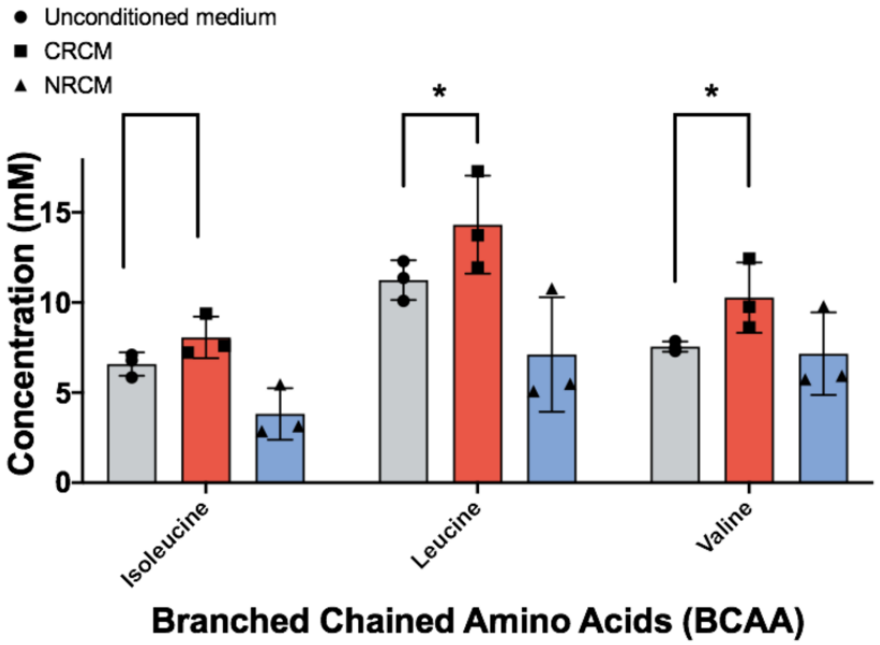

Figure 4.8 BCAAs in media seem higher in CRCM, suggesting lack of utilization, or synthesis and subsequent secretion. *Isoleucine, leucine, and valine measurements in unconditioned media CRCM, and NRCM isolated and concentrated 10-fold at day 5.*

Amino Acids Accumulate in CR media

The ZipChip data show that amino acids accumulate in CR conditioned stationary phase media, a finding that has not been reported elsewhere (Figure 4.6). We were intrigued by the potential for CR cells to use an alternative nitrogen source other than amino acids. In previous experiments, CR has been shown to slow down the aging process by reducing exposure to harmful metabolic byproducts like acetic acid (Burtner et al., 2009; Matecic et al., 2010; Smith Jr. et al., 2007; Wierman et al., 2017). Ammonia is another metabolite that can be toxic to yeast cells (Santos et al., 2012). CR could similarly promote ammonium assimilation as an additional strategy to protect against accumulation of harmful extracellular byproducts. This would also

potentially promote a shift in metabolism towards amino acid synthesis specifically glutamate or glutamine through the action of either glutamate dehydrogenase or glutamate synthetase respectively (Figure 4.9) (Magasanik, 2003).

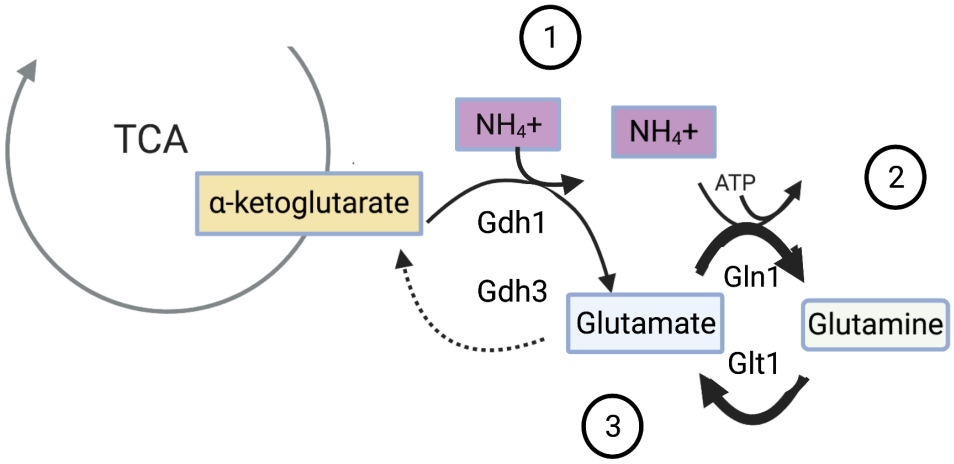

Figure 4.9 CR may promote strategic nitrogen utilization for the generation of glutamine and glutamate. *Diagram shows how ammonium (NH_4^+) could be assimilated to generate glutamate (1) and glutamine (2) via two routes. In the first pathway, glutamate is synthesized through glutamate dehydrogenase (Gdh1p) and utilized ammonia and alpha ketoglutarate. The second pathway utilizes glutamate reacting with ammonia to form glutamine via glutamine synthetase Gln1p. Glutamine can react with alpha-ketoglutarate to form glutamate via glutamate synthetase (Glt1p). This diagram shows how glutamate metabolism, nitrogen assimilation is linked to the tricarboxylic acid cycle (TCA cycle).*

This hypothesis suggests that glutamine accumulation in CR (Figure 4.6A & B) could be driven by the utilization of ammonia as a nitrogen source. Interestingly, in previous studies ammonia addition has resulted in higher expression of genes involved in amino acid biosynthesis (Jimenez-Marti & del Olmo, 2008). Specifically, BCAAs synthesis has been linked with ammonium assimilation as they together play a critical role in generating α-ketoglutarate (Kingsbury et al., 2015). In SC medium, and hence in the presence of ammonia, the CR cells in our system could perhaps promote amino acid synthesis, specifically BCAAs biosynthesis. To

begin testing this hypothesis of ammonia utilization we monitored ammonium in the media over time, but no significant changes in ammonia were detected in NR or CR (Figure 4.10A). Since 10 g of ammonium sulfate/500 mL for standard SC media were used it was difficult to distinguish small differences in ammonium amount between NR and CR medium (Figure 4.10A). We decided to switch our approach and use media with less ammonium sulfate.

First, we monitored ammonia production in a custom synthetic growth medium (HL) designed to support longevity that does not have ammonium sulfate as a nitrogen source (Hartman et al., 2015; Smith Jr. et al., 2016). Surprisingly, we saw higher levels of ammonia over time in the CR compared to NR condition (Figure 4.10B). This suggested that perhaps CR cells were relying on ammonia as a nitrogen source and in its absence, cells were catabolizing amino acids. If indeed ammonia was the main nitrogen source in CR, no ammonia in the medium would force cells to augment their consumption of amino acids in the media. For now, this remains unresolved.

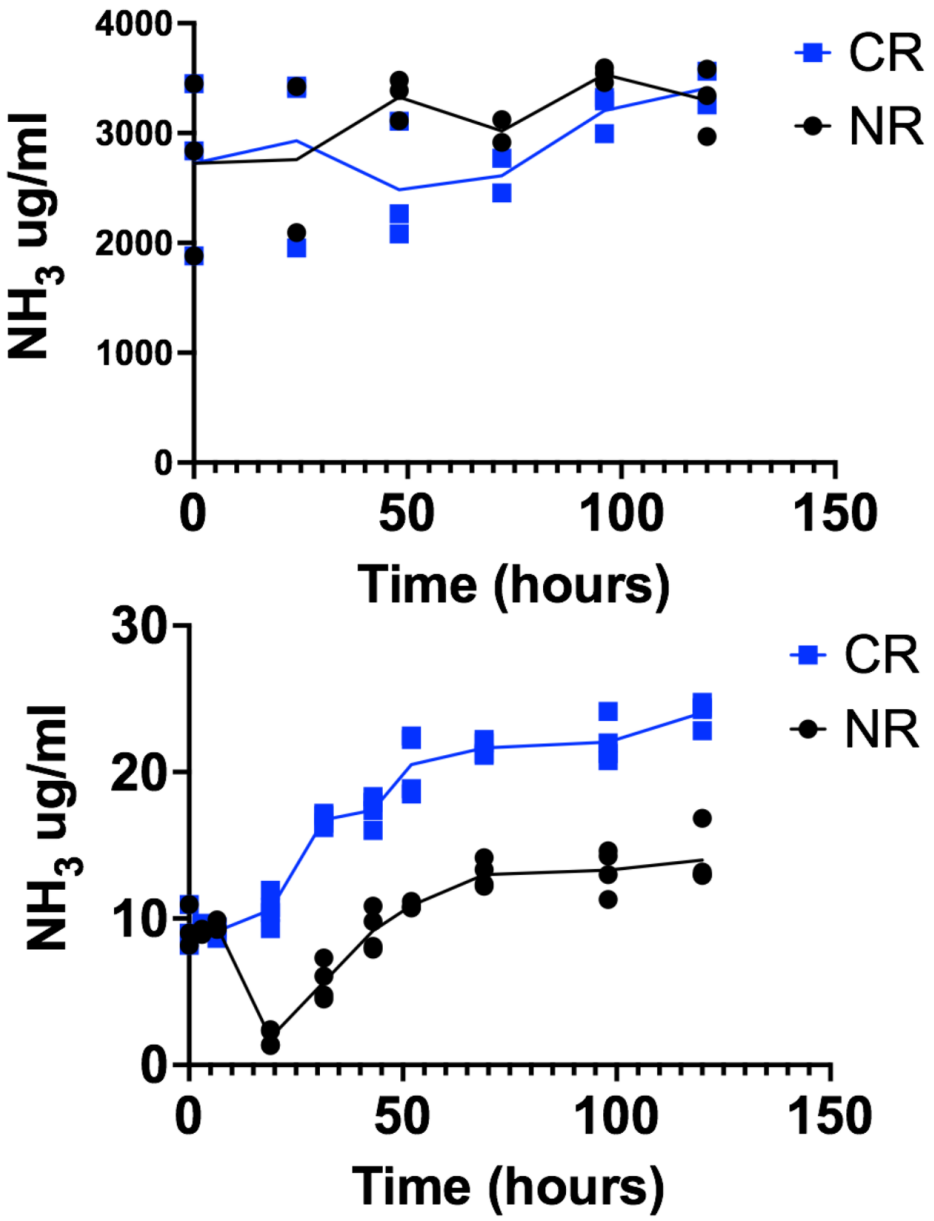

Figure 4.10 Detection of ammonia in HL media. A) *Levels of ammonia detected in the media of CR and NR treated cells using ammonia assay kit. BY4741 strain grown in SC media (n=3) B) Quantification of ammonia in the media. BY4741 strain grown in HL media (n=3).*

Supplementation of specific amino acids is sufficient to extend CLS

Since most amino acids were depleted from stationary phase NR cultures, we reasoned that one or more of them were critical for maintaining longevity. We initially focused on L-serine because the biosynthesis gene *SER1* was previously identified as a strong quantitative trait

locus (QTL) for CLS in the BY4741 background (Jung et al., 2018), and *CHA1* expression was strongly induced by CRCM supplementation during the diauxic shift (Figure 4.4G). The concentration of L-serine in our standard SC media is 1 mM (Burke et al., 2000; Matecic et al., 2010), so we tested the effect of supplementing an additional 1 mM or 5 mM L-serine into NR cultures at the time of inoculation. 5 mM L-serine significantly extended CLS, while 1 mM did not (Figure 4.11A and B). To confirm the L-serine effect was not specific to SC media, we also tested for CLS extension in HL medium (Hartman et al., 2015; Smith Jr. et al., 2016). BY4741 had significantly longer CLS in non-restricted HL medium compared to SC medium, and 5 mM L-serine further extended it (Figure 4.11 and B). Although we did not test SD medium, it has been reported that L-serine does not extend CLS in SD medium (Alvers et al., 2009). We next tested whether other amino acids could extend CLS at 5 mM (Figure 4.11C and D). Some amino acids did extend CLS, but not always as predicted based on abundance/depletion ratio in the conditioned media of both CR and NR. For example, L-asparagine had a similar depletion/enrichment profile as L-serine in NR (Figure 4.11A), but it did not extend CLS of NR when added back (Figure 4.11C and D). We also tested supplementation with 5 mM L-glycine, a component of one-carbon metabolism that can be derived from L-serine, but it was not depleted from the NR media (Figure 4.11A). L-glycine had no effect on CLS at this concentration (Figure 4.11C and D). L-cysteine supplementation at 5 mM dramatically slowed cell growth such that CFUs were increasing until day 10, after which the decline in CLS was parallel to the NR control, suggesting a delay rather than a true extension of survival (Figure 4.11C and D). Like cysteine, histidine at 5 mM was also inhibitory towards growth. This agrees with similar studies, which suggests that excess cysteine could interfere with ubiquitylation of proteins (Ruiz et al.,

2020). It is likely that each amino acid will have unique concentration dependence in regulating CLS.

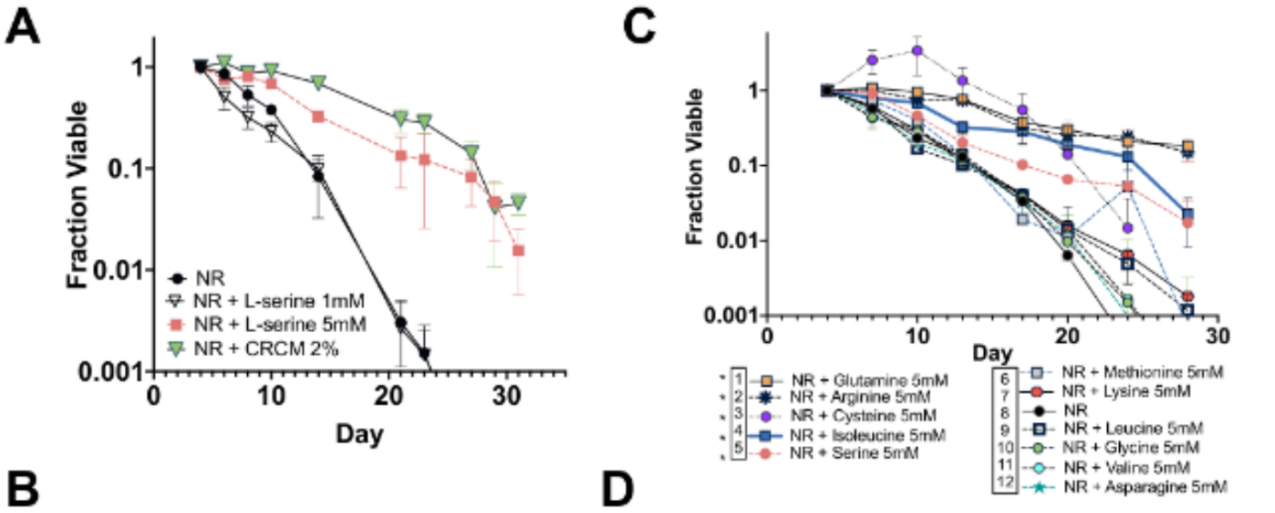

B

Condition	Mean lifespan (days)	SEM	95% Confidence Interval
NR + 2% CRCM	18.42	0.38	17.67 ~ 19.17
NR	10.84	0.26	10.33 ~ 11.35
NR + Serine 1mM	9.25	0.27	8.72 ~ 9.77
NR + Serine 5mM	14.66	0.4	13.87 ~ 15.45

D

Amino acid	# of CFUs Day 3	Mean lifespan Days	SEM	95% Confidence Interval
Glutamine	289	16.51	0.26	16.00 ~ 17.02
Arginine	281	16.40	0.31	15.79 ~ 17.01
Cysteine*	24	14.88	0.52	13.85 ~ 15.90
Isoleucine	262	14.53	0.40	13.74 ~ 15.32
Serine	272	12.42	0.26	11.91 ~ 12.92
Methionine	266	10.88	0.21	10.47 ~ 11.30
Lysine	298	10.24	0.21	9.83 ~ 10.66
NR	203	10.11	0.26	9.60 ~ 10.61
Leucine	213	9.80	0.22	9.37 ~ 10.23
Glycine	244	9.82	0.25	9.33 ~ 10.32
Valine	240	9.77	0.25	9.28 ~ 10.26
Asparagine	230	9.67	0.24	9.20 ~ 10.13

Figure 4.11 L-serine supplementation extends lifespan of NR cultures. *(A) CLS of non-restricted BY4741 supplemented with 2% CRCM, 1 mM L-serine, or 5 mM L-serine. (B) Mean CLS statistics from panel A calculated using OASIS 2. (C) CLS of non-restricted BY4741 supplemented with 5 mM of each indicated amino acid. *Amino acids 1-5 significantly extended lifespan compared to the NR control (sample 8) (D) Mean CLS statistics from panel C calculated using OASIS 2.*

L-serine extends CLS through catabolic pathways and non-catabolic pathways

An earlier study of cellular response to L-serine supplementation found that its uptake was linear with increasing extracellular concentrations up to at least 100 mM (Lee et al., 2013), suggesting to us that L-serine concentrations higher than 5 mM may induce stronger CLS extension. To test this idea, we supplemented NR cultures of BY4741 with 5-, 10-, 20-, or 30-mM L-serine and observed progressively improved longevity with increasing concentration (Figure 4.12 A and B). Survival with 30 mM L-serine was even slightly better than the CR control, showing minimal loss of viability during the experiment. A similar positive correlation between L-serine concentration and CLS was observed with FY4 (Figure 4.12 E and F) and with HL media (Figure 4.12 C and D).

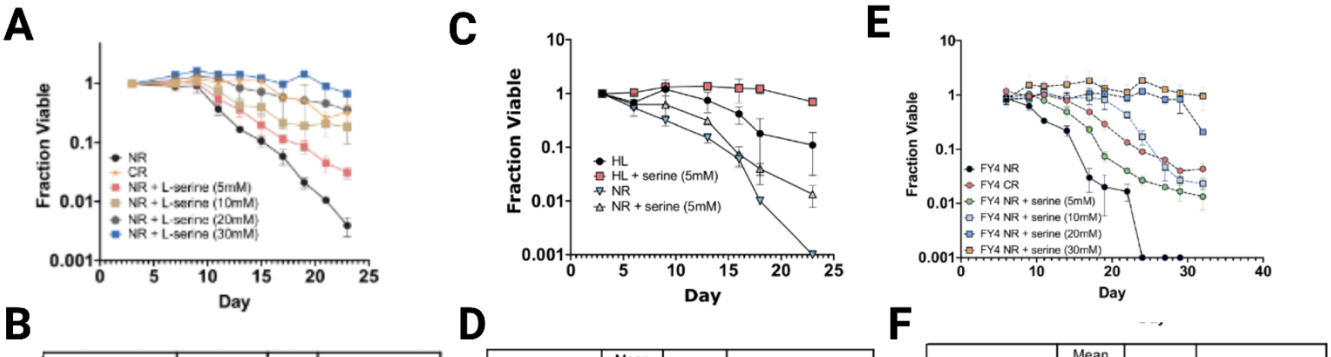

B

Condition	Mean Lifespan (days)	SEM	95% Confidence Interval
CR	19.02	0.47	18.11 ~ 19.93
NR	11.91	0.21	11.49 ~ 12.33
NR + L-serine (5mM)	13.48	0.29	12.90 ~ 14.05
NR + L-serine (10mM)	15.77	0.45	14.88 ~ 16.65
NR + L-serine (20mM)	18.53	0.46	17.63 ~ 19.43
NR + L-serine (30mM)	20.82	0.34	20.15 ~ 21.49

D

Condition	Mean Lifespan (days)	SEM	95% Confidence Interval
HL	13	0.40	12.44 ~ 14.01
HL + serine 5mM	21.38	0.32	20.75 ~ 22.00
NR	8.88	0.25	8.38 ~ 9.38
NR + serine 5mM	11.49	0.33	10.84 ~ 12.14

F

Condition	Mean Lifespan (days)	SEM	95% Confidence Interval
CR FY4	16.94	0.49	15.99 ~ 17.89
NR FY4	16.88	0.41	16.07 ~ 17.68
NR + serine FY4	12.2	0.32	11.57 ~ 12.82
NR + serine 10mM FY4	19.43	0.4	18.65 ~ 20.21
NR + serine 20mM FY4	26.48	0.49	25.52 ~ 27.44
NR + serine 30mM FY4	27.25	0.41	26.45 ~ 28.04

Figure 4.12 L-serine supplementation extends lifespan in HL media and FY4 strain *(A) CLS of non-restricted BY4741 supplemented with 5mM, 10mM, 20mM and 30mM serine. (B) Mean CLS statistics from panel A calculated using OASIS 2. (C) CLS of non-restricted BY4741 supplemented with 5 mM of L-serine. Cultures were grown in HL media or SC media. (D) Mean CLS statistics from panel C calculated using OASIS 2. (E) CLS of non-restricted FY4 supplemented with 5 mM, 10mM, 20mM, and 30mM of L-serine. (F) Mean CLS statistics from panel C calculated using OASIS 2.*

CR buffers the acidification of conditioned media by promoting consumption of acetate and acetic acid *via* Snf1/AMPK-dependent activation of gluconeogenesis and glyoxylate cycle gene transcription (Maqani et al., 2018; Wierman et al., 2017). An independent report concluded that exogenous amino acids, including L-serine, support CLS by preventing hyper-acidification of the media (Maruyama et al., 2016). We therefore tested whether 10 mM L-serine had the same pH buffering effect when supplemented into NR cultures. Compared to the CR positive control, 10 mM L-serine partially prevented acidification during CLS assays (Figure 4.13 A), consistent with the earlier report (Maruyama et al., 2016). We next tested whether supplementing L-serine into NR media also promoted acetic acid consumption. As shown in Figure 4.13 B, adding 5-, 10-, or 20-mM L-serine did not significantly reduce acetic acid levels in the NR media, indicating that pH buffering due to L-serine is unrelated to acetic acid. The result also implied that serine extends CLS through a mechanism different from CR. Indeed, L-serine further extended CLS when added to CR cultures (Figure 4.13 C and D). We also tested whether L-serine supplementation decreases culture density using growth assays (Figure 4.13 E). These efforts support the idea of independent mechanisms.

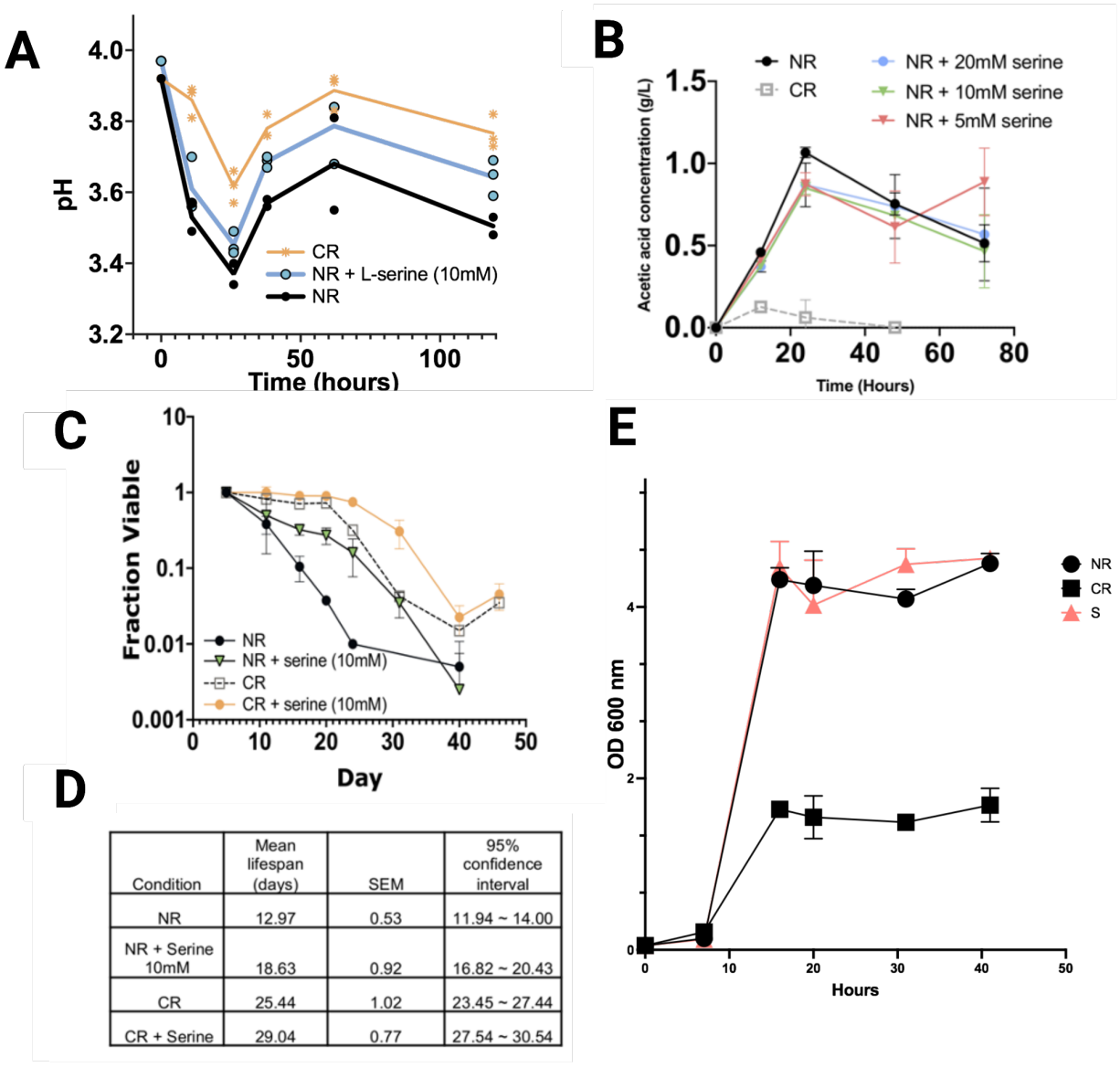

Condition	Mean lifespan (days)	SEM	95% confidence interval
NR	12.97	0.53	11.94 ~ 14.00
NR + Serine 10mM	18.63	0.92	16.82 ~ 20.43
CR	25.44	1.02	23.45 ~ 27.44
CR + Serine	29.04	0.77	27.54 ~ 30.54

Figure 4.13 CR and L-serine supplementation mediate longevity by independent mechanisms. *A) L-serine buffers liquid culture slightly compared to NR, like CR. B) Acetic acid content in the media of CR, NR, NR + L-serine (5, 10, 20 mM) cultures was measured over the first 72 hours of the aging assays (mean ± SD, n=3). (C) CLS of BY4741 growing in the NR or CR media condition supplemented with 10 mM L-serine (n=3). (D) Mean CLS statistics from panel B calculated using OASIS 2. E) Growth curves of liquid cultures of CR, NR, NR+10mM L-serine. Culture density was measured using a spectrophotometer over time (n=3).*

What is the mechanism by which serine extends lifespan?

The most obvious candidate to test was *CHA1* since it was the most upregulated gene in the CRCM media (Figure 4.14 A). *CHA1* is a catabolic deaminase that turns serine into pyruvate in the mitochondria (Figure 4.14 B). We reasoned that this production of pyruvate would be beneficial in driving longevity. However, when we tested *CHA1* mutant, serine still elicited a longevity response (Figure 4.14 C, E and D). This suggested that *CHA1* was not the major player driving longevity.

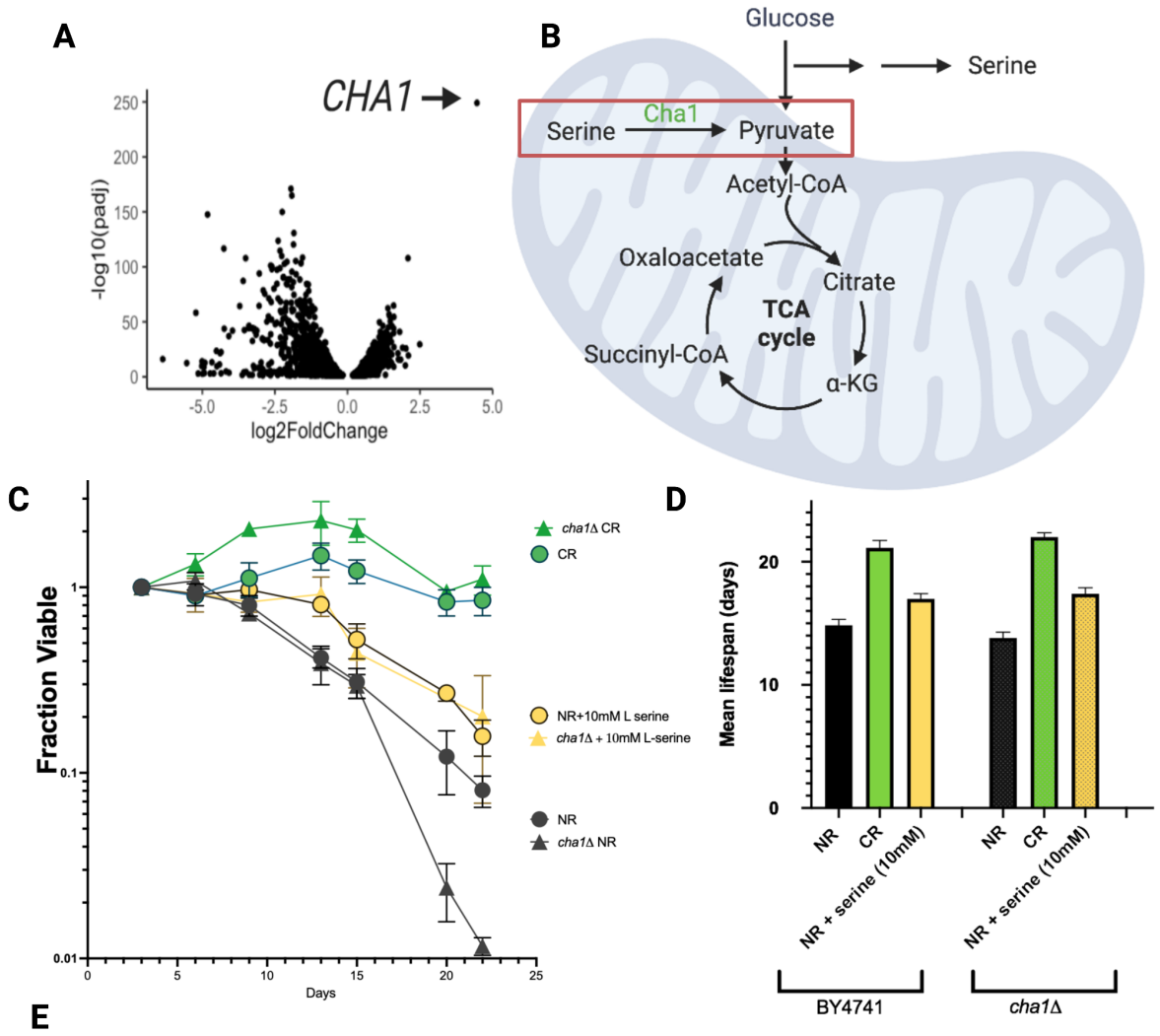

E

strain	Condition	Mean Lifespan (days)	SEM	95% CI
BY4141	NR	14.84	0.48	13.90~15.78
	CR	21.14	0.59	19.99~22.29
	NR + L serine	16.98	0.43	16.13~17.83
cha1Δ	NR	13.81	0.48	12.86~14.77
	CR	22	0.35	21.31~22.89
	NR + L serine	17.4	0.49	16.44~18.35

Figure 4.14 CHA1 is not the main driver of L-serine-mediated longevity.

A) Volcano plot showing CHA1 is the most upregulated gene in NR+CRCM/NR at 24 hours B) schematic of the role of Cha1p in the mitochondria C) CLS of CHA1 mutants respond to supplementation of 10mM L-serine comparable to control (n=3) D) Mean CLS statistics from panel A calculated using OASIS 2. E) Mean CLS statistics from B displayed visually.

L-serine extends lifespan *via* the one-carbon metabolism pathway

Since L-serine is the predominant donor of carbon units to folate in one-carbon metabolism (OCM) (Zeng et al., 2019), we hypothesized its depletion would constrain this route of utilization in supporting CLS, which could explain extension by exogenous L-serine. If true, then mutations that impair OCM should attenuate the effect. The OCM pathway for *S. cerevisiae* is depicted in Figure 4.15 A, including serine hydroxy methyltransferases (SHMTs), Shm1 and Shm2, that interconvert L-serine and L-glycine in the mitochondria or cytoplasm, respectively. Shm2 is the major isozyme for converting L-serine to L-glycine and one-carbon units on tetrahydrofolate, whereas Shm1 is the predominant isozyme for the reverse reaction, though their relative activities are strongly influenced by nutrient availability and growth conditions (Kastanos et al., 1997). We therefore supplemented NR cultures of *shm1*Δ or *shm2*Δ mutants from the YKO collection with 5 mM L-serine to observe any effects on CLS. Without L-serine supplementation, the *shm1*Δ mutant showed moderate extension of mean CLS when compared to WT NR cultures (Figure 4.15 B and Table 4.4), while the *shm2*Δ mutant only showed modest improvements in survival at the later time points (Figure 4.15 C and Table 4.4). Importantly, both deletions prevented further CLS extension induced by 5 mM L-serine, but did not attenuate the strong positive lifespan effect of CR. A similar result was obtained for a strain lacking *MTD1* (Figure 4.15 D and Table 4.4), which encodes a cytoplasmic NAD^+-dependent 5,10-methylenetetrahydrofolate dehydrogenase.

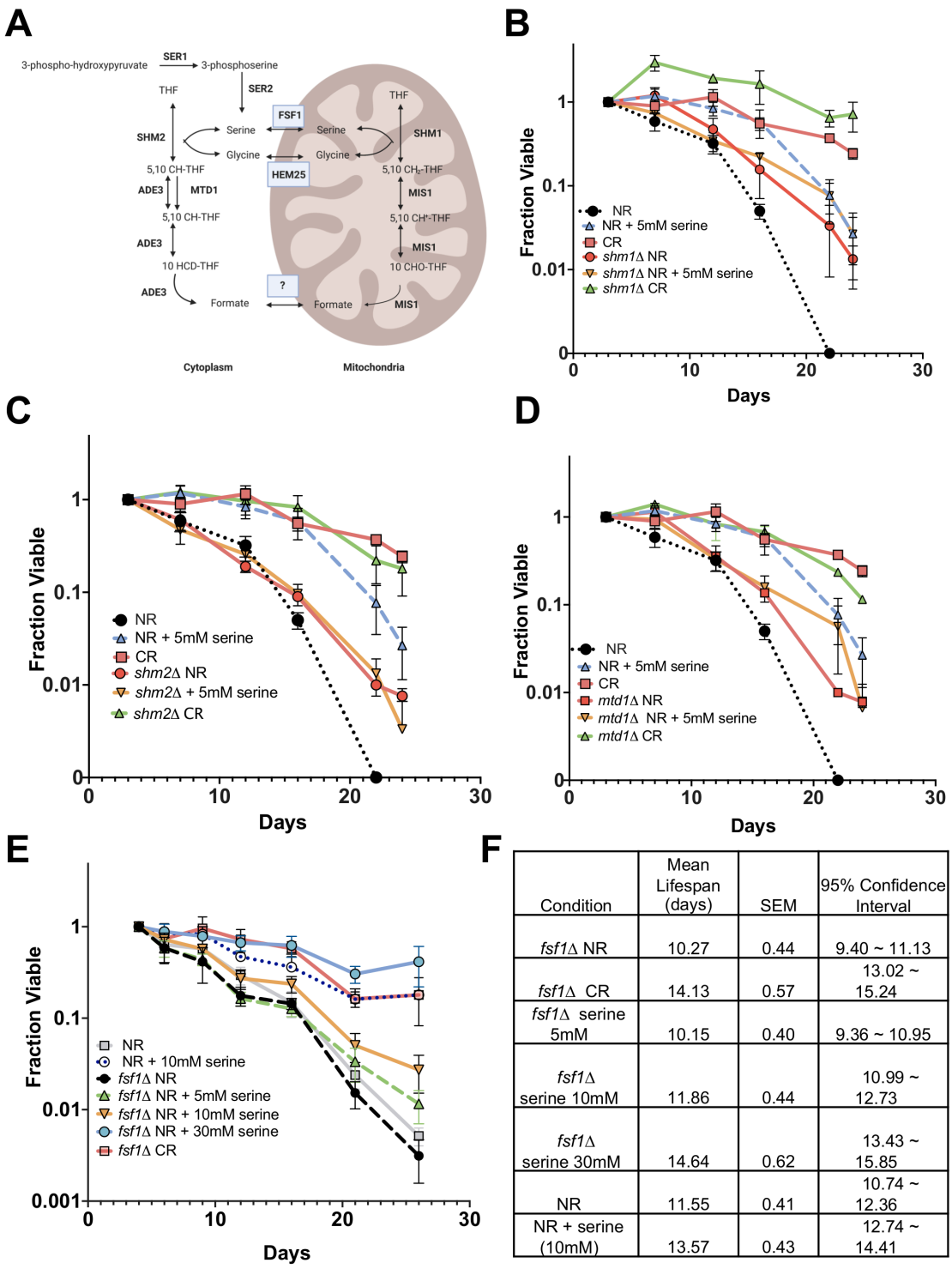

Condition	Mean Lifespan (days)	SEM	95% Confidence Interval
*fsf1*Δ NR	10.27	0.44	9.40 ~ 11.13
*fsf1*Δ CR	14.13	0.57	13.02 ~ 15.24
*fsf1*Δ serine 5mM	10.15	0.40	9.36 ~ 10.95
*fsf1*Δ serine 10mM	11.86	0.44	10.99 ~ 12.73
*fsf1*Δ serine 30mM	14.64	0.62	13.43 ~ 15.85
NR	11.55	0.41	10.74 ~ 12.36
NR + serine (10mM)	13.57	0.43	12.74 ~ 14.41

Figure 4.15 L-serine extends CLS through the one-carbon metabolism pathway*. (A) Schematic diagram of one-carbon metabolism (OCM) in Saccharomyces cerevisiae. Enzymes that catalyze specific reactions are in bold. Transporters are boxed. (B) CLS of BY4741 and shm1Δ mutant under NR and CR conditions or supplemented with 5 mM L-serine. (C) CLS of BY4741 and*

shm2Δ mutant under NR and CR conditions or supplemented with 5 mM L-serine. (D) CLS of BY4741 and mtd1Δ mutant under NR and CR conditions or supplemented with 5 mM L-serine. (E) CLS of BY4741 and fsf1Δ mutant under NR and CR conditions or supplemented with 5 mM L-serine. (F) Mean CLS statistics from panel E calculated using OASIS 2. All CLS assays were run in triplicate.

Condition	Mean Lifespan (days)	SEM	95% Confidence Interval
NR	11.24	0.53	10.20 ~ 12.27
CR	17.14	0.51	16.15 ~ 18.14
NR + 5mM serine	17.71	0.56	16.61 ~ 18.81
*shm1*Δ NR	14.93	0.34	14.26 ~ 15.60
*shm1*Δ CR	16.72	0.44	15.85 ~ 17.58
*shm1*Δ NR + 5mM serine	13.08	0.58	11.94 ~ 14.22
*shm2*Δ NR	11.26	0.55	10.18 ~ 12.34
*shm2*Δ CR	18.64	0.59	17.50 ~ 19.79
*shm2*Δ NR + 5mM serine	10.69	0.45	9.82 ~ 11.57
*mtd1*Δ NR	13.43	0.40	12.65 ~ 14.21
*mtd1*Δ CR	17.05	0.52	16.04 ~ 18.07
*mtd1*Δ NR+ 5mM serine	13.92	0.42	13.09 ~ 14.75

Table 4.4 Statistical analysis of CLS assays for one-carbon metabolism deletion mutants. *Statistics for CLS assays presented in Figure 4.15, panels B, C, and D. The mean CLS, SEMs, and 95% confidence intervals were calculated using OASIS 2.*

The mechanism of L-serine transport across the mitochondrial membrane for one-carbon metabolism was unknown until recently, when the Sideroflexin-1 protein (SFXN-1) was unexpectedly identified as the relevant transporter in human cells (Kory et al., 2018). Moreover, ectopic expression of the related yeast mitochondrial protein *Fsf1* rescued the L-serine transport

and *de novo* purine synthesis defects of a *SFXN-1* mutant cell line, suggesting that Fsf1p has the same function in yeast cells. We therefore hypothesized that the CLS of *fsf1*Δ yeast cells would be unresponsive to L-serine supplementation, similar to the *shm1*Δ, *shm2*Δ, and *mtd1*Δ mutants. There was no indication of CLS extension for the *fsf1*Δ mutant under the NR condition (Figure 4.11E and F). However, the effects of 5 mM and 10 mM L-serine on CLS were blocked or attenuated, respectively (Figure 4.11E and F). CLS was still strongly extended by 30 mM L-serine, perhaps through alternative catabolic pathways such as deamination by Cha1p, which is upregulated by high exogenous L-serine and the CRCM, or through the unknown D-serine induced mechanism. We conclude that L-serine catabolism through the cytoplasmic and mitochondrial arms of the one-carbon metabolism pathway promotes chronological longevity/stationary phase survival under non-restricted conditions.

Discussion

Herein, we found that conditioned media collected from stationary phase CR cultures extends CLS when supplemented into NR cultures at the time of inoculation, suggesting a potential cell non-autonomous mechanism of CR-induced lifespan regulation. At the onset of this study, we hypothesized that CR may induce the production of one or more longevity factors, perhaps small molecules, peptides, or even proteins, that are released into the growth medium either through secretion from live cells, or breakdown products from dying cells.

Chromatography of CRCM and NRCM clearly indicated the longevity factors were water soluble small molecules, but we were surprised to find the major differences between the two types of conditioned media were amino acids. Several unannotated compounds were more enriched in the CRCM, so at this time we cannot rule out the existence of other compounds with weaker effects on longevity. Although the focus of this study was on identifying factors

extending longevity in the CRCM, NRCM contained factors that decreased longevity. We speculate that acetic acid and low media pH could certainly be a negative longevity factor in the NRCM.

Amino acids as extracellular regulators of lifespan

CR in the context of this study consists of glucose restriction. However, dietary composition, not just overall caloric reduction, plays a critical role in modulating lifespan in multicellular organisms. In *Drosophila*, for example, lower dietary concentrations of yeast (amino acid source) or sugar generally improve lifespan, but moderate concentrations in combination are more optimal (Skorupa et al., 2008). Most cells in *Drosophila* or other multicellular organisms are not directly exposed to the environment, so they rely on specialized nutrient 'sensing' cells that relay messages about nutrient availability, typically in the form of hormones (Fromentin et al., 2012). Unicellular organisms, on the other hand, must directly respond to nutrient fluctuations in the environment, making them dependent on both rapid detection and subsequent response to changes in nutrients. Yeast cells have multiple amino acid permeases that are under tight transcriptional and translational control, in order to properly regulate uptake (Ljungdahl & Daignan-Fornier, 2012). For example, when amino acids are scarce, translation of the *GCN4* mRNA is derepressed. Since Gcn4p is a transcriptional activator for these genes (Hope & Struhl, 1985), this leads to transcriptional induction of most genes encoding amino acid biosynthetic enzymes, a regulatory process known as general amino acid control (GAAC) (Hinnebusch, 2005). The GAAC pathway also integrates with the TOR signaling pathway, which senses nitrogen availability (Staschke et al., 2010), and links amino acid availability to lifespan regulation (Powers et al., 2006). Activation of GAAC generally reduces CLS, while suppression of GAAC extends CLS (Alvers et al., 2009). This fits well with

our finding that supplementing non-restricted cultures with CRCM, which contains abundant amino acids, extends CLS. This is in stark contrast to supplementing with NRCM, which is depleted for amino acids, and consequently does not extend CLS.

Links between CR and Amino acid Restriction

Amino acid uptake has been genetically implicated in regulation of chronological aging. Chronological lifespan QTL analysis of outbred strains from a cross between S288C and a vineyard yeast strain revealed a polymorphism in the *BUL2* gene (Kwan et al., 2011). *BUL2* encodes a subunit of an E3 ubiquitin ligase that controls trafficking of high affinity amino acid permeases to the vacuole for degradation (Helliwell et al., 2001). Reduction in Bul2p function therefore stabilizes the permeases and increases intracellular amino acids, thus increasing TOR activity and shortening CLS. Thus, minimal amino acid consumption through multiple ways could mediate longevity. A recent study showed that myriocin, which targets the first step in sphingolipid synthesis, extends lifespan by lowering the rate of amino acid uptake (Hepowit et al., 2021). CR and amino acid restriction could have overlapping mechanisms.

Availability of non-essential amino acids in the growth medium was also shown to be important for chronological longevity (Maruyama et al., 2016). Specific amino acids were not critical, but rather the total amount of amino acids functioned to prevent hyper-acidification of the growth medium (Maruyama et al., 2016). This scenario could also be at play with the numerous amino acids enriched in CRCM. Perhaps part of CR's benefits due to this reservoir of amino acids sequestered in the media. In the case of L-serine we found that it was indeed capable of modestly buffering pH, but the CLS extension was independent of accumulated acetic acid levels in the media. Other amino acids have a significant impact on lifespan as well.

Branched chain amino acids

Branched chain amino acid (BCAA) supplementation has been shown to extend CLS of *S. cerevisiae* by downregulating the GAAC (Alvers et al., 2009) as described above, and *C. elegans* (Mansfeld et al., 2015). This availability of BCAAs is associated with increased synthesis and release of glycerol, which is inhibited by sustained growth signaling (Ruckenstuhl et al., 2010). This extension of lifespan effect is consistent with the abundance of BCAAs we observed under the CR condition. This abundance of BCAAs may act as a signal (perhaps of autophagy) rather than nutritional support for NR cells receiving the CRCM (Alvers et al., 2009). The authors also argue that levels of BCAAs are paramount for protein synthesis because leucine codons are the most numerous annotated open reading frames (ORFs) in the yeast genome (Alvers et al., 2009) (Figure 4.16). Noteworthy, L-serine codons rank second in relative abundance (Figure 4.16). However, the authors in this study did not assess the uptake of these amino acids, as was done in our study.

On the other hand, BCAA restriction improves late-life healthspan and lifespan in *Drosophila* and mice (Fontana et al., 2016; Juricic et al., 2020). In a way, CR cells in our experiment could be restricting BCAA uptake. Given such large differences in effects between species, this could reflect changes in amino acid balance, rather than direct effects due to BCAA levels (Fontana et al., 2016; Juricic et al., 2020). In type 2 diabetes (T2DM), where cells are starved for glucose, abundant BCAAs serve as a biomarker for developing insulin resistance and reduced metabolism in humans (Lynch & Adams, 2014) (Broer & Gauthier-Coles, 2022). High BCAAs could represent low metabolic activity within the cell under glucose starvation. Herein, our yeast system, CR cells are also ‘starving’ for glucose in a similar way to mammalian cells that are insulin resistant and the effects on BCAAs metabolism could be conserved.

Considering Auxotrophies

Common laboratory yeast strains such as W303, YPH499, and BY4741/BY4742 have several amino acid auxotrophies due to mutations in genes like *HIS3*, *LYS2*, *LEU2*, *TRP1*, or *MET15*. It has been shown that BY4741 genotype has consequences for longevity and amino acid uptake.

Leucine

Strains with *LEU2* mutations have been shown to be defective in transporting amino acid leucine into the cell, despite the cell's inability to synthesize it (Cohen & Engelberg, 2007). However, our results show that while leucine remains underutilized by BY4741 under CR conditions, leucine is depleted from the media in NR conditions. This does not suggest impaired import of leucine by this strain. Moreover, in FY4, these results were recapitulated, suggesting that leucine uptake might be more dependent on glucose level than the *leu2Δ* mutation in BY4741. Intriguingly, leucine availability appears to be an important factor in full extension of CLS during CR in BY4742 which is autotrophic for lysine and still has the *leu2Δ* mutation (Aris et al., 2013). The authors in this study found that autophagy levels are elevated in *LEU2* strains and may contribute to increased respiration proficiency compared to *leu2*Δ strains (Aris et al., 2013). Furthermore, it has been shown that *LEU2* mutation could also contribute to longevity of BY4741 (Alvers et al., 2009), much like *MET15* mutation. In our experiments using 5mM concentrations we did not observe that leucine supplementation increased longevity, so the effect remains unresolved. An important difference is that they focused on SD media, which is minimal only supplemented with the AAs needed for survival of the auxotrophic strain. In contrast, we used SC media, which has all the BCAAs.

Methionine

Methionine restriction also extends lifespan in all model organisms tested thus far (McIsaac et al., 2016). It should be noted that BY4741 is auxotrophic for methionine due to the *met15*Δ mutation, indicating that this strain is already relatively long-lived compared to a strain that is *MET15*$^{+}$ (Johnson & Johnson, 2014). Even with the *met15*Δ mutation, L-methionine or L-cysteine supplementation had little effect on CLS (Figure 4.11C). Furthermore, since CRCM and L-serine both extended CLS of FY4 (prototrophic strain), the *met15*Δ mutation does not appear to be a major determinant for this cell extrinsic mechanism of lifespan regulation.

L-serine

Less attention has been placed on L-serine within the aging research community. In addition to our work here and others showing that L-serine supplementation extends yeast CLS (Maruyama et al., 2016), L-serine was among the best amino acids at extending *C. elegans* lifespan when supplemented to the worms in a dose dependent manner (Edwards et al., 2015). L-serine supplementation to mice was also recently shown to reduce food intake, improve oxidative stress, and SIRT1 signaling in the hypothalamus of aging mice, though lifespan was not tested (Zhou et al., 2018). L-serine has the potential to induce a conserved effect in mammals. Lastly, L-serine is also being studied as a possible neuroprotectant in the treatment of ALS and other neurodegenerative disorders (Dunlop & Carney, 2020; Dunlop et al., 2018; Wang et al., 2019). Despite these beneficial effects, supplementing with L-serine was reported to be pro-aging in yeast when the only other amino acids added to the media were those covering the auxotrophies (Mirisola et al., 2014). As with BCAAs, these discrepancies could be due to the combination of auxotrophies and media content, which has been shown to be a major variable driving different CLS results from different labs (Mirisola et al., 2014; Santos et al., 2020; Smith et al., 2016).

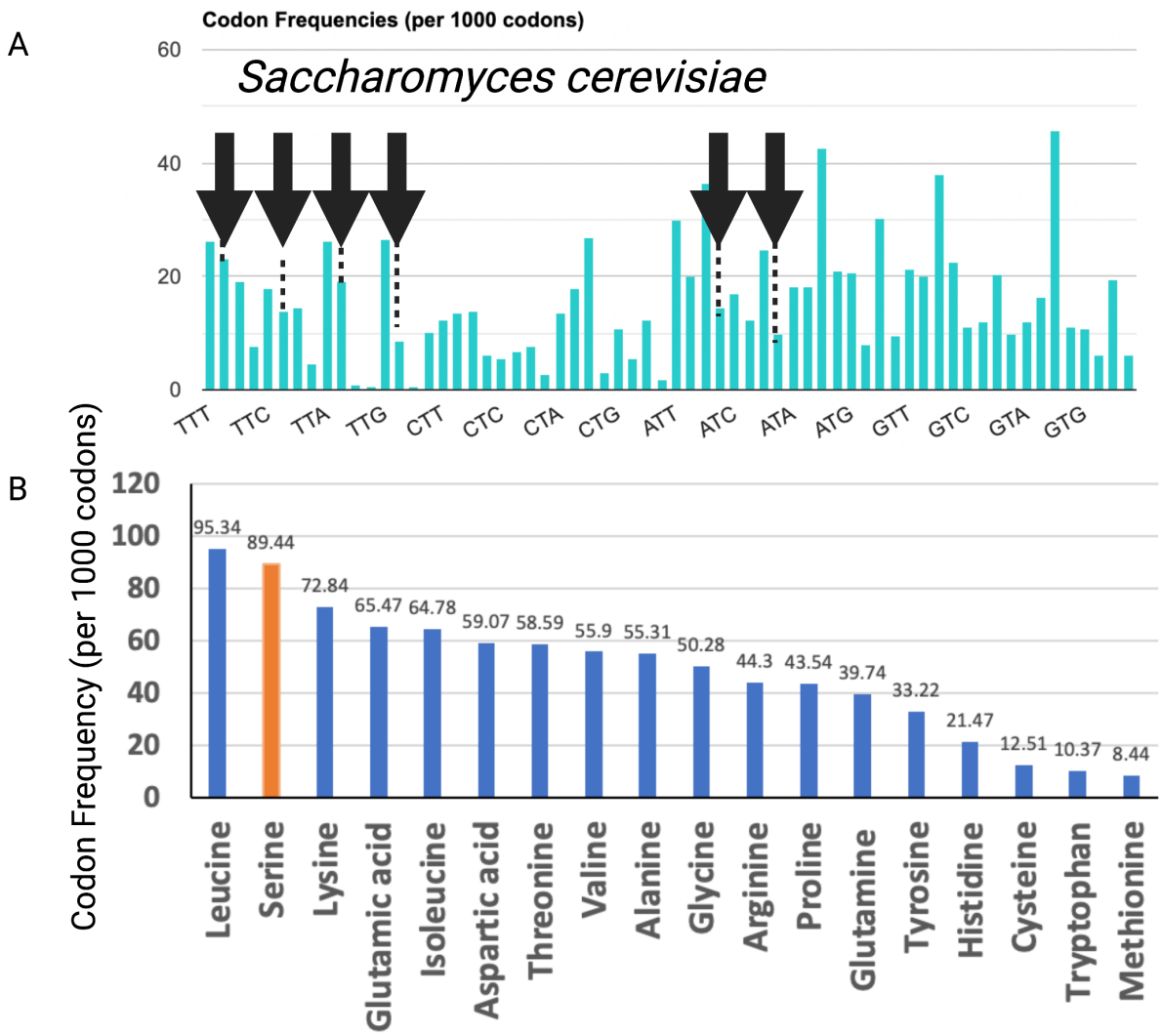

Figure 4.16. ***L-serine is an important amino acid for protein synthesis****. (A) Bar graph of codon relative frequency in yeast (S288C) (per 1000 codons). Arrows indicate codons specifying amino acid L-serine B) The data for the bar graph were derived from a codon usage table generated by CoCoPUTs, taken from Refseq, updated September, 2021(Alexaki et al., 2019). It shows the codon frequency per 1000 codons at the top of each amino acid. Similar results were obtained from Alvers et al. 2009.*

Why do amino acids accumulate in the conditioned media of CR cultures?

In the presence of sufficient glucose, *S. cerevisiae* cells actively suppress respiratory metabolism and biomass production through the TCA cycle, a phenomenon known as the

Crabtree effect in yeast, and the Warburg effect in cancer cells (Diaz-Ruiz et al., 2011). When glucose becomes limiting, however, *S. cerevisiae* cells utilize oxidative metabolism over fermentative metabolism, resulting in elevated respiration and electron transport. Under such conditions, amino acids may be used to replenish TCA cycle intermediates through trans- and deamination reactions, a process called anaplerosis. Normally, in cells originally grown in 2% glucose (NR), glucose depletion triggers increased amino acid uptake that involves upregulation of permeases *via* TOR (Peter et al., 2006). Initial growth under CR (0.5% glucose) appears to generally reduce amino acid uptake as indicated by accumulation of amino acids we observe in the conditioned medium (Figure 4.6A-D), and instead prioritizes consumption of alternative carbon sources such as acetate (Figure 4.10A) (Matecic et al., 2010; Wierman et al., 2015), which yeast cells can convert into acetyl-CoA for TCA intermediate replenishment, or gluconeogenesis *via* the glyoxylate cycle (Chew et al., 2019). This likely better accommodates the increased storage of glycogen and trehalose induced by CR and associated with long-term cell survival in the stationary phase (Kyryakov et al., 2012). The higher cell densities (biomass) achieved by NR cultures instead places tremendous demand for synthesis of macromolecules associated with cell growth, such as nucleotides, lipids, and proteins, thus depleting amino acids from the media.

Ammonium utilization

One hypothesis explored was that CR could also potentially utilize ammonium sulfate, a preferred nitrogen source over the amino acids that are usually preferred under NR conditions. Ammonium is a preferred nitrogen source as it supports rapid growth similar to asparagine, glutamine, and serine (Godard et al., 2007). Ammonia is also a normal product of amino acid catabolism in cells (Jin et al., 2018). However, like acetic acid and ethanol, ammonium can be

toxic at high levels and can impair CLS (Burtner et al., 2009; Casatta et al., 2013; Santos et al., 2014). Due to this toxicity, it is left out of the custom HL medium designed to optimize CLS (Hartman et al., 2015; Smith Jr. et al., 2016). Indeed, others have shown that reducing ammonium in the media extends longevity in NR cultures (Hartman et al., 2015) . Therefore, assimilation of the ammonium under CR could potentially extend CLS by reducing ammonium toxicity, like the CR-induced consumption of acetic acid (Matecic et al., 2010; Wierman et al., 2015). Whether ammonium is utilized for biosynthesis of glutamine or other amino acids in the CR-treated cells remains unresolved. Not only were we interested in accumulation of amino acids in the CR condition, but we were also interested in why certain amino acids were depleted in the NR.

What amino acids are preferred by cells?

Lysine

Support for increased amino acid harvesting comes from studies of amino acid preference during fermentation by wine yeasts (Crepin et al., 2012). Of the 17 amino acids tracked, lysine was utilized the fastest, followed by a group of 10 (Asp, Thr, Glu, Leu, His, Met, Ile, Ser, Gln, Phe) that were consumed quicker than ammonium sulfate, and 6 (Val, Arg, Ala, Trp, Tyr, Gly) that were slower. In agreement with increased lysine harvesting (Viridiana Olin-Sandoval et al., 2019), lysine was the most depleted amino acid in BY4741 NR conditioned media, and was partially rescued by CR (Figure 4.6A and B). Interestingly, this extreme lysine harvesting from the media could A) promote synthesis of polyamine molecules *via* Spe1 decarboxylation and B) functions to channel NADPH (normally used for lysine biosynthesis) into glutathione production(Viridiana Olin-Sandoval et al., 2019).

L-asparagine

L-asparagine was the second most depleted amino acid in the NR condition, but had no effect when more was added, which was puzzling. It has been shown that cancer cells have a high demand of L-asparagine and prefer to import it since *de novo* synthesis is energetically expensive (Krall et al., 2016). However, it is considered a "metabolic dead-end" and can contribute to protein synthesis (Krall et al., 2016). So why is it in high demand? There is evidence to support that L-asparagine acts as an amino acid exchange factor in cancer cells, like glutamine, and it specifically helps cells uptake L-serine, L-threonine, and L-histidine (Krall et al., 2016). In this role, L-asparagine exits the cell while another amino acid enters the cell (Krall et al., 2016). If this role is conserved in our system that would explain why there is no longevity extension. Although L-asparagine may be required for amino acid uptake in mammalian systems, L-asparagine is not limiting in the CR conditioned media

L-arginine

Interestingly, arginine is one of the best amino acids in terms of extending lifespan when added at 5mM. As discussed in a previous chapter, arginine is a precursor of putrescine and other polyamines (Chapter II). We are beginning to conduct experiments on mechanisms underlying arginine-mediated lifespan extension. Our working hypothesis is that supplementing arginine extends lifespan *via* augmenting polyamines.

One-carbon metabolism in regulation of aging

Although multiple amino acids are more abundant in CRCM than NRCM, we focused on L-serine because the biosynthesis gene *SER1* is a QTL for CLS in the BY4741 background (Jung et al., 2018). L-serine is also a major entry point for the one-carbon metabolism (OCM) pathway, and a key component of the TSP (Kalhan & Hanson, 2012b), which has been implicated in longevity (Kabil et al., 2011). The OCM pathway supports multiple cellular processes such as

biosynthesis of purines, amino acid homeostasis (glycine, serine, and methionine), epigenetics through SAM and chromatin methylation, and redox defense (Ducker & Rabinowitz, 2017). However, few studies directly linked OCM to the regulation of aging. In one aging study, activation of naïve T cells from aged mice was attenuated because of a deficit in the induction of OCM enzymes (Ron-Harel et al., 2018).

In our current study, we identified a link between serine, OCM, and CLS. Specifically, we found that L-serine supplementation into NR cultures extended CLS in a manner dependent on the OCM pathway (Figure 4.15), which we interpret as the one-carbon units donated from L-serine allowing cells to complete biosynthesis processes required to effectively enter quiescence. Of note, L-glycine, a 1C donor, was not depleted from NR yeast cultures and had no effect on CLS when supplemented (Figure 4.11). In this sense, NR yeast cells may be similar to cancer cells that rely on exogenous serine, but not glycine, for proliferation (Labuschagne et al., 2014a). Overexpression of serine hydroxymethyltransferase SHMT2 is also associated with poor prognosis in cancer patients, while downregulating this enzyme suppresses tumorigenesis in human hepatocellular carcinoma (Woo et al., 2016).

Yeast cells lacking the mitochondrial serine hydroxymethyltransferase Shm1p, or the NAD-dependent 5,10-methylenetetrahydrofolate dehydrogenase Mtd1p, each displayed extended mean and maximum CLS. Cells lacking the cytoplasmic Shm2p enzyme also appeared to extend maximum CLS (Figure 4.15). These results suggest that perturbing flux through the OCM pathway under NR conditions can influence long term cell survival, perhaps by forcing metabolism toward gluconeogenesis and the glyoxylate cycle, thus mimicking CR. Interestingly, yeast RLS extension caused by deletion of the *RPL22A* gene was recently shown to correlate with reduced translation of OCM enzymes (Maitra et al., 2020a). Furthermore, deleting genes

involved in OCM moderately extended replicative lifespan, like what we observed for CLS. Taken all together, we hypothesize that CR may also reduce flux through the OCM pathway, consistent with reduced serine consumption from the media and strong CR-induced CLS extension that occurred even in the *shm1*Δ, *shm2*Δ, or *mtd1*Δ mutants. The impact of these perturbations, which represent evolutionarily conserved and highly connected pathways, may depend on genetic and environmental context, and thus the yeast model is ideal for further systematic experimental characterization (Hartman et al., 2001). Given the common effect of OCM on yeast RLS and CLS, and its strong conservation from yeast to mammals, future investigation of its roles in metazoan aging models is warranted.

Experimental procedures

Yeast strains and media

S. cerevisiae strains used in this study were BY4741 (*MAT***a** *his3*Δ*1 leu2*Δ*0 met15*Δ*0 ura3*Δ*0)*, FY4 (*MAT***a** prototrophic), and several deletion mutants from the Euroscarf yeast knockout (YKO) collection in the BY4741 background (Winzeler EA, 1999). Synthetic complete (SC) growth medium was used for all experiments except for the use of custom 'human-like' HL media (Hartman et al., 2015; Smith Jr. et al., 2016). A recipe for SC media with individual amino acid concentrations is provided in Supplemental Table S6 (Burke et al., 2000). Glucose was added to a final concentration of either 2.0% (non-restricted [NR]) or 0.5% (calorie restricted [CR]). To supplement amino acids, SC or HL medium was used containing 2% glucose (NR), and with amino acids added to a final concentration of 5, 10, 20, or 30 mM where indicated. Unless noted otherwise, all cultures (10 mL) were grown at 30°C in 15 mL glass culture tubes with loose fitting metal caps on a New Brunswick Scientific roller drum.

Semiquantitative (spot) and quantitative assays for measuring CLS

To assess CLS, overnight 10 mL SC 2% glucose (NR) cultures were started from single colonies in triplicate. Next, 200 µL of the overnight cultures was used to inoculate fresh 10 mL cultures of the indicated SC medium conditions (NR, CR, or NR + amino acid). For each time point, 20 µL aliquots were then removed from cultures at the indicated times in the stationary phase (starting at day 3) and serially diluted in 10-fold increments with sterile water in 96-well plates. For semi-quantitative spot assays, 2.5 µL of each dilution was spotted onto YPD 2% glucose agar plates as previously described (Smith Jr. et al., 2007). The plates were then digitally imaged on a gel documentation system after 2 days of colony growth and the time points were compiled together to visualize the changes in viability over time. For the quantitative CLS assays, 2.5 µL of the 1:10, 1:100, and 1:1,000 dilutions of each culture were spotted onto YPD plates that were then incubated at 30°C for 18 to 24 h to allow for microcolony formation (Wierman et al., 2017). We typically spot the three dilutions for 12 different cultures onto one YPD plate. Images of each dilution spot were captured on a Nikon Eclipse E400 tetrad dissection microscope at 30x magnification such that the entire spot fills the field of view. Microcolonies were then counted from the images either manually with a counting pen, or automatically using OrganoSeg, a program originally developed for counting mammalian organoids in culture (Borten et al., 2018), which we have adapted for counting yeast colonies (Enriquez-Hesles et al., manuscript in preparation). At the end of each experiment, percent viability was calculated for each time point by normalizing to the first day of colony forming unit (CFU) measurements. Standard deviation error bars on the survival curve graphs were determined from 3 biological replicates. Statistical analysis was performed using the online program OASIS 2 (Han et al., 2016), reporting mean lifespan (days), standard error of the mean (SEM), and 95th percentile

confidence interval (95% CI) of the mean for each strain or condition. Q-HTCP analysis was performed as previously described (Santos et al., 2020).

Chromatography

Fifteen BY4741 NR or CR cultures (10 ml SC each), were grown to saturation for 5 days at 30°C in 18 mm glass test tubes with loose fitting metal caps. The glassware was acid washed with 0.1N HCl before use. Cells were pelleted by centrifugation and the conditioned media pooled. The pooled media was then concentrated in a Büchi Rotavap from 150 ml down to approximately 2.5 ml (60-fold). The concentrates were centrifuged at 4,000 rpm (2,987 RCF) for 10 minutes in 15 ml conical tubes to remove any solid precipitates. Two ml of the clarified concentrate was loaded onto a 1 x 26 cm Sephadex G-10 column and fractionated with double distilled water. Two ml fractions were collected by gravity flow in a Pharmacia fraction collector and filter sterilized through 0.22µm syringe filters. The fractions were then added to new 5 ml CLS cultures at a 1:5 ratio (ml concentrate: ml culture) and semiquantitative CLS assays performed. NaCl (100 mM) was eluted through the column before and after the media concentrates to determine the gel size retention fractions as measured by electrical conductivity.

Preparation of conditioned media concentrates for CLS and amino acid assays.

To collect and concentrate conditioned media for CLS assays and amino acid profiling, BY4741 or FY4 strains were grown in 150 mL SC cultures (with either 2% glucose or 0.5% glucose) at 30°C for 5 days in a shaking water bath. The cultures were then centrifuged, and the supernatants were condensed from 150 mL down to 15 mL (10-fold) using a Büchi Rotavapor-R apparatus, then filtered by passing through a 0.22µm filter and stored at -20°C. For supplementation experiments, conditioned media concentrates (derived from NR or CR cultures) were added to 10 mL of non-restricted SC-NR media to final concentrations of 1%, 2%, or higher where indicated.

Metabolomics

BY4741 NR and CR cultures (10 ml SC each) were grown to stationary phase (day 5), then centrifuged in 15 ml disposable conical tubes (Falcon). The supernatant media was filter sterilized through 0.22µm syringe filters and frozen at -80°C. Untargeted metabolomics of conditioned media from 6 NR and 6 CR cultures was performed *via* gas chromatography/electron-ionization mass spectrometry (GC/ei-MS) in the Metabolomics Laboratory of the Duke Molecular Physiology Institute (DMPI), as described (McNulty et al., 2011). Metabolites were extracted by the addition of methanol. Dried extracts were methoximated, trimethylsilylated, and run on an 7890B GC-5977B ei-MS (Agilent Corporation, Santa Clara, CA), with the MS set to scan broadly from *m/z* 50 to 600 during a GC heat ramp spanning 60º to 325 ºC. Deconvoluted spectra were annotated as metabolites using an orthogonal approach that incorporates both retention time (RT) from GC and the fragmentation pattern observed in MS. Peak annotation was based primarily on DMPI's own RT-locked spectral library of metabolites, which is now one of the largest of its kind for GC/EI-MS. DMPI's library is built upon the Fiehn GC/MS Metabolomics RTL Library (a gift from Agilent, their part number G1676-90000; (Kind et al., 2009)). Quantities from the mass spectrometry were normalized to OD_{600} of the cultures to account for cell density. 160 metabolites were annotated based on matches with a spectral library. Another 115 metabolites were not matched in the library and remain unannotated.

Quantitative amino acid profiling

Conditioned NR and CR media from day 5 stationary phase cultures was collected and concentrated with the Rotavap as described above. As a control, SC media without glucose was also concentrated and analyzed. Samples were submitted to the UVA Biomolecular Analysis

Facility and then analyzed using a ZipChip system from 908 Devices that was interfaced with a Thermo Orbitrap QE HF-X Mass Spectrometer. Samples were prepared by diluting 10 µL with 490 µL of LC-MS grade water, which was then further diluted 1:10 with 90 µL of the ZipChip diluent (908 Devices Inc., P/N 810-00168). The samples were loaded onto ZipChip HR Chip (908 Devices Inc., P/N 810-00194) for analysis. The following ZipChip analysis settings were utilized: Field strength: 500V/cm, Injection volume: 7 nl, Chip Type: HR, BGE: Metabolite, Pressure assist: Enable at 7 minutes, Run time: 10 minutes, MS setting (Thermo Orbitrap QE HF-X), m/z range: 70-500, Resolution: 15000, 1 microscan, AGC target: 3E6, Max ion injection time: 20 ms, Inlet capillary temperature: 200°C, S Lens RF: 50.

RNA analysis

Cells from NR overnight cultures were inoculated into 75 ml of fresh NR SC medium that was supplemented with 1.5 ml of concentrated conditioned media (CRCM or NRCM) or 1.5 ml of sterile water as a control. The starting OD_{600} was 0.05 in 250 ml Erlenmeyer flasks. Cultures were grown at 30°C in a New Brunswick water bath shaker. For the log phase condition, 50 ml of the samples were collected at OD_{600} of 0.2. Equivalent numbers of cells were collected from smaller aliquots harvested at 24 hr and 96 hr. Total RNA from three biological replicates was isolated using the hot acid phenol method and then processed into Illumina DNA sequencing libraries as previously described (Maqani et al., 2018), with slight modifications. Briefly, total RNA was treated with DNase I for 10 min at 37°C and then measured for concentration and quality with an Agilent Bioanalyzer. PolyA mRNA selection was performed on 5 µg of the DNase-treated total RNA with the NEBNext Poly(A) mRNA magnetic isolation module (E7490). DNA sequencing libraries were then generated with the NEBNExt Ultra Directional RNA library Prep kit for Illumina (E7420). Libraries were sequenced on an Illumina

NextSeq 500 by the UVA Genome Analysis and Technology Core (GATC). Sequencing files are available at GEO (accession number GSE151185). Sequencing reads were mapped to the sacCer3 genome using bowtie2 with default settings (Langmead & Salzberg, 2012). We preprocessed sequencing data from the UVA GATC and analyzed differential gene expression in R using DESeq2 (Love et al., 2014).

Acetic acid measurements

100 µl aliquots were taken at designated time points from standard 10 ml CLS cultures. Cells were pelleted by centrifugation at 2,500 rpm at 4°C, and 50 µl of supernatant was removed and stored at −80°C, until further analysis. Acetic acid concentration for each sample was then later determined using an Acetic Acid Kit (Biopharm AG) per manufacturer's instructions. The acetic acid concentrations and standard deviations provided are an average of three biological replicates for each condition and reported as g/L.

Acknowledgments

We thank Joel Hockensmith for small molecule chromatography advice and Mark Okusa for use of a Rotavap apparatus. We also thank Arun Dutta, Katherine Owsiany, and David Martin for assistance with R and RNA-seq analysis, and Marty Mayo for noting the connection between yeast Fsf1p and L-serine.

Chapter V

Can L-serine promote cell cycle completion in post-mitotic cells experiencing DNA replication stress?

Abstract

In yeast, quiescence depends on initial nutrient conditions. Surprisingly, glucose concentration in the growth media that is rapidly utilized in the growth phase, impacts longevity days later, even when no glucose remains (Smith Jr. et al., 2007) . For example, cells initially exposed to excess glucose in the growth media (non-restriction, NR) fail to enter or maintain effective quiescence. Resembling neurons in degenerative diseases, many NR yeast cells arrest in S-phase of the cell cycle (Weinberger et al., 2007; Yurov et al., 2011). In contrast, most cells exposed to low glucose (Calorie-Restricted, CR) acquire a resilient quiescent state, as indicated by a more effective G_1 arrest and extended CLS (Smith Jr. et al., 2007; Weinberger et al., 2007). Experiments from our lab have shown that amino acids may be limiting in NR conditions in yeast (Enriquez-Hesles et al., 2021). We have also found that most nucleotides are depleted as cells enter the stationary phase (Kalita et al., 2021). We hypothesized that L-serine supplementation may help maintain nucleotide levels by fueling one-carbon metabolism (OCM) and *de novo* nucleotide synthesis. We also hypothesized that reduced nucleotide levels would augment DNA replication stress and prevent proper entry or maintenance of quiescence. CR or L-serine supplementation could potentially suppress such replication stress by allowing completion of replication and then proper cell cycle exit from G_1. Unsurprisingly CR extends viability of both budded and unbudded cells relative to NR-treated cells. Furthermore, we show that L-serine supplementation mimics these beneficial effects, but how exactly is additional L-serine mimicking CR? In this section, we explored whether L-serine could push the cells towards G_0 by augmenting intracellular nucleotide levels. Surprisingly, we found that CR maintains elevated nucleotide levels in the cell relative to NR, while L-serine supplementation elevated

nucleoside levels meaning that the L-serine perhaps is increasing flux through this pathway in the NR condition.

Introduction

DNA replication stress

DNA replication stress—inefficient DNA replication that arrests cells in the synthesis phase of the cell cycle—results in stalling the replication machinery and incomplete chromosome duplication (Burhans & Weinberger, 2007; Mazouzi et al., 2014). In post-mitotic cells like neurons, this DNA replication stress and inability to complete the cell cycle contributes to irreversible cell death, leading to neurodegenerative diseases like Alzheimer's Disease (AD)(Yang et al., 2001; Yurov et al., 2011). Similarly in yeast cells, DNA replication stress or improper S-phase entry causes cell death and short CLS (Weinberger et al., 2007). Furthermore, CR suppressed DNA replication stress, prevented premature S-phase entry, and extended CLS essentially enhancing quiescence (Weinberger et al., 2007).

One major cause of DNA replication stress is the limitation of nucleotide levels in the cell (Zeman & Cimprich, 2014). Despite this nucleotide deficit, post-mitotic, non-proliferative neurons in the G_0/G_1 phase can improperly re-enter the cell cycle (Lee et al., 2009), and experience DNA replication stress in the S-phase of the cell cycle. A better understanding of interventions to restore nucleotide levels for the DNA synthesis completion (S-phase) is essential to prevent this neuronal loss, implicated in AD. We hypothesized that L-serine could be such an intervention.

L-serine, like threonine, may contribute to nucleotides

It is known that L-serine is indispensable for proliferating cells by contributing to nucleotide synthesis *via* catabolism in the OCM pathway (Hartman, 2007; Kalhan & Hanson,

2012a; Labuschagne et al., 2014b). More recently, we showed that L-serine-dependent CLS extension depends on the OCM where L-serine is converted to glycine (Enriquez-Hesles et al., 2021). Glycine can also be synthesized from L-threonine *via* threonine aldolase, Gly1p. Glycine production from threonine has been shown to maintain nucleotide level homeostasis in the context of hydroxyurea (HU) treatment (Hartman, 2007). Based on these data and L-serine's role in proliferating cells, we hypothesize that supplemental L-serine may provide nucleotides similarly to threonine. Specifically, we hypothesized that L-serine promotes cell cycle completion of post-mitotic cells experiencing replication stress through its catabolism into nucleotides. In this study, we show that L-serine extends longevity independent of time added, suggesting a potential role in alleviating cells experiencing replication stress in the stationary-phase. Furthermore, through budding index measurements and flow cytometry we show that exogenous L-serine addition does not affect cell cycle progression but improves viability of budded cells, much like CR-treated cells. This suggested that perhaps L-serine is indeed benefiting arrested S-phase cells in some manner. Although L-serine does not raise nucleotide levels, it increases levels of ribonucleosides. This result was perplexing. Why ribonucleosides? Could these nucleosides be derived from autophagy? Follow-up studies are warranted to support the hypothesis that these ribonucleosides are derived from autophagy when L-serine is plentiful. Overall, these studies show that L-serine supplementation and CR elicit similar beneficial effects in terms of longevity and protecting budded cells, but we provide more evidence that they mediate these benefits through different mechanisms.

Results

L-serine addition improves viability of stationary phase cells

L-serine supplementation to BY4741 yeast liquid cultures demonstrates a strong correlation with extending the viability of post-mitotic cells (Enriquez-Hesles et al., 2021; Maruyama et al., 2016). Previous results show the Caloric Restriction conditioned media (CRCM) extended lifespan independent of time added—even to cultures that have been sitting in the stationary phase for over a week (Figure 5.1A), we wanted to see whether L-serine, a major component of CRCM, could also extend lifespan when added after cells already entered stationary phase. Surprisingly, L-serine also extends lifespan independent of time added, but not to the same extent as when added at the time of inoculation (Figure 5.1B). Herein, that late addition of L-serine to stationary phase cultures could promote enhanced quiescence, but how? Given serine's known role as a OCM input to supply nucleotides to cancer in proliferative cells, we hypothesized that L-serine may be utilized to maintain nucleotide level homeostasis in the stationary phase cells. This maintenance of nucleotides in turn would allow replication to complete in the case of deoxyribonucleotides. Alternatively, this pool would allow transcription of genes necessary for quiescence entry, in the case of ribonucleotides.

L-serine does not impact the budding index significantly

We set out to determine whether this increase in viability is also correlated with improved cell cycle completion, measured by quantification of G_0/G_1 arrest *via* flow and budding index (Figure 5.1C). This would tell us whether L-serine enhances G_1 arrest. We employed flow cytometry to determine relative measures of cell number that were arrested with a G_1 content of DNA or S phase content of DNA. We also used a fraction of budded cells to detect potential replication stress since cells with buds indicate the cells are in S-phase of the cell cycle. Fewer budded cells would signify efficient G_1 arrest. Thus, we administered extra L-serine to cultures and used flow cytometry and microscopy (Figure 5.1 D-F). For these experiments, yeast cells

were grown in three conditions: non-restricted (NR, normal glucose); calorie restricted (CR, low glucose positive control that extends viability and improves G_0/G_1 arrest); NR+ L-serine (30mM). The cells were allowed to reach the stationary phase without alterations to the liquid culture. Percentage of the cell population in G_0/G_1 arrest in the different conditions were compared at Day 8. We prepared samples in triplicate at the indicated time points and collected cell budding index data as a marker for G_0/G_1 arrest in viable cells. We hypothesized that extra L-serine addition (30mM), would more efficiently complete cell cycle and promote G_0/G_1 arrest. We expected to see a shift in the population proportion from budded cells (S-phase) to unbudded cells (G_0/G_1) compared to the NR. Although there was a slight decrease in the budding index over time, it was not significantly different between conditions (Figure 5.1 D). To complement the budding index measurements, we performed flow cytometry on the same samples, to analyze the populations' cell cycle distribution more closely, as indicated by 1N (G0/G1) vs 2N (G2/M) DNA content ratios. Consistent with budding indices, the flow cytometry measurements in CR, NR, and L-serine conditions detected a similar proportion of cells in S-phase. At day 8, cells in S-phase were 22% in NR, 18% in CR and 23% in NR + L-serine (Figure 5.2C). CR cells had the lowest percentage of cells in S-phase. At the same time, CR cells had a reduced budding index compared to NR as previously shown (Weinberger et al., 2007). As shown in Figure 5.1D, conditions with L-serine supplementation had a higher proportion of cells in S-phase compared to NR but had a lower budding index throughout the time course experiment. Although no large changes were observed in the budding index, perhaps CR and L-serine offer protection to unbudded cells.

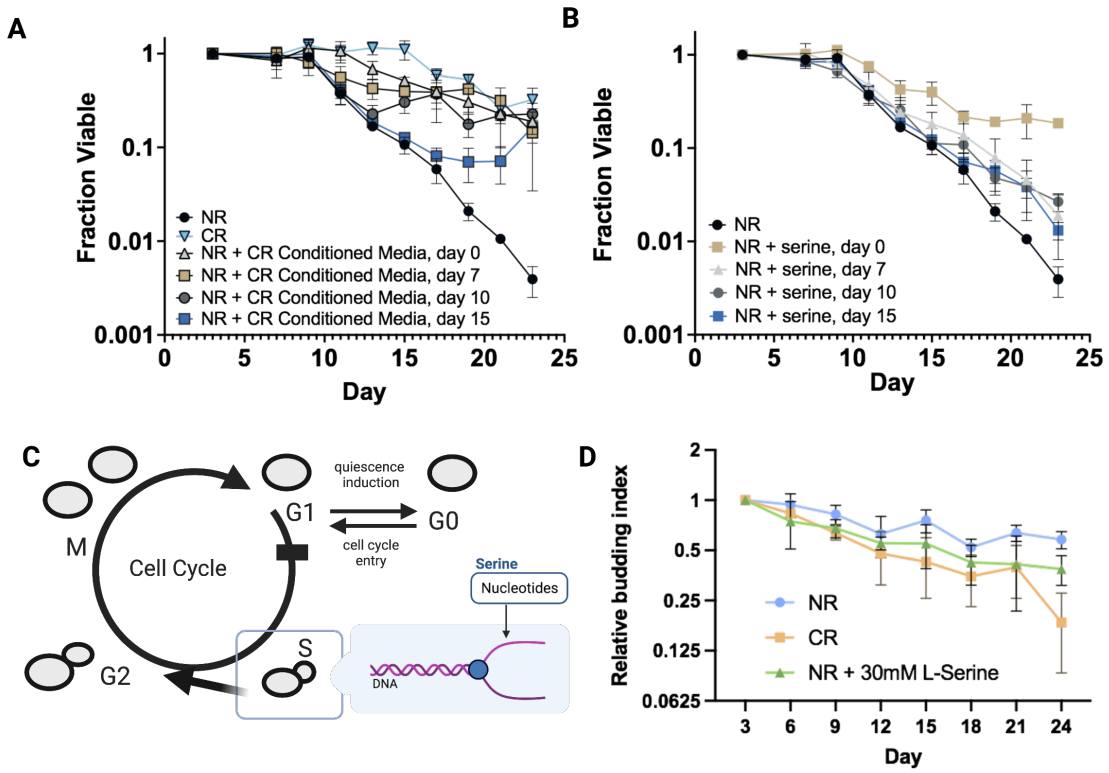

Figure 5.1 CRCM and L-serine improve quiescence in the stationary phase. *(A) Quantitative chronological lifespan (CLS) assay. Concentrated CRCM was supplemented at 2% (vol/vol) into NR cultures at time of inoculation (day 0), day 7, day 10 or day 15. B) Quantitative chronological lifespan (CLS) assay. 10mM serine was supplemented into NR cultures at time of inoculation (day 0), day 7, day 10 or day 15. C) Schematic representation of the cell quiescence cycle. Nutrient limitation causes cells to enter a non-proliferating state called quiescence. Cells that arrest in S-phase undergo DNA replication stress. Cells that arrest in G_0 are protected against DNA replication stress. We propose that L-serine fuels nucleotides that allow the cells to finish DNA replication D) Monitoring budding indices in CLS cultures over time.*

L-serine improves viability of budded cells

We wondered whether the budded cells were less viable than the unbudded G_1 arrested cells. We used methylene blue as a dye to quantify viability using a compound microscope. Methylene blue is a commonly used method to measure viability in yeast cells (Kwolek-Mirek & Zadrag-Tecza, 2014). This dye enters all cells, but only living cells enzymatically reduce the dye

to a colorless compound (Kwolek-Mirek & Zadrag-Tecza, 2014). Cells that remain blue are termed methylene blue positive and are counted as unviable (Figure 5.2 B). As expected, in the NR condition 43% of unbudded cells were methylene negative or alive, while in the CR condition, 63% of unbudded cells were methylene blue negative (Figure 5.2A). L-serine addition showed a similar viability profile to CR with 62% viability in unbudded yeast population (Figure 5.2A). Although we did not observe differences in budding index or flow cytometry (Figure 5.2C), we observed fewer budded cells that were blue in CR and with L-serine supplementation condition (Figure 5.2B). This suggests that CR and L-serine may offer some protection to budded cells. It is possible that both conditions help cells maintain higher levels of intracellular nucleotide levels. To test this hypothesis, we conducted target metabolomics of various nucleotides and intermediates.

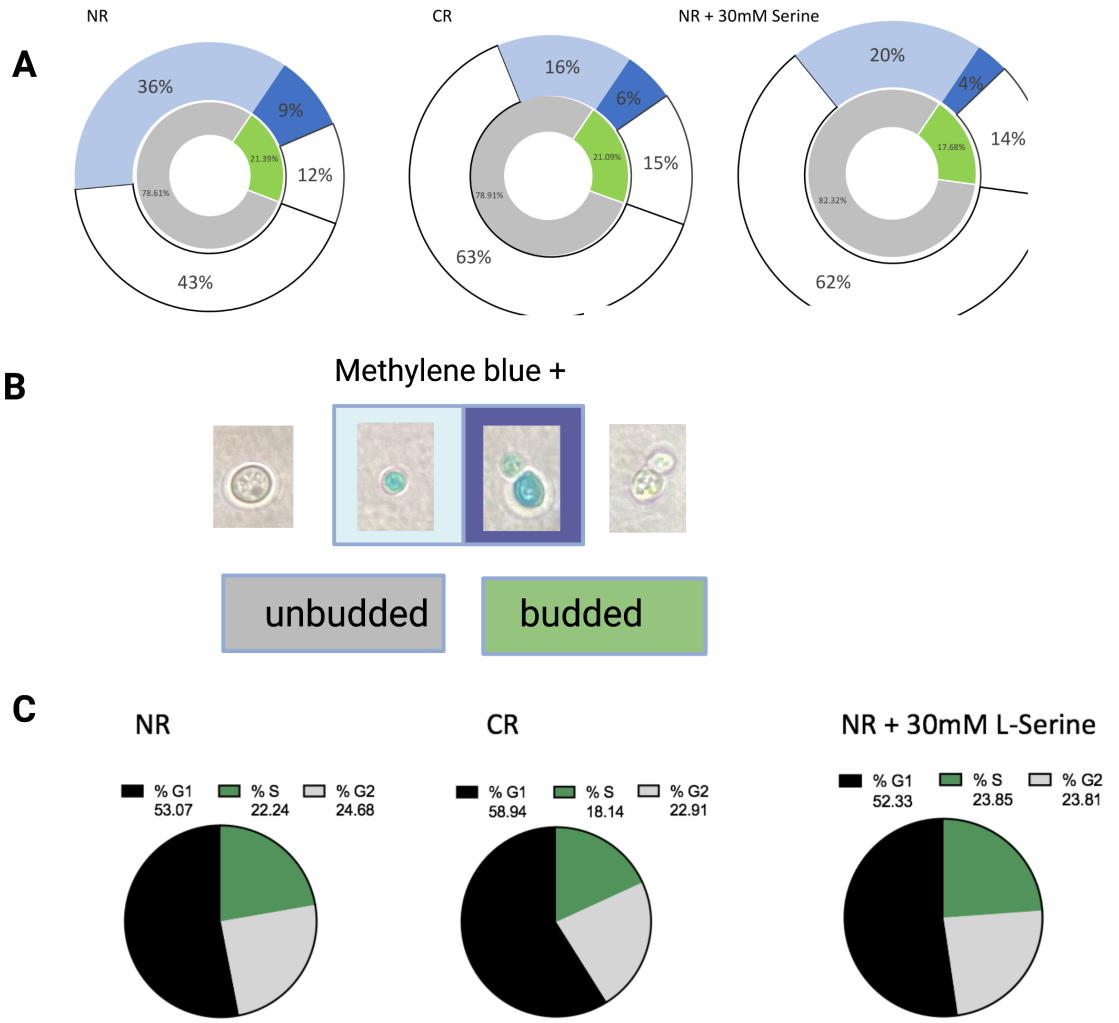

Figure 5.2 L-serine and CR both improve viability of budded cells. *A) Diagram showing the % viability in NR, CR, and NR + 30mM L-serine assessed at day 8. In the outer ring, the white indicates viability. Blue indicates unviable. The darker blue indicates % unviable in budded cells. The inner circle represents % budded (green) and % unbudded (blue). B) Pictures of single cells showing unbudded viable cell (clear cell), an unbudded cell stained with methylene blue representing an unbudded unviable cell (blue), the next picture shows a budded cell stained with methylene blue indicating a budded unviable cell. The last picture on the right is of a clear budded cell which indicates viability. C) Flow cytometry measurements of DNA content at day 8 of BY4741 cells treated with NR, CR or NR + 30 mM L-serine. This pie chart shows % in G1, S phase and G2.*

CR maintains intracellular nucleotide pools

Next, we conducted a targeted metabolomic analysis of various nucleotides and intermediates. BY4741 was grown to log phase, 24 hours or 96 hours under NR, CR, or NR+ serine, and NR+ threonine conditions. We used NR+ threonine, because a previous study showed that threonine availability and catabolism *via* Gly1p could maintain deoxyribonucleotide pool homeostasis (Hartman, 2007). We thought that L-serine may also contribute to *de novo* purine biosynthesis since L-serine also synthesizes glycine *via* Shm1p and Shm2p. In addition, L-threonine also extends CLS at day 0 and at day 7 consistent with the model of nucleotide production alleviating replication stress in arrested S-phase cells (Figure 5.3).

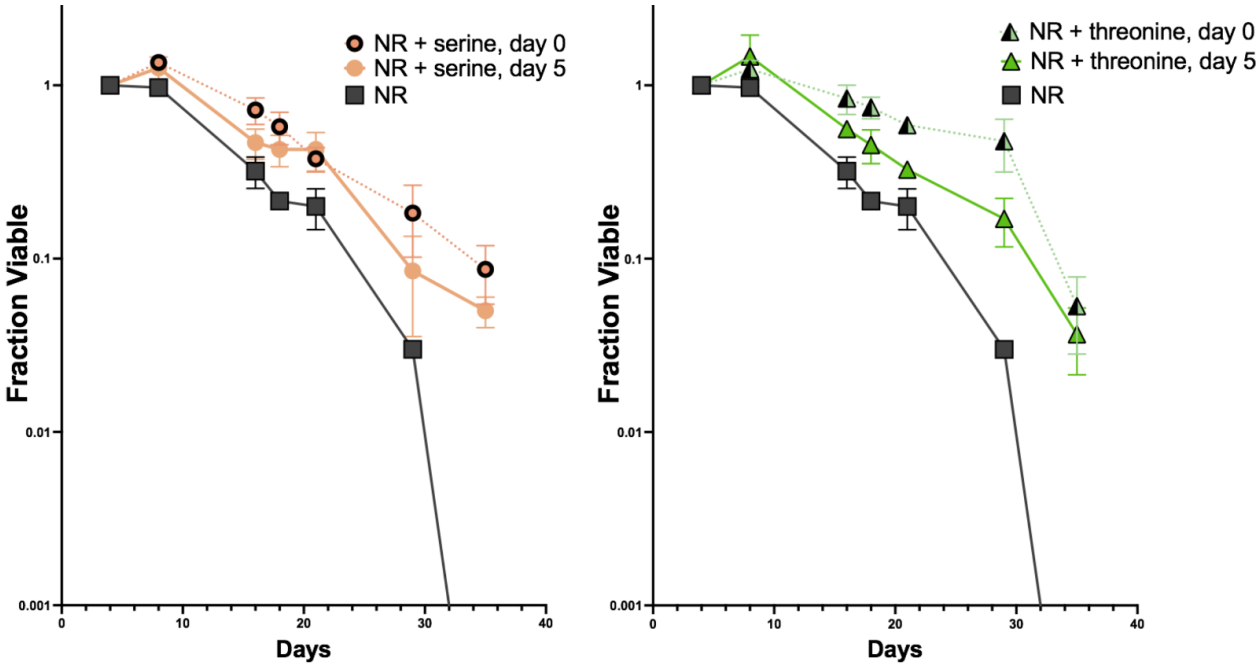

Figure 5.3 L-serine and L-threonine both improve CLS independent of time added*. CLS of non-restricted BY4741 supplemented with 10mM L-serine or L-threonine at inoculation (day 0) or day 5.*

In addition to testing threonine supplementation, we tested CR-treated cells. Under NR conditions, cells exhibited depletion of nucleotide pools relative to log phase, recapitulating

results in a previous study from our lab (Kalita et al., 2021). This depletion of intracellular nucleotide levels coincides with high replicative stress observed in the cells in previous studies (Weinberger et al., 2007). Surprisingly, under the CR conditions, CR cells, for the most part, maintained several nucleotides and associated molecules elevated relative NR in a time course experiment (Figure 5.4). For example, adenine, glutamine, dGDP, and CDP were all high in CR relative to NR at 96 hours (Figure 5.4). This elevation of nucleotides and precursors may not necessarily represent an increase in replication or transcription. These available nucleotides could be used for DNA repair and exit of quiescence. Accumulation could also represent underutilization. In mammalian cells it's been shown that nucleotide synthesis reduction may contribute to replicative senescence (Delfarah et al., 2019). Thus, maintaining nucleotide pools may be a currently unexplored mechanism essential to retain enhanced quiescence in CR-treated yeast cells. For now, this paradoxical effect of high nucleotide levels in G_1 arrested CR cells remains unresolved.

When we supplemented extra L-serine and L-threonine, we did not observe an increase in nucleotide pools as previously seen with hydroxyurea (HU) treatment (Hartman, 2007). HU inhibits deoxyribonucleotide reductase and stops further processing of dNTP substrates (Hartman, 2007). In this HU experiment, uptake of threonine from the environment and its subsequent metabolism into glycine is required for replenishing dNTP substrates. In our experiments L-serine and L-threonine conditions resembled NR condition except for UDP. UDP levels in L-serine, and L-threonine resembled levels in CR (Figure 5.4). Overall, this set of experiments further reinforced the conclusion that L-serine and CR extend lifespan *via* different mechanisms.

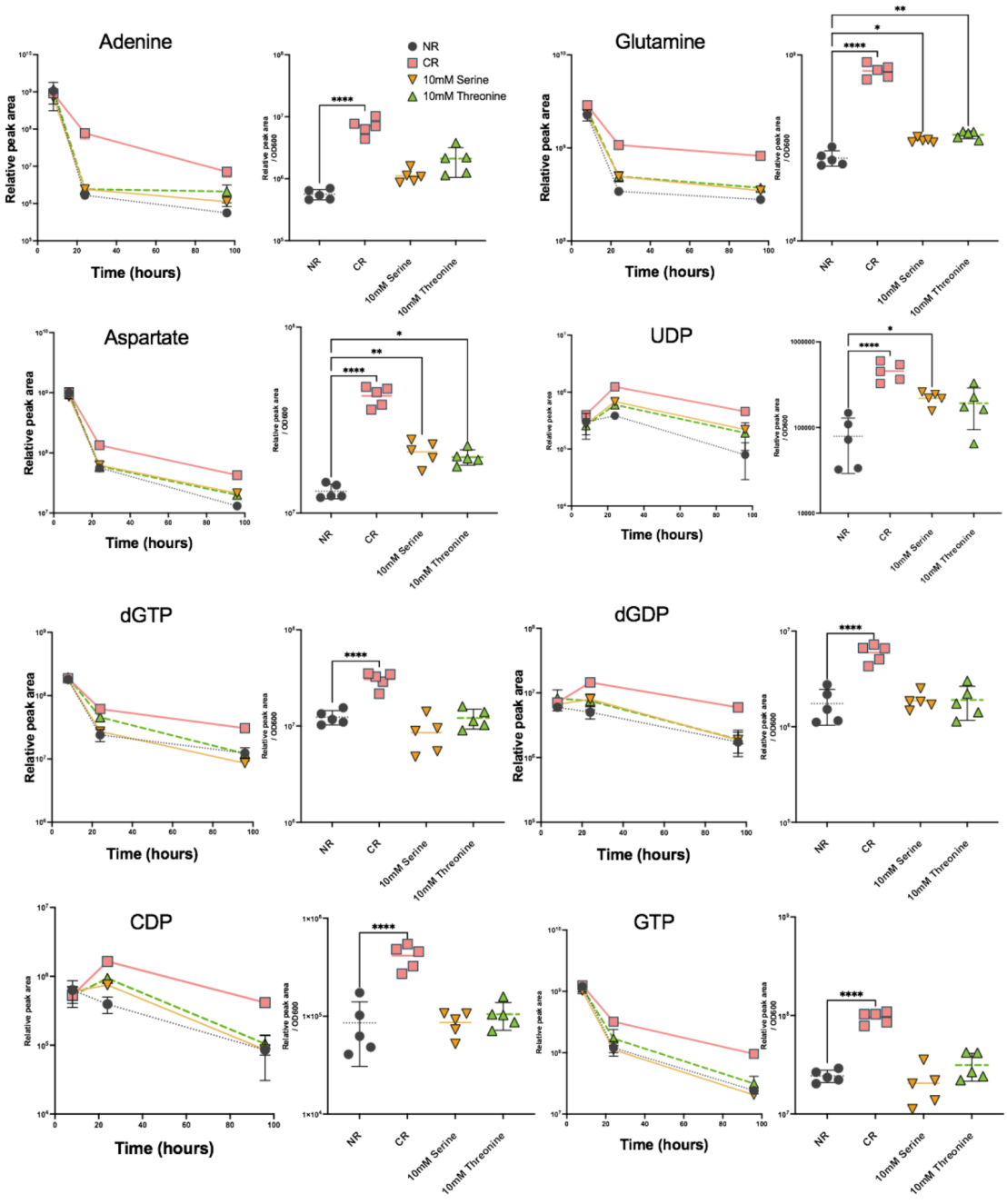

Figure 5.4 Caloric restriction increased nucleotide levels compared to Non-Restriction (NR) condition. *Intracellular nucleotide levels are shown for BY4741. Purines, pyrimidines, and associated precursors were measured at log, 24, 96 hours for NR, CR, NR+ serine and NR + threonine. In the time course, the x-axis represents hours post-inoculation, and the y-axis represents relative peak value normalized to optical density at time of collection. For these 96-hour values, statistical analysis was performed in PRISM 9 using ordinary one-way ANOVA*

followed by a Dunnett's multiple comparisons test. Data represent mean ±SD from five biological replicates normalized to log phase. L-serine and threonine were supplemented (10mM total concentration) to the NR condition at the time of inoculation.

Ribonucleosides were elevated with L-serine and L-threonine supplementation

Interestingly, we observed elevated ribonucleoside levels when cells were supplemented with 10mM L-serine or L-threonine at 96 hours. Ribonucleosides are derived from the degradation of ribosomes, which are composed of protein and RNA (Figure 5.5A) (Ben-Shem et al., 2011). Nutrient starvation triggers autophagic breakdown of ribosomes into nucleosides (Xu et al., 2013). With the addition of L-serine and L-threonine nucleosides including guanosine, uridine, and cytidine were significantly elevated (Figure 5.5 C). These may be preferentially used as energy sources during transition into stationary phase (Xu et al., 2013). Interestingly, nucleotide monophosphates including GMP, UMP, CMP nor AMP were not elevated, these are upstream of ribonucleosides (Figure 5.5 B). Similarly, hypoxanthine or guanine showed significant alterations, which are derived from nucleosides (Figure 5.5D). Phm8p is a nucleotidase that has been implicated as central in this breakdown as it converts nucleotide monophosphates into nucleosides (Figure 5.5A) (Xu et al., 2013). Ablation of Phm8p prevents effective nucleotide salvage and impaired survival of yeast in the stationary phase (Xu et al., 2013). Like Xu *et al.,* we interpreted this accumulation of nucleosides as active nucleotide degradation. We wanted to test whether L-serine-mediated-longevity hinged on this process. We conducted CLS assays with a *phm8*Δ mutant from the YKO and compared it to a control. Consistent with its central role, we also observed impaired quiescence in the absence of Phm8p (Figure 5.6A). L-serine was able to slightly extend the lifespan of *phm8*Δ, suggesting that L-serine does not depend on this pathway for its longevity effect. In the CR condition, viability dropped sharply after day 15 (Figure 5.6A) suggesting that CR depends on autophagy to extend

viability as culture ages. Another possible mechanism for nucleoside accumulation from RNA degradation is autophagy.

Does L-serine elevate ribonucleosides *via* Autophagy Activation?

Autophagy is a cell process activated upon nutrition stress. In this process cell components are recycled into basic metabolites. Although we have not tested L-serine's direct impact on AMPK, L-serine's activation of autophagy seemed unlikely given that L-serine and CR seem to extend CLS in diverse ways (Enriquez-Hesles et al., 2021). Despite this, we tested the hypothesis that extension of L-serine depended on activating autophagy. We used the *atg8*Δ deletion strain. Figure 5.6B shows that L-serine extends lifespan in this mutant which suggests that L-serine-life extension does not depend on autophagy. This is consistent with other studies showing that L-serine supplementation improves respiration in autophagy deficient strains (May et al., 2020).

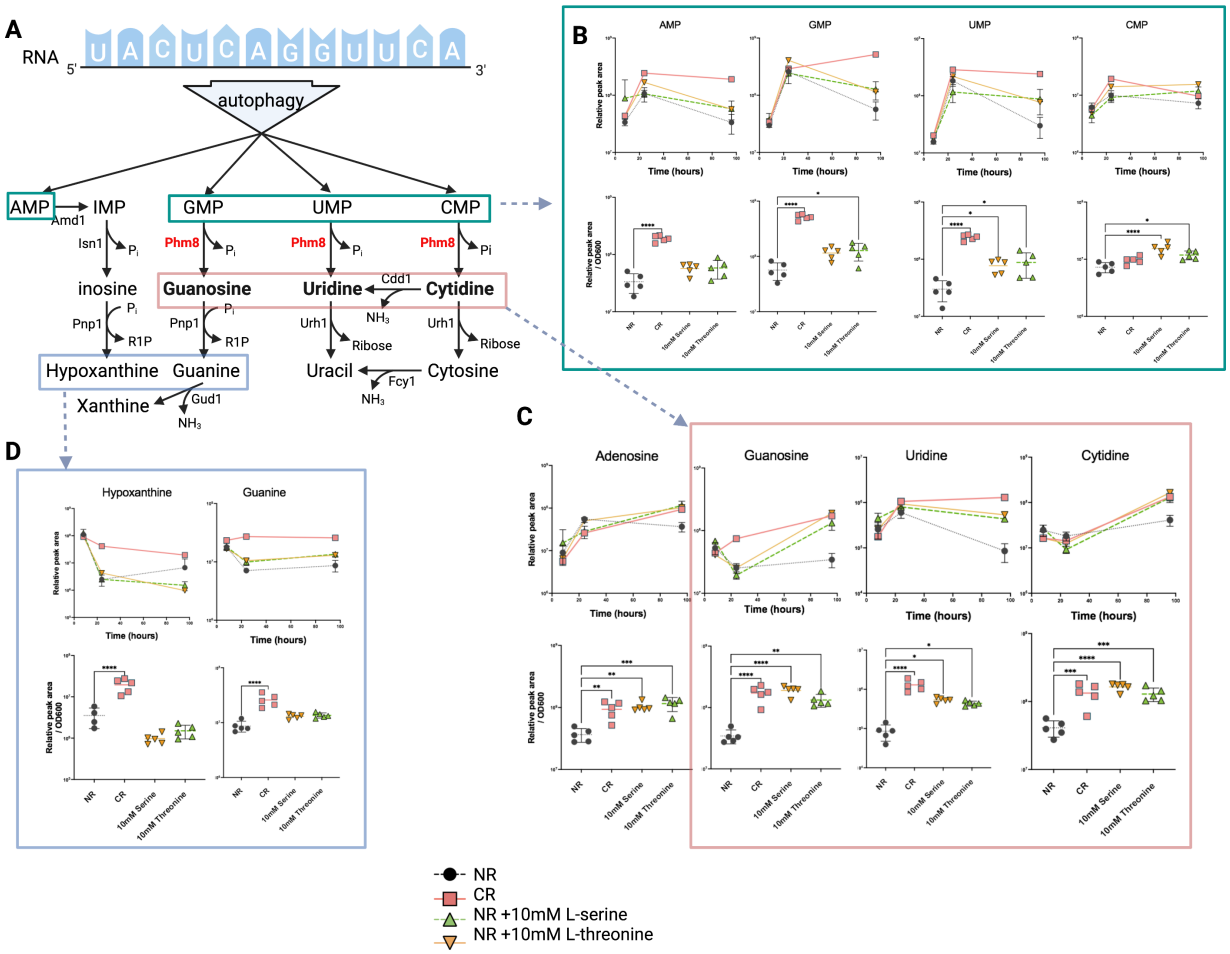

Figure 5.5 L-serine and threonine supplementation to Non-Restricted (NR) condition maintain levels of ribonucleosides. *A) Overview of nucleotide degradation and ribose salvage in Saccharomyces cerevisiae, which is induced by macroautophagy. Diagram shows breakdown of RNA into nucleotides (AMP, GMP, UMP and CMP) which are measured in B). These are then dephosphorylated into ribonucleosides: guanosine, uridine, and cytidine, which are measured in C). These are then converted into ribose and bases including hypoxanthine and guanine, which are measured in D). Intermediates of nucleotide degradation pathways were measured at log phase, 24, and 96 hours for NR, CR, NR+ serine and NR + threonine. Data represent the mean ±SD from five biological replicates normalized to Log phase. L-serine and threonine were supplemented (10mM total concentration) to the NR condition at the time of inoculation. Individual values of 96-hour time points are shown below each time course. For these 96-hour values, statistical analysis was performed in PRISM 9 using ordinary one-way ANOVA followed*

by a Dunnett's multiple comparisons test. In diagram A), measured metabolites are shown in bold. Phm8p is shown in red. Diagram in A) is adapted from (Xu et al., 2013).

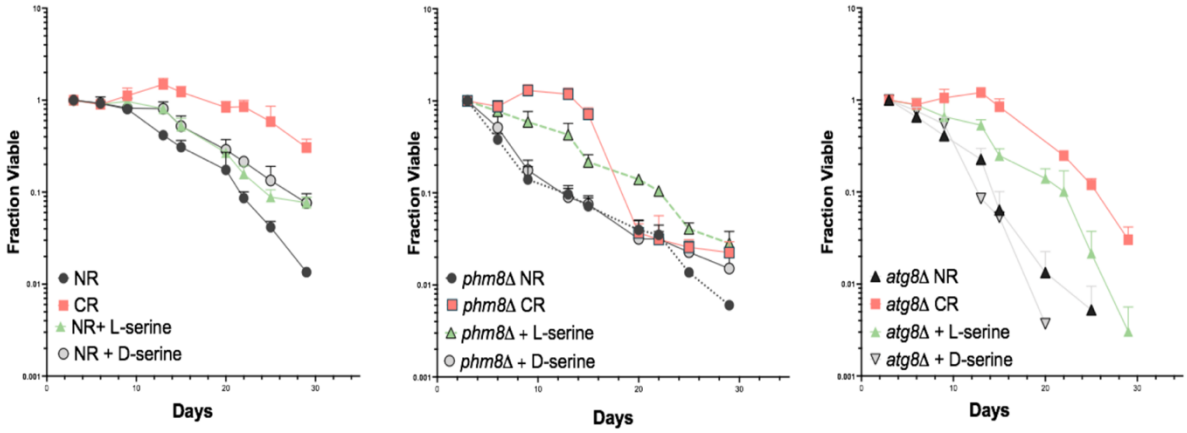

Figure 5.6 L-serine extends longevity independent of autophagy. *CLS of NR, CR, NR +L-serine and NR + D serine in BY4741 (left), phm8Δ (middle) or atg8Δ (right), n=3.*

Discussion

Thinking differently about quiescence and S-phase arrest

It was thought that cells entering the stationary phase also transition into G_0 or temporary quiescence, but evidence suggests that it is more flexible than that (Laporte et al., 2011; Wei et al., 1993). Quiescence is a cell state where cells enter due to glucose limitation and from all cell cycle states (Laporte et al., 2011). Both budded and unbudded cells subsequently reside in a temporary arrest of proliferation until glucose is reintroduced (Laporte et al., 2011). Data by Laporte *et al.* supports quiescence entry as a cell cycle independent process that can happen in a budded state or unbudded state—G_1 is not necessary nor sufficient for establishment of quiescence which differs from convention (Laporte et al., 2011). In the Smith lab, we also compared budded and unbudded in the stationary phase and that is independent of condition, like Laporte *et al.* suggest. Our data show that there are multiple cells that remain in S-phase even in

long-lived cells like CR. Although most papers indicate that this is a disadvantage as it is thought to cause replicative stress due to lack of nutrients. Granot *et al.* suggest that budded cells could induce faster growth upon transfer to rich media. However, perhaps staying in a budding state is a strategy giving the replicative older cells an advantage as they are paired with a replicative young cell—a condition emulating heterochronic parabiosis experiments.

DNA replication stress and L-serine is an alleviating factor

Due to many cells arrested in S-phase in the stationary phase and evidence of nutrient depletion in NR condition, we hypothesized that L-serine supplementation and CR maintain nucleotide levels. This could then potentially suppress such replication stress by allowing completion of replication and then proper cell cycle exit from G_1. Interestingly we observed that CR and L-serine protect budded cells in the stationary phase from dying. Although we failed to observe L-serine augmenting nucleotide levels, we found that CR maintains elevated nucleotide levels in the cell relative to NR, while L-serine supplementation elevated nucleoside levels. The significance of this observation remains unknown for now.

Experimental Procedures

To determine budding indices and cell cycle progression, aliquots from CLS cultures were taken at each time point were pelleted by centrifugation and resuspended in PBS (for determining budding index) or 70% ethanol (for flow cytometry).

Budding index

The budding status of at least 100 cells from each aliquot was visually determined using a compound microscope with a 40× phase oil immersion objective. Cells were spun down, conditioned media removed and resuspended in PBS. Methylene blue solution was added in a 1:1 volume to PBS. For example, 100ul of the cell suspension was mixed with 100ul of

methylene blue solution (0.1 mg/mL stock solution dissolved in a 2% dihydrate sodium citrate solution) as previously done (Kwolek-Mirek & Zadrag-Tecza, 2014). Methylene blue allows living cells to reduce the methylene blue stain to a colorless product. Dead cells are unable to reduce the compound and it remains oxidized (Cwalinski et al., 2020; Kwolek-Mirek & Zadrag-Tecza, 2014). Cells were incubated with methylene blue solution for less than 1 minute.

Cell cycle progression. To measure cell cycle progression *via* DNA content by flow cytometry, 1 million cells suspended in 70% ethanol were pelleted by centrifugation, washed with 50 mM sodium citrate (pH 7.5), and resuspended in 0.5 ml of this same buffer containing 0.5 mg/ml RNAse. After overnight incubation at 37°C, an additional 0.5 ml. of sodium citrate buffer containing 2 μM SYTOX Green was added to each sample. Stained cells were briefly sonicated as described above and DNA content was measured using a FacsCaliber flow at a maximum flow rate of 500 cells/s.

Chapter VI

Comparing the roles of L-serine and D-serine supplementation in promoting longevity

Abstract

L-serine is a versatile amino acid that has been implicated in longevity in various model organisms. L-serine can be synthesized *de novo via* the serine synthesis pathway (SSP), *via* one-carbon metabolism (OCM), or obtained from the extracellular environment, from degradation of proteins, or from glycine. By monitoring the conditioned media of stationary phase cultures (Enriquez-Hesles et al., 2021), we hypothesized that L-serine, like many other amino acids, was in high demand in the NR conditions, while it remained underutilized in the CR condition. We were intrigued with the high demand of serine in NR and tested the hypothesis that it was limiting (Enriquez-Hesles et al., 2021). Indeed, supplementation of L-serine to NR cells extended longevity in a dose-dependent manner (Enriquez-Hesles et al., 2021). L-serine-induced CLS extension was shown to be partially dependent on OCM enzymes. This chapter aims to continue understanding how L-serine supplementation improves longevity. Does it depend on autophagy? Does it increase oxygen consumption rate, does it promote catabolism through the OCM pathway? Here, we provide more evidence that L-serine supplementation extends lifespan via pathways that differ from the CR pathways. First, we show that most L-serine was not being harvested in CR conditions and that a small proportion was synthesized and subsequently secreted. This reduced utilization is the first indication of different mechanisms. While we conducted studies of L-serine, we also compared it with D-serine and found that it also extended longevity, albeit to a lesser extent than L-serine. In this Chapter we investigate the underlying mechanism driving longevity of L-serine and D-serine supplementation

Introduction

In the last decade, the connection between L-serine and health has been difficult to ignore. Although recent reports plead caution, L-serine has been shown to have a protective effect on health in various model organisms. L-serine-mediated extension was dependent on the OCM (Enriquez-Hesles et al., 2021). In *C. elegans*, 11 out of 20 amino acids extended lifespan when supplemented, with L-serine supplementation showing the largest effect (Edwards et al., 2015). In mice, impairment of glycolysis derived L-serine in astrocytes contributes to Alzheimer's Disease in a genetic model (Le Douce et al., 2020). In the yeast genome, L-serine codons are numerous in the annotated ORFs, suggesting it could contribute to proteostasis (Chapter IV). These benefits may extend to humans and offer benefits to neuronal tissues (Sinha et al., 2020). It has been shown that L-serine metabolism is in high demand in the retina (Sinha et al., 2020). There are ongoing clinical trials studying the effects of L-serine supplements on ALS and Alzheimer's patients (Stark, 2017; Stommel, 2018). Thus, any understanding of L-serine's function has immediate and direct implications on current clinical work. Additionally, the Ojimi village in Okinawa, Japan is famously named the "longevity village" for its higher-than-average lifespan among its population (Cox & Metcalf, 2017). Interestingly, it was discovered that the diet in this village has a L-serine content that is three-fold higher than that of the average United States citizen (Cox & Metcalf, 2017). How L-serine mediates longevity in this context remains unknown. These proposed mechanistic studies of L-serine will offer additional clues to its potential benefits. An inexpensive, low-toxicity supplement such as L-serine would be a major advancement in preventative medicine.

L-serine has been well described as the main donor for the OCM (Ducker et al., 2016). OCM has also been implicated as a central hub of longevity (Aon et al., 2020) and we provide

evidence that longevity in yeast acts via OCM and relies on transporters like Fsf1p. Fsf1p has been postulated to be the homologue of sideroflexin1 (SFXN1)— an inner mitochondrial membrane protein mediating transport of L-serine from cytoplasmic pools into the mitochondria (Kory et al., 2018). In other organisms, L-serine entry via SFXN1 into the mitochondria is an important source of NADH, nucleotides, and f-Met tRNA (Kory et al., 2018). This Chapter explores the link between L-serine, mitochondria, and longevity in yeast.

This work also explores the mechanism of the stereoisomer D-serine, which is well known for its role as a neurotransmitter in the brain. It has also been considered as a potential therapeutic agent or biomarker in schizophrenia and depression (MacKay et al., 2019). D-serine is a co-agonist for the N-methyl-D-aspartate (NMDA) receptors, produced from L-serine in metazoans by serine racemase (SR) in neurons (MacKay et al., 2019). This racemase is not present in yeast, but yeast have a D-serine hydratase called DSD1p that appears to detoxify D-serine (Ito et al., 2007). In yeast, we provide evidence that cells respond differently to addition of L-serine versus D-serine. Preliminary data show that D-serine may extend longevity in an autophagy-dependent manner.

Results And Discussion

An important regulation step in L-serine's mitochondrial catabolism must be the newly discovered transporter sideroflexin-1 (SFXN-1)which transports serine into the mitochondrial space (Kory et al., 2018). Once L-serine is imported, L-serine can donate one-carbon units to THF. It has been shown that the mitochondrial arm of OCM is preferred in most mammalian tissues (Ducker & Rabinowitz, 2017; Meiser & Vazquez, 2016) and the cytoplasmic arm can compensate when loss of mitochondrial pathway occurs (Ducker et al., 2016). Fungal sideroflexin-1 or *FSF1* is the predicted yeast homolog of *SFXN-1*. However, it is unknown if

Fsf1p performs the same function in yeast. It is not yet annotated as a L-serine transporter in Saccharomyces Genome Database (SGD). Using stable isotope labeled L-serine, we used BY4741, and isogenic strains deleted for *FSF1* to localize L-serine catabolism to either the cytosol or mitochondria.

How is L-serine metabolized in CR compared to NR?

In previous Chapters we provided evidence for L-serine being differentially consumed by cells under NR versus CR condition (Enriquez-Hesles et al., 2021). We wanted to understand whether L-serine is indeed being differentially consumed and differentially utilized in CR compared to NR. Isotope tracing is a tool to quantify the contribution of different pathways to the same product (Meiser & Vazquez, 2016). To directly test L-serine's utilization trajectory, we used [2,3,3-2H] serine, a stable isotope tracer to determine generation of 1C units for thymidine synthesis via cytosolic or mitochondrial L-serine catabolism. In this tracing experiments, unlabeled L-serine was omitted from the media and 1mM deuterated L-serine was added to both NR, CR conditions in BY4741 and *fsf1Δ* strains at inoculation. Cells were collected at log phase, 24 hours, and 96 hours. These measurements were normalized to optical density, a marker for cell number. Media also was collected at the start (time 0) and end of the experiment (time 96 hours). Detection of lower L-serine levels in the media of NR treated cells (Figure 5.1A and B) aligns with previous findings and the hypothesis that L-serine is in high demand in the NR condition (Enriquez-Hesles et al., 2021). There is no unlabeled L-serine detected in the media at the start of the experiment and only a small trace of L-serine present in both CR and NR media, suggesting that L-serine is being synthesized intracellularly and subsequently secreted, albeit in small amounts (Figure 6.1A and B). Most of the L-serine is being harvested from the environment. Intracellular tracing shows that L-serine is being imported in both NR and CR

conditions. In addition to L-serine being in high amounts in the extracellular space, labeled L-serine is also detected in CR condition at 24 and 96 hours (Figure 6.2). This suggests that perhaps L-serine is not being metabolized as quickly in the CR-treated cells. In later stages, L-serine detected in the cell is no longer labeled (Figure 6.2). There were no significant differences in L-serine's consumption of utilization between NR and the *fsf1Δ* (Figure 6.2).

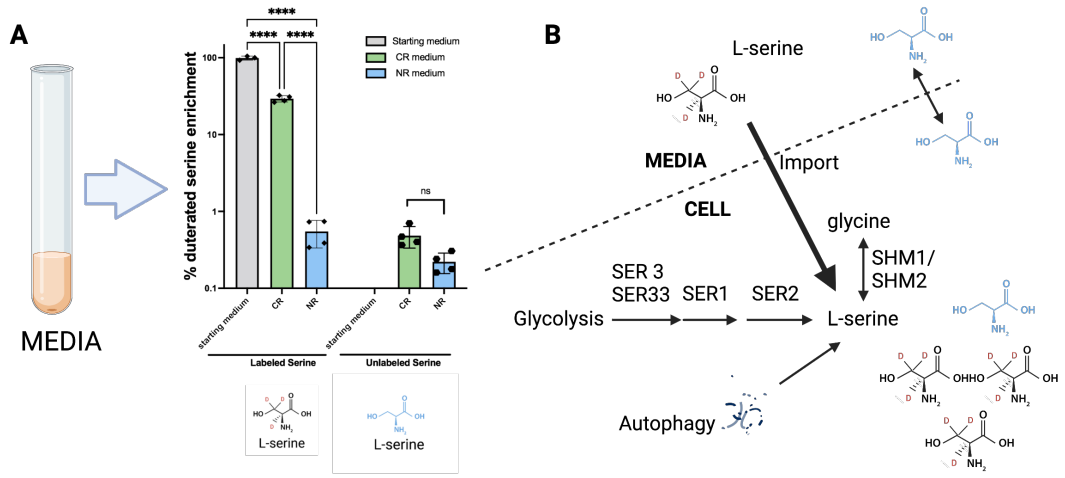

Figure 6.1 Tracing experiments show L-serine becomes depleted in NR and remains underutilized in CR. *(A) Levels of labeled and unlabeled L-serine in the media of NR and CR. Used [2,3,3-2H] serine, a stable isotope tracer to understand serine flux and found that [2,3,3-2H] serine levels are low at 96 hours in CR (green) and NR (blue) compared to starting medium (gray) (n=3). Unlabeled L-serine is also measured and found to be present at 95hours in the conditioned media. B) Schematic of unlabeled serine derived from glycolysis via the serine synthesis pathway (SSP), the one-carbon metabolism (OCM) or macroautophagy of proteins. This unlabeled serine could then be exported into the media where it is detected. Schematic also shows isotope labeled serine is removed from the media via import into the cell.*

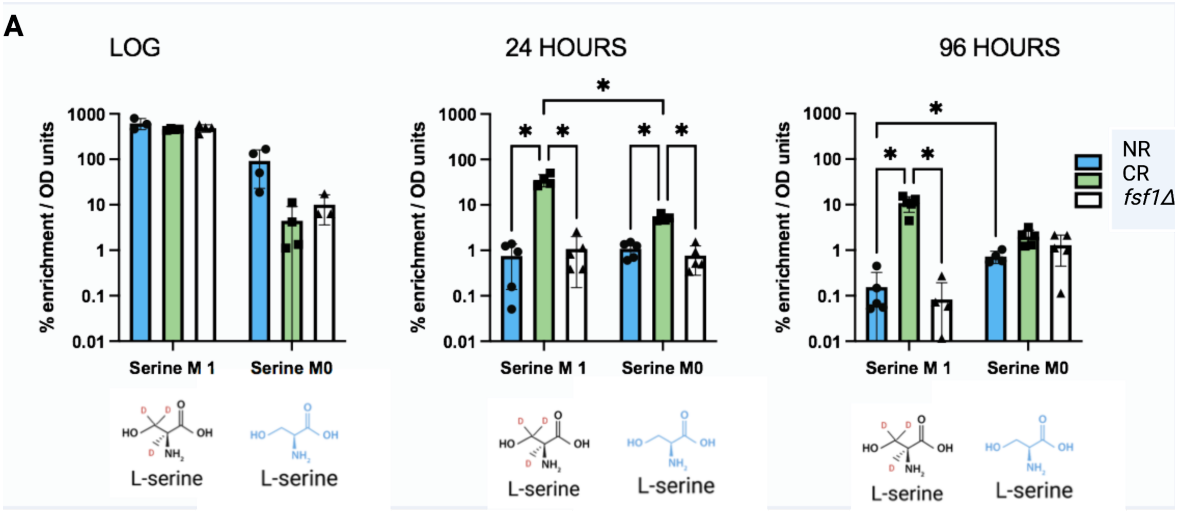

Figure 6.2 Tracing experiments show L-serine levels in the cell*. (A) Levels of labeled and unlabeled L-serine measured in cell extracts of NR and CR. Values are normalized to OD600 units. Used [2,3,3-2H] serine, a stable isotope tracer to understand serine flux and found that intracellular[2,3,3-2H] serine levels remain high (green), compared to NR (blue) and fsf1Δ (white) (n=5). M1 refers to labeled serine. M0 refers to unlabeled serine.*

Where is L-serine metabolized?

We previously showed that L-serine-mediated lifespan extension depended on the OCM enzymes like SHM1p and SHM2p (Enriquez-Hesles et al., 2021; Matecic et al., 2010). However, we wanted to understand whether the cell preferred the mitochondrial arm or the cytosolic arm of the OCM. By knowing how L-serine is catabolized we would derive additional clues on how it mediates longevity. We hypothesized that although L-serine was not increasing most nucleotide levels (previous Chapter), it may contribute to TMP via the OCM. We utilized deuterated serine ([2,3,3-2 H]serine) to enable compartment-specific analysis of one-carbon units (Ducker & Rabinowitz, 2017). In addition to measuring L-serine intracellular levels, we also detected TMP. Again, we exposed the cells to 1mM isotope labeled L-serine and omitted unlabeled L-serine from the SC media. At indicated time points we measured unlabeled TMP (TMP 0), which would indicate that TMP is being derived from unlabeled L-serine or another amino acid such as

glycine, or histidine (Meiser & Vazquez, 2016). We also measured TMP plus one deuterated hydrogen (TMP 1), and TMP plus two deuterated hydrogens (TMP 2). TMP 1 would suggest that L-serine is entering the mitochondria to be catabolized and TMP 2 would suggest that L-serine remains in the cytosol and is metabolized by OCM enzymes in the cytosol. Samples were collected at log, 24, and 96 hours. These measurements were normalized to Optical Density, a marker for cell number. We see that TMP levels peak at 24 hours (Figure 6.3B). These results suggest that TMP from L-serine is obtained through the mitochondria and cytoplasm in the NR and CR condition. Furthermore, it does not depend on the presence of Fsf1p (Figure 6.3B) suggesting that there is an alternative way for serine to be catabolized in the mitochondria. I propose that serine is being formed from glycine which, like serine, can also enter the mitochondria. In addition to serine-specific mitochondrial transport, there are also glycine specific transporters in yeast (Hem25p)(Dufay et al., 2017). I predict that knocking out Fsf1p augmented glycine flux through the Hem25p transporter. To observe an effect, both glycine and serine mitochondrial transported would have to be removed, and I expect this combination to be synthetically lethal.

Does L-serine enhance mitochondrial function?

It has been well established that yeast change their metabolism in the diauxic shift and rely on oxidative phosphorylation in the stationary phase to generate ATP and survive in the stationary phase (Dickinson, 1998; MacLean et al., 2001). CR-mediated longevity has partially been attributed to a shift in metabolism from fermentation to aerobic respiration (Lin et al., 2002; Wierman et al., 2017). Previous data from our lab show that non-fermentable carbon sources extend CLS at NR concentrations, which suggest respiration offers lifespan benefits (Smith Jr. et al., 2007). We have already shown that L-serine supplementation does not induce consumption

of acetic acid as CR cells (Enriquez-Hesles et al., 2021). Could L-serine improve mitochondrial function in some other way? Interestingly, a link exists between L-serine catabolism in the mitochondria, mitochondrial translation, and oxidative phosphorylation (Morscher et al., 2018). The tracing of stable isotope-labeled L-serine suggested that L-serine was not preferentially being catabolized through OCM in the mitochondria suggesting there may be little effect on respiration or ATP production. However, it has been shown that L-serine-derived lipids, ceramides, are essential for mitochondrial function (Gao et al., 2018). To further investigate the possibility that L-serine supplementation may enhance mitochondrial health we conducted ATP measurements and optimized Seahorse Assays for yeast. Studies from our lab suggest that L-serine supplementation has no effect on intracellular ATP levels (Figure 6.4 C).

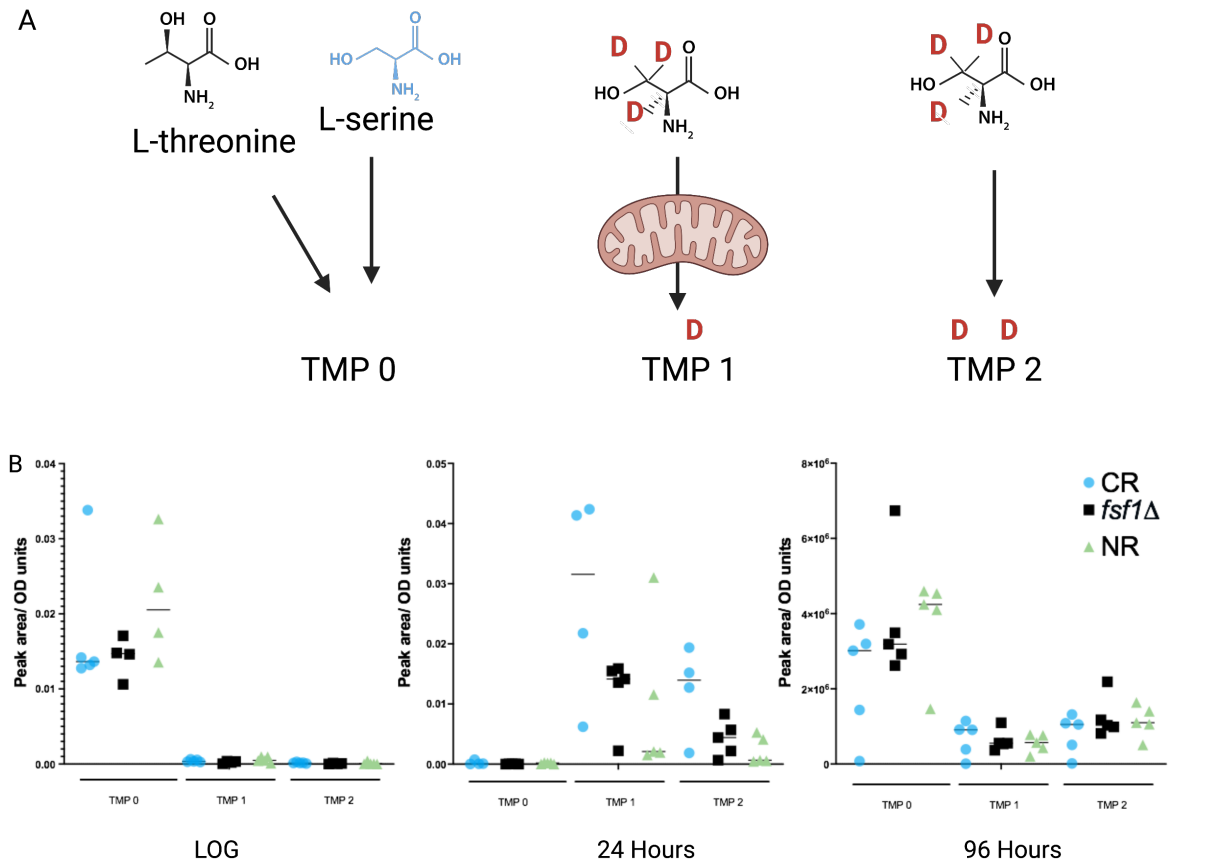

Figure 6.3 NR and CR treated cells use L-serine to derive TMP through the mitochondria and cytoplasm. *A) The left schematic shows sources of unlabeled TMP or TMP 0. The middle panel*

shows labeled L-serine being metabolized within the mitochondria to formate and losing two deuterons. In the right panel labeled L-serine is catabolized in the cytosol and loses one of the deuterium molecules. (B) Intracellular TMP0, TMP 1 and TMP 2 were accessed and normalized to OD units. Mean ± S.D. N=5.While using [2,3,3-2H] serine, an isotope tracer to understand serine flux, we observed that [2,3,3-2H] serine diminishes over time in CR and NR compared to starting medium (n=3).

In parallel to ATP studies, we optimized Seahorse Analyzer assays measuring mitochondria function as measured by their oxygen consumption rate (OCR) (Figure 6.4A-B). Although original assays were designed for mammalian cells, we optimized the system for measuring OCR in yeast. Based on our preliminary findings, we found that L-serine addition does not increase OCR using Seahorse Analyzer. However, CR cells have increased OCR as expected. These assays were conducted at 24 hours to ensure that all cells remained viable. The OCR profile was generated by injecting mitochondrial ATP synthase inhibitor oligomycin (10uM) and normalized to cell number. We also tested the difference between using conditioned medium or glucose free medium (data not shown). While we did not see a significant effect with L-serine, we now have the assay established for future studies thanks to Katie Pavelec and Norbert Leitinger's lab. Our results suggest that L-serine and CR extend lifespan *via* different mechanisms. While CR enhances respiration, L-serine addition does not. Although it's been shown that L-serine-mediated lifespan depends partially on the OCM, we had hoped to generate an in depth understanding of this mechanism. Future studies could utilize L-serine-3-^{13}C to conduct targeted metabolomic analysis.

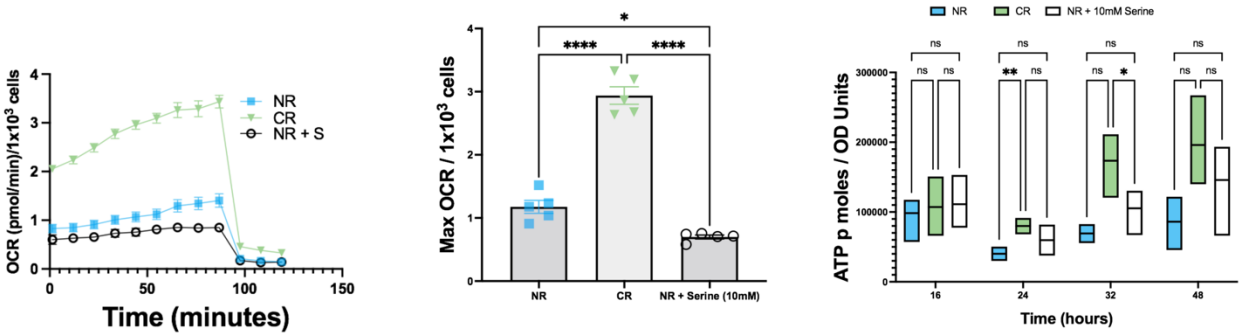

Figure 6.4 NR + L-serine and CR extend lifespan via different mechanisms. *(A) Oxygen Consumption rate (OCR) data normalized to cell number in NR, CR, and NR+ L-serine cultures grown to 24 hours. The Max OCR is shown in B with Mean ± S.D. N=5. C) In a separate experiment, intracellular ATP measurements were obtained in NR, CR, and NR + 10mM L-serine.*

D-serine extends longevity via an uncharacterized mechanism

We originally hypothesized that D-serine could potentially be utilized by yeast through an uncharacterized mechanism. To test this hypothesis, we first supplemented NR cultures of BY4741 with the presumably non-utilized stereoisomer D-serine (Enriquez-Hesles et al., 2021). We confirmed its inactivity by showing that 5- or 30-mM D-serine could not rescue the partial L-serine auxotrophic phenotype of a *ser2*Δ mutant in SC minus L-serine media (Figure 6.5 D-G). D-serine supplementation into BY4741 NR cultures had no effect on CLS at 5 mM (Figure 6.5 B). Consistent with the lack of D-serine utilization, titration of increasing concentrations did not further extend CLS unlike L-serine (Figure 6.5 E and F). Instead, we hypothesized that D-serine may have stronger media pH buffering capacity compared to L-serine. However, this was not the case as D-serine had absolutely no buffering capacity Figure 6.5 G. This suggested that the buffering capacity of L-serine is related to its metabolism. D-serine, on the other hand, extends CLS through an unknown mechanism.

In this Chapter as we explored the underlying longevity mechanisms, more questions than answers emerged. Consequently, the next step of this project is to conduct an untargeted mRNA-seq experiment and a tracing experiment to understand how L-serine and D-serine are being utilized.

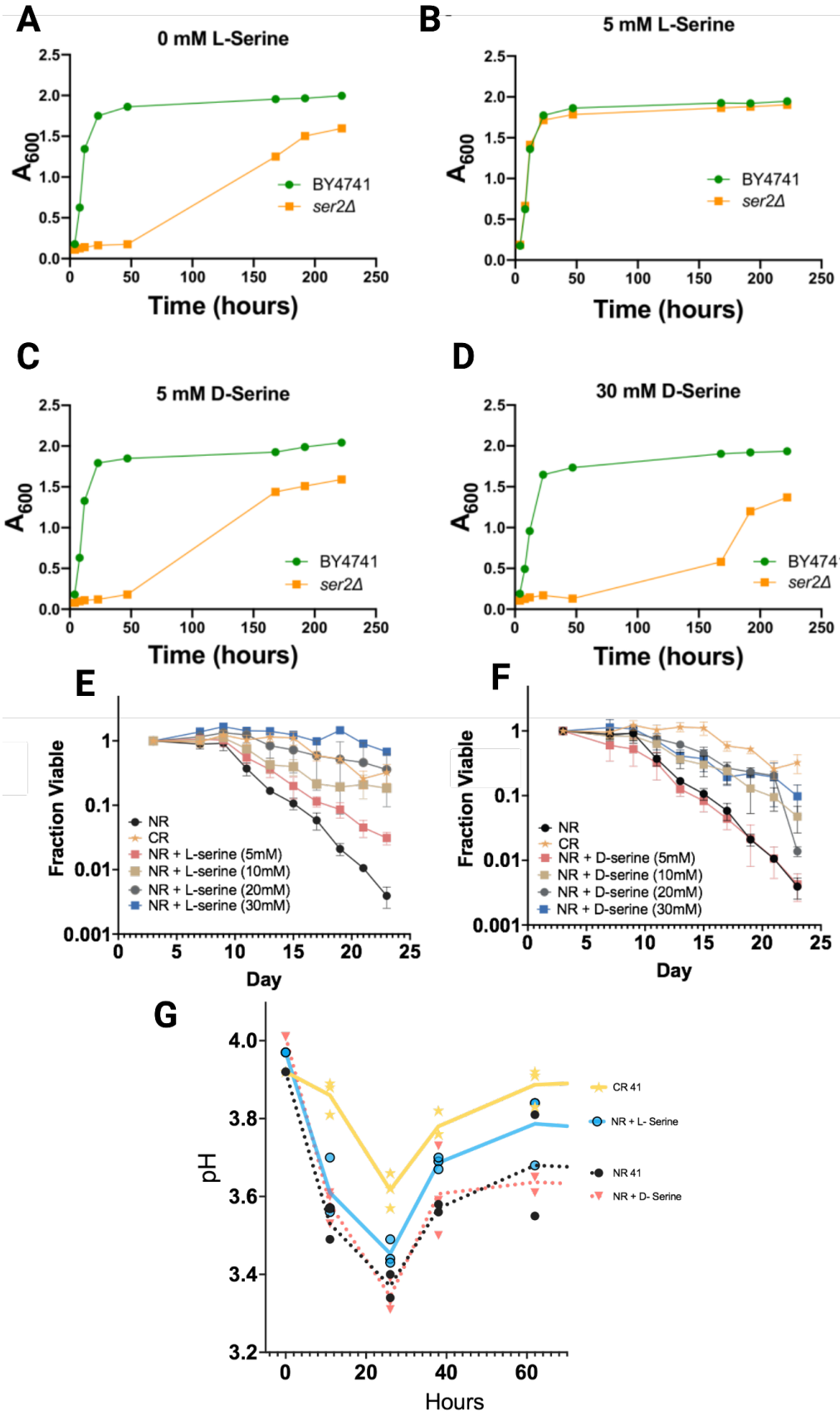
A
0 mM L-Serine
A600
Time (hours)
BY4741
ser2Δ
B
5 mM L-Serine
C
5 mM D-Serine
D
30 mM D-Serine
E
Fraction Viable
Day
NR
CR
NR + L-serine (5mM)
NR + L-serine (10mM)
NR + L-serine (20mM)
NR + L-serine (30mM)
F
NR + D-serine (5mM)
NR + D-serine (10mM)
NR + D-serine (20mM)
NR + D-serine (30mM)
G
pH
Hours
CR 41
NR + L- Serine
NR 41
NR + D- Serine

***Figure 6.5 D-serine and L-serine are not metabolized similarly**. Analysis of L-serine and D-serine effects on CLS and cell growth(A-D) Growth curves of BY4741 and ser2Δ mutant in SC-serine media supplemented with the indicated concentrations of L-serine or D-serine (mean, n=2). E) L-serine extends CLS of BY4741 in a dose-dependent manner. F) D-serine extends CLS of BY474. G) Although it initially elevates pH levels, D-serine fails to buffer liquid culture like CR or NR+L-serine.*

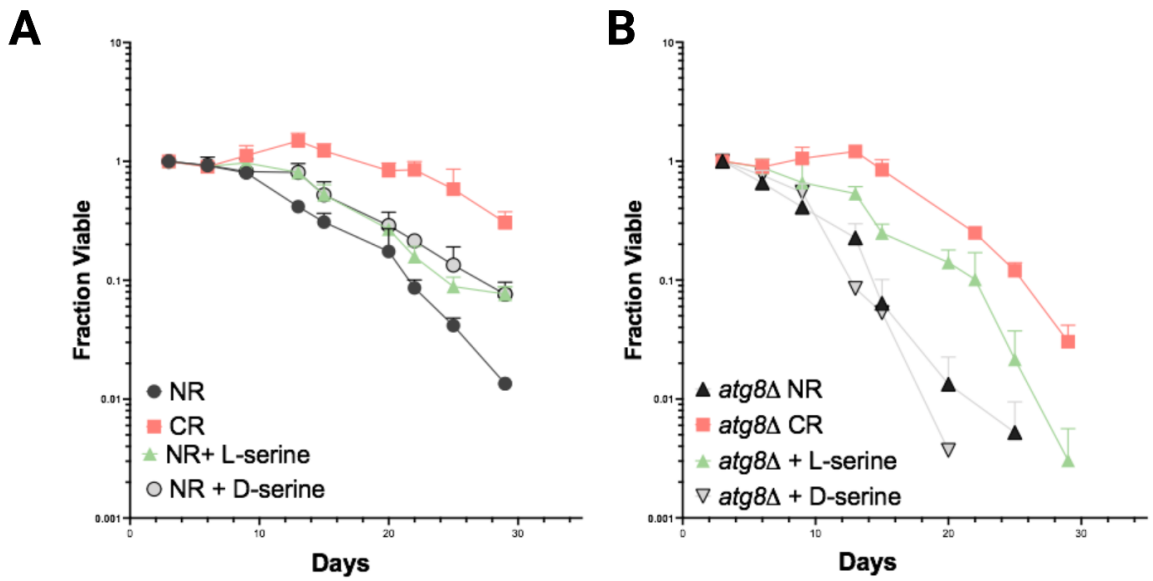

***Figure 6.6 Preliminary experiments show that D-serine-mediated longevity could rely on autophagy activation.** A) L-serine and D-serine supplementation extends CLS of BY4741 when added at 10mM concentration as previously shown. CR also extends lifespan relative to NR in By4741. B) L-serine supplementation, but not D-serine extends lifespan in atg8 mutant.*

Autophagy is essential for D-serine induced longevity

To further investigate the role of D-serine in CLS extension, we turned our attention to autophagy. Autophagy is well-established as being a mediator of other lifespan extending regimens in yeast and other models (Bareja et al., 2019). When we tested whether L-serine CLS extension required autophagy in the previous Chapter, we also tested D-serine. As shown in Figure 6.6, preliminary results show that D-serine mediated lifespan extension relies completely

on autophagy pathways. Deletion of *ATG8* completely abolished the gain in longevity that was conferred by D-serine. Considering this discovery, further experiments will be done to evaluate this connection. Other autophagy deficient mutants will be tested. Although D-serine addition has been studied in *C. elegans* (Edwards et al., 2015; Saitoh et al., 2012), the role of D-serine in yeast CLS has not been previously studied. This is potentially very interesting, and we are now conducting experiments in follow-up studies.

L-serine is classified as a non-essential amino acid that can be synthesized endogenously by cells, but rapidly proliferating cells and activated immune cells require an external supply (Amelio et al., 2014; Meiser & Vazquez, 2016). In fact, cancer cells harvest L-serine at a rate that exceeds the serine demand (Dolfi et al., 2013). L-serine serves as a precursor molecule for phospholipids, ATP, NADH and nucleic acid. L-serine has been shown to be a main one-carbon donor in the OCM, a process that occurs in the cytosol, mitochondria and nucleus (Ducker et al., 2016). The mitochondria have proved to be the main source where serine is catabolized (Ducker & Rabinowitz, 2017). In the mitochondria L-serine is a source for NADH generation, pyruvate, and one-carbon units (Maynard & Kanarek, 2020; Meiser & Vazquez, 2016). In the mitochondria, that one carbon results in the generation of methionyl-tRNA formyltransferase (MTFMT) which in turn increase f-Met tRNAs and foster mitochondrial protein synthesis (Lionaki et al., 2022). Based on this data, we hypothesized that L-serine is metabolized within the mitochondria while also enhancing mitochondrial health. However, tracing, ATP measurements, and Seahorse Assay results do not support this hypothesis.

To detect L-serine's utilization, ^{13}C labeled serine should be utilized to explore other possible pathways. With this approach we could look at whether serine contributes to sphingolipids and test whether this extends CLS. It has been reported that the uptake of

exogenous serine is important to maintain sphingolipid homeostasis in *S. cerevisiae* (Esch et al., 2020). However, it remains unknown if this homeostasis is important for CLS. If serine's effect on extending lifespan were mediated by sphingolipid synthesis, inhibiting sphingolipid synthesis would shorten lifespan. Interestingly, downregulation sphingolipid synthesis with myriocin *extends* CLS (Hepowit et al., 2021; Huang et al., 2012). Myriocin is a sphingolipid biosynthetic inhibitor that targets serine palmitoyltransferase (Huang et al., 2012). Perhaps lipids are a major product of serine in the NR condition and myriocin-treatment redirects serine utilization, slowing down growth.

Materials and Methods

Seahorse assays

Seahorse assays were performed with yeast cultures grown overnight in 2% SC media and in the morning new cultures 10 ml cultures were diluted to an OD600 of .05 in SC 2% (with or without L-serine) or SC 0.5% glucose. At 24 hours or indicated time points, 0.5 OD 600 of cells were collected by spinning them, removing expired media, and resuspended in 1 ml of expired media (filtered) or SC media without glucose. 20ul of the cell dilution was added to seed the wells of a Seahorse XF96 cell culture microplate (Agilent) that had been pre-treated with Concanavalin A to enable cell adhesion to the bottom. Plate was coated with Concanavalin A, the day prior by adding 50ul of Concanavalin A solution and incubating overnight in a 30˚C incubator. The wells were washed 3 times with ddH_20 prior to use. Six technical replicates were seeded leaving the background control wells empty. The plate was then centrifuged at 300x for 10 minutes (acceleration 0 and deceleration 0). The Seahorse XF96 Sensor Cartridge was prepared, and oxygen consumption rate (OCR) was measured.

Quantification of intracellular ATP

To extract nucleotides from yeast cells as previously described in (Wierman et al., 2017), an amount equal to 2.5 OD600 units of cells was transferred (at the indicated time points) from 50-ml cultures into 1.5-ml microcentrifuge tubes and pelleted at 1,500 rpm and 4°C. Cells were washed in 1 ml ice-cold Tris-EDTA (TE; 10 mM Tris, 1 mM EDTA, pH 8.0) and suspended in 250 µl LETS buffer (10 mM Tris [pH 8], 100 mM LiCl, 10 mM EDTA, 0.5% SDS). A 250-µl volume of 1:1 phenol-chloroform was added, and the samples were vortexed. The samples were then pelleted at 14,000 rpm in a microcentrifuge at 4°C, and the aqueous supernatants were transferred to a fresh microcentrifuge tube and diluted 1:10 with ice-cold TE buffer. To determine the ATP content of each sample, 4 µl of ATP buffer (30 mM KPO4 [pH 7.3], 40 mM MgSO4, 8% Tween 20) was added to 8 µl of sample. After incubation at room temperature for 10 min, 4 µl of AXP buffer (30 mM KPO4 [pH 7.3], 40 mM MgSO4) was added, and the samples were incubated for an additional 30 min at 30°C. A 10-µl volume of each sample was then pipetted into a white 96-well plate to determine ATP content using the ATP Determination kit (Invitrogen) in accordance with the manufacturer's instruction.

TMP and L-serine tracing

Cells were grown in 10 mL SC 2% glucose with 1 mM isotope labeled L-serine (unlabeled L-serine was omitted) on a roller drum. For each biological replicate three 10 mL cultures were grown so that 9 mL could be collected at each time point. Cultures were started from SC 2% overnight liquid cultures at OD_{600} adjusted to 0.05. ODs of cultures were measured before collection for normalization of metabolites. 1 mL of media was collected at the start and the end of the experiment. Cells were collected at log phase, 24 hr, and 96 hr. Intracellular metabolites were isolated as previously described in (Kalita et al., 2021).

Mass spectrometry

Metabolites were analyzed as at the UVA core. Peak areas were normalized to respective OD_{600} of each sample.

Acknowledgements

I thank Chris Prevost for pointing me to Shona Mukherjee. I thank Shona for sharing her Seahorse protocol with us. We also thank Katie Pavelec and the Leitinger lab for the use of the Seahorse apparatus and plate reader. We also thank Leah Gunnie for her work in optimizing these experiments.

Chapter VII

Discussion and Future Directions

Although age is often categorized as a non-modifiable risk factor, research suggests that the rate of aging in model organisms, ranging from yeast to mice, may be altered genetically or through dietary or CR (Belsky et al., 2017). CR consists of reduced food intake with adequate nutrition. This dietary regimen delays or prevents age-related diseases and improves cellular function in multiple model organisms, thus extending healthy aging, as well as lifespan (Belsky et al., 2017; Fontana et al., 2010). However, currently there are no nutritional regimens that are completely accepted by the scientific or medical community to prevent aging in humans with clinical trials only recently beginning for CR-mimetics, metformin in humans (ClinicalTrials.gov Identifier: NCT03477162) and rapamycin in dogs (Urfer et al., 2017). Thus, understanding CR at the cellular level would open the door to development of targeted therapies for the aging process. Targeting the aging process would have immense impacts on individuals' productivity, our health care system, and the economy. In the future, it seems possible that we will be able to promote longevity pathways and extend healthspan. There is a remarkable study showing that CRISPR-Cas9 was used therapeutically to alleviate suffering of sickle cell disease by targeting an enhancer within DNA (Frangoul et al., 2021). Could CRSPR-Cas 9 be an intervention that helps delay or reverse age associated-diseases? It remains to be seen. In the meantime, other studies suggested that altering the environment, not the cell itself, presents a more feasible opportunity to slow the aging process.

With this project, we have attempted to understand how extrinsic factors, conserved cellular pathways, and cell-non autonomous mechanisms modulate chronological lifespan in yeast. In Chapter II, we discussed the sensitivity of media composition and genetic background in longevity assays. We found that methionine restriction (MetR) via genetic modification (*met15*) and CR both activate polyamine synthesis. This agrees with the growing evidence that

CR and MetR work through overlapping pathways (Hepowit et al., 2021; Hine et al., 2015; Ogawa et al., 2022; Ogawa et al., 2016; Zou et al., 2020). Polyamines may be a point of convergence for longevity in CLS with these manipulations. Future experiments need to focus on understanding if and what aspects of the polyamine synthesis pathways are causative for longevity in BY4741 background and under CR conditions. It would be important to determine whether the long-lived *ADE* mutants also upregulate this pathway.

Scientists studying aging have focused on measuring lifespan, however, our goal in the aging field has shifted from looking for the fountain of longevity to looking for the fountain of health. Thus, we need to design our experiments to reflect this priority. How do we assess health in yeast? We set out to find a healthspan marker in yeast, a unicellular organism. We thought that quiescence, if uncoupled from viability, could represent a healthspan measurement that we could rely on. However, in this search for a healthspan marker we found that senescence in chronologically aged cells is negligible (Chapter III). This agrees with the previous studies (Alvers et al., 2009). Although this result discounts quiescence as a healthspan marker and may discount CLS as a good model for senescence, CLS could still serve as a tool to find senescent relevant genes. Genes promoting senescence in the chronological yeast population could be tested by finding discrepancies between proliferative capacity and viability using the YKO collection. Specifically, viable cells with low proliferative capacity would represent a population with a genetic profile that promotes senescence. Further studies need to ensure if this negligible senescence occurs across conditions and strains.

We identified amino acids as extending lifespan in a cell non-autonomous mechanism when CR conditioned media (CRCM) was transferred to NR cells (Chapter IV). This study showed that amino acids are depleted in the NR condition and limiting for longevity. One

unexplored possibility is that amino acids are being consumed during NR for translation and protein synthesis. Indeed, we found that replenishing specific amino acids such as L-serine extended lifespan in a dose-dependent manner. In the NR condition, we found that the effect of L-serine on lifespan hinges on the OCM pathway. However, this longevity effect was not specific to L-serine. Arginine was an amino acid with the most impact on longevity. Both amino acids have been shown to be overrepresented in codons in yeast (Alvers et al., 2009). Furthermore, D-serine emerged as an additional amino acid extending longevity. Understanding the mechanism by which arginine, D-serine, and L-serine mediate lifespan is an important goal of the laboratory. We have shown that L-serine supplementation and CR extend lifespan through different mechanisms (Chapter V). To continue understanding L-serine and D-serine's mechanism, we have isolated RNA samples for mRNAseq analysis at log, 24, and 96 hours. This study will be valuable as spike-in controls were utilized and we will be able to determine the relative transcript levels at each of these time points and whether their levels are influenced by NR, CR, and NR + L-serine or NR + D-serine. In addition, this RNA-seq will offer some clues to what genes are involved in mediating lifespan in each of these conditions. These RNA-seq data coupled with the YKO can play an important role in dissecting functional pathways in longevity. To my knowledge, D-stereoisomers have not been tested in yeast in the context of aging. Although benefits of D-serine supplementation are emerging in the brain via augmenting NMDA receptor function (Nava-Gomez et al., 2022), other mechanisms remain undiscovered. Preliminary studies in Chapter VI suggest that D-serine could perhaps mediate these benefits via autophagy activation. Autophagy will be assayed using a GFP-Atg8 expression plasmid which encodes a chimeric protein that is delivered to the vacuole. In the vacuole, Atg8p is degraded and GFP persists and has been used as a marker for activation of autophagy (Klionsky, 2011). We

will use CR as a control because autophagy has been observed in CR even when amino acids are abundant (Alvers et al., 2009).

Strain List

Strain	Relevant genotype
BY4741	*MAT**a**his3Δ1 leu2Δ0 met15Δ0 ura3Δ0*
atg8Δ	*MAT**a**his3Δ1 leu2Δ0 met15Δ0 ura3Δ0 atg8Δ::kanMX*
cha1 Δ	*MAT**a**his3Δ1 leu2Δ0 met15Δ0 ura3Δ0 cha1Δ::cloNAT*
fsf1Δ	*MAT**a**his3Δ1 leu2Δ0 met15Δ0 ura3Δ0 fsf1Δ::kanMX*
FY4	*Fully prototrophic*
mtd1Δ	*MAT**a**his3Δ1 leu2Δ0 met15Δ0 ura3Δ0 mtd1Δ::kanMX*
phm8Δ	*MAT**a**his3Δ1 leu2Δ0 met15Δ0 ura3Δ0 phm8Δ::kanMX*
ser2Δ	*MAT**a**his3Δ1 leu2Δ0 met15Δ0 ura3Δ0 ser2Δ::kanMX*
shm1Δ	*MAT**a**his3Δ1 leu2Δ0 met15Δ0 ura3Δ0 shm1Δ::kanMX*
shm2Δ	*MAT**a**his3Δ1 leu2Δ0 met15Δ0 ura3Δ0 shm2Δ::kanMX*
SY1083	*MAT**a**his3Δ1 leu2Δ0 ura3Δ0*

References

Agarwal, S., Sharma, S., Agrawal, V., & Roy, N. (2005). Caloric restriction augments ROS defense in S. cerevisiae, by a Sir2p independent mechanism. *Free Radical Research*, *39*(1), 55-62. https://doi.org/10.1080/10715760400022343

Alexaki, A., Kames, J., Holcomb, D. D., Athey, J., Santana-Quintero, L. V., Lam, P. V. N., Hamasaki-Katagiri, N., Osipova, E., Simonyan, V., Bar, H., Komar, A. A., & Kimchi-Sarfaty, C. (2019). Codon and Codon-Pair Usage Tables (CoCoPUTs): Facilitating Genetic Variation Analyses and Recombinant Gene Design. *Journal of Molecular Biology*, *431*(13), 2434-2441. https://doi.org/https://doi.org/10.1016/j.jmb.2019.04.021

Allen, C., Buttner, S., Aragon, A. D., Thomas, J. A., Meirelles, O., Jaetao, J. E., Benn, D., Ruby, S. W., Veenhuis, M., Madeo, F., & Werner-Washburne, M. (2006). Isolation of quiescent and nonquiescent cells from yeast stationary-phase cultures. *J Cell Biol*, *174*(1), 89-100. https://doi.org/10.1083/jcb.200604072

Alvers, A. L., Fishwick, L. K., Wood, M. S., Hu, D., Chung, H. S., Dunn, W. A., Jr., & Aris, J. P. (2009). Autophagy and amino acid homeostasis are required for chronological longevity in Saccharomyces cerevisiae. *Aging Cell*, *8*(4), 353-369. https://doi.org/10.1111/j.1474-9726.2009.00469.x

Amelio, I., Cutruzzola, F., Antonov, A., Agostini, M., & Melino, G. (2014). Serine and glycine metabolism in cancer. *Trends Biochem Sci*, *39*(4), 191-198. https://doi.org/10.1016/j.tibs.2014.02.004

Anderson, D. D., & Stover, P. J. (2009). SHMT1 and SHMT2 are functionally redundant in nuclear de novo thymidylate biosynthesis. *PloS one*, *4*(6), e5839. https://doi.org/10.1371/journal.pone.0005839

Aon, M. A., Bernier, M., Mitchell, S. J., Di Germanio, C., Mattison, J. A., Ehrlich, M. R., Colman, R. J., Anderson, R. M., & de Cabo, R. (2020). Untangling Determinants of Enhanced Health and Lifespan through a Multi-omics Approach in Mice. *Cell Metab*, *32*(1), 100-116 e104. https://doi.org/10.1016/j.cmet.2020.04.018

Aragon, A. D., Rodriguez, A. L., Meirelles, O., Roy, S., Davidson, G. S., Tapia, P. H., Allen, C., Joe, R., Benn, D., & Werner-Washburne, M. (2008). Characterization of differentiated quiescent and nonquiescent cells in yeast stationary-phase cultures. *Mol Biol Cell*, *19*(3), 1271-1280. https://doi.org/10.1091/mbc.e07-07-0666

Aris, J. P., Alvers, A. L., Ferraiuolo, R. A., Fishwick, L. K., Hanvivatpong, A., Hu, D., Kirlew, C., Leonard, M. T., Losin, K. J., Marraffini, M., Seo, A. Y., Swanberg, V., Westcott, J. L., Wood, M. S., Leeuwenburgh, C., & Dunn, W. A., Jr. (2013). Autophagy and leucine promote chronological longevity and respiration proficiency during calorie restriction in yeast. *Exp Gerontol*, *48*(10), 1107-1119. https://doi.org/10.1016/j.exger.2013.01.006

Ashrafi, K., Sinclair, D., Gordon, J. I., & Guarente, L. (1999). Passage through stationary phase advances replicative aging in Saccharomyces cerevisiae. *Proc Natl Acad Sci U S A*, *96*(16), 9100-9105. https://doi.org/10.1073/pnas.96.16.9100

Austad, S. N. (2016). The Geroscience Hypothesis: Is It Possible to Change the Rate of Aging? In F. Sierra & R. Kohanski (Eds.), *Advances in Geroscience* (pp. 1-36). Springer International Publishing. https://doi.org/10.1007/978-3-319-23246-1_1

Austad, S. N., & Hoffman, J. M. (2018). Is antagonistic pleiotropy ubiquitous in aging biology? *Evol Med Public Health*, *2018*(1), 287-294. https://doi.org/10.1093/emph/eoy033

Bach, B., Meudec, E., Lepoutre, J. P., Rossignol, T., Blondin, B., Dequin, S., & Camarasa, C. (2009). New insights into {gamma}-aminobutyric acid catabolism: Evidence for {gamma}-hydroxybutyric acid and polyhydroxybutyrate synthesis in Saccharomyces cerevisiae. *Appl Environ Microbiol*, *75*(13), 4231-4239. https://doi.org/10.1128/aem.00051-09

Bárcena, C., Quirós, P. M., Durand, S., Mayoral, P., Rodríguez, F., Caravia, X. M., Mariño, G., Garabaya, C., Fernández-García, M. T., Kroemer, G., Freije, J. M. P., & López-Otín, C. (2018). Methionine Restriction Extends Lifespan in Progeroid Mice and Alters Lipid and Bile Acid Metabolism. *Cell Reports*, *24*(9), 2392-2403. https://doi.org/https://doi.org/10.1016/j.celrep.2018.07.089

Bareja, A., Lee, D. E., & White, J. P. (2019). Maximizing Longevity and Healthspan: Multiple Approaches All Converging on Autophagy. *Front Cell Dev Biol*, *7*, 183. https://doi.org/10.3389/fcell.2019.00183

Bartke, A., & Quainoo, N. (2018). Impact of Growth Hormone-Related Mutations on Mammalian Aging. *Front Genet*, *9*, 586. https://doi.org/10.3389/fgene.2018.00586

Bartke, A., Sun, L. Y., & Longo, V. (2013). Somatotropic signaling: trade-offs between growth, reproductive development, and longevity. *Physiol Rev*, *93*(2), 571-598. https://doi.org/10.1152/physrev.00006.2012

Belak, Z. R., Harkness, T., & Eskiw, C. H. (2018). A rapid, high-throughput method for determining chronological lifespan in budding yeast. *J Biol Methods*, *5*(4), e106. https://doi.org/10.14440/jbm.2018.272

Bellantuono, A. J., Bridge, D., & Martínez, D. E. (2015). Hydra as a tractable, long-lived model system for senescence. *Invertebr Reprod Dev*, *59*(sup1), 39-44. https://doi.org/10.1080/07924259.2014.938196

Belsky, D. W., Huffman, K. M., Pieper, C. F., Shalev, I., & Kraus, W. E. (2017). Change in the Rate of Biological Aging in Response to Caloric Restriction: CALERIE Biobank Analysis. *J Gerontol A Biol Sci Med Sci*, *73*(1), 4-10. https://doi.org/10.1093/gerona/glx096

Ben-Shem, A., Garreau de Loubresse, N., Melnikov, S., Jenner, L., Yusupova, G., & Yusupov, M. (2011). The structure of the eukaryotic ribosome at 3.0 Å resolution. *Science*, *334*(6062), 1524-1529. https://doi.org/10.1126/science.1212642

Blagosklonny, M. V. (2010). Why human lifespan is rapidly increasing: solving "longevity riddle" with "revealed-slow-aging" hypothesis. *Aging (Albany NY)*, *2*(4), 177-182. https://doi.org/10.18632/aging.100139

Blagosklonny, M. V. (2021). The hyperfunction theory of aging: three common misconceptions. *Oncoscience*, *8*, 103-107. https://doi.org/10.18632/oncoscience.545

Bonafe, M., Barbieri, M., Marchegiani, F., Olivieri, F., Ragno, E., Giampieri, C., Mugianesi, E., Centurelli, M., Franceschi, C., & Paolisso, G. (2003). Polymorphic variants of insulin-like growth factor I (IGF-I) receptor and phosphoinositide 3-kinase genes affect IGF-I plasma levels and human longevity: cues for an evolutionarily conserved mechanism of life span

control. *J Clin Endocrinol Metab*, *88*(7), 3299-3304. https://doi.org/10.1210/jc.2002-021810
Borten, M. A., Bajikar, S. S., Sasaki, N., Clevers, H., & Janes, K. A. (2018). Automated brightfield morphometry of 3D organoid populations by OrganoSeg. *Sci Rep*, *8*(1), 5319. https://doi.org/10.1038/s41598-017-18815-8
Broer, S., & Gauthier-Coles, G. (2022). Amino Acid Homeostasis in Mammalian Cells with a Focus on Amino Acid Transport. *J Nutr*, *152*(1), 16-28. https://doi.org/10.1093/jn/nxab342
Brown-Borg, H. M. (2006). Longevity in mice: is stress resistance a common factor? *Age (Dordr)*, *28*(2), 145-162. https://doi.org/10.1007/s11357-006-9003-y
Brown-Borg, H. M., Borg, K. E., Meliska, C. J., & Bartke, A. (1996). Dwarf mice and the ageing process. *Nature*, *384*(6604), 33. https://doi.org/10.1038/384033a0
Burhans, W. C., & Weinberger, M. (2007). DNA replication stress, genome instability and aging. *Nucleic Acids Res*, *35*(22), 7545-7556. https://doi.org/10.1093/nar/gkm1059
Burke, D., Dawson, D., & Stearns, T. (2000). *Methods in Yeast Genetics* (2000 Edition ed.). Cold Spring Harbor Laboratory Press.
Burtner, C. R., Murakami, C. J., Kennedy, B. K., & Kaeberlein, M. (2009). A molecular mechanism of chronological aging in yeast. *Cell Cycle*, *8*(8), 1256-1270. https://doi.org/10.4161/cc.8.8.8287
Calahan, D., Dunham, M., DeSevo, C., & Koshland, D. E. (2011). Genetic analysis of desiccation tolerance in Sachharomyces cerevisiae. *Genetics*, *189*(2), 507-519. https://doi.org/10.1534/genetics.111.130369
Carpenter, A. E., Jones, T. R., Lamprecht, M. R., Clarke, C., Kang, I. H., Friman, O., Guertin, D. A., Chang, J. H., Lindquist, R. A., Moffat, J., Golland, P., & Sabatini, D. M. (2006). CellProfiler: image analysis software for identifying and quantifying cell phenotypes. *Genome Biology*, *7*(10), R100. https://doi.org/10.1186/gb-2006-7-10-r100
Casatta, N., Porro, A., Orlandi, I., Brambilla, L., & Vai, M. (2013). Lack of Sir2 increases acetate consumption and decreases extracellular pro-aging factors. *Biochimica et Biophysica Acta (BBA) - Molecular Cell Research*, *1833*(3), 593-601. https://doi.org/https://doi.org/10.1016/j.bbamcr.2012.11.008
Cerletti, M., Jang, Y. C., Finley, L. W., Haigis, M. C., & Wagers, A. J. (2012). Short-term calorie restriction enhances skeletal muscle stem cell function. *Cell Stem Cell*, *10*(5), 515-519. https://doi.org/10.1016/j.stem.2012.04.002
Chadwick, S. R., Pananos, A. D., Di Gregorio, S. E., Park, A. E., Etedali-Zadeh, P., Duennwald, M. L., & Lajoie, P. (2016). A Toolbox for Rapid Quantitative Assessment of Chronological Lifespan and Survival in Saccharomyces cerevisiae. *Traffic*, *17*(6), 689-703. https://doi.org/10.1111/tra.12391
Chaib, S., Tchkonia, T., & Kirkland, J. L. (2022). Cellular senescence and senolytics: the path to the clinic. *Nature Medicine*, *28*(8), 1556-1568. https://doi.org/10.1038/s41591-022-01923-y
Chan, P. Y., & Cossins, E. A. (1972). Regulation of arginase levels by urea and intermediates of the Krebs-Henseleit cycle in Saccharomyces cerevisiae. *FEBS Lett*, *19*(4), 335-339. https://doi.org/10.1016/0014-5793(72)80074-7

Chattopadhyay, M. K., Tabor, C. W., & Tabor, H. (2006). Methylthioadenosine and polyamine biosynthesis in a Saccharomyces cerevisiae meu1delta mutant. *Biochem Biophys Res Commun*, *343*(1), 203-207. https://doi.org/10.1016/j.bbrc.2006.02.144

Chen, H., & Fink, G. R. (2006). Feedback control of morphogenesis in fungi by aromatic alcohols. *Genes Dev*, *20*(9), 1150-1161. https://doi.org/10.1101/gad.1411806

Chew, S. Y., Chee, W. J. Y., & Than, L. T. L. (2019). The glyoxylate cycle and alternative carbon metabolism as metabolic adaptation strategies of Candida glabrata: perspectives from Candida albicans and Saccharomyces cerevisiae. *J Biomed Sci*, *26*(1), 52. https://doi.org/10.1186/s12929-019-0546-5

Choi, J. S., & Lee, C. K. (2013). Maintenance of cellular ATP level by caloric restriction correlates chronological survival of budding yeast. *Biochem Biophys Res Commun*, *439*(1), 126-131. https://doi.org/10.1016/j.bbrc.2013.08.014

Choi, K.-M., Hong, S.-J., van Deursen, J. M., Kim, S., Kim, K. H., & Lee, C.-K. (2017). Caloric Restriction and Rapamycin Differentially Alter Energy Metabolism in Yeast. *The Journals of Gerontology: Series A*, *73*(1), 29-38. https://doi.org/10.1093/gerona/glx024

Chong, J., Wishart, D. S., & Xia, J. (2019). Using MetaboAnalyst 4.0 for Comprehensive and Integrative Metabolomics Data Analysis. *Curr Protoc Bioinformatics*, *68*(1), e86. https://doi.org/10.1002/cpbi.86

Cohen, R., & Engelberg, D. (2007). Commonly used Saccharomyces cerevisiae strains (e.g. BY4741, W303) are growth sensitive on synthetic complete medium due to poor leucine uptake. *FEMS Microbiology Letters*, *273*(2), 239-243. https://doi.org/10.1111/j.1574-6968.2007.00798.x

Colman, R. J., Anderson, R. M., Johnson, S. C., Kastman, E. K., Kosmatka, K. J., Beasley, T. M., Allison, D. B., Cruzen, C., Simmons, H. A., Kemnitz, J. W., & Weindruch, R. (2009). Caloric restriction delays disease onset and mortality in rhesus monkeys. *Science*, *325*(5937), 201-204. https://doi.org/10.1126/science.1173635

Conboy, M. J., Conboy, I. M., & Rando, T. A. (2013). Heterochronic parabiosis: historical perspective and methodological considerations for studies of aging and longevity. *Aging Cell*, *12*(3), 525-530. https://doi.org/10.1111/acel.12065

Cooper, E. L. (1994). Invertebrates can tell us something about senescence. *Aging (Milano)*, *6*(1), 5-23. https://doi.org/10.1007/bf03324208

Coppe, J. P., Desprez, P. Y., Krtolica, A., & Campisi, J. (2010). The senescence-associated secretory phenotype: the dark side of tumor suppression. *Annu Rev Pathol*, *5*, 99-118. https://doi.org/10.1146/annurev-pathol-121808-102144

Cox, P. A., & Metcalf, J. S. (2017). Traditional Food Items in Ogimi, Okinawa: l-Serine Content and the Potential for Neuroprotection. *Curr Nutr Rep*, *6*(1), 24-31. https://doi.org/10.1007/s13668-017-0191-0

Crepin, L., Nidelet, T., Sanchez, I., Dequin, S., & Camarasa, C. (2012). Sequential use of nitrogen compounds by Saccharomyces cerevisiae during wine fermentation: a model based on kinetic and regulation characteristics of nitrogen permeases. *Appl Environ Microbiol*, *78*(22), 8102-8111. https://doi.org/10.1128/aem.02294-12

Croft, T., Venkatakrishnan, P., & Lin, S. J. (2020). NAD(+) Metabolism and Regulation: Lessons From Yeast. *Biomolecules*, *10*(2). https://doi.org/10.3390/biom10020330

Cwalinski, T., Polom, W., Marano, L., Roviello, G., D'Angelo, A., Cwalina, N., Matuszewski, M., Roviello, F., Jaskiewicz, J., & Polom, K. (2020). Methylene Blue-Current Knowledge, Fluorescent Properties, and Its Future Use. *J Clin Med*, *9*(11). https://doi.org/10.3390/jcm9113538

D'Mello, N. P., & Jazwinski, S. M. (1991). Telomere length constancy during aging of Saccharomyces cerevisiae. *J Bacteriol*, *173*(21), 6709-6713. https://doi.org/10.1128/jb.173.21.6709-6713.1991

da Cunha, F. M., Demasi, M., & Kowaltowski, A. J. (2011). Aging and calorie restriction modulate yeast redox state, oxidized protein removal, and the ubiquitin–proteasome system. *Free Radical Biology and Medicine*, *51*(3), 664-670. https://doi.org/https://doi.org/10.1016/j.freeradbiomed.2011.05.035

Dańko, M. J., Kozłowski, J., & Schaible, R. (2015). Unraveling the non-senescence phenomenon in Hydra. *Journal of Theoretical Biology*, *382*, 137-149. https://doi.org/https://doi.org/10.1016/j.jtbi.2015.06.043

Davey, H. M., & Hexley, P. (2011). Red but not dead? Membranes of stressed Saccharomyces cerevisiae are permeable to propidium iodide. *Environmental Microbiology*, *13*(1), 163-171. https://doi.org/https://doi.org/10.1111/j.1462-2920.2010.02317.x

de Cabo, R., & Mattson, M. P. (2019). Effects of Intermittent Fasting on Health, Aging, and Disease. *N Engl J Med*, *381*(26), 2541-2551. https://doi.org/10.1056/NEJMra1905136

Delfarah, A., Parrish, S., Junge, J. A., Yang, J., Seo, F., Li, S., Mac, J., Wang, P., Fraser, S. E., & Graham, N. A. (2019). Inhibition of nucleotide synthesis promotes replicative senescence of human mammary epithelial cells. *Journal of Biological Chemistry*, *294*(27), 10564-10578. https://doi.org/10.1074/jbc.RA118.005806

DeRisi, J. L., Iyer, V. R., & Brown, P. O. (1997). Exploring the metabolic and genetic control of gene expression on a genomic scale. *Science*, *278*(5338), 680-686. https://doi.org/10.1126/science.278.5338.680

Dhawan, J., & Laxman, S. (2015). Decoding the stem cell quiescence cycle--lessons from yeast for regenerative biology. *J Cell Sci*, *128*(24), 4467-4474. https://doi.org/10.1242/jcs.177758

Diaz-Ruiz, R., Rigoulet, M., & Devin, A. (2011). The Warburg and Crabtree effects: On the origin of cancer cell energy metabolism and of yeast glucose repression. *Biochim Biophys Acta*, *1807*(6), 568-576. https://doi.org/10.1016/j.bbabio.2010.08.010

Dickinson, J. R. (1998). *Metabolism and molecular physiology of Saccharomyces cerevisiae*. Taylor & Francis.

Dolfi, S. C., Chan, L. L.-Y., Qiu, J., Tedeschi, P. M., Bertino, J. R., Hirshfield, K. M., Oltvai, Z. N., & Vazquez, A. (2013). The metabolic demands of cancer cells are coupled to their size and protein synthesis rates. *Cancer & Metabolism*, *1*(1), 20. https://doi.org/10.1186/2049-3002-1-20

Dong, Z., Richie, J. P., Gao, X., Al-Shaar, L., Nichenametla, S. N., Shen, B., & Orentreich, D. (2022). Cumulative Consumption of Sulfur Amino Acids and Risk of Diabetes: a Prospective Cohort Study. *J Nutr*. https://doi.org/10.1093/jn/nxac172

Ducker, G. S., Chen, L., Morscher, R. J., Ghergurovich, J. M., Esposito, M., Teng, X., Kang, Y., & Rabinowitz, J. D. (2016). Reversal of Cytosolic One-Carbon Flux Compensates for Loss of

the Mitochondrial Folate Pathway. *Cell Metab*, *23*(6), 1140-1153. https://doi.org/10.1016/j.cmet.2016.04.016
Ducker, G. S., & Rabinowitz, J. D. (2017). One-Carbon Metabolism in Health and Disease. *Cell Metab*, *25*(1), 27-42. https://doi.org/10.1016/j.cmet.2016.08.009
Dufay, J. N., Fernández-Murray, J. P., & McMaster, C. R. (2017). SLC25 Family Member Genetic Interactions Identify a Role for HEM25 in Yeast Electron Transport Chain Stability. *G3 (Bethesda)*, *7*(6), 1861-1873. https://doi.org/10.1534/g3.117.041194
Dunlop, R. A., & Carney, J. M. (2020). Mechanisms of L-Serine-Mediated Neuroprotection Include Selective Activation of Lysosomal Cathepsins B and L. *Neurotox Res*. https://doi.org/10.1007/s12640-020-00168-2
Dunlop, R. A., Powell, J., Guillemin, G. J., & Cox, P. A. (2018). Mechanisms of L-Serine Neuroprotection in vitro Include ER Proteostasis Regulation. *Neurotox Res*, *33*(1), 123-132. https://doi.org/10.1007/s12640-017-9829-3
Duthie, S. J., Narayanan, S., Brand, G. M., Pirie, L., & Grant, G. (2002). Impact of folate deficiency on DNA stability. *J Nutr*, *132*(8 Suppl), 2444S-2449S. https://doi.org/10.1093/jn/132.8.2444S
Edwards, C., Canfield, J., Copes, N., Brito, A., Rehan, M., Lipps, D., Brunquell, J., Westerheide, S. D., & Bradshaw, P. C. (2015). Mechanisms of amino acid-mediated lifespan extension in Caenorhabditis elegans. *BMC Genet*, *16*, 8. https://doi.org/10.1186/s12863-015-0167-2
Eisenberg, T., Knauer, H., Schauer, A., Büttner, S., Ruckenstuhl, C., Carmona-Gutierrez, D., Ring, J., Schroeder, S., Magnes, C., Antonacci, L., Fussi, H., Deszcz, L., Hartl, R., Schraml, E., Criollo, A., Megalou, E., Weiskopf, D., Laun, P., Heeren, G., . . . Madeo, F. (2009). Induction of autophagy by spermidine promotes longevity. *Nature Cell Biology*, *11*(11), 1305-1314. https://doi.org/10.1038/ncb1975
Eisenberg, T., Knauer, H., Schauer, A., Buttner, S., Ruckenstuhl, C., Carmona-Gutierrez, D., Ring, J., Schroeder, S., Magnes, C., Antonacci, L., Fussi, H., Deszcz, L., Hartl, R., Schraml, E., Criollo, A., Megalou, E., Weiskopf, D., Laun, P., Heeren, G., . . . Madeo, F. (2009). Induction of autophagy by spermidine promotes longevity. *Nat Cell Biol*, *11*(11), 1305-1314. https://doi.org/10.1038/ncb1975
Enriquez-Hesles, E., Smith, D. L., Jr., Maqani, N., Wierman, M. B., Sutcliffe, M. D., Fine, R. D., Kalita, A., Santos, S. M., Muehlbauer, M. J., Bain, J. R., Janes, K. A., Hartman, J. L. t., Hirschey, M. D., & Smith, J. S. (2021). A cell-nonautonomous mechanism of yeast chronological aging regulated by caloric restriction and one-carbon metabolism. *Journal of Biological Chemistry*, *296*, 100125. https://doi.org/10.1074/jbc.RA120.015402
Esch, B. M., Limar, S., Bogdanowski, A., Gournas, C., More, T., Sundag, C., Walter, S., Heinisch, J. J., Ejsing, C. S., Andre, B., & Frohlich, F. (2020). Uptake of exogenous serine is important to maintain sphingolipid homeostasis in Saccharomyces cerevisiae. *PLoS Genet*, *16*(8), e1008745. https://doi.org/10.1371/journal.pgen.1008745
Fabrizio, P., Battistella, L., Vardavas, R., Gattazzo, C., Liou, L. L., Diaspro, A., Dossen, J. W., Gralla, E. B., & Longo, V. D. (2004). Superoxide is a mediator of an altruistic aging program in Saccharomyces cerevisiae. *J Cell Biol*, *166*(7), 1055-1067. https://doi.org/10.1083/jcb.200404002

Fabrizio, P., Liou, L. L., Moy, V. N., Diaspro, A., Valentine, J. S., Gralla, E. B., & Longo, V. D. (2003). SOD2 functions downstream of Sch9 to extend longevity in yeast. *Genetics*, *163*(1), 35-46. https://doi.org/10.1093/genetics/163.1.35

Fabrizio, P., & Longo, V. D. (2003). The chronological life span of Saccharomyces cerevisiae. *Aging Cell*, *2*(2), 73-81. https://doi.org/10.1046/j.1474-9728.2003.00033.x

Fabrizio, P., & Longo, V. D. (2007). The chronological life span of Saccharomyces cerevisiae. *Methods Mol Biol*, *371*, 89-95. https://doi.org/10.1007/978-1-59745-361-5_8

Fabrizio, P., Pozza, F., Pletcher, S. D., Gendron, C. M., & Longo, V. D. (2001). Regulation of longevity and stress resistance by Sch9 in yeast. *Science*, *292*(5515), 288-290. https://doi.org/10.1126/science.1059497

Fehrmann, S., Paoletti, C., Goulev, Y., Ungureanu, A., Aguilaniu, H., & Charvin, G. (2013). Aging yeast cells undergo a sharp entry into senescence unrelated to the loss of mitochondrial membrane potential. *Cell Reports*, *5*(6), 1589-1599. https://doi.org/10.1016/j.celrep.2013.11.013

Feyder, S., De Craene, J. O., Bar, S., Bertazzi, D. L., & Friant, S. (2015). Membrane trafficking in the yeast Saccharomyces cerevisiae model. *Int J Mol Sci*, *16*(1), 1509-1525. https://doi.org/10.3390/ijms16011509

Fontana, L., Cummings, N. E., Arriola Apelo, S. I., Neuman, J. C., Kasza, I., Schmidt, B. A., Cava, E., Spelta, F., Tosti, V., Syed, F. A., Baar, E. L., Veronese, N., Cottrell, S. E., Fenske, R. J., Bertozzi, B., Brar, H. K., Pietka, T., Bullock, A. D., Figenshau, R. S., . . . Lamming, D. W. (2016). Decreased Consumption of Branched-Chain Amino Acids Improves Metabolic Health. *Cell Reports*, *16*(2), 520-530. https://doi.org/10.1016/j.celrep.2016.05.092

Fontana, L., Partridge, L., & Longo, V. D. (2010). Extending healthy life span--from yeast to humans. *Science*, *328*(5976), 321-326. https://doi.org/10.1126/science.1172539

Frangoul, H., Altshuler, D., Cappellini, M. D., Chen, Y. S., Domm, J., Eustace, B. K., Foell, J., de la Fuente, J., Grupp, S., Handgretinger, R., Ho, T. W., Kattamis, A., Kernytsky, A., Lekstrom-Himes, J., Li, A. M., Locatelli, F., Mapara, M. Y., de Montalembert, M., Rondelli, D., . . . Corbacioglu, S. (2021). CRISPR-Cas9 Gene Editing for Sickle Cell Disease and beta-Thalassemia. *N Engl J Med*, *384*(3), 252-260. https://doi.org/10.1056/NEJMoa2031054

Fromentin, G., Darcel, N., Chaumontet, C., Marsset-Baglieri, A., Nadkarni, N., & Tome, D. (2012). Peripheral and central mechanisms involved in the control of food intake by dietary amino acids and proteins. *Nutr Res Rev*, *25*(1), 29-39. https://doi.org/10.1017/s0954422411000175

Gao, X., Lee, K., Reid, M. A., Sanderson, S. M., Qiu, C., Li, S., Liu, J., & Locasale, J. W. (2018). Serine Availability Influences Mitochondrial Dynamics and Function through Lipid Metabolism. *Cell Reports*, *22*(13), 3507-3520. https://doi.org/10.1016/j.celrep.2018.03.017

Gao, X., Sanderson, S. M., Dai, Z., Reid, M. A., Cooper, D. E., Lu, M., Richie, J. P., Jr., Ciccarella, A., Calcagnotto, A., Mikhael, P. G., Mentch, S. J., Liu, J., Ables, G., Kirsch, D. G., Hsu, D. S., Nichenametla, S. N., & Locasale, J. W. (2019). Dietary methionine influences therapy in mouse cancer models and alters human metabolism. *Nature*, *572*(7769), 397-401. https://doi.org/10.1038/s41586-019-1437-3

Garay, E., Campos, S. E., Gonzalez de la Cruz, J., Gaspar, A. P., Jinich, A., & Deluna, A. (2014). High-resolution profiling of stationary-phase survival reveals yeast longevity factors and

their genetic interactions. *PLoS Genet*, *10*(2), e1004168. https://doi.org/10.1371/journal.pgen.1004168

Gasch, A. P., Spellman, P. T., Kao, C. M., Carmel-Harel, O., Eisen, M. B., Storz, G., Botstein, D., & Brown, P. O. (2000). Genomic expression programs in the response of yeast cells to environmental changes. *Mol Biol Cell*, *11*(12), 4241-4257. https://doi.org/10.1091/mbc.11.12.4241

Gavrilov, L. A., & Gavrilova, N. S. (2002). Evolutionary theories of aging and longevity. *ScientificWorldJournal*, *2*, 339-356. https://doi.org/10.1100/tsw.2002.96

Geissmann, Q. (2013). OpenCFU, a new free and open-source software to count cell colonies and other circular objects. *PloS one*, *8*(2), e54072. https://doi.org/10.1371/journal.pone.0054072

Gems, D., & de Magalhaes, J. P. (2021). The hoverfly and the wasp: A critique of the hallmarks of aging as a paradigm. *Ageing Res Rev*, *70*, 101407. https://doi.org/10.1016/j.arr.2021.101407

Godard, P., Urrestarazu, A., Vissers, S., Kontos, K., Bontempi, G., van Helden, J., & Andre, B. (2007). Effect of 21 different nitrogen sources on global gene expression in the yeast Saccharomyces cerevisiae. *Mol Cell Biol*, *27*(8), 3065-3086. https://doi.org/10.1128/MCB.01084-06

Goldberg, A. A., Bourque, S. D., Kyryakov, P., Gregg, C., Boukh-Viner, T., Beach, A., Burstein, M. T., Machkalyan, G., Richard, V., Rampersad, S., Cyr, D., Milijevic, S., & Titorenko, V. I. (2009). Effect of calorie restriction on the metabolic history of chronologically aging yeast. *Experimental Gerontology*, *44*(9), 555-571. https://doi.org/https://doi.org/10.1016/j.exger.2009.06.001

Gonzalez-Gualda, E., Baker, A. G., Fruk, L., & Munoz-Espin, D. (2021). A guide to assessing cellular senescence in vitro and in vivo. *FEBS J*, *288*(1), 56-80. https://doi.org/10.1111/febs.15570

Gottlieb, S., & Esposito, R. E. (1989). A new role for a yeast transcriptional silencer gene, SIR2, in regulation of recombination in ribosomal DNA. *Cell*, *56*(5), 771-776. https://doi.org/https://doi.org/10.1016/0092-8674(89)90681-8

Gray, J. V., Petsko, G. A., Johnston, G. C., Ringe, D., Singer, R. A., & Werner-Washburne, M. (2004). "Sleeping beauty": quiescence in Saccharomyces cerevisiae. *Microbiol Mol Biol Rev*, *68*(2), 187-206. https://doi.org/10.1128/mmbr.68.2.187-206.2004

Haber, J. E. (2012). Mating-type genes and MAT switching in Saccharomyces cerevisiae. *Genetics*, *191*(1), 33-64. https://doi.org/10.1534/genetics.111.134577

Hammad, N., Rosas-Lemus, M., Uribe-Carvajal, S., Rigoulet, M., & Devin, A. (2016). The Crabtree and Warburg effects: Do metabolite-induced regulations participate in their induction? *Biochimica et Biophysica Acta (BBA) - Bioenergetics*, *1857*(8), 1139-1146. https://doi.org/https://doi.org/10.1016/j.bbabio.2016.03.034

Han, S. K., Lee, D., Lee, H., Kim, D., Son, H. G., Yang, J. S., Lee, S. V., & Kim, S. (2016). OASIS 2: online application for survival analysis 2 with features for the analysis of maximal lifespan and healthspan in aging research. *Oncotarget*, *7*(35), 56147-56152. https://doi.org/10.18632/oncotarget.11269

Hartman. (2007). Buffering of deoxyribonucleotide pool homeostasis by threonine metabolism. *Proc Natl Acad Sci U S A*, *104*(28), 11700-11705. https://doi.org/10.1073/pnas.0705212104

Hartman, Stisher, C., Outlaw, D. A., Guo, J., Shah, N. A., Tian, D., Santos, S. M., Rodgers, J. W., & White, R. A. (2015). Yeast Phenomics: An Experimental Approach for Modeling Gene Interaction Networks that Buffer Disease. *Genes*, *6*(1), 24-45. https://www.mdpi.com/2073-4425/6/1/24

Hartman, J. L. t., Garvik, B., & Hartwell, L. (2001). Principles for the buffering of genetic variation. *Science*, *291*(5506), 1001-1004. https://doi.org/10.1126/science.291.5506.1001

Heitman, J., Movva, N. R., & Hall, M. N. (1991). Targets for cell cycle arrest by the immunosuppressant rapamycin in yeast. *Science*, *253*(5022), 905-909. https://doi.org/10.1126/science.1715094

Helliwell, S. B., Losko, S., & Kaiser, C. A. (2001). Components of a ubiquitin ligase complex specify polyubiquitination and intracellular trafficking of the general amino acid permease. *J Cell Biol*, *153*(4), 649-662. https://doi.org/10.1083/jcb.153.4.649

Hepowit, N. L., Macedo, J. K. A., Young, L. E. A., Liu, K., Sun, R. C., MacGurn, J. A., & Dickson, R. C. (2021). Enhancing lifespan of budding yeast by pharmacological lowering of amino acid pools. *Aging (Albany NY)*, *13*(6), 7846-7871. https://doi.org/10.18632/aging.202849

Herker, E., Jungwirth, H., Lehmann, K. A., Maldener, C., Frohlich, K. U., Wissing, S., Buttner, S., Fehr, M., Sigrist, S., & Madeo, F. (2004). Chronological aging leads to apoptosis in yeast. *J Cell Biol*, *164*(4), 501-507. https://doi.org/10.1083/jcb.200310014

Hine, C., Harputlugil, E., Zhang, Y., Ruckenstuhl, C., Lee, B. C., Brace, L., Longchamp, A., Trevino-Villarreal, J. H., Mejia, P., Ozaki, C. K., Wang, R., Gladyshev, V. N., Madeo, F., Mair, W. B., & Mitchell, J. R. (2015). Endogenous hydrogen sulfide production is essential for dietary restriction benefits. *Cell*, *160*(1-2), 132-144. https://doi.org/10.1016/j.cell.2014.11.048

Hinnebusch, A. G. (2005). Translational regulation of GCN4 and the general amino acid control of yeast. *Annu Rev Microbiol*, *59*, 407-450. https://doi.org/10.1146/annurev.micro.59.031805.133833

Hobbs, C. A., & Gilmour, S. K. (2000). High levels of intracellular polyamines promote histone acetyltransferase activity resulting in chromatin hyperacetylation. *J Cell Biochem*, *77*(3), 345-360.

Hope, I. A., & Struhl, K. (1985). GCN4 protein, synthesized in vitro, binds HIS3 regulatory sequences: implications for general control of amino acid biosynthetic genes in yeast. *Cell*, *43*(1), 177-188. https://doi.org/10.1016/0092-8674(85)90022-4

Hu, J., Wei, M., Mirisola, M. G., & Longo, V. D. (2013). Assessing chronological aging in Saccharomyces cerevisiae. *Methods Mol Biol*, *965*, 463-472. https://doi.org/10.1007/978-1-62703-239-1_30

Hu, L., Li, H., Zi, M., Li, W., Liu, J., Yang, Y., Zhou, D., Kong, Q.-P., Zhang, Y., & He, Y. (2022). Why Senescent Cells Are Resistant to Apoptosis: An Insight for Senolytic Development [Review]. *Frontiers in Cell and Developmental Biology*, *10*. https://doi.org/10.3389/fcell.2022.822816

Huang, X., Liu, J., & Dickson, R. C. (2012). Down-Regulating Sphingolipid Synthesis Increases Yeast Lifespan. *PLOS Genetics*, *8*(2), e1002493. https://doi.org/10.1371/journal.pgen.1002493

Hwangbo, D. S., Gershman, B., Tu, M. P., Palmer, M., & Tatar, M. (2004). Drosophila dFOXO controls lifespan and regulates insulin signalling in brain and fat body. *Nature*, *429*(6991), 562-566. https://doi.org/10.1038/nature02549

Imai, S.-i., Armstrong, C. M., Kaeberlein, M., & Guarente, L. (2000). Transcriptional silencing and longevity protein Sir2 is an NAD-dependent histone deacetylase. *Nature*, *403*(6771), 795-800. https://doi.org/10.1038/35001622

Ito, T., Takahashi, K., Naka, T., Hemmi, H., & Yoshimura, T. (2007). Enzymatic assay of D-serine using D-serine dehydratase from Saccharomyces cerevisiae. *Anal Biochem*, *371*(2), 167-172. https://doi.org/10.1016/j.ab.2007.07.030

Jakoby, W. B., & Fredericks, J. (1959). Pyrrolidine and putrescine metabolism: gamma-aminobutyraldehyde dehydrogenase. *Journal of Biological Chemistry*, *234*(8), 2145-2150.

Jazwinski, S. M. (2002). Growing old: metabolic control and yeast aging. *Annu Rev Microbiol*, *56*, 769-792. https://doi.org/10.1146/annurev.micro.56.012302.160830

Jazwinski, S. M. (2005). Yeast longevity and aging--the mitochondrial connection. *Mech Ageing Dev*, *126*(2), 243-248. https://doi.org/10.1016/j.mad.2004.08.016

Jiang, J. C., Jaruga, E., Repnevskaya, M. V., & Jazwinski, S. M. (2000). An intervention resembling caloric restriction prolongs life span and retards aging in yeast. *Faseb j*, *14*(14), 2135-2137. https://doi.org/10.1096/fj.00-0242fje

Jimenez-Marti, E., & del Olmo, M. L. (2008). Addition of ammonia or amino acids to a nitrogen-depleted medium affects gene expression patterns in yeast cells during alcoholic fermentation. *FEMS Yeast Res*, *8*(2), 245-256. https://doi.org/10.1111/j.1567-1364.2007.00325.x

Jin, Y. Y., Singh, P., Chung, H. J., & Hong, S. T. (2018). Blood Ammonia as a Possible Etiological Agent for Alzheimer's Disease. *Nutrients*, *10*(5). https://doi.org/10.3390/nu10050564

Jing, Y.-H., Yan, J.-L., Wang, Q.-J., Chen, H.-C., Ma, X.-Z., Yin, J., & Gao, L.-P. (2018). Spermidine ameliorates the neuronal aging by improving the mitochondrial function in vitro. *Experimental Gerontology*, *108*, 77-86. https://doi.org/https://doi.org/10.1016/j.exger.2018.04.005

Jo, M. C., & Qin, L. (2016). Microfluidic Platforms for Yeast-Based Aging Studies. *Small*, *12*(42), 5787-5801. https://doi.org/10.1002/smll.201602006

Johnson, J. E., & Johnson, F. B. (2014). Methionine restriction activates the retrograde response and confers both stress tolerance and lifespan extension to yeast, mouse and human cells. *PLoS One*, *9*(5), e97729. https://doi.org/10.1371/journal.pone.0097729

Jones, D. L., & Rando, T. A. (2011). Emerging models and paradigms for stem cell ageing. *Nat Cell Biol*, *13*(5), 506-512. https://doi.org/10.1038/ncb0511-506

Jung, P. P., Zhang, Z., Paczia, N., Jaeger, C., Ignac, T., May, P., & Linster, C. L. (2018). Natural variation of chronological aging in the Saccharomyces cerevisiae species reveals diet-dependent mechanisms of life span control. *NPJ Aging Mech Dis*, *4*, 3. https://doi.org/10.1038/s41514-018-0022-6

Juricic, P., Gronke, S., & Partridge, L. (2020). Branched-Chain Amino Acids Have Equivalent Effects to Other Essential Amino Acids on Lifespan and Aging-Related Traits in Drosophila. *J Gerontol A Biol Sci Med Sci*, *75*(1), 24-31. https://doi.org/10.1093/gerona/glz080

Kabil, H., Kabil, O., Banerjee, R., Harshman, L. G., & Pletcher, S. D. (2011). Increased transsulfuration mediates longevity and dietary restriction in Drosophila. *Proc Natl Acad Sci U S A*, *108*(40), 16831-16836. https://doi.org/10.1073/pnas.1102008108

Kaeberlein, M. (2018). How healthy is the healthspan concept? *Geroscience*, *40*(4), 361-364. https://doi.org/10.1007/s11357-018-0036-9

Kaeberlein, M. (2019). It is Time to Embrace 21st-Century Medicine. *Public Policy & Aging Report*, *29*(4), 111-115. https://doi.org/10.1093/ppar/prz022

Kaeberlein, M., Burtner, C. R., & Kennedy, B. K. (2007). Recent developments in yeast aging. *PLoS Genet*, *3*(5), e84. https://doi.org/10.1371/journal.pgen.0030084

Kaeberlein, M., McVey, M., & Guarente, L. (1999). The SIR2/3/4 complex and SIR2 alone promote longevity in Saccharomyces cerevisiae by two different mechanisms. *Genes Dev*, *13*(19), 2570-2580. https://doi.org/10.1101/gad.13.19.2570

Kaeberlein, M., McVey, M., & Guarente, L. (2001). Using yeast to discover the fountain of youth. *Sci Aging Knowledge Environ*, *2001*(1), pe1. https://doi.org/10.1126/sageke.2001.1.pe1

Kalhan, S. C., & Hanson, R. W. (2012a). Resurgence of Serine: An Often Neglected but Indispensable Amino Acid. *Journal of Biological Chemistry*, *287*(24), 19786-19791. https://doi.org/10.1074/jbc.R112.357194

Kalhan, S. C., & Hanson, R. W. (2012b). Resurgence of serine: an often neglected but indispensable amino Acid. *J Biol Chem*, *287*(24), 19786-19791. https://doi.org/10.1074/jbc.R112.357194

Kalita, A., Hesles, E. E., Power, L. N., Wang, D., Singh, P. K., & Smith, J. S. (2021). Isonicotinamide extends yeast chronological lifespan through a mechanism that diminishes nucleotides. *bioRxiv*, 2021.2007.2011.451986. https://doi.org/10.1101/2021.07.11.451986

Kapahi, P., Kaeberlein, M., & Hansen, M. (2017). Dietary restriction and lifespan: Lessons from invertebrate models. *Ageing Res Rev*, *39*, 3-14. https://doi.org/10.1016/j.arr.2016.12.005

Karp, P. D., Billington, R., Caspi, R., Fulcher, C. A., Latendresse, M., Kothari, A., Keseler, I. M., Krummenacker, M., Midford, P. E., Ong, Q., Ong, W. K., Paley, S. M., & Subhraveti, P. (2019). The BioCyc collection of microbial genomes and metabolic pathways. *Brief Bioinform*, *20*(4), 1085-1093. https://doi.org/10.1093/bib/bbx085

Kastanos, E. K., Woldman, Y. Y., & Appling, D. R. (1997). Role of mitochondrial and cytoplasmic serine hydroxymethyltransferase isozymes in de novo purine synthesis in Saccharomyces cerevisiae. *Biochemistry*, *36*(48), 14956-14964. https://doi.org/10.1021/bi971610n

Kennedy, B. K., Austriaco, N. R., Jr., Zhang, J., & Guarente, L. (1995). Mutation in the silencing gene SIR4 can delay aging in S. cerevisiae. *Cell*, *80*(3), 485-496. https://doi.org/10.1016/0092-8674(95)90499-9

Kenyon, C. (2011). The first long-lived mutants: discovery of the insulin/IGF-1 pathway for ageing. *Philos Trans R Soc Lond B Biol Sci*, *366*(1561), 9-16. https://doi.org/10.1098/rstb.2010.0276

Kenyon, C., Chang, J., Gensch, E., Rudner, A., & Tabtiang, R. (1993). A C. elegans mutant that lives twice as long as wild type. *Nature*, *366*(6454), 461-464. https://doi.org/10.1038/366461a0

Kim, D., Fiske, B. P., Birsoy, K., Freinkman, E., Kami, K., Possemato, R. L., Chudnovsky, Y., Pacold, M. E., Chen, W. W., Cantor, J. R., Shelton, L. M., Gui, D. Y., Kwon, M., Ramkissoon, S. H., Ligon, K. L., Kang, S. W., Snuderl, M., Vander Heiden, M. G., & Sabatini, D. M. (2015). SHMT2 drives glioma cell survival in ischaemia but imposes a dependence on glycine clearance. *Nature*, *520*(7547), 363-367. https://doi.org/10.1038/nature14363

Kim, J., & Guan, K. L. (2019). mTOR as a central hub of nutrient signalling and cell growth. *Nat Cell Biol*, *21*(1), 63-71. https://doi.org/10.1038/s41556-018-0205-1

Kimura, K. D., Tissenbaum, H. A., Liu, Y., & Ruvkun, G. (1997). daf-2, an insulin receptor-like gene that regulates longevity and diapause in Caenorhabditis elegans. *Science*, *277*(5328), 942-946. https://doi.org/10.1126/science.277.5328.942

Kind, T., Wohlgemuth, G., Lee, D. Y., Lu, Y., Palazoglu, M., Shahbaz, S., & Fiehn, O. (2009). FiehnLib: mass spectral and retention index libraries for metabolomics based on quadrupole and time-of-flight gas chromatography/mass spectrometry. *Anal Chem*, *81*(24), 10038-10048. https://doi.org/10.1021/ac9019522

Kingsbury, J. M., Sen, N. D., & Cardenas, M. E. (2015). Branched-Chain Aminotransferases Control TORC1 Signaling in Saccharomyces cerevisiae. *PLoS Genet*, *11*(12), e1005714. https://doi.org/10.1371/journal.pgen.1005714

Kirkland, J. L., & Tchkonia, T. (2017). Cellular Senescence: A Translational Perspective. *EBioMedicine*, *21*, 21-28. https://doi.org/10.1016/j.ebiom.2017.04.013

Kirkland, J. L., & Tchkonia, T. (2020). Senolytic drugs: from discovery to translation. *J Intern Med*, *288*(5), 518-536. https://doi.org/10.1111/joim.13141

Kishimoto, S., Uno, M., & Nishida, E. (2018). Molecular mechanisms regulating lifespan and environmental stress responses. *Inflamm Regen*, *38*, 22. https://doi.org/10.1186/s41232-018-0080-y

Kitada, M., Ogura, Y., Monno, I., Xu, J., & Koya, D. (2021). Effect of Methionine Restriction on Aging: Its Relationship to Oxidative Stress. *Biomedicines*, *9*(2). https://doi.org/10.3390/biomedicines9020130

Kitada, M., Xu, J., Ogura, Y., Monno, I., & Koya, D. (2020). Mechanism of Activation of Mechanistic Target of Rapamycin Complex 1 by Methionine. *Front Cell Dev Biol*, *8*, 715. https://doi.org/10.3389/fcell.2020.00715

Korsmo, H. W., & Jiang, X. (2021). One carbon metabolism and early development: a diet-dependent destiny. *Trends Endocrinol Metab*, *32*(8), 579-593. https://doi.org/10.1016/j.tem.2021.05.011

Korstanje, R., Peters, L. L., Robinson, L. L., Krasinski, S. D., & Churchill, G. A. (2021). The Jackson Laboratory Nathan Shock Center: impact of genetic diversity on aging. *Geroscience*, *43*(5), 2129-2137. https://doi.org/10.1007/s11357-021-00421-2

Kory, N., Wyant, G. A., Prakash, G., Uit de Bos, J., Bottanelli, F., Pacold, M. E., Chan, S. H., Lewis, C. A., Wang, T., Keys, H. R., Guo, Y. E., & Sabatini, D. M. (2018). SFXN1 is a mitochondrial

serine transporter required for one-carbon metabolism. *Science*, *362*(6416). https://doi.org/10.1126/science.aat9528

Krall, A. S., Xu, S., Graeber, T. G., Braas, D., & Christofk, H. R. (2016). Asparagine promotes cancer cell proliferation through use as an amino acid exchange factor. *Nat Commun*, *7*, 11457. https://doi.org/10.1038/ncomms11457

Kwan, E. X., Foss, E., Kruglyak, L., & Bedalov, A. (2011). Natural polymorphism in BUL2 links cellular amino acid availability with chronological aging and telomere maintenance in yeast. *PLoS Genet*, *7*(8), e1002250. https://doi.org/10.1371/journal.pgen.1002250

Kwolek-Mirek, M., & Zadrag-Tecza, R. (2014). Comparison of methods used for assessing the viability and vitality of yeast cells. *FEMS Yeast Res*, *14*(7), 1068-1079. https://doi.org/10.1111/1567-1364.12202

Kyryakov, P., Beach, A., Richard, V. R., Burstein, M. T., Leonov, A., Levy, S., & Titorenko, V. I. (2012). Caloric restriction extends yeast chronological lifespan by altering a pattern of age-related changes in trehalose concentration. *Front Physiol*, *3*, 256. https://doi.org/10.3389/fphys.2012.00256

La Grotta, R., Frige, C., Matacchione, G., Olivieri, F., de Candia, P., Ceriello, A., & Prattichizzo, F. (2022). Repurposing SGLT-2 Inhibitors to Target Aging: Available Evidence and Molecular Mechanisms. *Int J Mol Sci*, *23*(20). https://doi.org/10.3390/ijms232012325

Labuschagne, C. F., van den Broek, N. J., Mackay, G. M., Vousden, K. H., & Maddocks, O. D. (2014a). Serine, but not glycine, supports one-carbon metabolism and proliferation of cancer cells. *Cell Rep*, *7*(4), 1248-1258. https://doi.org/10.1016/j.celrep.2014.04.045

Labuschagne, C. F., van den Broek, N. J. F., Mackay, G. M., Vousden, K. H., & Maddocks, O. D. K. (2014b). Serine, but Not Glycine, Supports One-Carbon Metabolism and Proliferation of Cancer Cells. *Cell Reports*, *7*(4), 1248-1258. https://doi.org/10.1016/j.celrep.2014.04.045

Langmead, B., & Salzberg, S. L. (2012). Fast gapped-read alignment with Bowtie 2. *Nat Methods*, *9*(4), 357-359. https://doi.org/10.1038/nmeth.1923

Laporte, D., Courtout, F., Tollis, S., & Sagot, I. (2016). Quiescent Saccharomyces cerevisiae forms telomere hyperclusters at the nuclear membrane vicinity through a multifaceted mechanism involving Esc1, the Sir complex, and chromatin condensation. *Mol Biol Cell*, *27*(12), 1875-1884. https://doi.org/10.1091/mbc.E16-01-0069

Laporte, D., Gouleme, L., Jimenez, L., Khemiri, I., & Sagot, I. (2018). Mitochondria reorganization upon proliferation arrest predicts individual yeast cell fate. *Elife*, *7*. https://doi.org/10.7554/eLife.35685

Laporte, D., Lebaudy, A., Sahin, A., Pinson, B., Ceschin, J., Daignan-Fornier, B., & Sagot, I. (2011). Metabolic status rather than cell cycle signals control quiescence entry and exit. *J Cell Biol*, *192*(6), 949-957. https://doi.org/10.1083/jcb.201009028

Le Douce, J., Maugard, M., Veran, J., Matos, M., Jego, P., Vigneron, P. A., Faivre, E., Toussay, X., Vandenberghe, M., Balbastre, Y., Piquet, J., Guiot, E., Tran, N. T., Taverna, M., Marinesco, S., Koyanagi, A., Furuya, S., Gaudin-Guerif, M., Goutal, S., . . . Bonvento, G. (2020). Impairment of Glycolysis-Derived l-Serine Production in Astrocytes Contributes to Cognitive Deficits in Alzheimer's Disease. *Cell Metab*, *31*(3), 503-517 e508. https://doi.org/10.1016/j.cmet.2020.02.004

Lee, B. C., Kaya, A., Ma, S., Kim, G., Gerashchenko, M. V., Yim, S. H., Hu, Z., Harshman, L. G., & Gladyshev, V. N. (2014). Methionine restriction extends lifespan of Drosophila melanogaster under conditions of low amino-acid status. *Nat Commun*, *5*, 3592. https://doi.org/10.1038/ncomms4592

Lee, H. G., Casadesus, G., Zhu, X., Castellani, R. J., McShea, A., Perry, G., Petersen, R. B., Bajic, V., & Smith, M. A. (2009). Cell cycle re-entry mediated neurodegeneration and its treatment role in the pathogenesis of Alzheimer's disease. *Neurochem Int*, *54*(2), 84-88. https://doi.org/10.1016/j.neuint.2008.10.013

Lee, J. C., Tsoi, A., Kornfeld, G. D., & Dawes, I. W. (2013). Cellular responses to L-serine in Saccharomyces cerevisiae: roles of general amino acid control, compartmentalization, and aspartate synthesis. *FEMS Yeast Res*, *13*(7), 618-634. https://doi.org/10.1111/1567-1364.12063

Lee, J. H., Kim, J. H., Kim, S., Cho, K. S., & Lee, S. B. (2018). Chromatin Changes Associated with Neuronal Maintenance and Their Pharmacological Application. *Curr Neuropharmacol*, *16*(2), 118-125. https://doi.org/10.2174/1570159X15666170601124220

Leontieva, O. V., & Blagosklonny, M. V. (2011). Yeast-like chronological senescence in mammalian cells: phenomenon, mechanism and pharmacological suppression. *Aging (Albany NY)*, *3*(11), 1078-1091. https://doi.org/10.18632/aging.100402

Lin, S. J., Defossez, P. A., & Guarente, L. (2000). Requirement of NAD and SIR2 for life-span extension by calorie restriction in Saccharomyces cerevisiae. *Science*, *289*(5487), 2126-2128. https://doi.org/10.1126/science.289.5487.2126

Lin, S. J., Kaeberlein, M., Andalis, A. A., Sturtz, L. A., Defossez, P. A., Culotta, V. C., Fink, G. R., & Guarente, L. (2002). Calorie restriction extends Saccharomyces cerevisiae lifespan by increasing respiration. *Nature*, *418*(6895), 344-348. https://doi.org/10.1038/nature00829

Lionaki, E., Ploumi, C., & Tavernarakis, N. (2022). One-Carbon Metabolism: Pulling the Strings behind Aging and Neurodegeneration. *Cells*, *11*(2). https://doi.org/10.3390/cells11020214

Ljungdahl, P. O., & Daignan-Fornier, B. (2012). Regulation of amino acid, nucleotide, and phosphate metabolism in Saccharomyces cerevisiae. *Genetics*, *190*(3), 885-929. https://doi.org/10.1534/genetics.111.133306

Loewith, R., & Hall, M. N. (2011). Target of rapamycin (TOR) in nutrient signaling and growth control. *Genetics*, *189*(4), 1177-1201. https://doi.org/10.1534/genetics.111.133363

Longo, V. D., Gralla, E. B., & Valentine, J. S. (1996). Superoxide dismutase activity is essential for stationary phase survival in Saccharomyces cerevisiae. Mitochondrial production of toxic oxygen species in vivo. *Journal of Biological Chemistry*, *271*(21), 12275-12280. https://doi.org/10.1074/jbc.271.21.12275

Longo, V. D., Shadel, G. S., Kaeberlein, M., & Kennedy, B. (2012). Replicative and chronological aging in Saccharomyces cerevisiae. *Cell Metab*, *16*(1), 18-31. https://doi.org/10.1016/j.cmet.2012.06.002

López-Maury, L., Marguerat, S., & Bähler, J. (2008). Tuning gene expression to changing environments: from rapid responses to evolutionary adaptation. *Nature Reviews Genetics*, *9*(8), 583-593. https://doi.org/10.1038/nrg2398

Lopez-Otin, C., Blasco, M. A., Partridge, L., Serrano, M., & Kroemer, G. (2013). The hallmarks of aging. *Cell*, *153*(6), 1194-1217. https://doi.org/10.1016/j.cell.2013.05.039

Love, M. I., Huber, W., & Anders, S. (2014). Moderated estimation of fold change and dispersion for RNA-seq data with DESeq2. *Genome Biol*, *15*(12), 550. https://doi.org/10.1186/s13059-014-0550-8

Lynch, C. J., & Adams, S. H. (2014). Branched-chain amino acids in metabolic signalling and insulin resistance. *Nat Rev Endocrinol*, *10*(12), 723-736. https://doi.org/10.1038/nrendo.2014.171

Macchiarini, F., Miller, R. A., Strong, R., Rosenthal, N., & Harrison, D. E. (2021). Chapter 10 - NIA Interventions Testing Program: A collaborative approach for investigating interventions to promote healthy aging. In N. Musi & P. J. Hornsby (Eds.), *Handbook of the Biology of Aging (Ninth Edition)* (pp. 219-235). Academic Press. https://doi.org/https://doi.org/10.1016/B978-0-12-815962-0.00010-X

MacKay, M. B., Kravtsenyuk, M., Thomas, R., Mitchell, N. D., Dursun, S. M., & Baker, G. B. (2019). D-Serine: Potential Therapeutic Agent and/or Biomarker in Schizophrenia and Depression? *Front Psychiatry*, *10*, 25. https://doi.org/10.3389/fpsyt.2019.00025

MacLean, M., Harris, N., & Piper, P. W. (2001). Chronological lifespan of stationary phase yeast cells; a model for investigating the factors that might influence the ageing of postmitotic tissues in higher organisms. *Yeast*, *18*(6), 499-509. https://doi.org/10.1002/yea.701

Magasanik, B. (2003). Ammonia assimilation by Saccharomyces cerevisiae. *Eukaryot Cell*, *2*(5), 827-829. https://doi.org/10.1128/EC.2.5.827-829.2003

Maitra, N., He, C., Blank, H. M., Tsuchiya, M., Schilling, B., Kaeberlein, M., Aramayo, R., Kennedy, B. K., & Polymenis, M. (2020a). Translational control of methionine and serine metabolic pathways underpin the paralog-specific phenotypes of Rpl22 ribosomal protein mutants in cell division and replicative longevity. *eLife*, *9*, e53127. https://doi.org/10.7554/eLife.53127

Maitra, N., He, C., Blank, H. M., Tsuchiya, M., Schilling, B., Kaeberlein, M., Aramayo, R., Kennedy, B. K., & Polymenis, M. (2020b). Translational control of one-carbon metabolism underpins ribosomal protein phenotypes in cell division and longevity. *Elife*, *9*. https://doi.org/10.7554/eLife.53127

Mansfeld, J., Urban, N., Priebe, S., Groth, M., Frahm, C., Hartmann, N., Gebauer, J., Ravichandran, M., Dommaschk, A., Schmeisser, S., Kuhlow, D., Monajembashi, S., Bremer-Streck, S., Hemmerich, P., Kiehntopf, M., Zamboni, N., Englert, C., Guthke, R., Kaleta, C., . . . Ristow, M. (2015). Branched-chain amino acid catabolism is a conserved regulator of physiological ageing. *Nat Commun*, *6*, 10043. https://doi.org/10.1038/ncomms10043

Maqani, N., Fine, R. D., Shahid, M., Li, M., Enriquez-Hesles, E., & Smith, J. S. (2018). Spontaneous mutations in CYC8 and MIG1 suppress the short chronological lifespan of budding yeast lacking SNF1/AMPK. *Microb Cell*, *5*(5), 233-248. https://doi.org/10.15698/mic2018.05.630

Martin-Montalvo, A., & de Cabo, R. (2013). Mitochondrial metabolic reprogramming induced by calorie restriction. *Antioxid Redox Signal*, *19*(3), 310-320. https://doi.org/10.1089/ars.2012.4866

Maruyama, Y., Ito, T., Kodama, H., & Matsuura, A. (2016). Availability of Amino Acids Extends Chronological Lifespan by Suppressing Hyper-Acidification of the Environment in Saccharomyces cerevisiae. *PloS one*, *11*(3), e0151894. https://doi.org/10.1371/journal.pone.0151894

Matecic, Smith, D. L., Pan, X., Maqani, N., Bekiranov, S., Boeke, J. D., & Smith, J. S. (2010). A microarray-based genetic screen for yeast chronological aging factors. *PLoS Genet*, *6*(4), e1000921. https://doi.org/10.1371/journal.pgen.1000921

Mattison, J. A., Colman, R. J., Beasley, T. M., Allison, D. B., Kemnitz, J. W., Roth, G. S., Ingram, D. K., Weindruch, R., de Cabo, R., & Anderson, R. M. (2017). Caloric restriction improves health and survival of rhesus monkeys. *Nat Commun*, *8*, 14063. https://doi.org/10.1038/ncomms14063

Mattison, J. A., Roth, G. S., Beasley, T. M., Tilmont, E. M., Handy, A. M., Herbert, R. L., Longo, D. L., Allison, D. B., Young, J. E., Bryant, M., Barnard, D., Ward, W. F., Qi, W., Ingram, D. K., & de Cabo, R. (2012). Impact of caloric restriction on health and survival in rhesus monkeys from the NIA study. *Nature*, *489*(7415), 318-321. https://doi.org/10.1038/nature11432

Mattocks, D. A. L., Mentch, S. J., Shneyder, J., Ables, G. P., Sun, D., Richie, J. P., Locasale, J. W., & Nichenametla, S. N. (2017). Short term methionine restriction increases hepatic global DNA methylation in adult but not young male C57BL/6J mice. *Experimental Gerontology*, *88*, 1-8. https://doi.org/https://doi.org/10.1016/j.exger.2016.12.003

May, A. I., Prescott, M., & Ohsumi, Y. (2020). Autophagy facilitates adaptation of budding yeast to respiratory growth by recycling serine for one-carbon metabolism. *Nature Communications*, *11*(1), 5052. https://doi.org/10.1038/s41467-020-18805-x

Maynard, A. G., & Kanarek, N. (2020). NADH Ties One-Carbon Metabolism to Cellular Respiration. *Cell Metab*, *31*(4), 660-662. https://doi.org/10.1016/j.cmet.2020.03.012

Mazouzi, A., Velimezi, G., & Loizou, J. I. (2014). DNA replication stress: causes, resolution and disease. *Exp Cell Res*, *329*(1), 85-93. https://doi.org/10.1016/j.yexcr.2014.09.030

McCay, C. M., Pope, F., Lunsford, W., Sperling, G., & Sambhavaphol, P. (1957). Parabiosis between old and young rats. *Gerontologia*, *1*(1), 7-17. https://doi.org/10.1159/000210677

McIsaac, R. S., Lewis, K. N., Gibney, P. A., & Buffenstein, R. (2016). From yeast to human: exploring the comparative biology of methionine restriction in extending eukaryotic life span. *Ann N Y Acad Sci*, *1363*, 155-170. https://doi.org/10.1111/nyas.13032

McNulty, N. P., Yatsunenko, T., Hsiao, A., Faith, J. J., Muegge, B. D., Goodman, A. L., Henrissat, B., Oozeer, R., Cools-Portier, S., Gobert, G., Chervaux, C., Knights, D., Lozupone, C. A., Knight, R., Duncan, A. E., Bain, J. R., Muehlbauer, M. J., Newgard, C. B., Heath, A. C., & Gordon, J. I. (2011). The impact of a consortium of fermented milk strains on the gut microbiome of gnotobiotic mice and monozygotic twins. *Sci Transl Med*, *3*(106), 106ra106. https://doi.org/10.1126/scitranslmed.3002701

Meiser, J., & Vazquez, A. (2016). Give it or take it: the flux of one-carbon in cancer cells. *The FEBS Journal*, *283*(20), 3695-3704. https://doi.org/https://doi.org/10.1111/febs.13731

Mercken, E. M., Crosby, S. D., Lamming, D. W., JeBailey, L., Krzysik-Walker, S., Villareal, D. T., Capri, M., Franceschi, C., Zhang, Y., Becker, K., Sabatini, D. M., de Cabo, R., & Fontana, L. (2013). Calorie restriction in humans inhibits the PI3K/AKT pathway and induces a

younger transcription profile. *Aging Cell*, *12*(4), 645-651. https://doi.org/10.1111/acel.12088
Messerer, J., Wrede, C., Schipke, J., Brandenberger, C., Abdellatif, M., Eisenberg, T., Madeo, F., Sedej, S., & Mühlfeld, C. (2023). Spermidine supplementation influences mitochondrial number and morphology in the heart of aged mice. *Journal of Anatomy*, *242*(1), 91-101. https://doi.org/https://doi.org/10.1111/joa.13618
Michael, A. J. (2016). Biosynthesis of polyamines and polyamine-containing molecules. *Biochem J*, *473*(15), 2315-2329. https://doi.org/10.1042/bcj20160185
Miles, S., Lee, C., & Breeden, L. (2023). BY4741 cannot enter quiescence from rich medium. *MicroPubl Biol*, *2023*. https://doi.org/10.17912/micropub.biology.000742
Millard, P. J., Roth, B. L., Thi, H. P., Yue, S. T., & Haugland, R. P. (1997). Development of the FUN-1 family of fluorescent probes for vacuole labeling and viability testing of yeasts. *Appl Environ Microbiol*, *63*(7), 2897-2905. https://doi.org/10.1128/aem.63.7.2897-2905.1997
Milman, S., Atzmon, G., Huffman, D. M., Wan, J., Crandall, J. P., Cohen, P., & Barzilai, N. (2014). Low insulin-like growth factor-1 level predicts survival in humans with exceptional longevity. *Aging Cell*, *13*(4), 769-771. https://doi.org/10.1111/acel.12213
Minois, N., Carmona-Gutierrez, D., & Madeo, F. (2011). Polyamines in aging and disease. *Aging (Albany NY)*, *3*(8), 716-732. https://doi.org/10.18632/aging.100361
Mirisola, M. G., Taormina, G., Fabrizio, P., Wei, M., Hu, J., & Longo, V. D. (2014). Serine- and threonine/valine-dependent activation of PDK and Tor orthologs converge on Sch9 to promote aging. *PLoS Genet*, *10*(2), e1004113. https://doi.org/10.1371/journal.pgen.1004113
Mitchell, S. J., Bernier, M., Mattison, J. A., Aon, M. A., Kaiser, T. A., Anson, R. M., Ikeno, Y., Anderson, R. M., Ingram, D. K., & de Cabo, R. (2019). Daily Fasting Improves Health and Survival in Male Mice Independent of Diet Composition and Calories. *Cell Metab*, *29*(1), 221-228.e223. https://doi.org/10.1016/j.cmet.2018.08.011
Mitchell, S. J., Madrigal-Matute, J., Scheibye-Knudsen, M., Fang, E., Aon, M., González-Reyes, J. A., Cortassa, S., Kaushik, S., Gonzalez-Freire, M., Patel, B., Wahl, D., Ali, A., Calvo-Rubio, M., Burón, M. I., Guiterrez, V., Ward, T. M., Palacios, H. H., Cai, H., Frederick, D. W., . . . de Cabo, R. (2016). Effects of Sex, Strain, and Energy Intake on Hallmarks of Aging in Mice. *Cell Metab*, *23*(6), 1093-1112. https://doi.org/10.1016/j.cmet.2016.05.027
Moger-Reischer, R. Z., & Lennon, J. T. (2019). Microbial ageing and longevity. *Nature Reviews Microbiology*, *17*(11), 679-690. https://doi.org/10.1038/s41579-019-0253-y
Mohammad, K., & Titorenko, V. I. (2021). Caloric restriction creates a metabolic pattern of chronological aging delay that in budding yeast differs from the metabolic design established by two other geroprotectors. *Oncotarget*, *12*(7), 608-625. https://doi.org/10.18632/oncotarget.27926
Morscher, R. J., Ducker, G. S., Li, S. H., Mayer, J. A., Gitai, Z., Sperl, W., & Rabinowitz, J. D. (2018). Mitochondrial translation requires folate-dependent tRNA methylation. *Nature*, *554*(7690), 128-132. https://doi.org/10.1038/nature25460
Mortimer, R. K., & Johnston, J. R. (1959). Life span of individual yeast cells. *Nature*, *183*(4677), 1751-1752. https://doi.org/10.1038/1831751a0
Mortimer, R. K., & Johnston, J. R. (1959). Life Span of Individual Yeast Cells. *Nature*, *183*(4677), 1751-1752. https://doi.org/10.1038/1831751a0

Mota-Martorell, N., Jové, M., Borrás, C., Berdún, R., Obis, È., Sol, J., Cabré, R., Pradas, I., Galo-Licona, J. D., Puig, J., Viña, J., & Pamplona, R. (2021). Methionine transsulfuration pathway is upregulated in long-lived humans. *Free Radic Biol Med*, *162*, 38-52. https://doi.org/10.1016/j.freeradbiomed.2020.11.026

Murakami, C., & Kaeberlein, M. (2009). Quantifying yeast chronological life span by outgrowth of aged cells. *J Vis Exp*(27). https://doi.org/10.3791/1156

Murakami, C. J., Burtner, C. R., Kennedy, B. K., & Kaeberlein, M. (2008). A method for high-throughput quantitative analysis of yeast chronological life span. *J Gerontol A Biol Sci Med Sci*, *63*(2), 113-121. https://doi.org/10.1093/gerona/63.2.113

Nagarajan, S., Kruckeberg, A. L., Schmidt, K. H., Kroll, E., Hamilton, M., McInnerney, K., Summers, R., Taylor, T., & Rosenzweig, F. (2014). Uncoupling reproduction from metabolism extends chronological lifespan in yeast. *Proc Natl Acad Sci U S A*, *111*(15), E1538-1547. https://doi.org/10.1073/pnas.1323918111

Nava-Gomez, L., Calero-Vargas, I., Higinio-Rodriguez, F., Vazquez-Prieto, B., Olivares-Moreno, R., Ortiz-Retana, J., Aranda, P., Hernandez-Chan, N., Rojas-Piloni, G., Alcauter, S., & Lopez-Hidalgo, M. (2022). Aging-Associated Cognitive Decline Is Reversed by D-Serine Supplementation. *eNeuro*, *9*(3). https://doi.org/10.1523/ENEURO.0176-22.2022

Newman, A. C., & Maddocks, O. D. K. (2017). One-carbon metabolism in cancer. *Br J Cancer*, *116*(12), 1499-1504. https://doi.org/10.1038/bjc.2017.118

Niccoli, T., & Partridge, L. (2012). Ageing as a Risk Factor for Disease. *Current Biology*, *22*(17), R741-R752. https://doi.org/https://doi.org/10.1016/j.cub.2012.07.024

Nichenametla, S. N., Mattocks, D. A. L., Cooke, D., Midya, V., Malloy, V. L., Mansilla, W., Øvrebø, B., Turner, C., Bastani, Nasser E., Sokolová, J., Pavlíková, M., Richie Jr, J. P., Shoveller, Anna K., Refsum, H., Olsen, T., Vinknes, K. J., Kožich, V., & Ables, G. P. (2022). Cysteine restriction-specific effects of sulfur amino acid restriction on lipid metabolism [https://doi.org/10.1111/acel.13739]. *Aging Cell*, *21*(12), e13739. https://doi.org/https://doi.org/10.1111/acel.13739

Novelle, M. G., Ali, A., Dieguez, C., Bernier, M., & de Cabo, R. (2016). Metformin: A Hopeful Promise in Aging Research. *Cold Spring Harb Perspect Med*, *6*(3), a025932. https://doi.org/10.1101/cshperspect.a025932

Ocampo, A., Liu, J., Schroeder, E. A., Shadel, G. S., & Barrientos, A. (2012). Mitochondrial respiratory thresholds regulate yeast chronological life span and its extension by caloric restriction. *Cell Metab*, *16*(1), 55-67. https://doi.org/10.1016/j.cmet.2012.05.013

Ogawa, T., Masumura, K., Kohara, Y., Kanai, M., Soga, T., Ohya, Y., Blackwell, T. K., & Mizunuma, M. (2022). S-adenosyl-L-homocysteine extends lifespan through methionine restriction effects. *Aging Cell*, *21*(5), e13604. https://doi.org/10.1111/acel.13604

Ogawa, T., Tsubakiyama, R., Kanai, M., Koyama, T., Fujii, T., Iefuji, H., Soga, T., Kume, K., Miyakawa, T., Hirata, D., & Mizunuma, M. (2016). Stimulating S-adenosyl-l-methionine synthesis extends lifespan via activation of AMPK. *Proc Natl Acad Sci U S A*, *113*(42), 11913-11918. https://doi.org/10.1073/pnas.1604047113

Ohsumi, Y. (2014). Historical landmarks of autophagy research. *Cell Res*, *24*(1), 9-23. https://doi.org/10.1038/cr.2013.169

Olin-Sandoval, V., Yu, J. S. L., Miller-Fleming, L., Alam, M. T., Kamrad, S., Correia-Melo, C., Haas, R., Segal, J., Pena Navarro, D. A., Herrera-Dominguez, L., Mendez-Lucio, O., Vowinckel,

J., Mulleder, M., & Ralser, M. (2019). Lysine harvesting is an antioxidant strategy and triggers underground polyamine metabolism. *Nature*, *572*(7768), 249-253. https://doi.org/10.1038/s41586-019-1442-6

Olin-Sandoval, V., Yu, J. S. L., Miller-Fleming, L., Alam, M. T., Kamrad, S., Correia-Melo, C., Haas, R., Segal, J., Peña Navarro, D. A., Herrera-Dominguez, L., Méndez-Lucio, O., Vowinckel, J., Mülleder, M., & Ralser, M. (2019). Lysine harvesting is an antioxidant strategy and triggers underground polyamine metabolism. *Nature*, *572*(7768), 249-253. https://doi.org/10.1038/s41586-019-1442-6

Olshansky, S. J. (2018). From Lifespan to Healthspan. *JAMA*, *320*(13), 1323-1324. https://doi.org/10.1001/jama.2018.12621

Orentreich, N., Matias, J. R., DeFelice, A., & Zimmerman, J. A. (1993). Low methionine ingestion by rats extends life span. *J Nutr*, *123*(2), 269-274. https://doi.org/10.1093/jn/123.2.269

Palkova, Z., Wilkinson, D., & Vachova, L. (2014). Aging and differentiation in yeast populations: elders with different properties and functions. *FEMS Yeast Res*, *14*(1), 96-108. https://doi.org/10.1111/1567-1364.12103

Peselj, C., Ebrahimi, M., Broeskamp, F., Prokisch, S., Habernig, L., Alvarez-Guerra, I., Kohler, V., Vögtle, F. N., & Büttner, S. (2022). Sterol Metabolism Differentially Contributes to Maintenance and Exit of Quiescence. *Front Cell Dev Biol*, *10*, 788472. https://doi.org/10.3389/fcell.2022.788472

Peter, G. J., During, L., & Ahmed, A. (2006). Carbon catabolite repression regulates amino acid permeases in Saccharomyces cerevisiae via the TOR signaling pathway. *J Biol Chem*, *281*(9), 5546-5552. https://doi.org/10.1074/jbc.M513842200

Petersen, J. G., Kielland-Brandt, M. C., Nilsson-Tillgren, T., Bornaes, C., & Holmberg, S. (1988). Molecular genetics of serine and threonine catabolism in Saccharomyces cerevisiae. *Genetics*, *119*(3), 527-534.

Pitt, J. N., & Kaeberlein, M. (2015). Correction: Why Is Aging Conserved and What Can We Do about it? *PLOS Biology*, *13*(5), e1002176. https://doi.org/10.1371/journal.pbio.1002176

Plummer, J. D., & Johnson, J. E. (2019). Extension of Cellular Lifespan by Methionine Restriction Involves Alterations in Central Carbon Metabolism and Is Mitophagy-Dependent [Original Research]. *Frontiers in Cell and Developmental Biology*, *7*. https://doi.org/10.3389/fcell.2019.00301

Postnikoff, S. D., & Harkness, T. A. (2014). Replicative and chronological life-span assays. *Methods Mol Biol*, *1163*, 223-227. https://doi.org/10.1007/978-1-4939-0799-1_17

Powers, R. W., 3rd, Kaeberlein, M., Caldwell, S. D., Kennedy, B. K., & Fields, S. (2006). Extension of chronological life span in yeast by decreased TOR pathway signaling. *Genes Dev*, *20*(2), 174-184. https://doi.org/10.1101/gad.1381406

Qin, Z., & Hubbard, E. J. (2015). Non-autonomous DAF-16/FOXO activity antagonizes age-related loss of C. elegans germline stem/progenitor cells. *Nat Commun*, *6*, 7107. https://doi.org/10.1038/ncomms8107

Quasem, I., J.Luby, C., R.Mace, C., & M.Fuchs, S. (2017). Density separation of quiescent yeast using iodixanol. *BioTechniques*, *63*(4), 169-173. https://doi.org/10.2144/000114596

Ramos, F., & Wiame, J. M. (1982). Occurrence of a catabolic L-serine (L-threonine) deaminase in Saccharomyces cerevisiae. *Eur J Biochem*, *123*(3), 571-576. https://doi.org/10.1111/j.1432-1033.1982.tb06570.x

Reverter-Branchat, G., Cabiscol, E., Tamarit, J., & Ros, J. (2004). Oxidative damage to specific proteins in replicative and chronological-aged Saccharomyces cerevisiae: common targets and prevention by calorie restriction. *J Biol Chem*, *279*(30), 31983-31989. https://doi.org/10.1074/jbc.M404849200

Richie, J. P., Jr., Leutzinger, Y., Parthasarathy, S., Malloy, V., Orentreich, N., & Zimmerman, J. A. (1994). Methionine restriction increases blood glutathione and longevity in F344 rats. *FASEB J*, *8*(15), 1302-1307. https://doi.org/10.1096/fasebj.8.15.8001743

Rochon, J., Bales, C. W., Ravussin, E., Redman, L. M., Holloszy, J. O., Racette, S. B., Roberts, S. B., Das, S. K., Romashkan, S., Galan, K. M., Hadley, E. C., Kraus, W. E., & Group, C. S. (2011). Design and conduct of the CALERIE study: comprehensive assessment of the long-term effects of reducing intake of energy. *J Gerontol A Biol Sci Med Sci*, *66*(1), 97-108. https://doi.org/10.1093/gerona/glq168

Ron-Harel, N., Notarangelo, G., Ghergurovich, J. M., Paulo, J. A., Sage, P. T., Santos, D., Satterstrom, F. K., Gygi, S. P., Rabinowitz, J. D., Sharpe, A. H., & Haigis, M. C. (2018). Defective respiration and one-carbon metabolism contribute to impaired naive T cell activation in aged mice. *Proc Natl Acad Sci U S A*, *115*(52), 13347-13352. https://doi.org/10.1073/pnas.1804149115

Rothschild, J., Hoddy, K. K., Jambazian, P., & Varady, K. A. (2014). Time-restricted feeding and risk of metabolic disease: a review of human and animal studies. *Nutrition Reviews*, *72*(5), 308-318. https://doi.org/10.1111/nure.12104

Ruckenstuhl, C., Carmona-Gutierrez, D., & Madeo, F. (2010). The sweet taste of death: glucose triggers apoptosis during yeast chronological aging. *Aging (Albany NY)*, *2*(10), 643-649. https://doi.org/10.18632/aging.100223

Ruckenstuhl, C., Netzberger, C., Entfellner, I., Carmona-Gutierrez, D., Kickenweiz, T., Stekovic, S., Gleixner, C., Schmid, C., Klug, L., Sorgo, A. G., Eisenberg, T., Buttner, S., Marino, G., Koziel, R., Jansen-Durr, P., Frohlich, K. U., Kroemer, G., & Madeo, F. (2014). Lifespan extension by methionine restriction requires autophagy-dependent vacuolar acidification. *PLoS Genet*, *10*(5), e1004347. https://doi.org/10.1371/journal.pgen.1004347

Ruetenik, A., & Barrientos, A. (2018). Exploiting Post-mitotic Yeast Cultures to Model Neurodegeneration. *Front Mol Neurosci*, *11*, 400. https://doi.org/10.3389/fnmol.2018.00400

Ruiz, S. J., van 't Klooster, J. S., Bianchi, F., & Poolman, B. (2020). Growth Inhibition by Amino Acids in Saccharomyces cerevisiae. *Microorganisms*, *9*(1). https://doi.org/10.3390/microorganisms9010007

Saitoh, Y., Katane, M., Kawata, T., Maeda, K., Sekine, M., Furuchi, T., Kobuna, H., Sakamoto, T., Inoue, T., Arai, H., Nakagawa, Y., & Homma, H. (2012). Spatiotemporal localization of D-amino acid oxidase and D-aspartate oxidases during development in Caenorhabditis elegans. *Mol Cell Biol*, *32*(10), 1967-1983. https://doi.org/10.1128/mcb.06513-11

Salmon, A. B., Murakami, S., Bartke, A., Kopchick, J., Yasumura, K., & Miller, R. A. (2005). Fibroblast cell lines from young adult mice of long-lived mutant strains are resistant to multiple forms of stress. *Am J Physiol Endocrinol Metab*, *289*(1), E23-29. https://doi.org/10.1152/ajpendo.00575.2004

Santos, J., Leitão-Correia, F., João Sousa, M., & Leão, C. (2014). Ammonium is a key determinant on the dietary restriction of yeast chronological aging in culture medium. *Oncotarget*, *6*(9). https://www.oncotarget.com/article/2989/text/

Santos, J., Sousa, M. J., & Leao, C. (2012). Ammonium is toxic for aging yeast cells, inducing death and shortening of the chronological lifespan. *PloS one*, *7*(5), e37090. https://doi.org/10.1371/journal.pone.0037090

Santos, S. M., Laflin, S., Broadway, A., Burnet, C., Hartheimer, J., Rodgers, J., Smith, D. L., Jr., & Hartman, J. I. (2020). High-resolution yeast quiescence profiling in human-like media reveals complex influences of auxotrophy and nutrient availability. *Geroscience*. https://doi.org/10.1007/s11357-020-00265-2

Santos, S. M., Laflin, S., Broadway, A., Burnet, C., Hartheimer, J., Rodgers, J., Smith, D. L., Jr., & Hartman, J. L. t. (2021). High-resolution yeast quiescence profiling in human-like media reveals complex influences of auxotrophy and nutrient availability. *Geroscience*, *43*(2), 941-964. https://doi.org/10.1007/s11357-020-00265-2

Schekman, R. (2002). Lasker Basic Medical Research Award. SEC mutants and the secretory apparatus. *Nat Med*, *8*(10), 1055-1058. https://doi.org/10.1038/nm769

nm769 [pii]

Sen, P., Shah, P. P., Nativio, R., & Berger, S. L. (2016). Epigenetic Mechanisms of Longevity and Aging. *Cell*, *166*(4), 822-839. https://doi.org/10.1016/j.cell.2016.07.050

Sequerra, E. B., Gardino, P., Hedin-Pereira, C., & de Mello, F. G. (2007). Putrescine as an important source of GABA in the postnatal rat subventricular zone. *Neuroscience*, *146*(2), 489-493. https://doi.org/https://doi.org/10.1016/j.neuroscience.2007.01.062

Shah, N. A., Laws, R. J., Wardman, B., Zhao, L. P., & Hartman, J. L. t. (2007). Accurate, precise modeling of cell proliferation kinetics from time-lapse imaging and automated image analysis of agar yeast culture arrays. *BMC Syst Biol*, *1*, 3. https://doi.org/10.1186/1752-0509-1-3

Sheldrake, A. R. (2022). Cellular senescence, rejuvenation and potential immortality. *Proc Biol Sci*, *289*(1970), 20212434. https://doi.org/10.1098/rspb.2021.2434

Sinclair, D. A., & Guarente, L. (1997). Extrachromosomal rDNA Circles— A Cause of Aging in Yeast. *Cell*, *91*(7), 1033-1042. https://doi.org/https://doi.org/10.1016/S0092-8674(00)80493-6

Sinha, T., Ikelle, L., Naash, M. I., & Al-Ubaidi, M. R. (2020). The Intersection of Serine Metabolism and Cellular Dysfunction in Retinal Degeneration. *Cells*, *9*(3). https://doi.org/10.3390/cells9030674

Skorupa, D. A., Dervisefendic, A., Zwiener, J., & Pletcher, S. D. (2008). Dietary composition specifies consumption, obesity, and lifespan in Drosophila melanogaster. *Aging Cell*, *7*(4), 478-490. https://doi.org/10.1111/j.1474-9726.2008.00400.x

Smith, D. L., Jr., Maharrey, C. H., Carey, C. R., White, R. A., & Hartman IV, J. L. (2016). Gene-nutrient interaction markedly influences yeast chronological lifespan. *Exp Gerontol*, *86*, 113-123. https://doi.org/10.1016/j.exger.2016.04.012

Smith, J., Daniel L., McClure, J. M., Matecic, M., & Smith, J. S. (2007). Calorie restriction extends the chronological lifespan of Saccharomyces cerevisiae independently of the Sirtuins. *Aging Cell*, *6*(5), 649-662. https://doi.org/10.1111/j.1474-9726.2007.00326.x

Smith Jr., Maharrey, C. H., Carey, C. R., White, R. A., & Hartman, J. L. (2016). Gene-nutrient interaction markedly influences yeast chronological lifespan. *Experimental Gerontology*, *86*, 113-123. https://doi.org/https://doi.org/10.1016/j.exger.2016.04.012

Smith Jr., D., McClure, J. M., Matecic, M., & Smith, J. S. (2007). Calorie restriction extends the chronological lifespan of Saccharomyces cerevisiae independently of the Sirtuins. *Aging Cell*, *6*(5), 649-662. https://doi.org/10.1111/j.1474-9726.2007.00326.x

Smith, J. S., & Boeke, J. D. (1997). An unusual form of transcriptional silencing in yeast ribosomal DNA. *Genes Dev*, *11*(2), 241-254. https://doi.org/10.1101/gad.11.2.241

Sousa-Victor, P., Neves, J., Cedron-Craft, W., Ventura, P. B., Liao, C. Y., Riley, R. R., Soifer, I., van Bruggen, N., Kolumam, G. A., Villeda, S. A., Lamba, D. A., & Jasper, H. (2019). MANF regulates metabolic and immune homeostasis in ageing and protects against liver damage. *Nat Metab*, *1*(2), 276-290. https://doi.org/10.1038/s42255-018-0023-6

Sousounis, K., Baddour, J. A., & Tsonis, P. A. (2014). Aging and regeneration in vertebrates. *Curr Top Dev Biol*, *108*, 217-246. https://doi.org/10.1016/B978-0-12-391498-9.00008-5

Stark, A. (2017). *Phase IIa L-serine trial for early Alzheimer's disease (AD)*. https://clinicaltrials.gov/ct2/show/NCT03062449

Staschke, K. A., Dey, S., Zaborske, J. M., Palam, L. R., McClintick, J. N., Pan, T., Edenberg, H. J., & Wek, R. C. (2010). Integration of general amino acid control and target of rapamycin (TOR) regulatory pathways in nitrogen assimilation in yeast. *J Biol Chem*, *285*(22), 16893-16911. https://doi.org/10.1074/jbc.M110.121947

Steinkraus, K. A., Kaeberlein, M., & Kennedy, B. K. (2008). Replicative aging in yeast: the means to the end. *Annu Rev Cell Dev Biol*, *24*, 29-54. https://doi.org/10.1146/annurev.cellbio.23.090506.123509

Stekovic, S., Hofer, S. J., Tripolt, N., Aon, M. A., Royer, P., Pein, L., Stadler, J. T., Pendl, T., Prietl, B., Url, J., Schroeder, S., Tadic, J., Eisenberg, T., Magnes, C., Stumpe, M., Zuegner, E., Bordag, N., Riedl, R., Schmidt, A., . . . Madeo, F. (2019). Alternate Day Fasting Improves Physiological and Molecular Markers of Aging in Healthy, Non-obese Humans. *Cell Metab*, *30*(3), 462-476 e466. https://doi.org/10.1016/j.cmet.2019.07.016

Stommel, E. W. (2018). *Tolerability and Efficacy of L-serine n Patients with Amyotrophic Lateral Scleroris (ALS)*. Retrieved 2020 from https://clinicaltrials.gov/ct2/show/NCT03580616

Suh, E., Choi, S.-W., & Friso, S. (2016). Chapter 36 - One-Carbon Metabolism: An Unsung Hero for Healthy Aging. In M. Malavolta & E. Mocchegiani (Eds.), *Molecular Basis of Nutrition and Aging* (pp. 513-522). Academic Press. https://doi.org/https://doi.org/10.1016/B978-0-12-801816-3.00036-4

Suh, Y., Atzmon, G., Cho, M. O., Hwang, D., Liu, B., Leahy, D. J., Barzilai, N., & Cohen, P. (2008). Functionally significant insulin-like growth factor I receptor mutations in centenarians. *Proc Natl Acad Sci U S A*, *105*(9), 3438-3442. https://doi.org/10.1073/pnas.0705467105

Sun, L., Sadighi Akha, A. A., Miller, R. A., & Harper, J. M. (2009). Life-span extension in mice by preweaning food restriction and by methionine restriction in middle age. *J Gerontol A Biol Sci Med Sci*, *64*(7), 711-722. https://doi.org/10.1093/gerona/glp051

Sun, S., & Gresham, D. (2021). Cellular quiescence in budding yeast. *Yeast*, *38*(1), 12-29. https://doi.org/10.1002/yea.3545

Sun, X., Chen, W. D., & Wang, Y. D. (2017). DAF-16/FOXO Transcription Factor in Aging and Longevity. *Front Pharmacol*, *8*, 548. https://doi.org/10.3389/fphar.2017.00548

Suppola, S., Heikkinen, S., Parkkinen, J. J., Uusi-Oukari, M., Korhonen, V. P., Keinanen, T., Alhonen, L., & Janne, J. (2001). Concurrent overexpression of ornithine decarboxylase and spermidine/spermine N(1)-acetyltransferase further accelerates the catabolism of hepatic polyamines in transgenic mice. *Biochem J*, *358*(Pt 2), 343-348. https://doi.org/10.1042/0264-6021:3580343

Svenkrtova, A., Belicova, L., Volejnikova, A., Sigler, K., Jazwinski, S. M., & Pichova, A. (2016). Stratification of yeast cells during chronological aging by size points to the role of trehalose in cell vitality. *Biogerontology*, *17*(2), 395-408. https://doi.org/10.1007/s10522-015-9625-5

Swygert, S. G., Kim, S., Wu, X., Fu, T., Hsieh, T. H., Rando, O. J., Eisenman, R. N., Shendure, J., McKnight, J. N., & Tsukiyama, T. (2019). Condensin-Dependent Chromatin Compaction Represses Transcription Globally during Quiescence. *Mol Cell*, *73*(3), 533-546.e534. https://doi.org/10.1016/j.molcel.2018.11.020

Tabor, C. W., & Tabor, H. (1985). Polyamines in microorganisms. *Microbiological Reviews*, *49*(1), 81-99. https://doi.org/doi:10.1128/mr.49.1.81-99.1985

Tahara, E. B., Cunha, F. M., Basso, T. O., Della Bianca, B. E., Gombert, A. K., & Kowaltowski, A. J. (2013). Calorie restriction hysteretically primes aging Saccharomyces cerevisiae toward more effective oxidative metabolism. *PLoS One*, *8*(2), e56388. https://doi.org/10.1371/journal.pone.0056388

Takagi, H. (2008). Proline as a stress protectant in yeast: physiological functions, metabolic regulations, and biotechnological applications. *Appl Microbiol Biotechnol*, *81*(2), 211-223. https://doi.org/10.1007/s00253-008-1698-5

Taormina, G., Ferrante, F., Vieni, S., Grassi, N., Russo, A., & Mirisola, M. G. (2019). Longevity: Lesson from Model Organisms. *Genes (Basel)*, *10*(7). https://doi.org/10.3390/genes10070518

Tooze, S. A., Hannan, L. A., Marks, M. S., Stevens, T. H., & Schroer, T. A. (2017). Fundamental mechanisms deliver the Nobel Prize to Ohsumi. *Traffic*, *18*(2), 93-95. https://doi.org/10.1111/tra.12460

Urfer, S. R., Kaeberlein, T. L., Mailheau, S., Bergman, P. J., Creevy, K. E., Promislow, D. E. L., & Kaeberlein, M. (2017). A randomized controlled trial to establish effects of short-term rapamycin treatment in 24 middle-aged companion dogs. *Geroscience*, *39*(2), 117-127. https://doi.org/10.1007/s11357-017-9972-z

Varady, K. A., & Hellerstein, M. K. (2007). Alternate-day fasting and chronic disease prevention: a review of human and animal trials. *The American Journal of Clinical Nutrition*, *86*(1), 7-13. https://doi.org/10.1093/ajcn/86.1.7

Wang, G., Ding, L., Gao, C., Zhang, N., Gan, D., Sun, Y., Xu, L., Luo, Q., & Jiang, Z. (2019). Neuroprotective effect of l-serine against white matter demyelination by harnessing and modulating inflammation in mice. *Neuropharmacology*, *146*, 39-49. https://doi.org/10.1016/j.neuropharm.2018.11.025

Wasko, B. M., & Kaeberlein, M. (2014). Yeast replicative aging: a paradigm for defining conserved longevity interventions. *FEMS Yeast Res*, *14*(1), 148-159. https://doi.org/10.1111/1567-1364.12104

Wei, W., Nurse, P., & Broek, D. (1993). Yeast cells can enter a quiescent state through G1, S, G2, or M phase of the cell cycle. *Cancer Res*, *53*(8), 1867-1870.

Weinberger, Feng, L., Paul, A., Smith, D. L., Jr., Hontz, R. D., Smith, J. S., Vujcic, M., Singh, K. K., Huberman, J. A., & Burhans, W. C. (2007). DNA replication stress is a determinant of chronological lifespan in budding yeast. *PloS one*, *2*(8), e748. https://doi.org/10.1371/journal.pone.0000748

Weinberger, M., Mesquita, A., Caroll, T., Marks, L., Yang, H., Zhang, Z., Ludovico, P., & Burhans, W. C. (2010). Growth signaling promotes chronological aging in budding yeast by inducing superoxide anions that inhibit quiescence. *Aging (Albany NY)*, *2*(10), 709-726. https://doi.org/10.18632/aging.100215

Werner-Washburne, M., Roy, S., & Davidson, G. S. (2012). Aging and the survival of quiescent and non-quiescent cells in yeast stationary-phase cultures. *Subcell Biochem*, *57*, 123-143. https://doi.org/10.1007/978-94-007-2561-4_6

Wierman, M. B., Maqani, N., Strickler, E., Li, M., & Smith, J. S. (2017). Caloric Restriction Extends Yeast Chronological Life Span by Optimizing the Snf1 (AMPK) Signaling Pathway. *Mol Cell Biol*, *37*(13). https://doi.org/10.1128/mcb.00562-16

Wierman, M. B., Matecic, M., Valsakumar, V., Li, M., Smith, D. L., Jr., Bekiranov, S., & Smith, J. S. (2015). Functional genomic analysis reveals overlapping and distinct features of chronologically long-lived yeast populations. *Aging (Albany NY)*, *7*(3), 177-194. https://doi.org/10.18632/aging.100729

Wierman, M. B., & Smith, J. S. (2014). Yeast sirtuins and the regulation of aging. *FEMS Yeast Research*, *14*(1), 73-88. https://doi.org/10.1111/1567-1364.12115

Williams, G. C. (1957). Pleiotropy, Natural Selection, and the Evolution of Senescence. *Evolution*, *11*(4), 398-411. https://doi.org/10.2307/2406060

Winzeler EA, e. a. (1999). Functional characterization of the *S. cerevisiae* genome by gene deletion and parallel analysis. *Science*, *285*, 901-906. https://doi.org/10.1126/science.285.5429.901

Woo, C. C., Chen, W. C., Teo, X. Q., Radda, G. K., & Lee, P. T. (2016). Downregulating serine hydroxymethyltransferase 2 (SHMT2) suppresses tumorigenesis in human hepatocellular carcinoma. *Oncotarget*, *7*(33), 53005-53017. https://doi.org/10.18632/oncotarget.10415

Wright, A. D., Hill, D. M., Lowy, C., & Fraser, T. R. (1970). Mortality in acromegaly. *Q J Med*, *39*(153), 1-16. https://www.ncbi.nlm.nih.gov/pubmed/5427331

Wu, Q., Cui, K., Lin, J., Zhu, Y., & Xu, Y. (2017). Urea production by yeasts other than Saccharomyces in food fermentation. *FEMS Yeast Research*, *17*(7). https://doi.org/10.1093/femsyr/fox072

Xu, Y. F., Létisse, F., Absalan, F., Lu, W., Kuznetsova, E., Brown, G., Caudy, A. A., Yakunin, A. F., Broach, J. R., & Rabinowitz, J. D. (2013). Nucleotide degradation and ribose salvage in yeast. *Mol Syst Biol*, *9*, 665. https://doi.org/10.1038/msb.2013.21

Yang, E. J., & Pon, L. A. (2022). Enrichment of aging yeast cells and budding polarity assay in Saccharomyces cerevisiae. *STAR Protocols*, *3*(3), 101599. https://doi.org/https://doi.org/10.1016/j.xpro.2022.101599

Yang, Y., Geldmacher, D. S., & Herrup, K. (2001). DNA replication precedes neuronal cell death in Alzheimer's disease. *J Neurosci*, *21*(8), 2661-2668. https://www.ncbi.nlm.nih.gov/pubmed/11306619

Yurov, Y. B., Vorsanova, S. G., & Iourov, I. Y. (2011). The DNA replication stress hypothesis of Alzheimer's disease. *ScientificWorldJournal*, *11*, 2602-2612. https://doi.org/10.1100/2011/625690

Zeman, M. K., & Cimprich, K. A. (2014). Causes and consequences of replication stress. *Nat Cell Biol*, *16*(1), 2-9. https://doi.org/10.1038/ncb2897

Zeng, J. D., Wu, W. K. K., Wang, H. Y., & Li, X. X. (2019). Serine and one-carbon metabolism, a bridge that links mTOR signaling and DNA methylation in cancer. *Pharmacol Res*, *149*, 104352. https://doi.org/10.1016/j.phrs.2019.104352

Zhang, G., Deighan, A., Raj, A., Robinson, L., Donato, H. J., Garland, G., Leland, M., Martin-McNulty, B., Kolumam, G. A., Riegler, J., Freund, A., Wright, K. M., & Churchill, G. A. (2021). Intermittent fasting and caloric restriction interact with genetics to shape physiological health in mice. *Genetics*, *220*(1). https://doi.org/10.1093/genetics/iyab157

Zhou, X., Zhang, H., He, L., Wu, X., & Yin, Y. (2018). Long-Term l-Serine Administration Reduces Food Intake and Improves Oxidative Stress and Sirt1/NFkappaB Signaling in the Hypothalamus of Aging Mice. *Front Endocrinol (Lausanne)*, *9*, 476. https://doi.org/10.3389/fendo.2018.00476

Zou, K., Rouskin, S., Dervishi, K., McCormick, M. A., Sasikumar, A., Deng, C., Chen, Z., Kaeberlein, M., Brem, R. B., Polymenis, M., Kennedy, B. K., Weissman, J. S., Zheng, J., Ouyang, Q., & Li, H. (2020). Life span extension by glucose restriction is abrogated by methionine supplementation: Cross-talk between glucose and methionine and implication of methionine as a key regulator of life span. *Sci Adv*, *6*(32), eaba1306. https://doi.org/10.1126/sciadv.aba1306